



The University of  
**Nottingham**

UNITED KINGDOM • CHINA • MALAYSIA

CARDAMONIN INDUCES APOPTOSIS IN HUMAN  
NASOPHARYNGEAL CARCINOMA CELLS VIA  
MITOCHONDRIAL DEATH PATHWAY MEDIATED BY  
CASPASE-3 AND CASPASE-8 ACTIVATION, INDEPENDENT OF  
CASPASE-9 SIGNALLING RESPONSES.

CHIANG MICHELLE

FEBRUARY 2016

SCHOOL OF PHARMACY

FACULTY OF SCIENCE

UNIVERSITY OF NOTTINGHAM MALAYSIA CAMPUS,

JALAN BROGA, 43500, SEMENYIH, SELANGOR.

## **ACKNOWLEDGEMENT**

First and foremost, I would like to express my deepest gratitude to my project supervisor, Dr. Khoo Teng Jin for his utmost support and guidance throughout my entire PhD project. I thank him for the freedom he has given to collaborate with other institutes and always encouraging me to attend overseas courses which have broaden my horizons in research world.

I wish to extend my heartfelt gratitude to Dr. Chin Chiew Foan for allowing me to utilize her laboratory in BRC and her guidance in molecular work. A special thank to the laboratory assistants in Faculty of Science who have helped me in many different ways.

This project was fully funded by scholarship awarded from Public Service Department (PSD) Malaysia.

My sincere gratitude also goes out to Dr. Khoo's team members who have generously guided me throughout my research and created an enjoyable environment to work in the lab.

Finally, I would like to express my gratitude to my family and friends who have morally supported me all along and for their inspiring voices.

Thank you.

## TABLE OF CONTENTS

PAGE	PAGE NUMBER
<b>TABLE OF CONTENTS</b>	i
<b>ABSTRACT</b>	xiii
<b>LIST OF FIGURES</b>	xv
<b>LIST OF TABLES</b>	xxi
<b>LIST OF ABBREVIATIONS</b>	xxii
<b>CHAPTER</b>	
<b>1.0 INTRODUCTION</b>	1
1.1 Phytochemical/secondary metabolite from edible plants as anticancer agent	1
1.2 Selection of plants	3
1.2.1 Curry leaf ( <i>Murraya koenigii</i> )	3
1.2.2 Temu kunci ( <i>Boesenbergia rotunda</i> )	5
1.2.3 Bunga kantan ( <i>Phaeomeria imperialis</i> )	7
1.2.4 Spring onion leaf ( <i>Allium fistulosum</i> )	8
1.2.5 Pearl/Pink bean ( <i>Phaseolus vulgaris</i> )	10
1.3 Understanding cancer	11
1.4 Cancer treatment	12
1.5 Nasopharyngeal carcinoma (NPC) cells	13
1.6 Plant phytochemicals/secondary metabolites extraction	15
1.7 Tetrazolium (MTT) assay for cellular viability	16
1.8 Selection of isolated compounds from temu kunci ( <i>Boesenbergia rotunda</i> )	17
1.9 Cardamonin	20
1.10 Apoptosis	21
1.11 DNA fragmentation: Hallmark of cell death	22
1.12 Caspase-activation: The initiation of mitochondrial-dependent apoptotic pathway	22
1.13 Cell cycle analysis: Stage of arrest	23
1.14 Overproduction of Reactive Oxygen Species (ROS): Promoter of cell death	24
1.15 Bcl-2 family proteins: Mitochondrial-dependent cell death pathway regulators	28
1.16 Mitochondrial outer membrane (OMM) permeabilization: Cell death execution	32
1.17 Malfunction of cell leads to drop in ATP synthesis: Will cardamonin affect level in HK-1 cells?	36
1.18 Do apoptosis occur dependent or independent of caspase-9?: Relative quantification of gene expression level	37
1.19 Objectives	38

<b>2.0</b>	<b>METHODOLOGY</b>	<b>40</b>
2.1	Materials	40
2.2	Edible plant crude extracts	42
2.3	Total phenolic and flavonoid content determination	43
2.3.1	Preparation of stock crude extracts	43
2.3.2	Total phenolic content determination by Folin-Ciocalteu assay	43
2.3.3	Total flavonoid content determination using Dowd method	44
2.4	Phytochemical analysis	44
2.4.1	Preparation of stock crude extracts	44
2.4.2	Tannins	45
2.4.3	Saponins	45
2.4.4	Phlobatannins	45
2.4.5	Flavonoids	45
2.4.6	Terpenoids	45
2.4.7	Steroids	46
2.4.8	Alkaloids	46
2.4.9	Glycosides	46
2.5	Cell culture	46
2.5.1	Cell propagation and its maintenance	46
2.5.2	Subculture	47
2.5.3	Cryopreservation	48
2.5.4	Cell thawing	48
2.6	Cytotoxic assay	49
2.6.1	Stock sample preparation	49
2.6.2	Cell seeding	49
2.6.3	Treatment preparation and dilutions	50
2.6.4	Cell viability using MTT assay	51
2.7	Cytotoxic effects of cardamonin, pinostrobin, naringin and hesperidin against HK-1 and NP-69 cell lines	52
2.8	Viable cell count using trypan blue	53
2.9	Fluorescence assay- cellular morphology microscopic observations	53
2.10	DNA fragmentation assay	54
2.11	Cell cycle analysis	55
2.12	Caspase-3 and caspase-8 activity	58
2.13	Reactive Oxygen Species (ROS) production using Cellular Antioxidant (CAA) assay	59
2.14	JC-1 Mitochondrial Membrane Potential Assay	60
2.15	ADP/ATP Ratio Assay	61
2.16	Detection of mitochondrial-dependent pathway associated proteins using western blotting	62
2.16.1	Preparation of cell lysate (proteins) from cardamonin-treated HK-1 cells	65
2.16.2	Protein concentration determination	65
2.16.3	Gel electrophoresis for protein separation in 24, 48 and 72 hrs cardamonin-induced HK-1 cells	66



2.16.4	Gel electrophoresis for protein separation in 0-24 hrs cardamonin-induced HK-1 cells through optimization of resolving gel percentage	66
2.16.5	Visualization of protein in gel	67
2.16.6	Protein transfer (Electro blotting)	67
2.16.7	Blocking and Detection	69
2.16.8	Loading control	69
2.17	Relative quantification of caspase-9 gene expression level using real-time PCR	70
2.18	Statistical analysis	77
<b>3.0</b>	<b>RESULTS</b>	78
3.1	Phytochemical analysis	78
3.2	Total phenolic content	81
3.3	Total flavonoid content	83
3.4	Cytotoxic activity	85
3.4.1	Effect of various crude extracts and positive control on HK-1 cell viability	85
3.4.1.1	Effect of methanol crude extract of bunga kantan on HK-1 cell viability	85
3.4.1.2	Effect of ethyl acetate crude extract of bunga kantan on HK-1 cell viability	87
3.4.1.3	Effect of hexane crude extract of bunga kantan on HK-1 cell viability	89
3.4.1.4	Effect of methanol solid 1 crude extract of bunga kantan on HK-1 cell viability	91
3.4.1.5	Effect of methanol crude extract of curry leaf on HK-1 cell viability	93
3.4.1.6	Effect of ethyl acetate crude extract of curry leaf on HK-1 cell viability	95
3.4.1.7	Effect of hexane crude extract of curry leaf on HK-1 cell viability	97
3.4.1.8	Effect of methanol crude extract of temu kunci on HK-1 cell viability	99
3.4.1.9	Effect of ethyl acetate crude extract of temu kunci on HK-1 cell viability	101
3.4.1.10	Effect of hexane crude extract of temu kunci on HK-1 cell viability	103
3.4.1.11	Effect of methanol crude extract of spring onion leaf on HK-1 cell viability	105
3.4.1.12	Effect of ethyl acetate crude extract of spring onion leaf on HK-1 cell viability	107
3.4.1.13	Effect of hexane crude extract of spring onion on HK-1 cell viability	109

3.4.1.14	Effect of methanol crude extract of mushroom bean on HK-1 cell viability	111
3.4.1.15	Effect of ethyl acetate crude extract of mushroom bean on HK-1 cell viability	113
3.4.1.16	Effect of hexane crude extract of mushroom bean on HK-1 cell viability	115
3.4.1.17	Effect of 5-fluorouracil on HK-1 cell viability	117
3.4.2	Effect of various crude extracts on NP-69 cell viability	119
3.4.2.1	Effect of methanol crude extract of bunga kantan on NP-69 cell viability	119
3.4.2.2	Effect of ethyl acetate crude extract of bunga kantan on NP-69 cell viability	121
3.4.2.3	Effect of hexane crude extract of bunga kantan on NP-69 cell viability	123
3.4.2.4	Effect of methanol solid 1 crude extract of bunga kantan on NP-69 cell viability	125
3.4.2.5	Effect of methanol crude extract of curry leaf on NP-69 cell viability	127
3.4.2.6	Effect of ethyl acetate crude extract of curry leaf on NP-69 cell viability	129
3.4.2.7	Effect of hexane crude extract of curry leaf on NP-69 cell viability	131
3.4.2.8	Effect of methanol crude extract of temu kunci on NP-69 cell viability	133
3.4.2.9	Effect of ethyl acetate crude extract of temu kunci on NP-69 cell viability	135
3.4.2.10	Effect of hexane crude extract of temu kunci on NP-69 cell viability	137
3.4.2.11	Effect of methanol crude extract of spring onion leaf on NP-69 cell viability	139
3.4.2.12	Effect of ethyl acetate crude extract of spring onion leaf on NP-69 cell viability	141
3.4.2.13	Effect of methanol crude extract of temu kunci on NP-69 cell viability	143
3.4.2.14	Effect of methanol crude extract of mushroom bean on NP-69 cell viability	145
3.4.2.15	Effect of ethyl acetate crude extract of mushroom bean on NP-69 cell viability	147
3.4.2.16	Effect of hexane crude extract of mushroom bean on NP-69 cell viability	149
3.4.3	IC <sub>50</sub> (Concentration that produces 50% growth inhibition) values of cytotoxic activity	151
3.5	Cytotoxic effects of cardamonin, pinostrobin, naringin and hesperidin against HK-1 and NP-69 cell lines	153
3.6	Cardamonin induces cell death and decreases cell viability in HK-1 cells	159

3.7	Cardamonin induces morphological changes in HK-1 cells	162
3.8	Cardamonin induces apoptosis in HK-1 cells stained with fluorescence dyes	164
3.9	Cardamonin induces apoptosis leading to DNA fragmentation	166
3.10	Cell cycle analysis: Cardamonin induces cell cycle arrest at G2/M phase and Sub-G1 (apoptotic) phase	167
3.11	Cardamonin induces up-regulation of both caspase-3 and caspase-8 in HK-1 cells	170
3.11.1	Cardamonin induces up-regulation of caspase-3	170
3.11.2	Cardamonin induces up-regulation of caspase-8	170
3.12	Cardamonin decreases intracellular ROS production and ROS does not contribute to HK-1 cell death	172
3.13	Cardamonin induces loss of mitochondrial membrane potential in HK-1 cells	176
3.14	Cardamonin decreases intracellular ATP levels in HK-1 cells	182
3.15	Cardamonin induces cell death <i>via</i> activation of mitochondrial-dependent pathway associated proteins	184
3.15.1	Protein separation using gel electrophoresis for 24, 48 and 72 hrs	184
3.15.2	Up-regulation of Bcl2-L1 anti-apoptotic protein level after 24 hrs cardamonin treatment	185
3.15.3	Protein separation using gel electrophoresis for untreated control and 3-24 hrs cardamonin-treated HK-1 cells	186
3.15.4	Changes in mitochondrial-dependent pathway associated proteins expression levels	187
3.16	Mitochondrial-dependent apoptotic pathway occurs independent of caspase-9	191
<b>4.0</b>	<b>DISCUSSION</b>	194
<b>5.0</b>	<b>CONCLUSION AND PROPOSED FUTURE STUDIES</b>	219
<b>6.0</b>	<b>REFERENCES</b>	227
<b>7.0</b>	<b>APPENDICES</b>	245
7.1	Total phenolic content of various crude extracts determined by Folin-Ciocalteu's assay	245
7.2	Total flavonoid content of various crude extracts using Dowd method	247
7.3	Cell viability of HK-1 and NP-69 cell lines	249
7.3.1	Template for cell treatment	249

7.3.2	Data of percentage of cell viability of HK-1 cells treated with crude methanolic extract of bunga kantan after 24 hrs treatment	249
7.3.3	Data of percentage of cell viability of HK-1 cells treated with crude ethyl acetate extract of bunga kantan after 24 hrs treatment	250
7.3.4	Data of percentage of cell viability of HK-1 cells treated with crude hexane extract of bunga kantan after 24 hrs treatment	250
7.3.5	Data of percentage of cell viability of HK-1 cells treated with crude methanolic solid 1 extract of bunga kantan after 24 hrs treatment	250
7.3.6	Data of percentage of cell viability of HK-1 cells treated with crude methanolic extract of bunga kantan after 48 hrs treatment	251
7.3.7	Data of percentage of cell viability of HK-1 cells treated with crude ethyl acetate extract of bunga kantan after 48 hrs treatment	251
7.3.8	Data of percentage of cell viability of HK-1 cells treated with crude hexane extract of bunga kantan after 48 hrs treatment	251
7.3.9	Data of percentage of cell viability of HK-1 cells treated with crude methanolic solid 1 extract of bunga kantan after 48 hrs treatment	252
7.3.10	Data of percentage of cell viability of HK-1 cells treated with crude methanolic extract of curry leaf after 24 hrs treatment	252
7.3.11	Data of percentage of cell viability of HK-1 cells treated with crude ethyl acetate extract of curry leaf after 24 hrs treatment	252
7.3.12	Data of percentage of cell viability of HK-1 cells treated with crude hexane extract of curry leaf after 24 hrs treatment	253
7.3.13	Data of percentage of cell viability of HK-1 cells treated with crude methanolic extract of curry leaf after 48 hrs treatment	253
7.3.14	Data of percentage of cell viability of HK-1 cells treated with crude ethyl acetate extract of curry leaf after 48 hrs treatment	253
7.3.15	Data of percentage of cell viability of HK-1 cells treated with crude hexane extract of curry leaf after 48 hrs treatment	254
7.3.16	Data of percentage of cell viability of HK-1 cells treated with crude methanolic extract of temu kunci after 24 hrs treatment	254
7.3.17	Data of percentage of cell viability of HK-1 cells treated with crude ethyl acetate extract of temu kunci after 24 hrs treatment	254

7.3.18	Data of percentage of cell viability of HK-1 cells treated with crude hexane extract of temu kunci after 24 hrs treatment	255
7.3.19	Data of percentage of cell viability of HK-1 cells treated with crude methanolic extract of temu kunci after 48 hrs treatment	255
7.3.20	Data of percentage of cell viability of HK-1 cells treated with crude ethyl acetate extract of temu kunci after 48 hrs treatment	255
7.3.21	Data of percentage of cell viability of HK-1 cells treated with crude hexane extract of temu kunci after 48 hrs treatment	256
7.3.22	Data of percentage of cell viability of HK-1 cells treated with crude methanolic extract of spring onion leaf after 24 hrs treatment	256
7.3.23	Data of percentage of cell viability of HK-1 cells treated with crude ethyl acetate extract of spring onion leaf after 24 hrs treatment	256
7.3.24	Data of percentage of cell viability of HK-1 cells treated with crude hexane extract of spring onion leaf after 24 hrs treatment	257
7.3.25	Data of percentage of cell viability of HK-1 cells treated with crude methanolic extract of spring onion leaf after 48 hrs treatment	257
7.3.26	Data of percentage of cell viability of HK-1 cells treated with crude ethyl acetate extract of spring onion leaf after 48 hrs treatment	257
7.3.27	Data of percentage of cell viability of HK-1 cells treated with crude hexane extract of spring onion leaf after 48 hrs treatment	258
7.3.28	Data of percentage of cell viability of HK-1 cells treated with crude methanolic extract of pink/mushroom bean after 24 hrs treatment	258
7.3.29	Data of percentage of cell viability of HK-1 cells treated with crude ethyl acetate extract of pink/mushroom bean after 24 hrs treatment	258
7.3.30	Data of percentage of cell viability of HK-1 cells treated with crude hexane extract of pink/mushroom bean after 24 hrs treatment	259
7.3.31	Data of percentage of cell viability of HK-1 cells treated with crude methanolic extract of pink/mushroom bean after 48 hrs treatment	259
7.3.32	Data of percentage of cell viability of HK-1 cells treated with crude ethyl acetate extract of pink/mushroom bean after 48 hrs treatment	259
7.3.33	Data of percentage of cell viability of HK-1 cells treated with crude hexane extract of pink/mushroom bean after 48 hrs treatment	260

7.3.34	Data of percentage of cell viability of HK-1 cells treated with 5-fluorouracil after 24 hrs treatment	260
7.3.35	Data of percentage of cell viability of HK-1 cells treated with 5-fluorouracil after 48 hrs treatment	260
7.3.36	Data of percentage of cell viability of NP-69 cells treated with crude methanolic extract of bunga kantan after 24 hrs treatment	261
7.3.37	Data of percentage of cell viability of NP-69 cells treated with crude ethyl acetate extract of bunga kantan after 24 hrs treatment	261
7.3.38	Data of percentage of cell viability of NP-69 cells treated with crude hexane extract of bunga kantan after 24 hrs treatment	261
7.3.39	Data of percentage of cell viability of NP-69 cells treated with crude methanolic extract of bunga kantan after 48 hrs treatment	262
7.3.40	Data of percentage of cell viability of NP-69 cells treated with crude ethyl acetate extract of bunga kantan after 48 hrs treatment	262
7.3.41	Data of percentage of cell viability of NP-69 cells treated with crude hexane extract of bunga kantan after 48 hrs treatment	262
7.3.42	Data of percentage of cell viability of NP-69 cells treated with crude methanolic solid 1 extract of bunga kantan after 24 hrs treatment	263
7.3.43	Data of percentage of cell viability of NP-69 cells treated with crude methanolic solid 1 extract of bunga kantan after 48 hrs treatment	263
7.3.44	Data of percentage of cell viability of NP-69 cells treated with crude methanolic extract of curry leaf after 24 hrs treatment	263
7.3.45	Data of percentage of cell viability of NP-69 cells treated with crude methanolic extract of curry leaf after 48 hrs treatment	264
7.3.46	Data of percentage of cell viability of NP-69 cells treated with crude ethyl acetate extract of curry leaf after 24 hrs treatment	264
7.3.47	Data of percentage of cell viability of NP-69 cells treated with crude ethyl acetate extract of curry leaf after 48 hrs treatment	264
7.3.48	Data of percentage of cell viability of NP-69 cells treated with crude hexane extract of curry leaf after 24 hrs treatment	265
7.3.49	Data of percentage of cell viability of NP-69 cells treated with crude hexane extract of curry leaf after 48 hrs treatment	265
7.3.50	Data of percentage of cell viability of NP-69 cells treated with crude methanolic extract of temu kunci after 24 hrs treatment	265

7.3.51	Data of percentage of cell viability of NP-69 cells treated with crude methanolic extract of temu kunci after 48 hrs treatment	266
7.3.52	Data of percentage of cell viability of NP-69 cells treated with crude ethyl acetate extract of temu kunci after 24 hrs treatment	266
7.3.53	Data of percentage of cell viability of NP-69 cells treated with crude ethyl acetate extract of temu kunci after 48 hrs treatment	266
7.3.54	Data of percentage of cell viability of NP-69 cells treated with crude hexane extract of temu kunci after 24 hrs treatment	267
7.3.55	Data of percentage of cell viability of NP-69 cells treated with crude hexane extract of temu kunci after 48 hrs treatment	267
7.3.56	Data of percentage of cell viability of NP-69 cells treated with crude methanolic extract of spring onion leaf after 24 hrs treatment	267
7.3.57	Data of percentage of cell viability of NP-69 cells treated with crude methanolic extract of spring onion leaf after 48 hrs treatment	268
7.3.58	Data of percentage of cell viability of NP-69 cells treated with crude ethyl acetate extract of spring onion leaf after 24 hrs treatment	268
7.3.59	Data of percentage of cell viability of NP-69 cells treated with crude ethyl acetate extract of spring onion leaf after 48 hrs treatment	268
7.3.60	Data of percentage of cell viability of NP-69 cells treated with crude hexane extract of spring onion leaf after 24 hrs treatment	269
7.3.61	Data of percentage of cell viability of NP-69 cells treated with crude hexane extract of spring onion leaf after 48 hrs treatment	269
7.3.62	Data of percentage of cell viability of NP-69 cells treated with crude methanolic extract of mushroom bean after 24 hrs treatment	269
7.3.63	Data of percentage of cell viability of NP-69 cells treated with crude methanolic extract of mushroom bean after 48 hrs treatment	270
7.3.64	Data of percentage of cell viability of NP-69 cells treated with crude ethyl acetate extract of mushroom bean after 24 hrs treatment	270
7.3.65	Data of percentage of cell viability of NP-69 cells treated with crude ethyl acetate extract of mushroom bean after 48 hrs treatment	270
7.3.66	Data of percentage of cell viability of NP-69 cells treated with crude hexane extract of mushroom bean after 24 hrs treatment	271

7.3.67	Data of percentage of cell viability of NP-69 cells treated with crude hexane extract of mushroom bean after 48 hrs treatment	271
7.4	Cytotoxic effects of cardamonin, pinostrobin, naringin and hesperidin against HK-1 and NP-69 cell lines	272
7.4.1	Data of percentage of cell viability of HK-1 cells treated with cardamonin after 24 hrs	272
7.4.2	Data of percentage of cell viability of HK-1 cells treated with cardamonin after 48 hrs	272
7.4.3	Data of percentage of cell viability of HK-1 cells treated with cardamonin after 72 hrs	273
7.4.4	Data of percentage of cell viability of HK-1 cells treated with hesperidin after 24 hrs	273
7.4.5	Data of percentage of cell viability of HK-1 cells treated with hesperidin after 48 hrs	273
7.4.6	Data of percentage of cell viability of HK-1 cells treated with hesperidin after 72 hrs	274
7.4.7	Data of percentage of cell viability of HK-1 cells treated with naringin after 24 hrs	274
7.4.8	Data of percentage of cell viability of HK-1 cells treated with naringin after 48 hrs	274
7.4.9	Data of percentage of cell viability of HK-1 cells treated with naringin after 72 hrs	275
7.4.10	Data of percentage of cell viability of HK-1 cells treated with pinostrobin after 24 hrs	275
7.4.11	Data of percentage of cell viability of HK-1 cells treated with pinostrobin after 48 hrs	275
7.4.12	Data of percentage of cell viability of HK-1 cells treated with pinostrobin after 72 hrs	276
7.4.13	Data of percentage of cell viability of NP-69 cells treated with cardamonin after 24 hrs	276
7.4.14	Data of percentage of cell viability of NP-69 cells treated with cardamonin after 48 hrs	276
7.4.15	Data of percentage of cell viability of NP-69 cells treated with cardamonin after 72 hrs	277
7.4.16	Tryphan blue cell counting	277
7.5	Cell cycle analysis	277
7.5.1	Histogram and forward scatter (FS) and side scatter (SS) dot plot of control group	278
7.5.2	Histogram and forward scatter (FS) and side scatter (SS) dot plot of cardamonin treated at 12 hrs	279
7.5.3	Histogram and forward scatter (FS) and side scatter (SS) dot plot of cardamonin treated at 24 hrs	280
7.6	Caspase-3,-8 assays	281
7.6.1	R110 standard curve	281
7.6.2	Caspase-3 assay	281



7.6.2.1	Cardamonin-treated HK-1 cells at 24, 48 and 72 hrs	281
7.6.2.2	Untreated HK-1 cells at 24, 48 and 72 hrs	282
7.6.2.3	Cardamonin treated HK-cells with inhibitor at 24, 48 and 72 hrs	282
7.6.3	Caspase-8 assay	282
7.6.3.1	Cardamonin-treated HK-1 cells at 24, 48 and 72 hrs	282
7.6.3.2	Untreated HK-1 cells at 24, 48 and 72 hrs	283
7.6.3.3	Cardamonin treated HK-cells with inhibitor at 24, 48 and 72 hrs	283
7.7	Cellular Antioxidant Activity (CAA) assay	283
7.7.1	Preparation of quercetin standard from 200µM stock	283
7.7.2	Preparation of cardamonin from 200µM stock	284
7.7.3	CAA assay at various concentrations of cardamonin-treated HK-1 cells	284
7.7.4	CAA assay at various concentrations of quercetin-treated HK-1 cells	287
7.8	Effect of cardamonin on mitochondrial membrane potential in HK-1 cells after 3 and 6 hrs	291
7.9	Effect of cardamonin on intracellular ATP levels in HK-1 cells after 3 and 6 hrs	291
7.9.1	ADP/ATP ratio	291
7.10	Western blotting	292
7.10.1	Protein quantification	292
7.10.1.1	BSA standard curve	292
7.10.2	Gel electrophoresis (SDS-PAGE)	293
7.10.2.1	Preparing gels at different resolving gel percentage	293
7.10.2.2	Separation of proteins on gel electrophoresis for 24, 48 and 72 hrs	293
7.10.2.3	Separation of proteins on gel electrophoresis 0-24 hrs	294
7.10.3	Electro blotting	294
7.10.3.1	Bcl2-L1 protein expression in 0-24 hrs cardamonin-induced HK-1 cells	294
7.10.3.2	Cytochrome c protein expression in 0-24hrs cardamonin-induced HK-1 cells	295
7.10.3.3	Bcl-2 protein expression in 0-24hrs cardamonin-induced HK-1 cells	295
7.10.3.4	Bad protein expression in 0-24hrs cardamonin-induced HK-1 cells	294
7.10.3.5	Bax protein expression in 0-24hrs cardamonin-induced HK-1 cells	296
7.10.3.6	GADPH (as loading control) protein expression in 0-24 hrs cardamonin-induced HK-1 cells	297

7.10.4	Quantification of protein bands intensities	297
7.10.4.1	Bcl2-L1 protein expression level	297
7.10.4.2	Cytochrome c protein expression level	298
7.10.4.3	Bcl-2 protein expression level	298
7.10.4.4	Bax protein expression level	298
7.11	Relative quantification of caspase-9 gene expression level using real-time PCR	299
7.11.1	Total RNA extraction from HK-1 cells	299
7.11.2	Gel electrophoresis for total RNA extraction in HK-1 cells after 24 hrs	299
7.11.3	Mix preparation	300
7.11.4	Amplification plot in control and cardamonin-treated HK-1 cells (by assay)	301
7.11.5	Amplification plot in control and cardamonin-treated HK-1 cells (by assay repeats)	301
7.11.6	Amplification plot in control and cardamonin-treated HK-1 cells (by sample)	301
7.11.7	Amplification plot in control and cardamonin-treated HK-1 cells (by sample repeats)	302
7.11.8	Derivative melt in control and cardamonin-treated HK-1 cell (by assay)	302
7.11.9	Derivative melt in control and cardamonin-treated HK-1 cells (by assay repeats)	303
7.11.10	Derivative melt in control and cardamonin-treated HK-1 cells (by sample)	303
7.11.11	Derivative melt in control and cardamonin-treated HK-1 cells (by sample repeats)	304
7.11.12	Component melt in control and cardamonin-treated HK-1 cells (by assay)	304
7.11.13	Component melt in control and cardamonin-treated HK-1 cells (by assay repeats)	305
7.11.14	Component melt in control and cardamonin-treated HK-1 cells (by sample)	305
7.11.15	Component melt in control and cardamonin-treated HK-1 cells (by sample repeats)	306
7.11.16	Gel electrophoresis of amplicons	307
7.11.17	Relative quantification using Livak method	308

<b>8.0</b>	<b>MANUSCRIPTS</b>	<b>309</b>
------------	--------------------	------------

## ABSTRACT

Nasopharyngeal cancer lies in the upper part of throat behind the nose and near the base of the skull called the nasopharynx. It is more commonly diagnosed in parts of Asia, particularly in the southern China. Five local edible plants from different families; namely curry leaf (*Murraya koenigii*), temu kunci (*Boesenbergia rotunda*), spring onion leaf (*Allium cepa*), mushroom bean (*Phaseolus vulgaris*) and bunga kantan (*Phaeomeria imperialis*) were macerated to obtain methanol, ethyl acetate and hexane crude extracts. Each crude extract was tested against nasopharyngeal carcinoma (HK-1) and normal nasopharyngeal epithelial (NP-69) cell lines. All crude extracts from temu kunci (*Boesenbergia rotunda*) were found to contain flavonoids, alkaloids and polyphenols. Both methanolic and hexane crude extracts were found to exhibit cytotoxic effects against HK-1 cells but non-toxic against NP-69 cell line. Of all the bioactive compounds previously extracted from *B. Rotunda*, we have selected four commercially available flavonoids and polyphenols to narrow down our search to one potential anticancer agent. These compounds were tested against HK-1 and NP-69 cell lines for cytotoxicity and it was found that cardamonin exhibits highest cytotoxic effect against HK-1 cells with IC<sub>50</sub> of 22 µg/mL.

Cardamonin, a naturally occurring chalcone from the rhizome of *Boesenbergia rotunda* (locally known as temu kunci) was found to induce apoptosis in human nasopharyngeal carcinoma (HK-1) cell line *in vitro*. It exhibits a significant cytotoxic effect against human nasopharyngeal carcinoma cell line without affecting normal immortalized nasopharyngeal epithelial cell line (NP-69) in MTT assay. Based on these results, HK-1 cell line was treated

with IC<sub>50</sub> 22 µg/mL in time-dependent manner 24, 48 and 72 hrs to further investigate the mechanisms of apoptosis. Apoptotic cells induced by cardamonin were illustrated by change in cellular morphology, increase in G2/M phase population and DNA fragmentation. Furthermore, up-regulation of caspase-3 and caspase-8 activities substantiated the induction of apoptosis through caspase-dependent pathway. Cardamonin leads to a decrease in overproduction of reactive oxygen species (ROS), disruption in mitochondrial membrane potential and drop in intracellular ATP level in HK-1 cells. Present study also revealed up-regulation of pro-apoptotic protein, Bax and apoptotic signalling factor, cytochrome c resulting in down-regulation of anti-apoptotic protein, Bcl-2. There was no fold change in caspase-9 gene expression level suggesting that HK-1 cellular apoptosis occurred independent of caspase-9. Activation of caspase-3 was directly regulated by caspase-8 and does not require caspase-9. Current findings on the mode of actions of cardamonin suggested its potential application as an anticancer agent against nasopharyngeal carcinoma.

## LIST OF FIGURES

FIGURE	PAGE NUMBER
<b>Figure 1:</b> Curry leaf ( <i>Murraya koenigii</i> )	5
<b>Figure 2:</b> Temu kunci ( <i>Boesenbergia rotunda</i> )	6
<b>Figure 3:</b> Bunga kantan ( <i>Phaeomeria imperialis</i> )	8
<b>Figure 4:</b> Spring onion leaf ( <i>Allium fistulosum</i> )	9
<b>Figure 5:</b> Pearl/Pink bean ( <i>Phaseolus vulgaris</i> )	11
<b>Figure 6:</b> Summary of screening for bioactive compounds from five local edible plants.	19
<b>Figure 7:</b> Structure of cardamonin.	21
<b>Figure 8:</b> Principle of Cellular Antioxidant Activity (CAA) assay.	26
<b>Figure 9:</b> Molecular structure of Quercetin and Cardamonin	27
<b>Figure 10:</b> Mitochondrial-dependent intrinsic and extrinsic apoptotic pathways.	31
<b>Figure 11:</b> Flow cytometry	57
<b>Figure 12:</b> The schemetic diagram above described the flow work of western blotting to detect protein being expressed.	64
<b>Figure 13:</b> Electro blotting arrangement.	68
<b>Figure 14:</b> Polymerase chain reaction (PCR) cycle.	73
<b>Figure 15:</b> Exponential curve of real-time PCR showing different phases.	74
<b>Figure 16:</b> Total phenolic content.	82
<b>Figure 17:</b> Total flavonoid content.	84
<b>Figure 18:</b> Effect of methanol crude extract of bunga kantan on HK-1 cell viability	86

<b>Figure 19:</b> Effect of ethyl acetate crude extract of bunga kantan on HK-1 cell viability	88
<b>Figure 20:</b> Effect of hexane crude extract of bunga kantan on HK-1 cell viability	90
<b>Figure 21:</b> Effect of methanol solid 1 crude extract of bunga kantan on HK-1 cell viability	92
<b>Figure 22:</b> Effect of methanol crude extract of curry leaf on HK-1 cell viability	94
<b>Figure 23:</b> Effect of ethyl acetate crude extract of curry leaf on HK-1 cell viability	96
<b>Figure 24:</b> Effect of hexane crude extract of curry leaf on HK-1 cell viability	98
<b>Figure 25:</b> Effect of methanol crude extract of temu kunci on HK-1 cell viability	100
<b>Figure 26:</b> Effect of ethyl acetate crude extract of temu kunci on HK-1 cell viability	102
<b>Figure 27:</b> Effect of hexane crude extract of temu kunci on HK-1 cell viability	104
<b>Figure 28:</b> Effect of methanol crude extract of spring onion leaf on HK-1 cell viability.	106
<b>Figure 29:</b> Effect of ethyl acetate crude extract of spring onion leaf on HK-1 cell viability.	108
<b>Figure 30:</b> Effect of methanol crude extract of temu kunci on HK-1 cell viability.	110
<b>Figure 31:</b> Effect of methanol crude extract of mushroom bean on HK-1 cell viability.	112
<b>Figure 32:</b> Effect of ethyl acetate crude extract of mushroom bean on HK-1 cell viability.	114
<b>Figure 33:</b> Effect of hexane crude extract of mushroom bean on HK-1 cell viability.	116
<b>Figure 34:</b> Effect of 5-fluorouracil on HK-1 cell viability.	118

<b>Figure 35:</b> Effect of methanol crude extract of bunga kantan on NP-69 cell viability.	120
<b>Figure 36:</b> Effect of ethyl acetate crude extract of bunga kantan on NP-69 cell viability	122
<b>Figure 37:</b> Effect of hexane crude extract of bunga kantan on NP-69 cell viability.	124
<b>Figure 38:</b> Effect of methanol solid 1 crude extract of bunga kantan on NP-69 cell viability	126
<b>Figure 39:</b> Effect of methanol crude extract of curry leaf on NP-69 cell viability.	128
<b>Figure 40:</b> Effect of ethyl acetate crude extract of curry leaf on NP-69 cell viability.	130
<b>Figure 41:</b> Effect of hexane crude extract of curry leaf on NP-69 cell viability.	132
<b>Figure 42:</b> Effect of methanol crude extract of temu kunci on NP-69 cell viability.	134
<b>Figure 43:</b> Effect of ethyl acetate crude extract of temu kunci on NP-69 cell viability.	136
<b>Figure 44:</b> Effect of hexane crude extract of temu kunci on NP-69 cell viability.	138
<b>Figure 45:</b> Effect of methanol crude extract of spring onion leaf on NP-69 cell viability.	140
<b>Figure 46:</b> Effect of ethyl acetate crude extract of spring onion leaf on NP-69 cell viability	142
<b>Figure 47:</b> Effect of methanol crude extract of temu kunci on NP-69 cell viability.	144
<b>Figure 48:</b> Effect of methanol crude extract of mushroom bean on NP-69 cell viability.	146
<b>Figure 49:</b> Effect of ethyl acetate crude extract of mushroom bean on NP-69 cell viability.	148
<b>Figure 50:</b> Effect of hexane crude extract of mushroom bean on NP-69 cell viability.	150

<b>Figure 51:</b> Cytotoxic effect of various concentrations of cardamonin on HK-1 cell viability at 24, 48 and 72 hrs.	154
<b>Figure 52:</b> Cytotoxic effect of various concentrations of hesperidin on HK-1 cell viability at 24, 48 and 72 hrs.	155
<b>Figure 53:</b> Cytotoxic effect of various concentrations of naringin on HK-1 cell viability at 24, 48 and 72 hrs.	156
<b>Figure 54:</b> Cytotoxic effect of various concentrations of pinostrobin on HK-1 cell viability at 24, 48 and 72 hrs.	157
<b>Figure 55:</b> Cell viability after 24, 48 and 72 hrs treatment with 22 µg/mL of cardamonin.	160
<b>Figure 56:</b> Cytotoxic effect of various concentrations of cardamonin against NP-69 cell lines after 24, 48 and 72 hrs.	161
<b>Figure 57:</b> Cardamonin induces HK-1 cellular apoptosis at 72 hrs in dose-dependent manner and microscopy observations after 6 hrs of treatment.	163
<b>Figure 58:</b> HK-1 cells stained with acridine orange and propidium iodide fluorescence dyes.	165
<b>Figure 59:</b> DNA fragmentation of HK-1 cells when untreated, treated with 19 µM of anticancer drug, 5-fluorouracil (5-FU) and 22 µg/mL of cardamonin at 24, 48 and 72 hrs.	166
<b>Figure 60:</b> Effects of cardamonin on cell cycle phase distribution in HK-1 cells.	168
<b>Figure 61:</b> Cardamonin induces cell cycle arrest at G2/M phase and sub-G1 (apoptosis) in HK-1 cells at 12 and 24 hrs.	169
<b>Figure 62:</b> Caspase-3 and caspase-8 activities in HK-1 cells when untreated, treated with 22 µg/mL of cardamonin and treated with 22 µg/mL of cardamonin then caspase-3 inhibitor at 24, 48 and 72 hrs.	171
<b>Figure 63:</b> Cellular Antioxidant Activity of Cardamonin in HK-1 cells.	173
<b>Figure 64:</b> Cellular Antioxidant Activity of Quercetin in HK-1 cells.	173
<b>Figure 65:</b> Dose-response curve of Quercetin standard and Cardamonin in HK-1 cells.	174
<b>Figure 66:</b> Effect of cardamonin on mitochondrial membrane potential in HK-1 cells after 3 and 6 hrs.	177



<b>Figure 67:</b> Mitochondrial membrane potential in HK-1 cells (control group) after 3 hrs.	178
<b>Figure 68:</b> Mitochondrial membrane potential in HK-1 cells (control group) after 6 hrs.	179
<b>Figure 69:</b> Effect of cardamonin on mitochondrial membrane potential in HK-1 cells after 3 hrs.	180
<b>Figure 70:</b> Effect of cardamonin on mitochondrial membrane potential in HK-1 cells after 6 hrs.	181
<b>Figure 71:</b> Effect of cardamonin on intracellular ATP levels and ADP/ATP ratio in HK-1 cells after 3 and 6 hrs.	183
<b>Figure 72:</b> Protein lysates extracted from HK-1 cells treated with cardamonin at 24, 48 and 72 hrs were separated on 4% stacking gel and 12% resolving gel.	184
<b>Figure 73:</b> Bcl2-L1 protein expression for 24, 48 and 72 hrs in cardamonin-induced HK-1 cells.	185
<b>Figure 74:</b> Protein lysates extracted from HK-1 cells treated with cardamonin at 3, 6, 9, 12, 18 and 24 hrs were separated on 4% stacking gel and 12% resolving gel.	186
<b>Figure 75:</b> Changes in mitochondrial dependent pathway-associated protein expression levels were analyzed qualitatively by Western blotting.	188
<b>Figure 76:</b> Effect of cardamonin on Bcl-2 protein expression level in time-dependent manner.	189
<b>Figure 77:</b> Effect of cardamonin on Bcl2-L1 protein expression level in time-dependent manner.	189
<b>Figure 78:</b> Effect of cardamonin on Bax protein expression level in time-dependent manner.	190
<b>Figure 79:</b> Effect of cardamonin on cytochrome c protein expression level in time-dependent manner.	190
<b>Figure 80:</b> Dowd method.	197
<b>Figure 81:</b> Structure of koenoline and ditercalinium.	199
<b>Figure 82:</b> Structure of mahanimbicine, murrayamine, mahanine, pyrayafoline and murrafoline.	201

<b>Figure 83:</b> This diagram illustrates mode of actions of cardamonin in activation of mitochondrial-dependent pathway mediated by caspase-8 against nasopharyngeal carcinoma (HK-1) cells.	216
<b>Figure 84:</b> Time Frame of HK-1 cell death.	217
<b>Figure 85:</b> Proposed addition of functional groups on cardamonin.	221
<b>Figure 86:</b> Apoptosis signalling <i>via</i> Fas/Fas L system.	225

## LIST OF TABLES

TABLE	PAGE NUMBER
<b>Table 1:</b> Phytochemical constituents of various crude extracts of curry leaf ( <i>Murraya koenigii</i> ), temu kunci ( <i>Boesenbergia rotunda</i> ), spring onion leaf ( <i>Allium cepa</i> ), mushroom bean ( <i>Phaseolus vulgaris</i> ), bunga kantan ( <i>Phaeomeria imperialis</i> ).	80
<b>Table 2:</b> IC <sub>50</sub> values of various crude extracts on HK-1 and NP-69 cell lines.	152
<b>Table 3:</b> IC <sub>50</sub> values for all four commercially available flavonoids and polyphenols tested against HK-1 cells.	158
<b>Table 4:</b> EC <sub>50</sub> values from dose-response curve.	175
<b>Table 5:</b> Rate of Cellular Antioxidant Activity of quercetin and cardamonin in HK-1 cells.	175
<b>Table 6:</b> Threshold cycle (C <sub>T</sub> ) values of caspase-9 and GADPH in control and cardamonin-treated groups.	193
<b>Table 7:</b> Normalized gene expression ratio and melting temperature of caspase-9 and GADPH in control and cardamonin-treated groups.	193
<b>Table 8:</b> Proposed addition of functional groups on cardamonin.	222

## LIST OF ABBREVIATIONS

°C	: Degree in Celcius
µg	: Microgram
µL	: Microliter
CGM	: Complete Growth Medium
DMSO	: Dimethyl sulfoxide
DMEM	: Dulbecco's Modified Eagle Medium
EDTA	: Ethylenediaminetetraacetic acid
MTT	: 3-[4,5-dimethyl-2-thiazolyl]-2,5-diphenyl tetrazolium bromide
WHO	: World Health Organization
PBS	: Phosphate Buffer Saline
FBS	: Foetal Bovine Serum
mg	: Miligram
mL	: Mililiter
S.D.	: Standard deviation
S.E.M.	: Standard Error of Mean
HK-1	: Human nasopharyngeal carcinoma
NP-69	: Immortalized nasopharyngeal epithelial cell line
IC <sub>50</sub>	: Concentration producing 50% growth inhibition
DNA	: Deoxyribonucleic acid
RNA	: Ribonucleic acid
TBE	: Tris-Borate EDTA
TBS	: Tris Buffered Saline
MeOH	: Methanol
EtOAc	: Ethyl acetate

TEMED	: Tetramethylethylenediamine
APS	: Ammonium persulfate
BSA	: Bovine Serum Albumin
TMB	: 3,3',5,5'-Tetramethylbenzidine (TMB)
JC-1	: 5,5'',6,6''-tetrachloro-1,1'',3,3''-tetraethylbenzimidazolylcarbocyanine iodide
PCR	: Polymerase Chain Reaction
RT-PCR	: Reverse Transcriptase PCR
SYBR Green	: N',N'-dimethyl-N-[4-[(E)-(3-methyl-1,3-benzothiazol-2-ylidene)methyl]-1-phenylquinolin-1-ium-2-yl]-N-propylpropane-1,3-diamine
GADPH	: Glyceraldehyde 3-phosphate dehydrogenase
Bcl2-L1 protein	: a protein that encodes <i>BCL2L1</i> gene, belongs to Bcl-2 family
Bax protein	: a protein that encodes <i>Bax</i> gene, belongs to Bcl-2 family
Bad	: a pro-apoptotic member of the Bcl-2 gene family which is involved in initiating apoptosis
RLU	: Relative Luminescence Units
UV	: Ultraviolet
cDNA	: complementary DNA
C <sub>T</sub>	: Threshold cycle
ANOVA	: Analysis of Variance

## **1.0 Introduction**

The inexhaustible supplies of natural resources allow scientists to explore into the world of natural products. Approximately two third of Malaysia tropical land is covered with rainforest which hosts 14,500 plant species (Richmond and Simon, 2010). Plants have been used as traditional remedies for centuries and were believed to have various therapeutic effects (Dalziel, 1937). Medicinal plants are rich in secondary metabolites which were potential sources for drug discovery. It is believed that plant-derived active compounds such as polyphenols exhibit the ability to inhibit tumor growth (Park and Pezzuto, 2002). The discovery of drugs produced from plant bioactive compounds has given an alternative treatment to patients instead of synthetically developed drugs which could eventually cause side effects on patients (Lazarus *et al.*, 2009). Therefore, the main aim of this study is to evaluate the potential of phytochemical compounds isolated from 5 local edible plants as a source of anticancer bioactive compounds and their effects against nasopharyngeal carcinoma.

### **1.1 Phytochemical/secondary metabolite from edible plants as anticancer agent**

Phytochemicals or secondary metabolites are organic compounds produced by plants in small quantity. The term “secondary” suggests that these metabolites do not directly influence normal development of plants. If these secondary metabolites are absent in plants, plants may still survive like they

normally do despite some may restrict some biological activities in plants. Phytochemicals are found mostly in plant-based food such as fruits and vegetables.

Bioactive compounds are secondary metabolites that contribute greatly for protection to plants in response to environmental stress. Phenolic compound is one of the most prominent phytochemicals that was found to exhibit anticancer activity. Phytochemicals from plants act by stimulation of non-specific and specific immunity in our body (Madhuri and Govind, 2009).

Phenolics and saponins are found most commonly as secondary metabolites or bioactive compounds in plants and have been proven to exhibit anticancer activity (Yu *et al.*, 2009). For instance, the inner bark of *Acacias* produces tannins which are used to treat kidney diseases and malaria (Elhefian *et al.*, 2012). More than 30 types of flavonoids were tested for cytotoxicity against colon cancer cell line and almost all were found to exhibit inhibition in cancer cell proliferation (Kuntz *et al.*, 1999). Curcubitacin B, an oxygenated triterpenes was found to decrease cell viability of human hepatocellular carcinoma, Hep G2 through apoptosis (Zhang *et al.*, 2009). Berberine isolated from *Rhizoma coptidis* is an isoquinoline alkaloid which kills cancer cells through cell cycle arrest (Sun *et al.*, 2009).

To develop a new antitumor agent from plant phytochemical requires long-term commitment. The process involves the discovery of potential natural products usually from plants, the screening process for cytotoxic activity, production and formulation of anticancer drug and finally clinical trials on animals and on human beings (Schwartzmann, 1988).

## 1.2 Selection of plants

Edible plants have long been used as traditional remedies and their therapeutic effects in various ailments and diseases have been established many decades ago. Moreover, edible plants are safe, economical and easily available (Parul *et al.*, 2012). Current research will focus on 5 edible plants from different families, namely; curry leaf (*Murraya koenigii*), temu kunci (*Boesenbergia rotunda*), spring onion leaf (*Allium cepa*), mushroom bean (*Phaseolus vulgaris*) and bunga kantan (*Phaeomeria imperialis*). These edible plants have been well researched for anticancer effect. In fact, most secondary metabolites have been isolated from these plants. However, lack of research of the plants mentioned above on nasopharyngeal carcinoma cells lead to an interest to study their anticancer effect.

### 1.2.1 Curry leaf (*Murraya koenigii*)

Curry leaf (*Murraya koenigii*) is a leafy vegetable which is used widely in Indian cuisine for aromatic flavouring (**Figure 1**). The plant originated from the Tarai region of Uttar Pradesh, India but has since been widely cultivated in the South East Asia. The shrub can grow as high as 2.5 meters in height and its leaf up to 30 cm long, each bearing an average of 24 leaflets (Parul *et al.*, 2012). Fresh leaves of *Murraya koenigii* have high volatile oil content. Gas chromatography-mass spectrometry analysis revealed 34 major constituents where 97.4% of essential oils were identified, namely alpha-pinene( (51.7%), sabinene (10.5%), beta-pinene (9.8%), beta-caryophyllene (5.5%), limonene



(5.4%), bornyl acetate (1.8%), terpinen-4-ol (1.3%), gamma-terpinene (1.2%) and alpha-humulene (1.2%) (Chowdhury *et al.*, 2008).

Curry leaf extracts possess various biological properties. Curry leaf extract was reported to lower the cholesterol level and blood glucose level in diabetic mice (Xie *et al.*, 2006). Methanolic extracts of 21 curry leaf species were screened for antibacterial activity and *S. epidermidis* was significantly inhibited (Thomas *et al.*, 1999). Carbazole alkaloids isolated using dichloromethane showed high antioxidant activity against 1,1-diphenyl-2-picrylhydrazyl (DPPH) (Kureel *et al.*, 1969). Alkaloids pyrafoline-D and murrafoline-I isolated from curry leaf showed a significant cytotoxic activity against human promyelocytic leukemia cells (HL-60) (Ito *et al.*, 2006). Curry leaf is high in calcium which was traditionally used as a supplement to cope with calcium deficiency. Also, essential nutrients such as Vitamin A, Vitamin B, Vitamin C, Vitamin B2, calcium and iron were found in curry leaf (Parul *et al.*, 2012). With present research and literature, the diversified chemical constituents of curry leaf have promising biological values and the potential of this plant has not been completely explored. Hence, current research focuses on cytotoxic effect of various extracts of curry leaf against nasopharyngeal carcinoma (HK-1) cells.



**Figure 1:** Curry leaf (*Murraya koenigii*)

### **1.2.2 Temu kunci (*Boesenbergia rotunda*)**

Temu kunci is an edible plant belonging to the ginger family, Zingiberaceae (**Figure 2**). It grows in the region of South East Asia and India. It is commonly used as a food ingredient to promote flavor and appetite. In Indonesia, it is used as herb for post-natal women (Chaudhury and Rafei, 2001). It is a perennial plant which can grow up to 40 cm in height. The plant consists of long tubers sprout from its rhizome with each tuber having a diameter of approximately 1.5 cm (Sirirugsa, 1992).

Over the years, researchers have discovered the potential and medicinal values of the plant. More than a hundred compounds were isolated and have shown positive results in various biological tests (Tan *et al.*, 2012). Temu

kunci was reported to exhibit highest anticancer activity towards breast cancer cells (MCF-7) and colon cancer cells (HT-29) with low inhibitory concentrations (Kirana *et al.*, 2007). Panduratin A isolated from temu kunci was found to decrease cell viability of prostate cancer cell lines (PC3 and DU145) in time- and dose-dependent manner (Yun *et al.*, 2003). In another study on ovarian cancer cell (CaOV<sub>3</sub>) and breast cancer cell (MDA-MB-231), temu kunci was reported to possess anticancer effect against both cancerous cell lines (Jing *et al.*, 2010). Rhizome of temu kunci was also reported to exhibit wound healing properties where extraction of rhizome using ethanol solvent sped wound and injury recovery (Mahmood *et al.*, 2010). Based on previous reported bioactive compounds found in temu kunci, it has lead to our current study on its potential to exhibit anticancer effect against nasopharyngeal carcinoma cell (HK-1).



**Figure 2:** Temu kunci (*Boesenbergia rotunda*)

### 1.2.3 Bunga kantan (*Phaeomeria imperialis*)

Bunga kantan is an edible plant belonging to the ginger family, Zingiberaceae (**Figure 3**). The inflorescence of bunga kantan is widely used for culinary as food flavouring in laksa and often made into ulam among the Malay community in the South East Asia. The perennial plant is widely cultivated in Malaysia and Indonesia and can grow up to 4.7 m in height (Lachumy *et al.*, 2010). The inflorescence cannot be eaten once it has bloomed, hence flower bud of bunga kantan is the key component that gives flavor, colour and aroma to local cuisines (Chan *et al.*, 2007).

Studies have reported that the flower shoots of the plant extracted from aqueous ethanol exhibit antimicrobial and antitumor activities (Murakami *et al.*, 2000) where as the dichloromethane and methanol extracts showed the presence of alpha-tocopherol in ferric thiocynate assay (FTC) (Habsah *et al.*, 2000). Ethanol extracts from flower shoots of bunga kantan revealed cytotoxic effect on glandular cervix cancer cells (HeLa) (Mackeen *et al.*, 1997). Rhizomes of bunga kantan were extracted with ethyl acetate and the fraction was reported to exhibit cytotoxic effect on human breast cancer cell (MCF-7) and human T-lymphoblatoid (CEM-SS) cancer cell. 2 compounds were isolated from the fraction and they showed high inhibitory effect against the 2 cell lines (Habsah *et al.*, 2005). Acetone extracts from the leaves, stems, rhizomes and inflorescences of bunga kantan were tested and leaf extract was proven to inhibit proliferation of human colorectal cancer (HT-29) cell line (Chun *et al.*, 2009). Hence, this plant was selected for current research to study the anticancer effect on nasopharyngeal carcinoma cancer (HK-1) cell line.



**Figure 3:** Bunga kantan (*Phaeomeria imperialis*)

#### **1.2.4 Spring onion leaf (*Allium fistulosum*)**

Spring onion leaf is an edible plant from the family of Amaryllidaceae (**Figure 4**). Spring onion consists of white bulb where straight and hollow leaves grow from. The plant can grow up to 40 cm high and have a stem thickness of 8-15 cm. It has been used in traditional Chinese cuisine for centuries in Asian countries like China and Japan. The leaves are edible and often added into salads for aroma and taste. The origin of the plant was believed to be from Siberia and Mongolia (Burt, 2007).



Although there is lack of research on anticancer activity of spring onion leaf, its genus *Alliums* has been proven to exhibit high therapeutic and medicinal values. Leaves of *Allium sativum* L., *Allium cepa* L., *Allium vineale* L., *Allium fistulosum* L., *Allium nutans* L., wild *Allium flavum* L. and *Allium ursinum* L. have been reported to exhibit high antioxidant activities (Stajner and Varga, 2003). Diallylsulfide (DAS) isolated from *Alliums* was tested for its antitumor properties on mouse skin carcinogenesis and showed inhibitory results (Singh and Shukla, 1998). Other allylsulfides such as 1,2-dimethylhydrazine has been proven to inhibit malignancies in gastrointestinal tract (Sumiyoshi and Wargovich, 1990). Quercetin was isolated from *Alliums* and treated to mice with tumors derived from human pharyngeal squamous cell carcinoma in dose-dependent manner. A significant inhibition in tumor growth was observed (Castillo *et al.*, 1989). Hence, *Allium fistulosum* was selected for current research to study its anticancer effect on nasopharyngeal carcinoma cancer (HK-1) cell line.

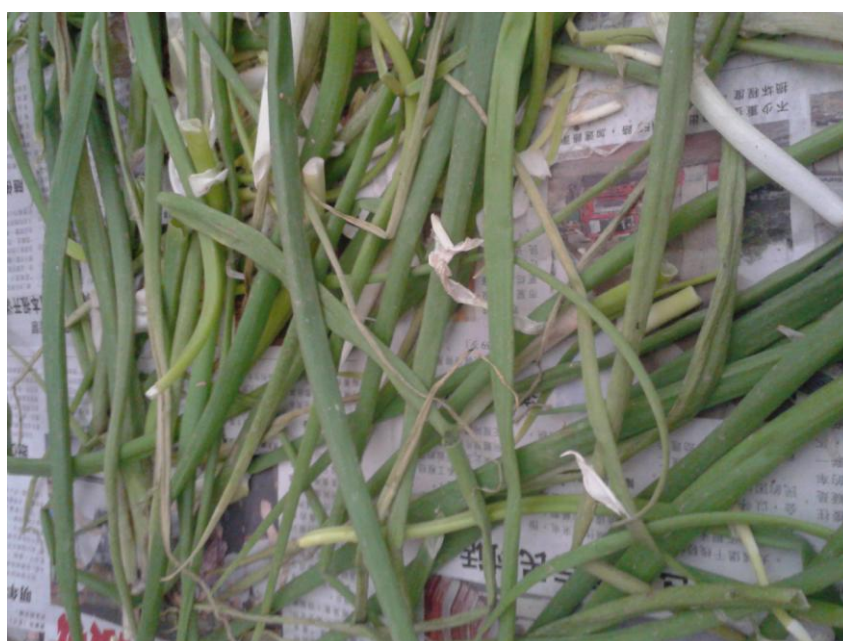


**Figure 4:** Spring onion leaf (*Allium fistulosum*)

### 1.2.5 Pearl/Pink bean (*Phaseolus vulgaris*)

Pearl/Pink bean is an edible legume belonging to the family of Fabaceae (**Figure 5**). It is sometimes known as mushroom bean or cranberry bean and is used in making soup in China. Beans are removed from pods and a slight pinkish hue on beans' surface will disappear once boiled. It gives a nutty flavouring to the soup and causes the soup to appear creamy.

Beans have long been recognized for high protein content, current research however focus on flavonoid content in beans due to various biological activities of flavonoid compounds. Flavonoid glycosides content found in Italian bean (*Phaseolus vulgaris* L.) ecotypes were high (Dinelli *et al.*, 2006). Most distributed flavonoids isolated from seed coats of beans are generally proanthocyanidins and exhibit antioxidant activity (Beninger and Hosfield, 2003). Phytohaemagglutinin, a type of lectin present in *Phaseolus vulgaris* was found to produce higher cytotoxic effect on human colon cancer cell CCL-220/Colo320DM than in human normal colon cells (Heinrich *et al.*, 2005). Legumes black and navy beans fed to tumor-induced rat were found to reduce total tumor incidence by 54% and 59% respectively (Hangen and Bennick, 2002). Hence, *Phaseolus vulgaris* was selected for current research to study its anticancer effect on nasopharyngeal carcinoma cancer (HK-1) cell line.



**Figure 5:** Pearl/Pink bean (*Phaseolus vulgaris*)

### 1.3 Understanding cancer

Generally, cancer occurs when a group of normal cells proliferate abnormally at an uncontrollable rate. In due course, these cells intrude adjacent cells and eventually spread to other body organs via lymph vessels or bloodstream. The severity of the disease includes abnormally proliferated cells which can be malignant. Malignant is closely related with the term metastasis whereby abnormal cells start to proliferate by invading nearby cells and spread uncontrollably to other organs (Dollinger *et al.*, 2002).

According to the World Health Organization (WHO), the world cancer rate can increase by 50% from current record to 15 million people in the year 2020. It was observed that deaths from cancer alone have taken up 12% of worldwide disease-related deaths. WHO reported that cancer appears to be a



major health issues in developing countries where industrialization is the main focus for economic growth. Since the millennium has started, for women, breast cancer has topped second place followed by lung cancer (World Health Organization, 2003). In year 2014, 14 million new cancer cases were reported and this alarming number is expected to rise in the next 2 decades (World Health Organization, 2014).

The reasons for cancer development can be varied. WHO has grouped them into three categories of external agents, including physical carcinogens such as ultraviolet rays, chemical carcinogen such as arsenic in untreated drinking water and biological carcinogens such as viruses and bacteria infection. Risk factors for cancer increase with age and unhealthy diet as well as lack of physical exercise (World Health Organization, 2014).

It is important to maintain a balanced lifestyle to reduce the risk of cancer to a minimum level. For example, running has been proven to reduce the risk of liver and lung cancers by inducing certain antioxidant activity (Duncan *et al.*, 1997).

#### **1.4 Cancer treatment**

Treatments for cancer range from surgery to different kinds of therapies depending on the type of cancer, the location and size of the growth and the seriousness of the cancer in which is classified in stages. Surgery is done to completely remove cancerous tissues from patients. However, there are cases

when some cancerous cells remained at the growth site leading to risk of re-occurrence of cancer (Harbeck *et al.*, 2010).

Ongoing research is done to treat cancer and apart from the above approach, other methods such as using combination of various therapies. However, this combination may result in higher overall response rates to disease progression than the usage of a single therapy (Wardley, 2008). Usually, it involves the combination of traditional chemotherapeutics and targeted biological agents. For example, recently paclitaxel and bevacizumab (act as inhibitors) work synergistically and result in significant improvement in the survival of cancer patients (Gray *et al.*, 2009).

### **1.5 Nasopharyngeal carcinoma (NPC) cells**

In current research, we are interested in Nasopharyngeal cancer is cancer that lies in the upper part of throat behind the nose and near the base of the skull called the nasopharynx. It is fairly rare in most part of the world, 7 in every 1 million people in North America were diagnosed in the year 2012. However, nasopharyngeal cancer is more common in parts of Asia, particularly in the southern China. There are three types of nasopharyngeal carcinoma; namely keratinizing squamous cell carcinoma, non-keratinizing differentiated carcinoma and undifferentiated carcinoma. These are epithelial cells that made up the lining of nasopharynx and are defined as carcinoma when cancerous. Other types of cancers can occur in the nasopharynx region such as lymphomas and adenocarcinoma. Dietary habits and lifestyle may increase the risk of

nasopharyngeal carcinoma (NPC) incidence rate (American Cancer Society, 2012). Infection of Epstein-Barr virus (EBV) may have cause the development of nasopharyngeal carcinoma. EBV-infected nasopharyngeal epithelial cells cause genetic alterations which will eventually transformed into cancerous cells (Tsao *et al.*, 2012).

Currently, NPC is treated by radiation and chemotherapy to remove tumor growth. Anticancer drugs such as paclitaxel and cetuximab have been working synergistically to enhance the antitumor effect in nasopharyngeal carcinoma cell lines which targets the over-expression of epidermal growth factor receptor (EGFR) (Sung *et al.*, 2005). Several compounds isolated from plants displayed anticancer effect against NPC. Cucurbitacin I isolated from *Iberis amara* seeds was proven to inhibit cellular invasion and exhibit high chemopreventive potential in over expressed signal transducer and activator of transcription 3 (STAT 3) genes (Lui *et al.*, 2009). Rhein isolated from rhizome of rhubarb was reported to induce apoptosis in NPC cells. Upon treatment with rhein, apoptosis-inducing factors which were observed through mitochondrial dependent pathways were detected (Lin *et al.*, 2007). Cucurmin-treated NPC demonstrates apoptotic cell death mediated by overproduction of ROS, mitochondrial depolarization and caspase-3 dependent pathway (Kuo *et al.*, 2011). Several other bioactive compounds have been isolated from naturally occurring resources and proven to be potent anticancer agent against nasopharyngeal carcinoma.

It is important to note that approximately 90% of cancers arise from epithelial cells which coat surfaces of colon, skin and nasopharynx. Hence, this

study is important to elucidate the cell death pathway of cancer that arose from epithelial cells. Normal cells and cancer cells are distinct in six different ways; one of them is abnormal and inaccurate cell death of cancer cells. Cellular death occurs at an abnormal rate compared to normal cells (Ravindran *et al.*, 2009). Hence, our research focuses on the discovery of a potential anticancer agent in triggering cancer cell death.

## **1.6 Plant phytochemicals/secondary metabolites extraction**

Essential secondary metabolites are removed through plant extractions. Secondary metabolites are removed from the plant tissue to its surrounding filled with organic solvent. This process is called maceration. After first maceration period, organic solvent containing extracted secondary metabolites is replaced with fresh medium (Mol *et al.*, 1990). When secondary metabolites have diffused from the plant substances into their surrounding solvent, the solvent will become more concentrated and saturated; hence the saturated solvent is removed and replaced by a fresh solvent (Wall *et al.*, 1996).

The choice of solvent is crucial for extraction and factors influencing extraction were taken into consideration. For example, the solubility of target secondary metabolites is vital to ensure that all specific metabolites are extracted from plant during maceration. Other important factors such as how easy it is for the solvent to work with and the purity of end products are taken into consideration when choosing the right solvent (Wall *et al.*, 1996). To maximise the yield of compounds of interest, the principle of “like attracts like” is used. Maceration is a common method used to extract smaller amount

of constituents from plant materials. It functions to soak plant materials in solvent to soften the plant materials and separate the desired constituents. When the plant materials are completely exhausted or dried, the desired constituents in the solvent are ready for screening (Jones and Kinghorn, 2005).

A specific extraction procedure is carried out to get more enriched fractions containing secondary metabolites. The procedure mainly uses the manipulation of compound's polarity. In current research, methanol, ethyl acetate and hexane organic solvents were used to extract fractions containing polar, semi-polar and non-polar compounds respectively.

### **1.7 Tetrazolium (MTT) assay for cellular viability**

3-[4,5-dimethylthiazol-2-yl]-2,5-diphenyl tetrazolium bromide (MTT) assay is a colorimetric assay to count viable cells and the reaction is based on the reduction of mitochondrial dehydrogenases. The reduced product is a water-insoluble blue formazan. Depending on how much uptake by viable cells, this blue formazan must be dissolved in order to be measured colorimetrically. There are several solvent to dissolve the blue formazan, however, DMSO is most suitable (Carmichael, 1987). The intracellular reduction of MTT ultimately indicates the estimation of viable cells after compound treatment.

The formation of blue formazan product measured in absorbance unit is plotted against concentration ( $\mu\text{g/mL}$ ) to obtain  $\text{IC}_{50}$ , an inhibitory concentration that reduces cell viability to 50% compared to control group. A

compound is considered to exhibit cytotoxic potential when its  $IC_{50}$  value in the presence of tested compound is significantly less than that occurs in its absence (Mosmann, 1983). For cytotoxic activity of crude extracts,  $IC_{50}$  will be classified as low for  $IC_{50} > 200\mu\text{g/mL}$ , moderate for  $100 < IC_{50} < 200$  and high for  $IC_{50} < 100\mu\text{g/mL}$ .

### **1.8 Selection of isolated compounds from temu kunci (*Boesebergia rotunda*)**

Based on results from current studies, all crude extracts from temu kunci (*Boesenbergia rotunda*) were found to contain flavonoids, alkaloids and polyphenols. Both methanolic and hexane crude extracts were found to exhibit cytotoxic effects against HK-1 cells but non-toxic against normal nasopharyngeal epithelial (NP-69) cell line. Various active compounds have been isolated from *B. Rotunda* (Tan *et al.*, 2012). Of all the bioactive compounds extracted from *B. Rotunda*, we have selected four commercially available flavonoids and polyphenols to narrow down our search to one potential anticancer agent. The screening for bioactive compounds is summarized in **Figure 6**.

All four compounds are flavonoids; cardamonin and pinostrobin and polyphenols; naringin and hesperidin. These compounds were tested against HK-1 and NP-69 cell lines for cytotoxicity and it was found that cardamonin exhibits highest cytotoxic effect against HK-1 cells with  $IC_{50}$  of  $22\mu\text{g/mL}$ .

Therefore, further studies on mode of actions of cardamonin in triggering HK-1 cell death will be conducted.

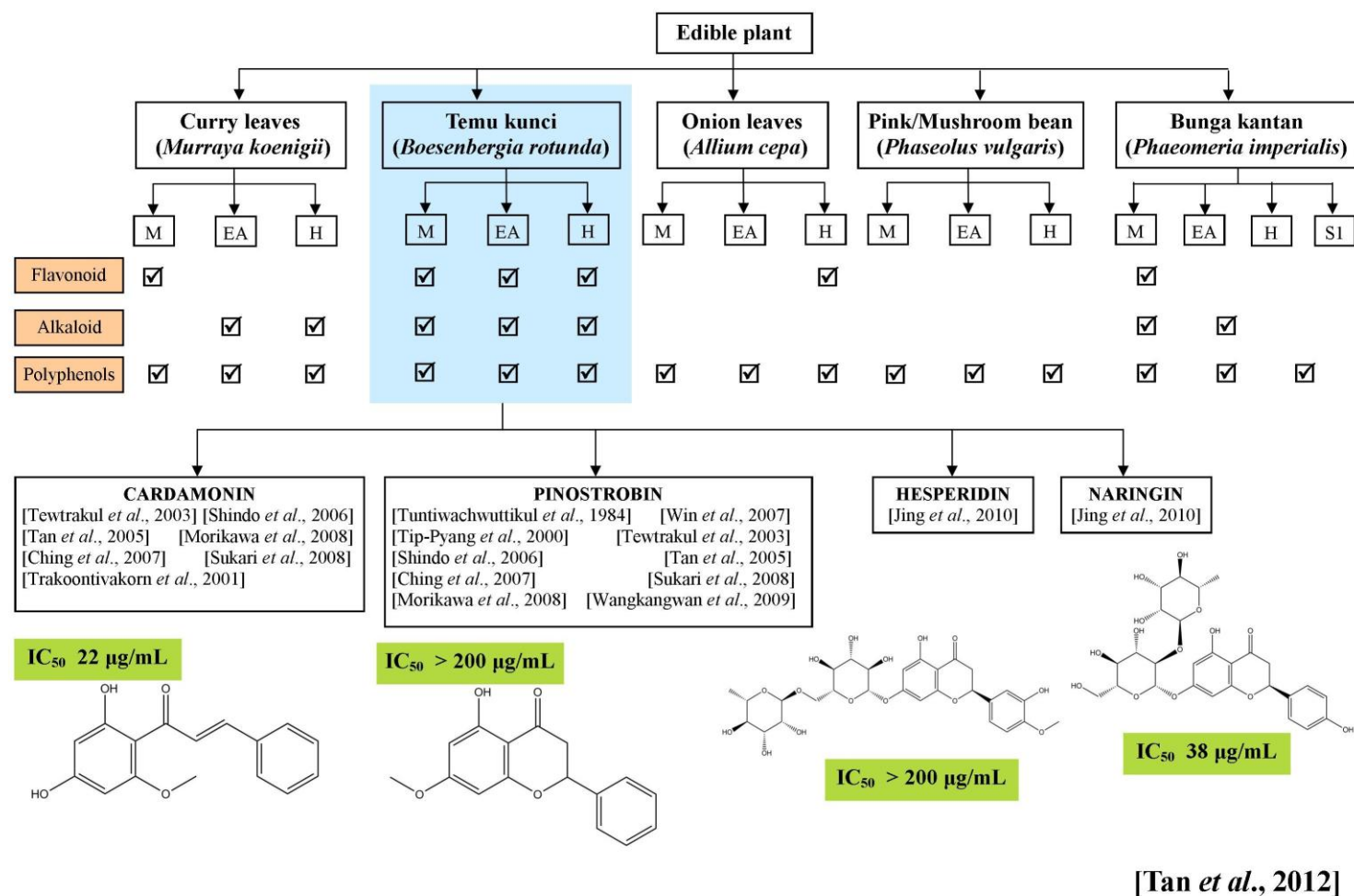


**Figure 6:** Summary of screening for bioactive compounds from five local edible plants.



## 1.9 Cardamonin

From preliminary MTT assays results of four bioactive compounds, it was found that cardamonin exhibit highest cytotoxic effect against HK-1 cells. Hence, cardamonin will be selected for further investigations on how it triggers HK-1 cell death.

Cardamonin was first extracted from cardamom spice and subsequently from other plants in Zingiberaceae family. It is classified as chalcone in flavonoid family whereby it contains two phenyl rings and an aromatic ketone and enone that forms the central core (**Figure 7**). Electroanalytical methodology was developed to quantify the amount of cardamonin in cardamom (Carvalho *et al.*, 2011). This naturally occurring chalcone has been known to display diverse biological activities such as anticancer and anti-inflammatory activities (Chow *et al.*, 2012). It was proven to repress nuclear factor (NF- $\kappa$ B) and its gene products, ICAM-1, COX-2 and VEGF were down-regulated in human multiple myeloma cells, which cause malignancy of plasma cells in bone marrow (Qin *et al.*, 2012). Cardamonin suppressed Wnt/ $\beta$ -catenin pathway by down regulation of intracellular  $\beta$ -catenin proteins. The degradation of proteins inhibits proliferation of several colon cancer cell lines in dose-dependent manner (Park S *et al.*, 2013). Cardamonin displayed anti-migration and anti-invasion properties against fibrosarcoma cell lines through suppression of transglutaminase 2 (Tgase-2) enzyme expressions (Park MK *et al.*, 2013). In this research, the potential of cardamonin in the activation of apoptosis in HK-1 cells will be investigated.

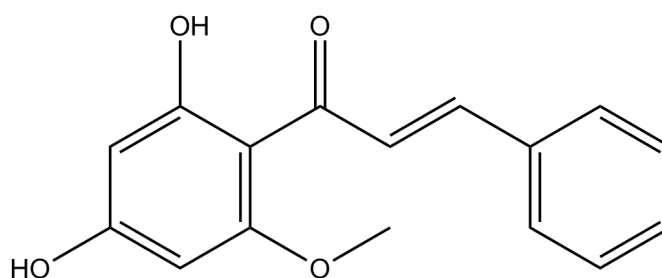


**Figure 7:** Structure of cardamonin.

### 1.10 Apoptosis

Apoptosis is essential for development and maintenance of cell homeostasis. Elimination of wrongly divided cells and cells that are undergoing senescence is a natural defensive mechanism in any living organisms. Malfunction of cell death can lead to various implications such as cancer and neurodegenerative diseases. It was initially assumed that programmed cell death was entirely controlled at nuclear level. However, it was later found that apoptosis occurs normally even in enucleated cells (Jacobson *et al.*, 1994). This suggests that cell death can also be regulated at cytoplasmic level (Wang and Youle, 2009). The localization of Bcl-2 family proteins between cytosol and mitochondria was later proven to be associated with cell death. It was observed that cytochrome c was released from mitochondria into cytosol thus loss of function in the electron transport chain causing cell death signal to be activated (Krippner *et al.*, 1996). Cytochrome c in cytosol will then bind to apoptosis protease activating factor (Apaf-1) to induce apoptosome formation, leading to caspases activation which are cell death stimuli (Wang and Youle, 2009). In cancer cells, apoptotic signaling is

triggered in response to various conditions such as chemotherapeutic agents, UV radiation and DNA damage. Hence, in current research we investigate the role of caspases in mediating apoptosis in HK-1 cells.

### **1.11 DNA fragmentation: Hallmark of cell death**

The characteristics of apoptotic cells are illustrated by nuclear envelope breakdown and chromatin condensation which lead to DNA fragmentation. Nuclear lamin B is degraded by proteolytic cleavage causing DNA to be digested to fragments. Proteins involved in regulation of DNA replication such as topoisomerases (enzymes that regulate winding of DNA), poly (ADP-ribose) polymerase (PARP) (enzymes involved in DNA repair and programmed cell death) and histone H1 (phosphorylates cyclin-dependent kinase 1, CDK-1 during mitosis) are cleaved into fragments (Krippner *et al.*, 1996). Hence, malfunction of these vital proteins in regulation of DNA replication leads to DNA being fragmented. In this study, fragmentations of DNA in NPC will be observed in a time-dependent manner after treatment with cardamonin.

### **1.12 Caspase-activation: The initiation of mitochondrial-dependent apoptotic pathway**

Caspases (cysteine aspartate-specific proteins) play an important role in mediation of nuclear apoptosis. They are structurally related to cysteine proteases that cleave peptide bonds through specific protein sequence recognitions. The protease enzyme is mainly associated with formation of apoptotic bodies which occurs from a series of biological events that triggers

cell death (Porter and Jänicke, 1999). Caspases are synthesized as inactive pro-caspases and regulated at post-translational level. Pro-caspases contains a pro-domain, a small and a large subunit. There are two classes of caspases, the initiator caspase and effector caspase. Initiator caspase are further divided into two subclasses; a longer pro-domain called caspase activation and recruitment domains (CARDs) and the death effector domain (DED) which has small pro-domain. Caspases that have CARDs are caspase-2 and caspase-9 whereas caspase-8 and caspase-10 contain DED. Effector caspases, on the other hand, are activated by initiator caspases to trigger cleavage of other substrates in apoptosis. Caspase-3, -6 and -7 belong to effector caspases family (Stennicke and Salvesen, 1998). In mammals, there are 14 caspases that have been identified to date and caspase-3 is highly associated with execution of cell death (Hu *et al.*, 1998).

Caspase-3 defective organisms are less likely to induce apoptosis although eventually typical signs of cell death do occur. Delay in cell death under deficiency of caspases significantly proved that caspases are important in the event to trigger apoptosis (Woo *et al.*, 1998). Therefore, in this study, we hypothesized that cardamonin might induce cell death via up-regulation of caspases which subsequently induces apoptosis; thereby potentially demonstrating anticancer effect against nasopharyngeal carcinoma (HK-1) cells.

### **1.13 Cell cycle analysis: Stages of arrest**

Flow cytometer is a fluorescence microscope equipped with a light source (UV or laser) which analyses moving particles in a liquid suspension. In

current research, we analyze moving cells stained with a propidium iodide (PI) fluorescent dye in a suspension buffer.

Each signal generated will be displayed on a histogram plot to quantify number of cells at different stages (G0/G1, G1, S and G2/M) in cell cycle. Significant increase in cell number of a certain cell cycle checkpoint relative to its control group demonstrates cell cycle is arrested and hence cells do not survive.

#### **1.14 Overproduction of intracellular Reactive Oxygen Species (ROS): Promoter of cell death**

Reactive Oxygen Species (ROS) has long been associated with formation of cancer. It appears that oxidative stress can induce cancer by transforming cells to generate more ROS than normal cells do. High intracellular ROS level induces cell death and activates pro-apoptotic signaling. On the contrary, inhibition of ROS production by an antioxidant will protect tumor cells against apoptosis (Skrzypski *et al.*, 2014). Despite some literature that report on overproduction of ROS leads to pro-apoptotic signaling in cancerous cells (Zhang *et al.*, 2008), reduction in ROS generation also mediates apoptosis in brain tumor cells (Lee *et al.*, 2000).

Cellular antioxidant activity can be evaluated using biological assay where its activity is measured *in vitro*. Cellular Antioxidant Activity (CAA) assay is a cell-based assay employed to measure antioxidant activity within a cell. A fluorogenic dye is used to quantify the reactive oxygen species (ROS) within the cell cytosol (Wolfe and Liu, 2007).

This method involves a fluorogenic probe dye 2',7'-dichlorohydrofluorescein diacetate (DCFA-DA) that is able to diffuse into cells. Esterases in cells deacetylate DCFA-DA (non-flourescent) to flourescent 2',7'-dichlorodihydrofluorescein (DCF). Cells will be incubated with cell-permeable DCFA-DA fluorescence probe and quercetin (antioxidant standard) or cardamonin followed by 2,2'-Azo-bis-amidinopropane (ABAP), a free radical initiator that initiates the generation of peroxy radicals. The presence of ROS generated from cancerous cells leads to a rapid oxidation of DCFH to highly fluorescent 2'7'-dichlorodihydrofluorescein (DCF). An oxidized DCF produces fluorescence which can be measured and its fluorescence intensity is proportional to the level of oxidation. However, the presence of an antioxidant (quercetin or cardamonin) might quench these peroxy radicals by preventing the generation of DCF (**Figure 8**). Therefore, CAA assay measures the ability of antioxidants to inhibit oxidation of DCFH to DCF. The conversion of non-flourescent DCFH to fluorescent DCF acts as an oxidative stress indicator. (Wolfe and Liu, 2007).

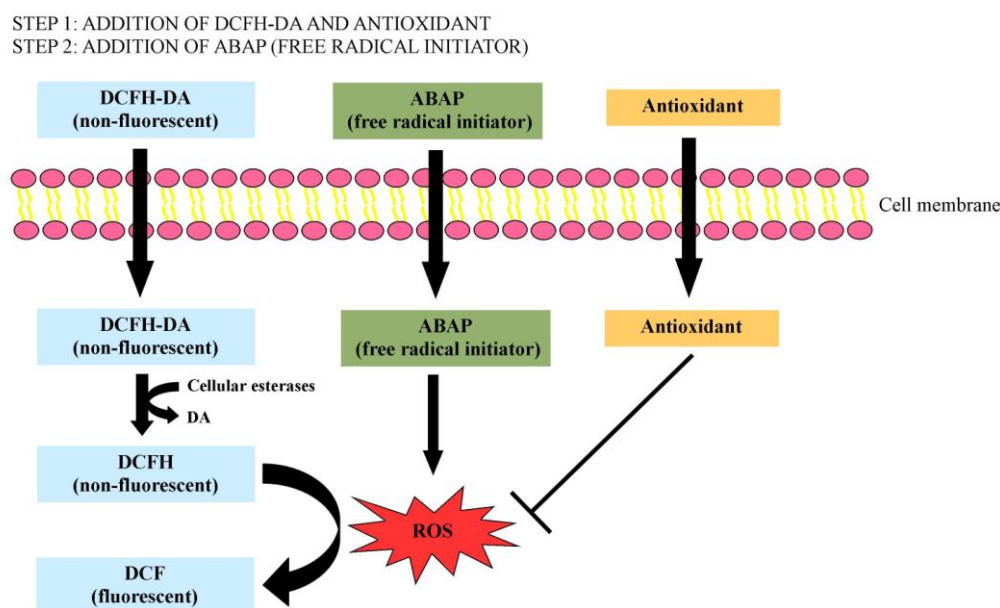


**Figure 8:** Principle of Cellular Antioxidant Activity (CAA) assay.

CAA assay is greatly dependent on the properties of antioxidants and their interactions with cells. Antioxidant can react by inhibiting peroxyl radical chain on cell surface or react intracellularly. There are several advantages of CAA. It was chosen over other antioxidant assays such as Oxygen Radical Absorbance Capacity (ORAC), Total Radical Trapping Antioxidant Parameter (TRAP) and Ferric Reducing Ability of Plasma (FRAP) due to the limitations of these assays which they lack of representations of the complexity of biological system. In addition, the radical initiator, ABAP has a half-life of about 175 hrs and the rate is constant for the first few hours (Niki, 1990). Quercetin was employed as standard for CAA assay in current research because it is pure, relatively stable, easily obtainable and widely found in fruits and vegetables. Studies have proven that quercetin exhibit high CAA values compared to other phytochemicals (Wolfe and Liu, 2007).

Structural properties of flavonoids and other phytochemicals such as polarity also determine the interactions on the cell membrane (Oteiza *et al.*, 2005). It is proven previously that flavonoid such as quercetin contains 2,3-double bond and 4-oxo group displayed high CAA (Wolfe and Liu, 2007). In this research, we propose that cardamonin (with antioxidant properties) will exhibit high CAA as it is a flavonoid which has an oxo- group and structurally similar to quercetin (**Figure 9**). However, in current research, cancer cell line will be employed to evaluate free radicals level using CAA assay. ROS are products of biological metabolism and generally there is an overproduction of ROS in cancerous cells. Under normal condition, depending on the level of ROS, it can be detrimental or favorable to cells (Circu and Aw, 2010). ROS may be an important chemical messenger in activating growth factor receptors which ensures cell survival (Huang *et al.*, 1996). At the same time, ROS has been proven to regulate cell death through tumor necrosis factor (TNF) receptors family and mitochondria (Simon *et al.*, 2000). Hence, in this study, it will be interesting to observe the regulation of ROS generated by HK-1 cancer cells in the presence of cardamonin; which may either demonstrates as a protective agent against HK-1 cell death or promote HK-1 cell apoptosis.

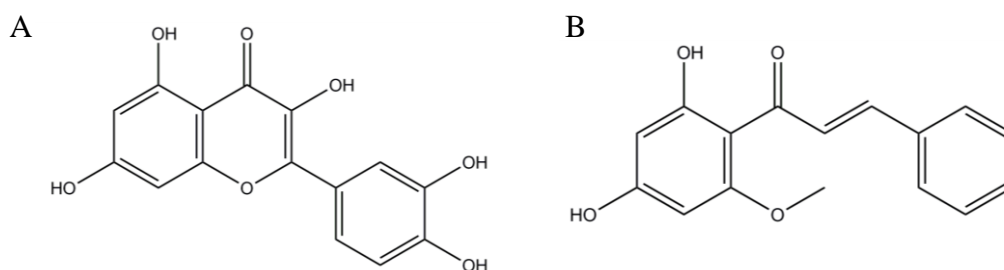


**Figure 9:** Molecular structure of (A) Quercetin (B) Cardamonin



### **1.15 Bcl-2 family proteins: Mitochondrial-dependent cell death pathway regulators**

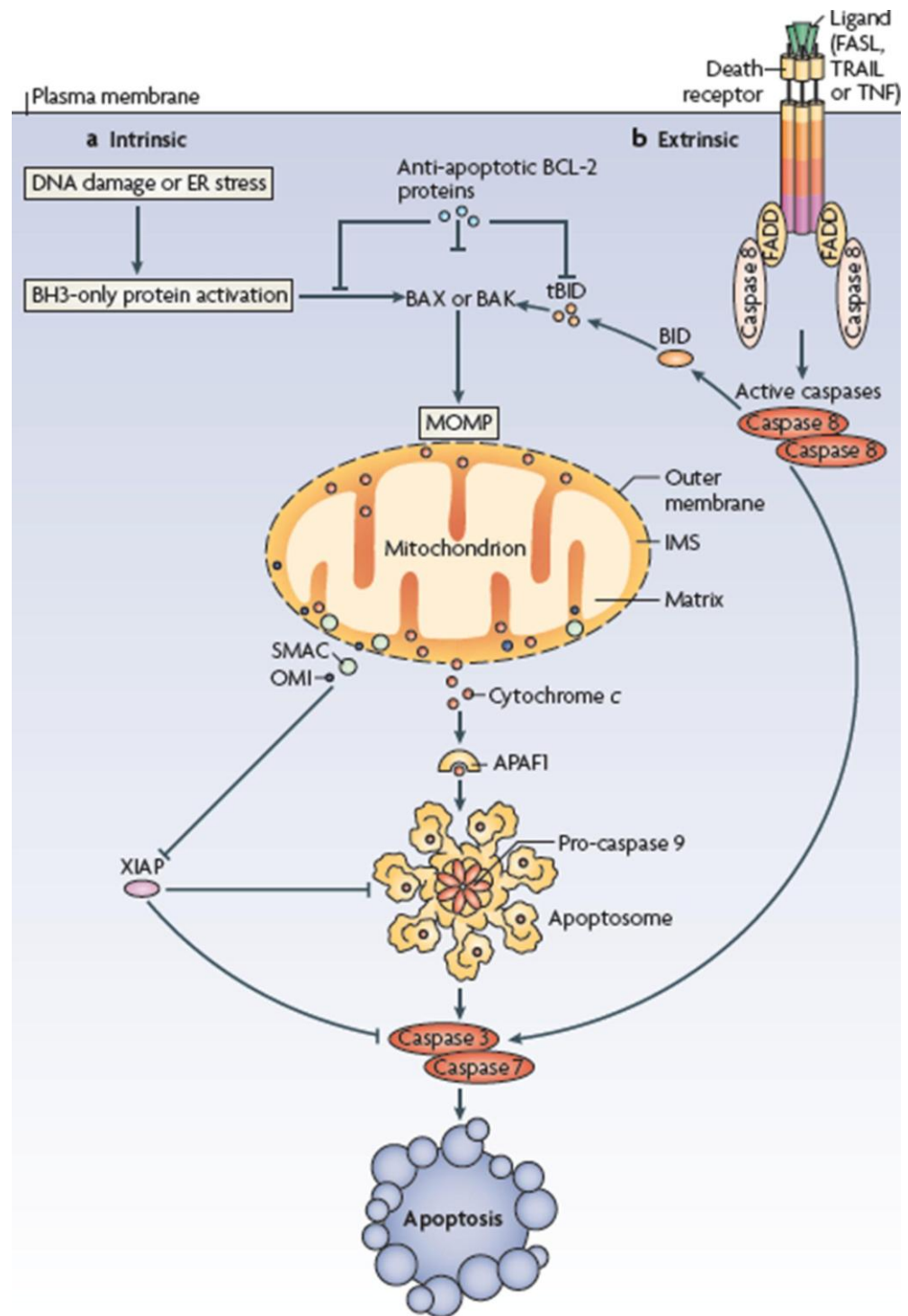
The family of B cell lymphoma-2 (Bcl-2) proteins play crucial role as regulators in apoptosis. These proteins control permeability of mitochondrial membrane to either trigger or inhibit apoptosis. The members of Bcl-2 proteins are divided into three groups depending on their homology and functions. Antiapoptotic proteins (Bcl-2 and Bcl-xL) contain four BH domains (BH1 to BH4) located in outer mitochondrial wall whereas proapoptotic proteins (Bax and Bak) possess three BH domains (BH1 to BH3) and reside in cytosol. The third group has only one BH3 domain and they are proapoptotic proteins (Bid, Bad and Bim) (Rong and Distelhorst, 2008). These three classes of proteins are able to form homo-oligomers or heterodimers in response to cell death signaling. The reorganization of proapoptotic proteins within cytosol is essential before proteins are being translocated across outer mitochondrial membrane (OMM) (Breckenridge and Xue, 2004). The permeability of mitochondrial membrane to allow protein translocation is greatly dependent on the activity of caspase. Caspase activation induces permeabilization of mitochondrial membrane to allow protein BID cleavage to an active fragment, tBID and thus being translocated to OMM. The initial signal triggered from caspase activation will be transmitted to release apoptogenic factors such as cytochrome c (Luo *et al.*, 1998). These factors bind to apoptosis activating factor to form complex in order to activate the release of caspase-9 and hence stimulates apoptosis. Based on current findings, results demonstrate an up-

regulation of caspase-3 and caspase-8 which substantiate future investigation on the regulation of Bcl-2 proteins.

This research focuses on the identification of proteins that are being up- or down-regulated during apoptosis through mitochondrial-dependent pathway in nasopharyngeal carcinoma (HK-1) cells. In 1990, it was found that apoptosis occurred and regulated at mitochondrial level when Bcl-2 family proteins were localized in mitochondrial inner membrane in cancer cells (Hockenbery et al., 1990). Mitochondria play important roles in activating apoptosis in mammalian cells as cell death is being regulated at cytosolic level (Wang and Youle. 2009). Studies have suggested that caspase-8 activation in cancerous cells leads to activation in mitochondrial dependent pathway through regulations of Bcl-2 family proteins (Lin *et al.*, 2010). We have proven the up-regulation of these caspases using Caspase-3 DEVD-R110 and Caspase-8 IETD-R110 Fluorometric and Colorimetric Assay Kits in HK-1 cells being treated with 22  $\mu$ M of cardamonin. These findings substantiate the investigation on the regulations and localizations of Bcl-2 family proteins between the cytosol and mitochondria.

Mitochondrial-dependent pathway commences following a signal at Fas ligand to trigger caspase-8 to cleave cytosolic Bid to truncated tBid active fragments in extrinsic pathway of apoptosis (**Figure 10**). Typically, apoptosis occurs through extrinsic or intrinsic pathway. In extrinsic pathway (receptor-mediated), it involves extracellular binding of a ligand on transmembrane death receptors such as Fas receptor that activates death-inducing signaling complex (DISC) by recruiting Fas-associated death domain (FADD). Subsequently,

caspase-8 is activated which initiate the activation of caspase-3. This leads to cleavage of protein Bid, a mediator of mitochondrial damage. Bid is localized in cytosol while truncated Bid (tBid) translocate to mitochondria membrane. First, tBid induces clustering of mitochondria around the nuclei which then causes release of cytochrome c. This is followed by the collapse of mitochondrial membrane potential and cell shrinkage. Eventually, this leads to nuclear condensation and cell death (Li *et al.*, 1998). On the other hand, an intrinsic pathway involves Bcl-2 family proteins on mitochondria to regulate the release of cytochrome c. A series of reaction will activate caspase-9 which in turn activates caspase-3 leading to apoptosis (Hengartner, 1997). Hence, caspases are considered as an early target of apoptosis. In order to evaluate expression level of protein associated with this cell death pathway, western blotting is conducted.



(Tait and Green, 2010)

**Figure 10:** Mitochondrial-dependent intrinsic and extrinsic apoptotic pathways.

### **1.16 Mitochondrial outer membrane (OMM) permeabilization: Cell death execution**

In healthy growing cells, it is important to maintain mitochondrial membrane potential as several key activities require this dynamic organelle for cell survival. Mitochondria function as energy production machinery as it is generally known, regulate translocations of specific proteins from mitochondrial inner membrane to outer membrane and play crucial role in deciding the life and death of a cell. Unfortunately cancer cells too can grow healthily like normal cells for survival and mitochondria function as usual to maintain regular activities of cancer cells. Hence, it is a long and never ending battle for scientist to discover ways to disrupt the usual biological activity in healthy cancer cells.

During apoptosis, there are series of events that occur in mitochondria. Mitochondrial outer membrane permeabilization triggers the activation of caspase (death protease) which leads to apoptotic cell death. Activation of caspases requires translocation of pro-apoptotic proteins from cytosol to mitochondrial intermembrane space (IMS) following permeabilization of mitochondrial outer membrane. This translocation promotes the release of IMS proteins such as cytochrome c which then binds to apoptotic protease-activating factor 1 (Apaf-1) (**Figure 10**). This induces oligomerization from both monomers forming a complex called apoptosome. Apoptosome recruits caspase-9 which in turn activates executioner caspase, caspase-3. This eventually leads to an irreversible cell death (Tait and Green, 2010). Here, we focus on the importance of mitochondrial outer membrane permeabilization in regulation of mitochondrial membrane potential and hence cellular apoptosis.

Recent findings demonstrate the importance of initial response which is loss of mitochondrial membrane potential to trigger cell death. Salinomycin isolated from *Streptomyces albus* has been proven to inhibit tumor growth and metastasis *in vivo* via loss of mitochondrial membrane potential (Kim *et al.*, 2011). Tualang honey induces apoptosis in several human breast and cervical cancer cell lines through disruption of mitochondrial membrane potential (Fauzi *et al.*, 2011). A well-known food spice, cinnamon has been shown to induce loss of mitochondrial membrane potential in human cervical carcinoma and hence cellular apoptosis (Koppikar *et al.*, 2010).

There are several key features in disruption mitochondrial membrane potential which have been discovered previously. One of these features is opening of mitochondrial permeability transition pore (PTP) which is essential to allow exchange and movements of molecules. Mitochondrial PTP is a voltage-dependent mitochondrial channel that allows release of certain apoptogenic factors during apoptosis. PTP opening regulates calcium ( $\text{Ca}^{2+}$ ) ions efflux pathway across mitochondria inner membrane. PTP is formed from a complex of voltage-dependent anion channel (VDAC) with adenine nucleotide translocase and cyclophilin-D (CyP-D) (Crompton, 1999). When there is an unbalance charge between mitochondrial matrix and cytosol, PTP becomes more permeable to mitochondrial solutes with molecular weight of less than 1,500 kDa which describes the loss mitochondrial membrane potential ( $\Delta\Psi_m$ ) (Velde *et al.*, 2000).

Opening of mitochondrial PTP causes more water and solutes ( $\text{K}^+$ ,  $\text{Mg}^{2+}$  and  $\text{Ca}^{2+}$ ) to draw into mitochondria and causes swelling of cells and therefore leads to cell death. A drop in mitochondrial membrane potential leads

to release of cytochrome c and at the same time rupture of outer membrane. As proposed by Ly *et al.*, PTP opening is influenced by change in mitochondrial membrane potential (caused by  $\text{Ca}^{2+}$  ions), pH of the mitochondrial matrix, actions of kinases and formation of Bax channel (Ly *et al.*, 2003). Indeed opening of mitochondrial PTP is able to induce depolarization of mitochondrial membrane potential.

Although there are several mechanisms on how mitochondrial outer membrane permeabilization occurs, the involvements of Bax and Bak (Bcl-2 family proteins) are highly regarded in mitochondrial outer membrane permeabilization (Tait and Green, 2010). Kuwana *et al.* concluded that opening of mitochondrial PTP and outer membrane permeabilization only requires Bcl-2 family proteins by regulating macromolecular efflux. Pro-apoptotic protein Bax in monomeric form is activated by Bid protein to stimulate channel opening for translocation of large mitochondrial proteins (Kuwana *et al.*, 2002). Another member of pro-apoptotic proteins such as Bid that exists as an inactive form in cytosol translocates to mitochondria upon cleavage by caspase-8. The active form of Bid promotes the release of death-inducing factor, cytochrome c. It is also believed that high levels of cardiopilin in cleaved Bid provide a hydrophobic surface to mediate the insertion of activated Bid to membrane of mitochondria (Lutter *et al.*, 2000).

The ultimate goal for cellular apoptosis lies in collaboration between mitochondrial membrane and Bcl-2 family proteins. Bcl-2 family proteins play crucial roles in activation of mitochondrial outer membrane permeabilization. In fact, it is suggested that loss of mitochondrial membrane potential is an early requirement for cellular apoptosis (Petit *et al.*, 1995).

Opening of mitochondrial PTP not only affects loss of mitochondrial membrane potential, it also causes depletion in ATP as mitochondria can no longer generate energy to sustain cellular activities. In fact, it is proposed that drop in ATP leads to accumulation of inorganic phosphates which is an ideal condition for mitochondrial PTP opening (Duchen, 2004). There is an alteration in energy supply during cancer cells growth and proliferation. Cancer cells are fast proliferating and as such there is an inadequate amount of oxygen supply causing a condition termed hypoxia. Under this condition, cancer cells up-regulate glycolytic pathway to compensate ATP production. (Gogvadze *et al.*, 2008). The shift of glycolytic pathway consequently leads to resistance to cellular apoptosis which means it is less susceptible to mitochondrial outer membrane permeabilization. This condition is not favourable to cancer patients as cancer cells are able to proliferate uncontrollably and increase the possibility of metastasis.

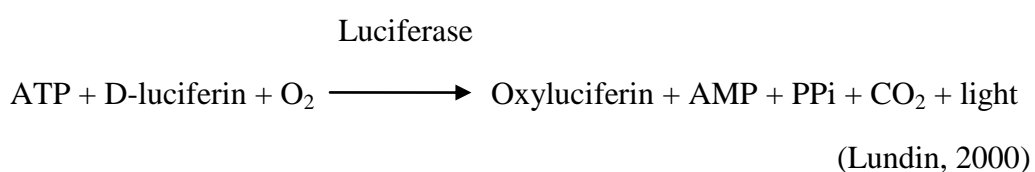
Hence, in current research we evaluate the potential of cardamonin to trigger opening of mitochondrial PTP leading to impairment in mitochondrial membrane, thus disruption of ATP production. A decrease in ATP generation affects the entire cellular functions of cancer cells. Both apoptotic events require tremendous assistance from Bcl-2 family proteins. An imbalance of Bcl-2 proteins determines the commencement of life or death of a cancer cell.



### **1.17 Malfunction of cell leads to drop in ATP synthesis: Will cardamonin affect ATP level in HK-1 cells?**

Loss of mitochondrial membrane potential will tremendously affect entire system of a cell. Mitochondrion acts as energy generator for cell to function regularly. Disruption in HK-1 cell mitochondrial membrane potential mediates apoptosis as cell is unable to function without ATP. Hence, we quantify amount of intracellular ATP in cardamonin-treated HK-1 cells and in control group.

ATP/ADP assay kit was employed to measure levels of intracellular ATP and ADP levels in two steps. Firstly, assay buffer in the ATP reagent lyses cells to release ATP and ADP. Released ATP reacts immediately with substrate D-luciferin and oxidized to oxyluciferin and produces light (luminescence). This reaction is catalysed by luciferase enzyme and ATP-Mg<sup>2+</sup> as co-substrate. Light intensity generated is measured as the ATP concentration (RLU A).



In second step, ADP is converted to ATP catalyzed by ADP enzyme (ATP synthase). Newly formed ATP reacts with D-luciferin from the first step. Luminescence reading was measured and intracellular ATP was quantified after 3 and 6 hrs of cardamonin treatment.

Changes in intracellular ATP level was further analysed by interpretation of ADP/ATP ration. No significant increase in ADP levels with

an elevated ATP levels in cardamonin-treated cells in relative to control cells signify cells proliferation (ADP=, ATP↑). Decrease in ATP levels with an increase in ADP levels in treated cells compared to control group show cells are undergoing apoptosis (ADP↑, ATP↓). As for cells that are undergoing necrosis, it will result in a distinctly low ATP levels with a greatly increased ADP levels compared to control cells (ADP↑↑, ATP↓↓).

### **1.18 Do apoptosis occur dependent or independent of caspase-9? :**

#### **Relative quantification of gene expression level**

Caspase-9 is an initiator protein that contains caspase activation and recruitment domains (CARDs) that plays a crucial role during events of cell death (Stennicke and Salvesen, 1998). Upon release of cytochrome c in mitochondrial –dependent apoptotic pathway, apoptotic peptidase activating factor (Apaf-1) oligomerizes to recruit caspase-9 to form a large complex called apoptosome. Activated apoptosome cleaves and activates downstream effector caspase, caspase-3. Caspase-3 will then target key events in triggering cell death such as nuclear fragmentation (Allan and Clarke, 2009). Hence, caspase-9 plays an important role in cell death. There have been studies that showed that caspase-9 activation induces apoptosis in Jurkat cells but not caspase-2 or caspase-8 (Shelton *et al.*, 2010). Promising data shown that caspase-9 is actively involved in remodelling of mitochondria and efficiently execute cellular apoptosis (Brentnall *et al.*, 2013). Sanguinarine, an alkaloid induces apoptosis in human colon cancer cells *via* caspase-9-dependent pathway (Lee *et al.*, 2012).

However, several publications revealed that mitochondrial-dependent cell death pathway occurs independent of caspase-9 (Wu *et al.*, 2011; Marsden *et al.*, 2002; Ekert *et al.*, 2002). In fact, caspase-3, an executioner caspase was proven to be activated directly by caspase-8 and not caspase-9 during hydrogen peroxide (H<sub>2</sub>O<sub>2</sub>)-induced apoptosis in HeLa cells. Caspase-9 was activated alongside with caspase-3 but merely as a side effect and does not play significant role in cell death pathway (Wu *et al.*, 2011).

### **1.19 Objectives**

1) to macerate five local edible plants into three different crude extracts through sequential extraction; determine the presence of phytochemical in each crude extract; evaluate cytotoxic effect of various crude extracts against nasopharyngeal carcinoma (HK-1) cells and immortalized nasopharyngeal epithelial cells.

Crude extracts with highest cytotoxic activity against HK-1 cells will be further investigated for actions of cell death.

2) to evaluate cytotoxic effects of commercially available compounds isolated from methanol and hexane crude extracts of temu kunci (*Boesebergia rotunda*); namely cardamonin, hesperidin, narignin and pinostrobin against HK-1 and NP-69 cell lines; to validate preliminary cell death bioassays using cell exclusion assay, DNA fragmentation, cell cycle analysis, changes in cellular

morphology using fluorescence dyes; to quantify caspase activities in cardamonin-treated HK-1 cells.

Caspase activation will lead to studies of cellular apoptosis through mitochondrial dependent pathway.

3) to quantify level of intracellular reactive oxygen species (ROS); change in mitochondrial membrane potential (MMP); intracellular ATP/ADP level and expression level of mitochondrial-dependent apoptotic pathway associated protein; fold difference of caspase-9 gene expression level relative to reference gene in cardamonin-treated HK-1 cells.

Current research will report on cytotoxic effect of various crude extracts of edible plants against nasopharyngeal carcinoma (HK-1) cells. Mode of actions of cardamonin *via* mitochondrial-dependent apoptotic pathway will be explored in search for a potential anticancer agent.

## 2.0 METHODOLOGY

### 2.1 Materials

Human nasopharyngeal carcinoma (HK-1) and immortalized nasopharyngeal epithelial cell line (NP-69) cell lines were material transfer upon signing of collaboration with The University of Hong Kong through local collaboration with Institute of Medical Research (IMR) Malaysia. HK-1 was established from differentiated squamous carcinoma of nasopharynx of a Chinese male 17 ½ years after radiation therapy (Huang *et al.*, 1980).

Cell culture media RPMI 1640 containing L-glutamine, Keratinocyte-SFM, Penicillin-Streptomycin, Fetal Bovine Serum, Trypsin-EDTA with phenol red, Bovine Pituitary Extract, EGF Recombinant Human, Phosphate Buffered Saline (PBS) pH 7.2 and MTT (3-[4,5-dimethylthiazol-2-yl]-2,5-diphenyltetrazolium bromide), 250 bp DNA ladder, SYBR Safe DNA stain, ApoTarget Quick Apoptotic DNA Ladder Detection Kit, Tris-Borate-EDTA (TBE) buffer were purchased from Gibco, Life Technologies, USA. Gallic acid, quercetin, iron (III) chloride, chemotherapy drug 5-fluorouracil, cardamonin  $\geq 98\%$  purity, pinostrobin  $\geq 99\%$  purity, naringin  $\geq 95\%$ , hesperidin  $\geq 80\%$ , trypan blue and agarose were purchased from Sigma-Aldrich Co. (Saint Louis, Missouri, USA). Dimethyl sulfoxide (DMSO), sulphuric acid ( $\text{H}_2\text{SO}_4$ ), sodium carbonate ( $\text{Na}_2\text{CO}_3$ ), Folin Ciocalteu's phenol reagent, methanol (MeOH), ethyl acetate (EtOAc), hexane, hydrochloric acid (HCl), ethanol (EtOH), acetic acid, glycerol, sodium hydroxide (NaOH), chloroform, Dragendorff's reagent, aluminum trichloride ( $\text{AlCl}_3$ ) were purchased from Merck & Co., Inc. (Germany). 100% extra virgin olive oil (Filippo Berio) was

purchased from local supermarket. All chemicals were of analytical grade. Ethanol, acetone, methanol and dimethyl sulfoxide (DMSO) were obtained from RCI Labscan. Propidium iodide, acridine orange, Caspase-3 DEVD-R110 Fluorometric and Colorimetric assay kit, Caspase-8 IETD-R110 Fluorometric and Colorimetric assay kit were purchased from Biotium Inc., Canada.

For evaluation of ROS production: 2X DCFH-DA probe, free radical initiator, 50 mM quercetin as standard (OxiSelect Cellular Antioxidant Activity Assay Kit (Green Fluorescence), Cell Biolabs, Inc., USA)

For protein extraction: PRO-PREP protein extraction kit (iNtRON Biotechnology, Inc.), protein markers, pre-stained, Ez-Run *Rec* Ladder (Fisher Scientific), PageRuler Unstained Protein Ladder (Thermo Scientific), 30% Acrylamide/Bis solution, 10X Tris/Glycine/SDS running buffer, 10X Tris/Glycine transfer buffer, Tetramethylethylenediamine (TEMED), ammonium persulfate (APS), Bio-Safe Coomassie Stain, 1X Bradford dye reagent (Bio-rad Laboratories). Trizma base, Tween20, sodium chloride, 2-Mercaptoethanol, bromophenol blue sodium salt, bovine serum albumin (BSA) (Sigma Aldrich), TMB Membrane Peroxidase Substrate Ready-To-Use (Rockland Immunochemicals Inc.), Hybond ECL nitrocellulose blotting membrane (GE Healthcare and Life Sciences) and non-fat milk (Anlene). Anti-Bcl-2, Anti-Bcl2-L1, Anti-Bax, Anti-Bad, Anti-cytochrome c primary antibodies and Goat Anti-Rabbit IgG peroxidase-conjugated secondary antibodies were purchased from Abgent, Inc..

For mitochondrial assays: JC-1 Mitochondrial Membrane Potential Assay Kit and ADP/ATP Ratio Assay Kit were obtained from Abnova.

For real-time PCR: RNAqueous®-4PCR Total RNA Isolation Kit, SuperScript® III Platinum® SYBR® Green One-Step qRT-PCR Kit were purchased from Invitrogen, Life Technologies, USA. Homo caspase-9 forward (F) primer (5' TGTCTACTCTACTTTCCCAGGTTTT 3'), homo caspase-9 reverse (R) primer (5' GTGAGCCCACTGCTCAAAGAT 3'), GADPH forward (F) primer (5' ACACCCACTCCTCCACCTTT 3') and GADPH reverse (R) primer (5' TAGCCAAATTCGTTGTCATACC) (Yu *et al.*, 2010).

## **2.2 Edible plant crude extracts**

Five edible local plants; curry leaf (*Murraya koenigii*), temu kunci (*Boesenbergia rotunda*), spring onion leaf (*Allium cepa*), mushroom bean (*Phaseolus vulgaris*) and bunga kantan (*Phaeomeria imperialis*) were purchased from a local market Pasar Tani Prima Saujana, Semenyih, Malaysia [Coordinate location Decimal Degree (DD) 3.010558, 101.808302]. Plants were dried for 2 weeks in low humidity area to remove all moisture. Plants were then pulverized using a Philips food processor into powder and kept in an airtight bag. 20 g of dry mass of plant was weighed and placed in a 250 mL conical flask sealed with aluminium foil. 200 mL of hexane was added and macerated for 3 days to promote elution of non polar compounds from the plants into surrounding organic solvent. After 3 days, hexane was filtered through filter paper (BRAND) into a 250-mL round bottom flask for evaporation. The extract was concentrated using BUCHI rotavapor R-2100 at 37°C at rotation speed of 3-4. Evaporated hexane was recycled for another 3 days of maceration and this step was repeated twice. All successive extracts

were pooled and kept in the desiccators for 2 weeks until it is completely dried from organic solvent. After 2 weeks, extracts were sealed in a glass vial and kept in 2°C fridge until further analysis.

To obtain semi polar and polar compounds, the procedure was repeated using ethyl acetate and methanol respectively. Sequential extraction was used by collecting bioactive compounds using organic solvent at increasing polarity. In methanol extraction, reddish brown solid was found and filtered using filter paper. Methanolic solid 1 was obtained.

## **2.3 Total phenolic and flavonoid content determination**

### **2.3.1 Preparation of stock crude extracts**

A total of 100 mg of dried sample was weighed and diluted in 1 mL of 100% DMSO. Then, 4 µL was dissolved in 1 mL of methanol to make 400 µg/mL stock crude extracts for total phenolic content determination and total flavonoid content determination assays.

### **2.3.2 Total phenolic content determination by Folin-Ciocalteu assay**

A total of 100 µL of stock crude extract was placed in a test tube. Then, 2 mL of 2% (w/v) sodium carbonate ( $\text{Na}_2\text{CO}_3$ ) was added to test tube. Test tube was mixed vigorously using a vortex mixer. While mixing, 100 µL of 1:1 dilution of Folin-Ciocalteu reagent was added and test tube was allowed to stand for a minimum of 30 mins at room temperature (not more than an hour).



The absorbance against blank (0  $\mu\text{L}$  of the standard gallic acid standard solution) was determined at 750 nm using Thermo Scientific Varioskan Flash multimode plate reader. Gallic acid with concentrations 25, 50, 100, 200 and 400  $\mu\text{g/mL}$  were used as standard for determination of total phenolic compounds in plant samples. Total phenolic content was expressed as mg gallic acid equivalents per g of sample.

### **2.3.3 Total flavonoid content determination using Dowd method**

A total of 100  $\mu\text{L}$  of stock crude extract was placed in a test tube. 100  $\mu\text{L}$  of 2% (w/v) aluminium trichloride ( $\text{AlCl}_3$ ) was added to test tube and incubate for 10 mins in the dark at room temperature. The absorbance against prepared reagent blank (0  $\mu\text{L}$  of the standard quercetin standard solution) was determined at 415 nm using Thermo Scientific Varioskan Flash multimode plate reader. Quercetin with concentrations 25, 50, 100, 200 and 400  $\mu\text{g/mL}$  were used as standard for determination of total flavonoid content in plant samples. Total flavonoid content was expressed as mg quercetin equivalents per g of sample.

## **2.4 Phytochemical analysis**

### **2.4.1 Preparation of stock crude extracts**

A total of 0.01 g of dried extract was weighed and diluted in 1 mL of 100% DMSO to make stock crude extracts with concentration of 0.01 g/mL.

#### **2.4.2 Presence of tannins**

A total of 1 mL of crude extract was stirred in 1 mL of distilled water. A few drops of 10% iron (III) chloride solution were added. Formation of green precipitate indicates presence of tannins.

#### **2.4.3 Presence of saponins**

About 2-3 drops of olive oil were added into 1 mL of crude extract and shaken vigorously (Emulsion test). Formation of stable emulsions indicates the presence of saponins.

#### **2.4.4 Presence of phlobatannins**

A total of 1 mL of crude extract was added to 1 mL of 1% hydrochloric acid (HCl) and mixture is boiled. Depositions of red precipitates indicate the presence of phlobatannins.

#### **2.4.5 Presence of flavonoids**

A total of 1 mL of crude extract was added into 1 mL of 10% sodium hydroxide (NaOH) solution. Formation of yellow precipitates indicates presence of flavonoids.

#### **2.4.6 Presence of terpenoids**

A total of 1 mL of crude extract was added into 1 mL of chloroform and evaporated to dryness. Then, 1 mL of concentrated sulphuric acid ( $\text{H}_2\text{SO}_4$ ) was added and heated for 2 mins. Greyish colour indicates the presence of terpenoids.

#### **2.4.7 Presence of steroids**

A total of 1 mL of chloroform and 1 mL of concentrated sulphuric acid ( $\text{H}_2\text{SO}_4$ ) were added into 1 mL of crude extract. Red coloration produced in lower chloroform layer indicates the presence of steroids.

#### **2.4.8 Presence of alkaloids**

A total of 1 mL of crude extract was stirred in 1 mL of 1% hydrochloric acid (HCl) on steam bath. A few drops of Dragendorff's reagent were added. Turbidity in resulting precipitate indicates presence of alkaloids.

#### **2.4.9 Presence of glycosides**

A total of 1 mL of crude extract was added into 1 mL of chloroform. Then, 1 mL of sulphuric acid is added carefully and shaken gently. Reddish brown colour indicates the presence of steroidal ring (glycone portion of glycoside).

### **2.5 Cell culture**

#### **2.5.1 Cell propagation and its maintenance**

Human nasopharyngeal carcinoma (HK-1) cell line was maintained with 90% RPMI 1640 containing L-glutamine with 10% Foetal Bovine Serum (FBS) and 5% Penicillin-Streptomycin in a 75 cm<sup>2</sup> culture flask. The cells were incubated at 37°C in an incubator with 95% air humidity and 5% CO<sub>2</sub> supply. Immortalized nasopharyngeal epithelial cell line (NP69) cell line was maintained with Keratinocyte-SFM containing 0.025% bovine pituitary extract,

0.014% recombinant epidermal growth factor (EGF) and 5% Penicillin-Streptomycin. When the cells have reached 80-90% confluence, usually within 3-4 days, sub-culturing was conducted to split cells into 2 flasks or to collect cells for storage in liquid nitrogen. Sub-culture can be done on the 5<sup>th</sup> day of incubation. All cell works were conducted in Biohazard Cabinet Type II (Esco) to prevent contamination to the cells.

### **2.5.2 Subculture**

Both HK-1 and NP-69 cell lines are adherent-dependent cells and hence trypsinization was done to detach the cells from the culture flask's bottom surface. First, growth media in the culture flask was removed and discarded. Then, the layer of cells was washed with 5 mL of phosphate buffered saline (PBS). PBS was removed and this step was repeated once. Then, 2 mL of trypsin-EDTA was added into the culture flask to remove any residues of serum which contain trypsin inhibitor. The cells were incubated in the incubator for 5 mins at 37°C with 5% CO<sub>2</sub>. After incubation, the cells were observed under microscope to see if the cells have detached from the flask's bottom surface. If the cells have detached, 4 mL of growth media was added to arrest trypsinization (1:2 trypsin to growth media ratio). For NP-69, 98% PBS and 2% fetal bovine serum (FBS) was added to deactivate the trypsin. The cells were then centrifuged for 5 mins at 1,800 rpm (Eppendorf 5810-R). Supernatant was discarded and cell pellet was re-suspended in 1mL CGM. 500 µL of the cell suspension was transferred into a new culture flask. In the new culture flask, 9.5 mL of CGM was added to make up to final volume of 10 mL.

### **2.5.3 Cryopreservation**

When cells have reached confluence of more than 80%, it can be cryopreserved and kept in liquid nitrogen. Cells were detached using PBS, trypsin-EDTA and growth media using the method mentioned in section 2.5.2. After trypsinization, the aliquot cell suspension was transferred into a 50-mL centrifuge tube. The aliquot cell suspension was then spun down at 1,800 rpm for 5 mins. Then, the supernatant was discarded. The cell pellet was re-suspended with 1 mL of freezing media (90% FBS and 10% DMSO for HK-1 cells and 75% FBS, 10% DMSO and 15% bovine pituitary extract for NP-69 cells). Cryovial was stored in -80°C Heto Ultra Freezer UF 460 (Rich-Mond, UK) overnight before being transferred to liquid nitrogen tank for longer storage.

### **2.5.4 Cell thawing**

15 mL of growth media was added into a 75 cm<sup>2</sup> culture flask. The culture flask was allowed to stand upright. Then, a cryovial containing the required cell was removed from the liquid nitrogen tank and thawed in 37°C water bath by carefully swirling it in the water bath. Immediately after the cells in cryovial have thawed, the cell aliquot was transferred using micropipette into the culture flask. The culture flask was observed under an inverted microscope and incubated at 37°C in an incubator with 95% air humidity and under 5% CO<sub>2</sub> supply.

## **2.6 Cytotoxic assay**

### **2.6.1 Stock sample preparation**

Plant crude extracts were dissolved in 100% DMSO. However, toxicity of DMSO against cell lines is taken into consideration in stock preparation. Crude extracts were diluted in media at highest concentration of 0.1% DMSO. It has been previously tested that this concentration of DMSO did not reveal any significant effect on the proliferation of cells compared to their respective control (Kumi-Diaka *et al.*, 2000).

Except bunga kantan (which dissolved completely in growth media), other 4 plant crude extracts (crude methanolic, ethyl acetate and hexane extracts) and positive control 5-fluorouracil were dissolved in 100% DMSO to obtain stock crude extracts with concentration of 100 mg/mL. 2  $\mu$ L of each stock crude extract was then dissolved in 1 mL of growth media to obtain concentration of 200  $\mu$ g/mL. All crude extracts prepared were stored in -20°C freezer.

### **2.6.2 Cell seeding**

When the cells were ready for seeding, the cells were harvested from culture flask and centrifuged at 1,800 rpm for 5 mins. After centrifugation, the supernatant was removed. The cell pellet was re-suspended with 1 mL of growth media. Then, the cell concentration in the 1 mL suspension was determined using standard trypan blue cell counting technique (haemocytometer). 10  $\mu$ L of cell suspension was mixed well with 10  $\mu$ L of trypan blue. Then, 10  $\mu$ L from the mixture was transferred to haemocytometer.

Cells were counted using an inverted microscope and an average number of cells were determined. Then the cell concentration was obtained using the formula below:

$$\begin{aligned}\text{Average cell count} &= \left[ \frac{\text{Area A+B+C+D}}{4} \times 2 \times 10^4 \right] \text{cells/mL} \\ &= x \text{ cells /mL}\end{aligned}$$

Then, the volume, V of cells suspension in 1 mL was calculated using the following formula:

Number of cells in 1 mL of stock =  $x$  cells/mL

$$(x \text{ cells /mL}) \times \text{Volume, V} = \text{Number of cells/well} \times 100 \mu\text{L of cells/well} \\ \times \text{Total volume of cells for 96-well plate}$$

$7 \times 10^3$  cells per well were seeded into each well on a 96-well tissues culture plate. The 96-well tissue culture plate was incubated at 37°C under 5% CO<sub>2</sub> in a humidified atmosphere for 24 hrs to allow cell adherence.

### 2.6.3 Treatment preparation and dilutions

For sample dilution, each well from row B to G were filled with 100  $\mu$ L of growth media. Then, 100  $\mu$ L of sub-stock sample was transferred into row B. For 3 replicates, B1 to B4 were filled with crude methanolic extracts, B5 to B8 were filled with crude ethyl acetate extract and B9 to B12 were filled with crude hexane extract. Next, two-fold dilution was carried out from row B to G and row H was the final waste. Row A was filled with 100  $\mu$ L of 200  $\mu$ g/mL

stock crude extract. The concentrations of each row of wells were shown in **Appendix 7.3.1.**

After 24 hrs cells incubation, the spent medium was removed. The stock samples that underwent serial dilutions earlier in the sample plate were transferred into the 96-well culture plate. All samples from rows B to G of sample plate were transferred into row B to G of 96-well culture plate. For row A, 100  $\mu$ L from the sub-stock with initial concentration of 200  $\mu$ g/mL was transferred into each well. For row H, wells H1 to H3 were filled with growth media. Wells H1 to H3 were blank with untreated cells. The culture plate was incubated for another 24 and 48 hrs.

#### **2.6.4 Cell viability using MTT assay**

After 24-hour incubation, an estimation of number of cells that are viable was determined relatively to the untreated cell population through MTT (3-[4,5-dimethylthiazol-2-yl]-2,5-diphenyltetrazolium bromide) assay. The MTT is a water-soluble blue formazan that is readily taken up by viable cells and the action was due to reduction of mitochondrial dehydrogenases. DMSO is used to dissolve it for colorimetric measurement (Slater *et al.*, 1963).

5 mg/mL MTT in sterile PBS pH 7.2 was prepared and for every 1 mL, 10 mL of growth media were added. The spent media in the 96-well plate were removed. Each well was then filled with 110  $\mu$ L of MTT solution. This was done in the dark (by turning off the light in the biosafety cabinet) because MTT is light sensitive. Then, the culture plate was incubated for 4 hrs at 37°C under



5% CO<sub>2</sub> in a humidified atmosphere. After 4-hour incubation, 85 µL of the growth media and MTT were removed from each well. Then, 50 µL of 100% DMSO was added to dissolve the purple formazan salt. The absorbance of each well was read at 540 nm using Thermo Scientific Varioskan Flash multimode plate reader. The percentage of cell viability was calculated using the following equation:

$$\text{Cell viability (\%)} = \frac{\text{Optical Density (OD)}_{\text{sample}}}{\text{Optical Density (OD)}_{\text{control}}} \times 100\%$$

The concentration that produced 50% inhibition concentration (IC<sub>50</sub>) was determined from absorbance (OD) versus concentration curve.

5-fluorouracil (5-FU) is a chemopreventive drug used as a positive control in comparison to all crude extracts in MTT assay. 5-fluorouracil has been previously proven to induce apoptosis in NPC (Qin *et al.*, 2008).

## **2.7 Cytotoxic effects of cardamonin, pinostrobin, naringin and hesperidin against HK-1 and NP-69 cell lines**

Nasopharyngeal carcinoma (HK-1) and immortalized epithelial nasopharyngeal (NP-69) cell lines were seeded in a 96-well plate at  $1 \times 10^4$  cells per well. After 24 hrs, compound was dissolved in DMSO at various concentrations (0, 3.125, 6.25, 12.5, 25, 50, 100 and 200 µg/mL) before treated on the cells. After incubation times of 24, 48 and 72 hrs, 5 mg/ml MTT in sterile PBS pH 7.2 was added to each well and incubated for 4 hours at 37°C under 5% CO<sub>2</sub> in a humidified atmosphere. After 4-h incubation, 100% DMSO was added to dissolve the purple formazan salt. The absorbance of each well

was read at 540 nm using Thermo Scientific Varioskan Flash multimode plate reader. 50% inhibition concentration (IC<sub>50</sub>) was determined from absorbance (OD) versus concentration curve. Of all four compounds tested, cardamonin exhibits highest cytotoxic effect against HK-1 cells without affecting normal nasopharyngeal cells, NP-69. Hence, cardamonin will be selected for further biological assays to determine the mode of actions in HK-1 cell death.

## **2.8 Viable cell count using trypan blue**

HK-1 cells were seeded on a 6-well plate at cell density  $3 \times 10^5$  cells per well. Untreated cells and cells treated with IC<sub>50</sub> 22 µg/mL cardamonin (based on result from MTT assay) were incubated for 24, 48 and 72 hrs at 37°C under 5% CO<sub>2</sub>. Cells were then spun down at 1,800 rpm for 5 mins and resuspended with 500 µL of PBS. To 500 µL of trypan blue, 500 µL of cell suspension were added. At microscope magnification of 100×, viable cells were counted at 3,000 cells per chamber of haemocytometer. Non-viable cells were stained blue as viable cells will not take up trypan blue dye. Results were recorded in triplicates.

## **2.9 Fluorescence assay- cellular morphology microscopic observation**

HK-1 cells were seeded on a chamber slide (Thermo Scientific Nunc Lab Tek II) at cell density of  $6 \times 10^4$  cells per chamber. Untreated cells and cells treated with 22 µg/mL cardamonin were incubated for 24 and 48 hrs at 37°C under 5% CO<sub>2</sub>. After respective incubation hours, media were removed. Cells were washed with PBS twice. For cell fixation, 1 mL of 100% cold methanol was added and incubated in -20°C freezer for 10 mins. Methanol was

removed prior to addition of 1 mL of cold acetone for cell permeabilization and incubated for 1 min in -20°C freezer. Cells were washed twice with PBS. 10 µg/mL of acridine orange (AO) and 10 µg/mL of propidium iodide (PI) were added to each chamber. Chamber slide was incubated at 37°C for 15 mins for staining. It was then observed under Fluoview 1000 laser scanning confocal microscope (Olympus IX 81 Motorized Inverted Microscope).

## **2.10 DNA fragmentation assay**

HK-1 cells were seeded on a 6-well plate at cell density  $1 \times 10^5$  cells per well. Untreated cells and cells treated with 22 µg/mL cardamonin were incubated for 24, 48 and 72 hrs at 37°C under 5% CO<sub>2</sub>. Cells were then spun down at 1,800 rpm for 5 mins and washed twice with PBS. Then, *ApoTarget* Quick Apoptotic DNA Ladder Detection Kit (Invitrogen) was used for cell DNA extraction. Cells were first lysed using 35 µL of TE lysis buffer followed by 5 µL of Enzyme A and vortex gently. The lysate was then incubated in 37°C water bath for 10 mins before adding 5 µL of Enzyme B. Lysate was then further incubated for another 30 mins at 50°C. 5 µL of ammonium acetate solution and 100 µL of cold absolute ethanol were added to lysate and kept at -20°C for 10-15 mins to precipitate DNA. Supernatant was then discarded and 0.5 mL of cold 70% ethanol was added to wash DNA pellet and re-centrifuged for 10 mins at 12,500 rpm. The DNA pellet was subsequently air-dried for 10 mins at room temperature. Extracted DNA was suspended in 25 µL of sterile distilled water. A total of 5 µL of loading dye was added into the DNA sample and 20 µL of the sample was loaded on 1.2% agarose gel in TBE buffer stained

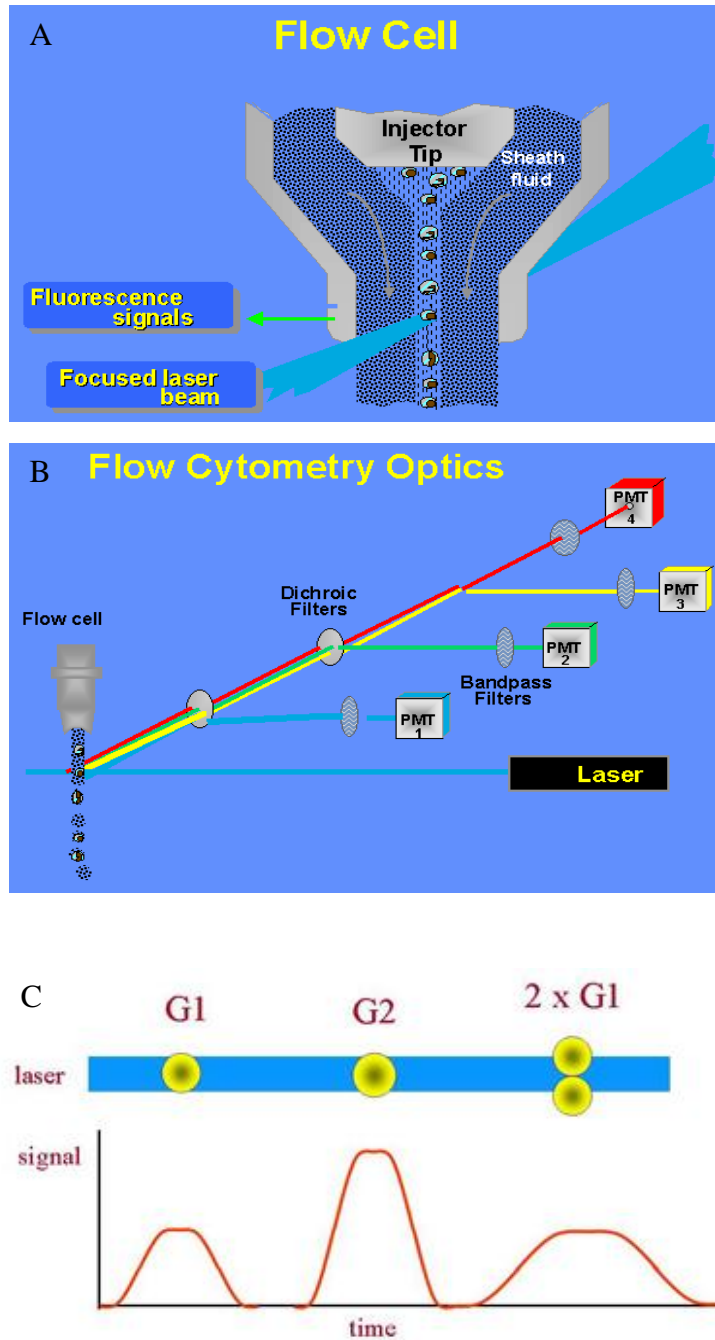
with SYBR safe. Electrophoresis was run at 70V for 1-2 hrs and visualized under UV light illuminator (ChemiDoc XRS system, BioRad).

## **2.11 Cell cycle analysis**

Flow cytometer consists of three parts; first is fluidics part where cells in suspension pass through a needle using hydrodynamic focusing (**Figure 11A**). Hydrodynamic focusing introduces each cell to a convergence point where each cell is line parallel to the sheath fluid filling the flow cell. Each of these cells carries a fluorophore, absorbs light from laser or UV and emits photons in range of wavelengths. This part is called optics. Two types of optical signals are generated and detected by a photomultiplier tube; namely fluorescence and scattered light. Both are separated using respective filters and directed to individual photomultiplier tube for measurement (**Figure 11B**). Forward scattered channel (FSC) detects size of a single cell whereas side scattered channel (SSC) detects granularity or internal complexity of a single cell. At the same time, fluorescent dye that stained cells emits different fluorescence intensities and these intensities will be received by its photomultiplier tube. Third part of flow cytometer is the electronics. Fluorescence signal emitted from fluorophore is converted from analog to digital in photomultiplier (Ochatt, 2006). This will produce a one-parameter (in our research, we employed propidium iodide fluorescent dye to analyze cell cycle) or a two-parameter dot-plot diagram.

The amount of DNA content in each cell is directly proportional to the intensity of emission from fluorophore. Each emission generates signal and represents one dot on dot-plot (FSC vs. SSC). In cell cycle G1 stage, cell will

contain DNA content of  $2n$  (diploid) whereas DNA content in G2 phase after synthesis (S) phase is  $4n$ . When cells are analyzed using flow cytometry, it is probable that 2 cells with 2 nuclei in G1 phase are clumped together. Hence, the signal generated will be the same as a single cell in G2 phase. However, 2 cells clump will generate a peak signal with narrower width compared to a single cell in G2 phase where a sharp and higher peak will be displayed (**Figure 11C**). It is important to exclude these cells clump to prevent false positive results. This phenomenon is called doublet discrimination and can be prevented by gating the cells in FSC-SSC dot plot. Gating allows selection of cells of interest to be analyzed. Dead cells are often represented by lower forward scatter and higher side scatter than viable cells on dot plot. This allows a group of cells to be excluded from analysis and only cells that are gated will be included for analysis (Ormerod, 2008).



(Robinson, 2006)

**Figure 11:** (A) Each cell flows by hydrodynamic focusing manner. (B) Once excited by laser beam, each cell emits fluorescence and scattered light which will be separated by different filters. (C) Signals generated after cells are excited by laser. 2 cells clump together will cause false positive in DNA content cell cycle analysis.

HK-1 cells were seeded on a 6-well plate at cell density  $1 \times 10^6$  cells per well. Untreated cells and cells treated with 22  $\mu\text{g/mL}$  cardamonin were incubated for 12 and 24 hrs at 37°C under 5%  $\text{CO}_2$ . Cells were then spun down at 2,500 rpm for 5 mins and washed twice with PBS. Cell pellet was re-suspended in 1 mL PBS and transferred to 15-mL centrifuge tube. Cells were allowed cool on ice for 10 mins. 3 mL of cold ethanol was added drop wise while gently shaking the tube. Cells were fixed in -20°C overnight prior to cell cycle analysis. After fixation, cells were washed twice with PBS to remove ethanol. Cells were centrifuge at higher centrifugal force at 2,500 rpm as cells tend to be flocculent. 425  $\mu\text{L}$  of PBS was added to cell pellet and mixed well before transferred to round bottom tube. 50  $\mu\text{L}$  of RNase A solution (1 mg/mL) was added and incubate at 37°C for 15 mins. Then, 25  $\mu\text{L}$  of propidium iodide (PI) (1 mg/mL) was added to cells and left on ice in the dark for 10 mins prior to cell cycle analysis using CyAn™ ADP Analyzer flow cytometer (Beckman Coulter). The PI stained cells were analyzed using ModFit LT software for DNA cell cycle distribution and sub-G1 group as representative group of apoptosis.

## **2.12 Caspase-3 and caspase-8 activity**

Caspase-3 and caspase-8 fluorometric assays were evaluated using Caspase-3 DEVD-R110 Fluorometric and Colorimetric Assay Kit and Caspase-8 IETD-R110 Fluorometric and Colorimetric Assay Kit (Biotium). HK-1 cells were seeded on a black 96-well plate at cell density  $2 \times 10^4$  cells per well. Untreated cells and cells treated with 22  $\mu\text{g/mL}$  cardamonin were incubated for 24, 48 and 72 hrs at 37°C under 5%  $\text{CO}_2$ . Cells were then spun

down at 1,800 rpm for 5 mins. Culture medium was aspirated from each well and 50  $\mu$ L of cell lysis buffer was added to each well. The 96-well plate was then incubated on ice for 10 mins before cell lysates were being transferred to microcentrifuge tubes. The tubes were centrifuged at 4°C to pellet the insoluble cell debris. A total of 50  $\mu$ L of Assay Buffer was added to each tube and mixed well. To verify that signal detected was due to caspase activity, an induced sample was added with 1  $\mu$ L of enzyme inhibitor. All samples were then incubated at room temperature for 15 mins. Subsequently, 5  $\mu$ L of 1mM enzyme substrate was added to each sample and mixed well. All samples were incubated at 37°C for 2 hrs and fluorescence was measured at 470 nm excitation and 520 nm emission. A R110 reference standard was prepared to generate a standard curve to quantify the amount of caspase generated.

### **2.13 Reactive Oxygen Species (ROS) production using Cellular Antioxidant Activity (CAA) assay**

$1 \times 10^4$  cells were seeded in a 96-well clear bottom black plate. After 24 hrs, media were removed from all wells. Cells were washed gently with sterile phosphate buffered saline (PBS) for three times. 50  $\mu$ L of 2',7'-dichlorohydrofluorescein diacetate (DCFH-DA) probe were added to each well. 50  $\mu$ L of quercetin standard and cardamonin (at various concentrations of 0, 12.5, 25, 50, 100 and 200  $\mu$ M) were added to respective wells in triplicates. The plate was incubated for 60 mins at 37°C. After incubation, all solutions were carefully removed. Cells were washed gently with sterile PBS for three times. 100  $\mu$ L of free radical initiator were added to each well. Immediately, fluorescence reading was taken using Thermo Scientific Varioskan Flash



multimode plate reader at 37°C with excitation wavelength of 480 nm and emission wavelength of 530 nm. Fluorescence was read at five-minute interval for a total one hour. Using the data generated from fluorescence values, the area under the curve (AUC) were integrated versus time. AUC values were used to determine cellular antioxidant activity (CAA) according to the formula below:

$$\text{CAA units} = 100 - [(\text{AUC}_{\text{antioxidant}} / \text{AUC}_{\text{control}}) \times 100]$$

From CAA versus concentration curve, half maximal effective concentration (EC<sub>50</sub>) values were generated. All results were analyzed using Microsoft Excel 2007.

#### **2.14 JC-1 Mitochondrial Membrane Potential Assay**

5×10<sup>4</sup> cells per 100 µL were seeded in a 96-well clear bottom black microplate. After 24 hours, media were removed from all wells and treated with cardamonin (IC<sub>50</sub> = 22 µg/mL). After 3 and 6 hrs of treatment, 10 µL of JC-1 staining solution was added to each well and gently mixed. Cells were incubated at 37°C for 20 mins for staining. After incubation, the plate was centrifuged at 1,800 rpm at room temperature for 5 mins. Supernatant in each well was removed prior to addition of 200 µL of assay buffer. The plate was centrifuged at 1,800 rpm at room temperature for 5 mins. This washing step was repeated twice. Finally, 100 µL of assay buffer was added to each well. Fluorescence reading was taken using Thermo Scientific Varioskan Flash multimode plate reader with excitation wavelength of 485 nm and emission wavelength of 535 nm for JC-1 monomers (apoptotic or unhealthy cells) and

excitation wavelength of 560 nm and emission wavelength of 595 nm for J-aggregate (healthy cells). The ratio of fluorescent intensity of J-aggregates to monomers is used as an indicator of cell health.

Changes in mitochondrial membrane potential stained with JC-1 were analyzed using Fluoview 1000 laser scanning confocal microscope (Olympus IX 81 Motorized Inverted Microscope). 100  $\mu$ L of JC-1 staining solution per mL of CGM was added to each chamber on chamber slide and incubated in the dark for 15 mins at 37°C. JC-1 can selectively enter into mitochondria and forms J-aggregates in healthy cells with high mitochondrial membrane potential. J-aggregates will emit intense red fluorescence whereas in cells with low mitochondrial membrane potential, JC-1 remains as monomers and emit green fluorescence.

## **2.15 ADP/ATP Ratio Assay**

$1 \times 10^4$  cells were seeded in a 96-well clear bottom white opaque microplate. After 24 hrs, media were removed from all wells and treated with cardamonin ( $IC_{50} = 22 \mu\text{g/mL}$ ). All media were removed after 3 and 6 hours of exposure to cardamonin. 90  $\mu$ L of ATP reagent (A pre-mixture of 95  $\mu$ L of assay buffer, 1  $\mu$ L of luciferin substrate, 1  $\mu$ L of ATP- $Mg^{2+}$  cosubstrate and 1  $\mu$ L of ATP enzyme) was added to each well and mixed by tapping the sides of the plate. After 1 min, luminescence (RLU A) was read using Thermo Scientific Varioskan Flash multimode plate reader. After 10 mins, luminescence was read again (RLU B). RLU B measures the background prior to ADP luminescence reading, also known as ATP residual signal. For ADP measurement, 5  $\mu$ L of ADP reagent (A pre-mixture of 5  $\mu$ L of sterile distilled

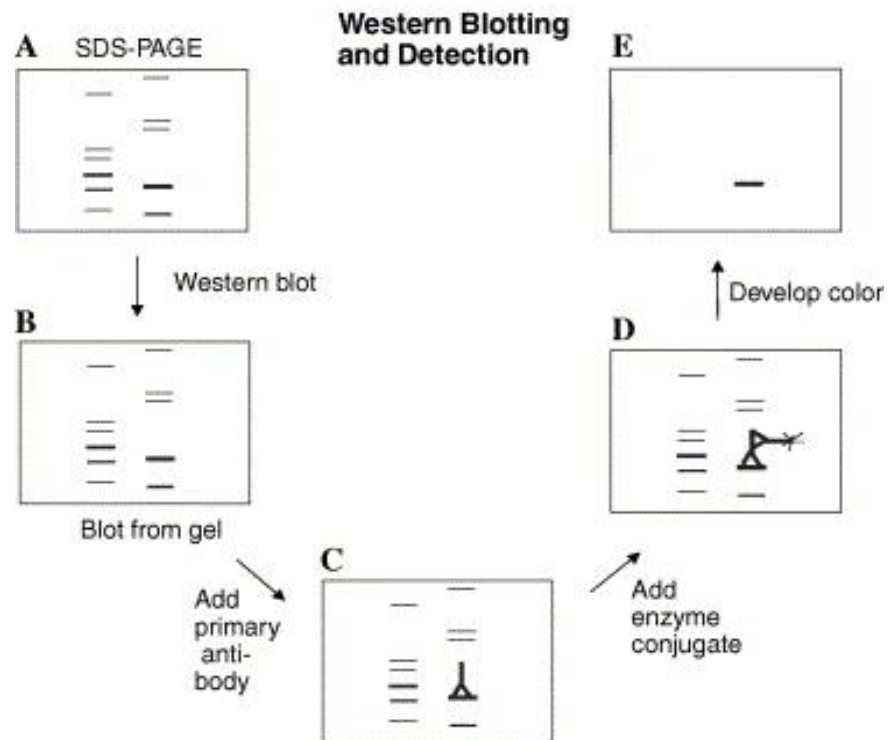
water and 1  $\mu$ L of ADP enzyme) was added to each well and mixed well by tapping the sides of the plate. After 1 min, luminescence (RLU C) was read. ADP/ATP ratio of each sample was calculated using the formula below:

$$\text{ADP/ATP} = \frac{\text{RLU C} - \text{RLU B}}{\text{RLU A}}$$

## **2.16 Detection of mitochondrial-dependent pathway associated proteins using western blotting**

Western blot is a method to separate and identify protein of interest expressed in cells. Proteins extracted from tissues or cells are separated based on different molecular weight through gel electrophoresis (Sodium Dodecyl Sulfate Polyacrylamide Gel Electrophoresis, SDS-PAGE). Polyacrylamide gel is formed from polymerization of acrylamide and N,N-methylenebisacrylamide (Bis) which consists of a three dimensional networks of long hydrocarbon by crosslink of methylene groups. Separated proteins are then transferred to blotting membrane (nitrocellulose) where proteins retain the same arrangement (mirror image) of separation they had on gel. Then, the membrane is incubated with a generic protein (such as milk proteins) to bind non specific proteins on the nitrocellulose membrane. The membrane is incubated with antibody that binds specifically to protein of interest. This antibody is known as primary antibody. The membrane is washed to remove all unbound primary antibody prior to incubation with secondary antibody. Secondary antibody is labeled with a dye or an enzyme (usually horseradish peroxidase) which develop colour with substrate and can be directly viewed and scanned with a densitometer (**Figure 12**). Theoretically, antibodies specific to the protein of

interest should produce a single band and the thickness of the band is highly dependent on the amount of proteins present (Mahmood and Yang, 2012).



(Kurien and Scofield, 2006)

**Figure 12:** The schemetic diagram above described the flow work of western blotting to detect protein being expressed. (A) Proteins extracted were separated using SDS-PAGE. Multiple bands can be viewed after proteins of different molecular weight migrate. (B) A mirror image of SDS-PAGE gel is being transferred to blotting membrane through electro blotting system. (C) Primary antibody binding to a specific band (known as antigen which can be a polypeptide or carbohydrate) on the blot. (D) Secondary antibody conjugated with horse radish peroxidase (HRP) binding to primary antibody. HRP (for amplification of signal detection) converts chromogenic subtrates (eg. 3,3',5,5'-Tetramethylbenzidine, TMB) into colored products. (E) Color of the specific band being developed and can be detected colorimetrically.

### **2.16.1 Preparation of cell lysate (proteins) from cardamonin-treated HK-1 cells**

HK-1 cells were treated with 22 µg/mL of cardamonin at 24, 48 and 72 hrs. Cells were harvested and centrifuged at 2,500 rpm for 5 mins. Cells were counted to approximately  $5 \times 10^6$  cells before being washed with PBS in a 1.5 mL tube. Cell pellet was then re-suspended in 400 µL of PRO-PREP solution (volume differs depending on number of cells harvested). The cells are incubated in -20°C freezer for 15 mins to induce cell lysis. After incubation, the cells were spun down at 13,000 rpm at 4°C for 5 mins. The supernatant was transferred to a new 1.5 mL tube and labeled as cell lysate which contains highly purified proteins. Protein extraction was repeated for control and 3, 6, 9, 12, 18 hrs exposure to cardamonin against HK-1 cell line to identify the expression of proteins an extended period of time.

### **2.16.2 Protein concentration determination**

5 µL of protein sample or bovine serum albumin (BSA) protein standard was mixed well with 200 µL of 1X Bradford dye reagent in 96-microplate wells on plate shaker for 30 seconds. Plate is incubated for 10 mins at room temperature (RT). After incubation, absorbance is measured at 595 nm using Thermo Scientific Varioskan Flash multimode plate reader. A BSA standard curve was plotted to quantify the concentration of proteins in the extracted samples. Three repeats were measured for all samples and standard.

### **2.16.3 Gel electrophoresis for protein separation in 24, 48 and 72 hrs cardamonin-induced HK-1 cells**

11.9 µg of extracted protein samples (control and 22 µg/mL of cardamonin-treated HK-1 cells) (**Appendices 7.10.2.2**) were heated in 90°C water bath for 10 mins to unfold and expose its long polypeptide chain. A total of 18 µL from each sample was loaded on 10-well gel casted with 4% of stacking gel and 12% of resolving gel. 6 µL of PageRuler unstained protein ladder was loaded as a reference to determine molecular weights of proteins. Gel electrophoresis was run at 120V for 1 hr 20 mins. Gel was carefully removed from casting plates and washed three times with distilled water. After washing, gel was left to shake overnight at 60 rpm in 30 mL of 1X Bio-Safe Coomassie Stain. Next day, Coomassie stain was replaced with destaining solution (67.5% distilled water, 25% methanol and 7.5% acetic acid) to destain Coomassie Stain and this step was repeated at least three times at 1 hr interval until protein bands are completely visible. Gel was washed with distilled water before being viewed using a GS-800 calibrated densitometer (Bio-Rad Laboratories).

### **2.16.4 Gel electrophoresis for protein separation in 0 to 24 hrs cardamonin-induced HK-1 cells through optimization of resolving gel percentage**

Proteins were separated on polyacrylamide gel based on gel pore size by manipulation of cross linkage agent, Bis. The smaller the size of protein, the

higher the percentage of PAGE gel is used to retain protein. Because the molecular weight of proteins of interest varied, an optimization of gel percentage was conducted. Resolving gels were casted at four different percentages of Bis (**Appendices 7.10.2.1**). 30 µg of protein samples extracted from cardamonin-treated HK-1 cells at 0-24 hrs (**Appendices 7.10.2.3**) were heated at 90°C for 10 mins and loaded on 8%, 10%, 12% and 15% resolving gels to separate proteins according to different molecular weight of proteins. Gel electrophoresis was run at 120V between 1 hr and 1hr 20 mins.

#### **2.16.5 Visualization of proteins in gel**

After gel electrophoresis, gel was carefully removed from casting plates and washed three times with distilled water. After washing, gel was left to shake overnight at 60 rpm in 30 mL of 1X Bio-Safe Coomassie Stain. Next day, Coomassie stain was replaced with destaining solution (67.5% distilled water, 25% methanol and 7.5% acetic acid) to destain Coomassie Stain and this step was repeated at least three times at 1 hr interval until protein bands are completely visible. Gel was washed with distilled water before being viewed using a GS-800 calibrated densitometer (Bio-Rad Laboratories).

#### **2.16.6 Protein transfer (Electro blotting)**

Proteins were transferred from gel to blotting membrane (nitrocellulose) through wet transfer. In wet transfer, the gel and membrane are sandwiched between filter paper and blotting pad. The sandwich will then be submerged in



transfer buffer where an electrical field is applied to the system. Negatively-charged proteins will travel towards anode, a positively-charged electrode until all proteins are being transferred onto the nitrocellulose membrane. Filter papers, blotting pads and nitrocellulose membrane were fully saturated in transfer buffer (10X Tris/Glycine) before being sandwiched in an arrangement shown in **Figure 13**. Before placing the last two blotting pads, a pipette was used to gently roll over the surface of the filter paper to ensure all air bubbles were removed. Sandwich was carefully placed into the blot module and positioned in the electro-blotting tank. Transfer buffer was fully filled into blot module and distilled water was filled into the gel tank to cool the electro-blotting system. Electro-blotting was allowed to run at 25V for 80 mins (after at least three replicate of optimization).

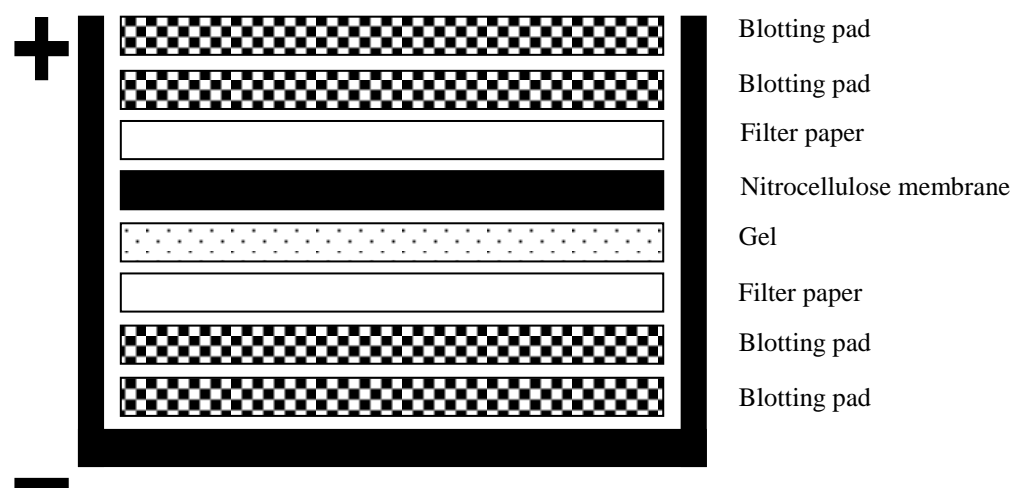


**Figure 13:** Electro blotting arrangement.

### **2.16.7 Blocking and Detection**

The membrane was soaked in Tris Buffered Saline (TBS) containing 5% low fat milk (Anlene) and 1% Tween-20 (blocking buffer) overnight with agitation (60 rpm) at 4°C. Primary antibody (1:1500 dilution) added in a fresh 15 mL of blocking buffer was incubated with membrane for 2 hrs with agitation (60 rpm) at room temperature. Membrane was washed for three times with 5-minute intervals with 10 mL of TBS-Tween. A secondary antibody (1:1500 dilution) prepared in a fresh 15 mL blocking buffer was added to membrane and allowed agitation (60 rpm) for another 1 hr 30 mins at room temperature. Membrane was washed four times, three with TBS-Tween and finally with distilled water at 5-minute intervals. Lastly, membrane was washed with 1 mL of TMB Membrane Peroxidase Substrate Ready-To-Use (Rockland Immunochemicals Inc.) until protein bands were observed (usually 5-10 mins). Membrane was dried at room temperature before being viewed using GS-800 calibrated densitometer (Bio-Rad Laboratories).

### **2.16.8 Loading control**

Glyceraldehyde 3-phosphate dehydrogenase (GADPH) is an enzyme involved in glycolysis. It acts as a housekeeping protein and hence it was used as loading control to ensure uniform and equal loading efficiency of protein lysate. The membrane was blocked overnight in TBS-Tween containing 3% Bovine Serum Albumin (BSA). Membrane was then incubated with Anti-GADPH primary antibody (1:6000 dilution) for 1 hr at room temperature with

agitation (60 rpm). Washing was done with TBS-Tween according to Method 2.5.2. Secondary antibody, Rabbit Anti-Mouse (1:6000 dilution) was incubated for another hour before detection using GS-800 calibrated densitometer (Bio-Rad Laboratories). Signal intensities were quantified using Quantity One 1-D Analysis software (Bio-Rad).

## **2.17 Relative quantification of caspase-9 gene expression level using real-time PCR**

In current research, caspase-9 expression level will be evaluated using real time reverse transcriptase polymerase chain reaction (RT-PCR). PCR is a biochemical process using a relatively small quantity of starting material (short DNA sequences) to amplify specific DNA sequences of interest on a longer double-stranded DNA. Real-time PCR (qPCR) is used to quantify amount of amplified products (amplicons) by incorporation of a fluorescent reporter molecule. Real-time assay is the time point where first PCR product is detected during thermal cycling. Fluorescence intensity is proportional to each DNA molecule amplified. Amplification of a specific DNA sequence during PCR mimics the process of DNA replication. It requires thermophilic DNA polymerase and primers to synthesis new DNA copies (Bustin, 2005). In current research, qPCR is done in a single tube reaction using a thermal cycler machine for DNA synthesis. Ribonucleic acid (RNA) will be used as starting material to synthesis complementary DNA (cDNA). cDNA is synthesized using Invitrogen Superscript III reverse transcriptase enzyme (Life

Technologies). Target gene of interest on cDNA will be amplified in three steps.

These 3 steps complete one PCR cycle whereby specific DNA sequence expressing gene of interest is amplified (**Figure 14**). Step 1 involves denaturing of double-stranded DNA at high temperature (95°C) to yield single-stranded DNA (Step 1: Denaturation). Single-stranded DNA containing base pairs is now exposed and ready for step 2. Step 2 involves attachment of primers to specific DNA sequence on single stranded DNA. Primers are oligonucleotides that are short, single-stranded and complementary to a defined sequence on each strand of double-stranded DNA. It allows DNA polymerase (*Taq* polymerase) to attach at its site to extend and replicate complementary strand (Step 2: Annealing). Final step of PCR cycle is extension of primers by adding deoxynucleotide triphosphates (dNTPs) specifically at the phosphate backbone (Elongation) (Mullis and Faloona, 1987).

The fluorescence intensity emitted during qPCR is directly proportional to the amount of amplicons produced. In this research, SYBR Green I (Life Technologies) is used as a fluorescent dye that binds directly to double stranded DNA synthesized from each qPCR cycle. As amplicons are generated fluorescence intensity increases exponentially with each qPCR cycle. After a few initial qPCR cycles where baseline fluorescence are generated (threshold level), following cycles will generate fluorescence signal that crosses threshold level which is where true amplification is quantified (**Figure 15**). This is when reaction reaches exponential phase. Eventually when the fluorescence intensity saturates the detector of qPCR machine, amplicons become abundant and

reaches plateau phase. The cycle number at which reaction reaches exponential phase is termed threshold cycle ( $C_T$ ).  $C_T$  represents the beginning of exponential phase where first significant fluorescent signal is taken into account for quantification (Fraga *et al.*, 2008).

$C_T$  value is important for relative quantification of gene expression level. In current research, we are interested in relative quantification of caspase-9 gene expression level compared to level of expression in control group. In addition, we utilized a reference gene (GADPH) as a normalization of the assay. Fold difference expressed in relative level is obtained based on  $C_T$  values. Non-template control will be used as negative control containing no RNA template (Livak and Schmittgen, 2001).

Livak method is used for relative quantification of caspase-9 gene expression level. It is also known as  $2^{-\Delta\Delta C_T}$  method where this equation is used for relative quantification. This method requires a target (caspase-9) and a reference gene (GADPH). Calculations of gene expression relative quantification require 3 steps. Step 1 is to normalize  $C_T$  value of target gene to  $C_T$  value of reference gene ( $\Delta C_T$ ). Step 2 involves normalization of  $\Delta C_T$  of test sample to  $\Delta C_T$  of control group ( $\Delta\Delta C_T$ ). In step 3, normalization of expression ratio based on  $\Delta\Delta C_T$  obtained in step 2 using formula  $2^{-\Delta\Delta C_T}$  derived by Livak and Schmittgen (Livak and Schmittgen, 2001).

Melting curve analysis will be run at the end of qPCR thermal cycles at 40°C for 1 min to determine the dissociation-characteristics of amplicons by increasing temperature to dissociate double-stranded DNA synthesized. Melting point of amplicon can be determined where 50% of the

DNA is denatured. The energy required to break hydrogen bonding between base pair of double-stranded DNA is dependent on their length, GC (guanine-cytosine) content and complementary. Hence, melting point of amplicon is specific to the product of interest. It acts as a reference if amplicon is the product expressing gene of interest. In addition, pattern of melting curve can be used to determine purity of amplicons and the presence of primer-dimer effect (Ririe *et al.*, 1997). qPCR product will be analyzed on agarose gel electrophoresis to estimate the length of the amplicons.

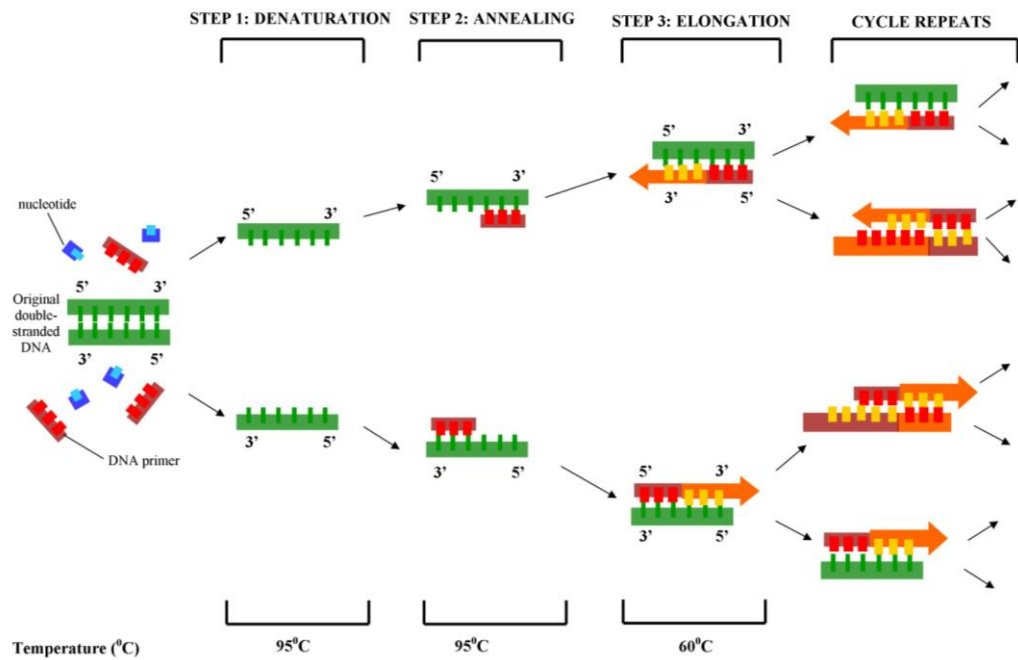


**Figure 14:** Polymerase chain reaction (PCR) cycle.

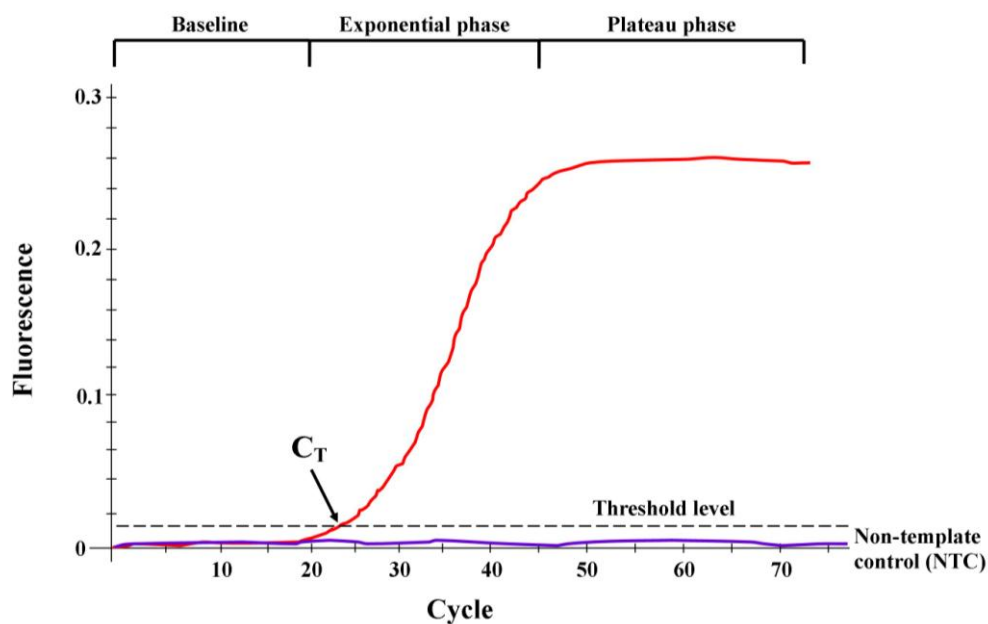


**Figure 15:** Exponential curve of real-time PCR showing different phases.

$1 \times 10^6$  HK-1 cells treated with cardamonin were harvested after 24 hrs of exposure. Cells were washed with PBS prior to total RNA extraction using RNeasy®-4PCR Total RNA Isolation Kit (Invitrogen). 350  $\mu$ L of lysis/binding buffer was added to cell pellet and vortex vigorously by pipetting until lysate is homogenous. 350  $\mu$ L (equal volume) of 64% ethanol (EtOH) solution was added to the lysate and mixed gently by pipetting and inverting tube. Lysate/EtOH mixture was filtered through filter cartridge and collection tube by applying centrifugal force at 13,000 rpm for 1 min. Flow-through was discarded and filter cartridge was washed with 700  $\mu$ L of wash solution #1 by centrifugation at 13,000 rpm for 1 min. Flow-through was discarded and washed with again with wash solution #2/3 by centrifugation at 13,000 rpm for 1 min. This washing step was repeated once. Filter cartridge was placed on a

new collection tube. 60  $\mu\text{L}$  of pre-heated ( $80^{\circ}\text{C}$ ) elution solution was applied to the centre of filter cartridge and centrifuged at 13,000 rpm for 30 secs. 40  $\mu\text{L}$  of elution solution was added to the filter cartridge and centrifuged again. Both eluted solutions contain RNA needed for real-time PCR. Next, 10  $\mu\text{L}$  of DNase 1 buffer and 1  $\mu\text{L}$  of DNase 1 were added to the eluted RNA and incubated for 30 mins at  $37^{\circ}\text{C}$  to remove contaminating DNA. Next, 11  $\mu\text{L}$  of DNase inactivation reagent was added and incubated at room temperature for 2 mins by gently flicking the collection tube. This step is crucial to prevent DNase 1 from degrading products (DNA) during PCR. Then, the tube was centrifuged at 13,000 rpm for 1 min to pellet DNase inactivation reagent. The supernatant containing RNA was transferred to a new tube for storage.

Purity and quantification of RNA was determined using UV absorbance. Aliquot of RNA was diluted in Tris-EDTA (TE) buffer at ratio 1:50 (2  $\mu\text{L}$  of RNA aliquot to 100  $\mu\text{L}$  of TE buffer). Absorbance was read at 260 nm and 280 nm with TE buffer as blank using Thermo Scientific Varioskan Flash multimode plate reader. The concentration of RNA aliquot was quantified using the equation below:

Since  $A_{260}$  of 1 is equivalent to 40  $\mu\text{g}$  RNA/mL,

Hence,  $A_{260} \times \text{dilution factor} \times 40 = \mu\text{g RNA/mL}$

Purity of eluted RNA is determined by ratio of  $A_{260}/A_{280}$  where it should fall in the range of 1.8-2.1.

Agarose gel electrophoresis was conducted to estimate the integrity and purity of total RNA extracted. Total RNA was separated on 1% agarose gel containing 1.5  $\mu\text{L}$  SYBR Safe at 80V for 90 mins. Separated RNA molecules



were visualized under UV light illuminator (ChemiDoc XRS system, BioRad). 28S and 18S ribosomal RNA bands should be observed with intensity of upper band is twice of the lower band.

To evaluate expression of caspase-9, quantitative RT-PCR was performed using Eco Real-Time PCR system (Illumina). Superscript III Platinum SYBR Green One-Step qRT-PCR kit (Invitrogen) combines proprietary Superscript III Reverse Transcriptase (RT) and Platinum *Taq* DNA polymerase in a single enzyme mix together with SYBR Green I fluorescent dye. Hence, cDNA synthesis and PCR are performed in a single tube by using RNA as starting material. cDNA was synthesized in a single 20- $\mu$ L reaction containing 0.4  $\mu$ L of Superscript III RT/Platinum *Taq*Mix, 10  $\mu$ L of 2X SYBR Green Reaction Mix (containing 0.4 mM of each dNTP and 3.2 mM of  $\text{MgSO}_4$ ), 0.4  $\mu$ L of 10  $\mu$ M forward primer and reverse primer each and 1 ng/ $\mu$ L of RNA aliquot. Thermal cycling conditions were set for cDNA synthesis for 3 mins hold at 50°C, followed by 5 mins activation of DNA polymerase and denaturation at 90°C. 40 cycles of annealing and amplification were performed at 95°C for 15 secs and 60°C for 30 secs respectively. The products were incubated for 1 min at 40°C prior to melting curve analysis.

Amplicons were separated on a 2% agarose gel electrophoresis at 80V for 60 mins. Gel was visualized under UV light illuminator (ChemiDoc XRS system, BioRad).

Specific primers used were: Homo caspase-9 forward (F) primer (5' TGTCTACTCTACTTTCCCAGGTTTT 3'), homo caspase-9 reverse (R) primer (5' GTGAGCCCACTGCTCAAAGAT 3'), GAPDH forward (F)

primer (5' ACACCCACTCCTCCACCTTT 3') and GADPH reverse (R) primer (5' TAGCCAAATTCGTTGTCATACC).

Eco Real-Time PCR system software v5.0 was employed for relative quantification to generate a real-time amplification plot based on the normalized fluorescence signal. Threshold cycle ( $C_T$ ); cycle number at which detectable signal is significant was used as a relative quantification to initial number of target copies in the starting material. GADPH was used as a reference gene to quantify the number of fold decrease or increase in caspase-9 expression level.

## **2.18 Statistical Analysis**

The results of triplicate experiments were obtained and the values were presented in the form of mean  $\pm$  standard deviation (S.D.). One-way analysis of variance (ANOVA)'s Dunnett's Multiple Comparison Test and t-test were applied to analyze the difference from the respective controls for each experiment. All analyses were done using GraphPad Prism 5 software and Microsoft Excel 2007. The signal intensities of various protein bands were quantified using Quantity One 1-D Analysis Software (Bio-Rad Laboratories, Munich, Germany).

### 3.0 RESULTS

#### 3.1 Phytochemical analysis

Methanolic crude extract of curry leaf (*Murraya koenigii*) revealed the presence tannins and flavonoids where as both ethyl acetate and hexane crude extracts of curry leaf (*Murraya koenigii*) showed the presence of alkaloids (Table 1). Steroids were also present in hexane crude extract of curry leaf (*Murraya koenigii*).

As for temu kunci (*Boesenbergia rotunda*), all three crude extracts revealed the presence of flavonoids and alkaloids. Other phytochemicals were not present in these crude extracts.

In spring onion leaf (*Allium cepa*), both methanolic and ethyl acetate crude extracts contained tannins where as hexane crude extract revealed the presence of flavonoids. Only methanolic crude extract of mushroom bean (*Phaseolus vulgaris*) gave positive results in phytochemical tests compared to the crude extracts of mushroom bean (*Phaseolus vulgaris*) with the presence of phlobatannins and steroids.

All crude extracts of bunga kantan (*Phaeomeria imperialis*) revealed the presence of saponins. Methanolic solid (S1) contained phlobatannins where as alkaloids were present in ethyl acetate and hexane crude extracts of bunga kantan (*Phaeomeria imperialis*). Flavonoids were present in methanolic crude extract of bunga kantan (*Phaeomeria imperialis*).

Glycosides and terpenoids were not present in all crude extracts.

It is important to note that both flavonoid and alkaloid contribute greatly as backbone in development of anticancer drug. In current research, all

three crude extracts of temu kunci (*Boesenbergia rotunda*) revealed the presence of flavonoids and alkaloids which suggests further investigate on the roles of these phytochemicals in search for a single anticancer agent.

**Table 1: Phytochemical constituents of various crude extracts of curry leaf (*Murraya koenigii*), temu kunci (*Boesenbergia rotunda*), spring onion leaf (*Allium cepa*), mushroom bean (*Phaseolus vulgaris*), bunga kantan (*Phaeomeria imperialis*).**

Phytochemical test	Edible plant															
	Curry leaf ( <i>Murraya koenigii</i> )			Temu kunci ( <i>Boesenbergia rotunda</i> )			Spring onion leaf ( <i>Allium cepa</i> )			Mushroom bean ( <i>Phaseolus vulgaris</i> )			Bunga kantan ( <i>Phaeomeria imperialis</i> )			
	M	EA	H	M	EA	H	M	EA	H	M	EA	H	M	EA	H	S1
Tannins	■	■	-	-	-	-	■	■	-	-	-	-	■	-	-	-
Saponins	-	-	-	-	-	-	-	-	-	-	-	-	■	■	■	■
Phlobatannins	-	-	-	-	-	-	-	-	-	■	-	-	-	-	-	■
Flavonoids	■	-	-	■	■	■	-	-	■	-	-	-	■	-	-	-
Steroids	-	-	■	-	-	-	-	-	-	■	-	-	-	-	-	-
Alkaloids	-	■	■	■	■	■	-	-	-	-	-	-	■	■	-	-
Glycosides	-	-	-	-	-	-	-	-	-	-	-	-	-	-	-	-
Terpenoids	-	-	-	-	-	-	-	-	-	-	-	-	-	-	-	-

■ represents the presence of the constituent; - represents the absence of the constituent; M represents the methanolic crude extract;

EA represents ethyl acetate crude extract; H represents hexane crude extract; S1 represents methanolic solid 1

### 3.2 Total phenolic content

Both crude ethyl acetate of curry leaf (*Murraya koenigii*) and temu kunci (*Boesenbergia rotunda*) showed highest amount of phenolic content compared to other plant crude extracts with  $86.15 \pm 2.156$  mg gallic acid equivalents/g of sample and  $113.9 \pm 0.7315$  mg gallic equivalents/g of sample respectively (**Figure 16**). As for bunga kantan (*Phaeomeria imperialis*), crude methanolic extract showed highest phenolic content with  $67.92 \pm 1.381$  mg gallic acid equivalents/g of sample. All crude extracts of spring onion leaf (*Allium cepa*) and mushroom bean (*Phaseolus vulgaris*) were reported to exhibit low phenolic content.

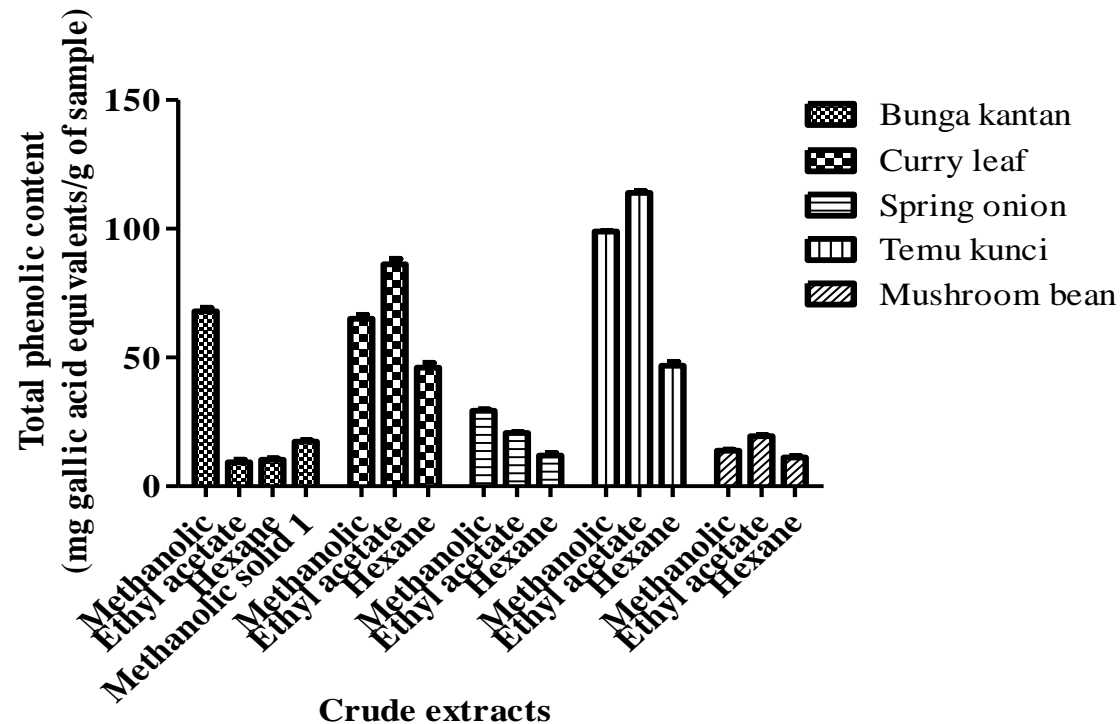


**Figure 16:** Total phenolic content (mg gallic acid equivalents/g of sample) of various crude extracts of curry leaf (*Murraya koenigii*), temu kunci (*Boesenbergia rotunda*), spring onion leaf (*Allium cepa*), mushroom bean (*Phaseolus vulgaris*) and bunga kantan (*Phaeomeria imperialis*). All values are  $\pm$  S.D. of 3 independent experiments.

### 3.3 Total flavonoid content

Crude ethyl acetate of temu kunci (*Boesenbergia rotunda*) showed highest amount of flavonoid content compared to other plant crude extracts with  $833.0 \pm 12.63$  mg quercetin equivalents/g of sample (**Figure 17**). For curry leaf (*Murraya koenigii*), temu kunci (*Boesenbergia rotunda*) and spring onion leaf (*Allium cepa*), crude ethyl acetate extracts showed highest flavonoid content compared to methanolic and hexane crude extracts. All crude extracts of bunga kantan (*Phaeomeria imperialis*) and mushroom bean (*Phaseolus vulgaris*) were reported to exhibit low flavonoid content.



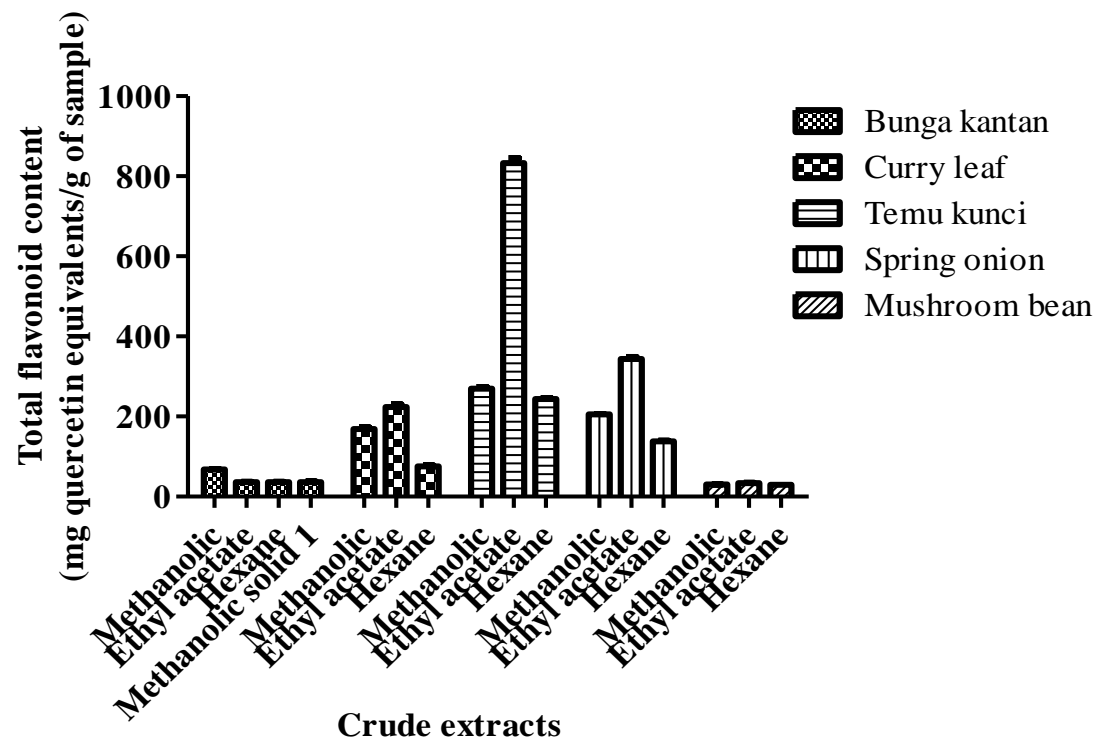


**Figure 17:** Total flavonoid content (mg quercetin equivalents/g of sample) of various crude extracts of curry leaf (*Murraya koenigii*), temu kunci (*Boesenbergia rotunda*), spring onion leaf (*Allium cepa*), mushroom bean (*Phaseolus vulgaris*) and bunga kantan (*Phaeomeria imperialis*). All values are  $\pm$  S.D. of 3 independent experiments.

### **3.4 Cytotoxic activity**

#### **3.4.1 Effect of various crude extracts and positive control on HK-1 cell viability**

##### **3.4.1.1 Effect of methanol crude extract of bunga kantan on HK-1 cell viability**

HK-1 cell line was treated with various concentrations of crude methanol extract of bunga kantan from 3.13 µg/mL to 200 µg/mL at 24 and 48 hrs and cell viability was evaluated (**Figure 18**). Control group was not treated with the crude extract. At 24 hrs, the percentage of cell viability in each concentration was high, ranging from 88.62±0.51% to 107.1±1.33%. None of the concentrations gave cell viability lower than 50%. At 48 hrs, none of the concentrations showed more than 50% cell inhibition with cell viability ranging from 61.85±3.12% to 96.90±1.20%. Extract concentrations of more than 50 µg/mL had significant ( $p<0.001$ ) decrease in viable cells when compared to untreated control group. Thus, it can be concluded that crude methanolic extract of bunga kantan has low cytotoxic activity against HK-1 cell line.

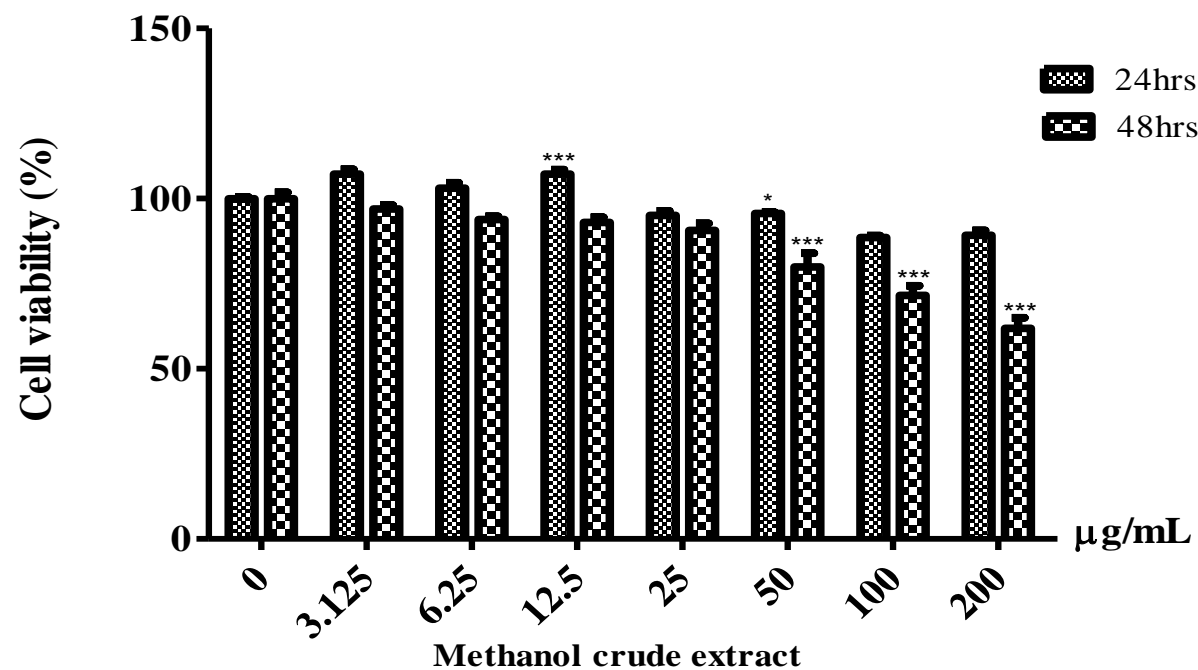


**Figure 18 : Effect of methanol crude extract of bunga kantan on HK-1 cell viability. Each bar represents the mean  $\pm$  standard deviation (S.D.) from 3 independent experiments (n=3). \*\*\* $P < 0.001$  and \* $P < 0.05$  indicate the statistical significant difference with respect to untreated control group.**

### **3.4.1.2 Effect of ethyl acetate crude extract of bunga kantan on HK-1 cell viability**

HK-1 cell line was treated with various concentrations of crude ethyl acetate extract of bunga kantan from 3.13 µg/mL to 200 µg/mL at 24 and 48 hrs and cell viability was evaluated (**Figure 19**). Control group was not treated with the crude extract. At 24 hrs, the percentage of cell viability in each concentration was high, ranging from 91.25±4.06% to 123.80±2.13%. None of the concentrations gave cell viability lower than 50%. At 48 hrs, none of the concentrations showed more than 50% cell inhibition with cell viability ranging from 71.47±0.61% to 97.63±1.21%. Extract concentrations of 100 and 200 µg/mL had significant ( $p<0.001$ ) decrease in viable cells when compared to untreated control group. Thus, it can be concluded that crude ethyl acetate extract of bunga kantan has low cytotoxic activity against HK-1 cell line.

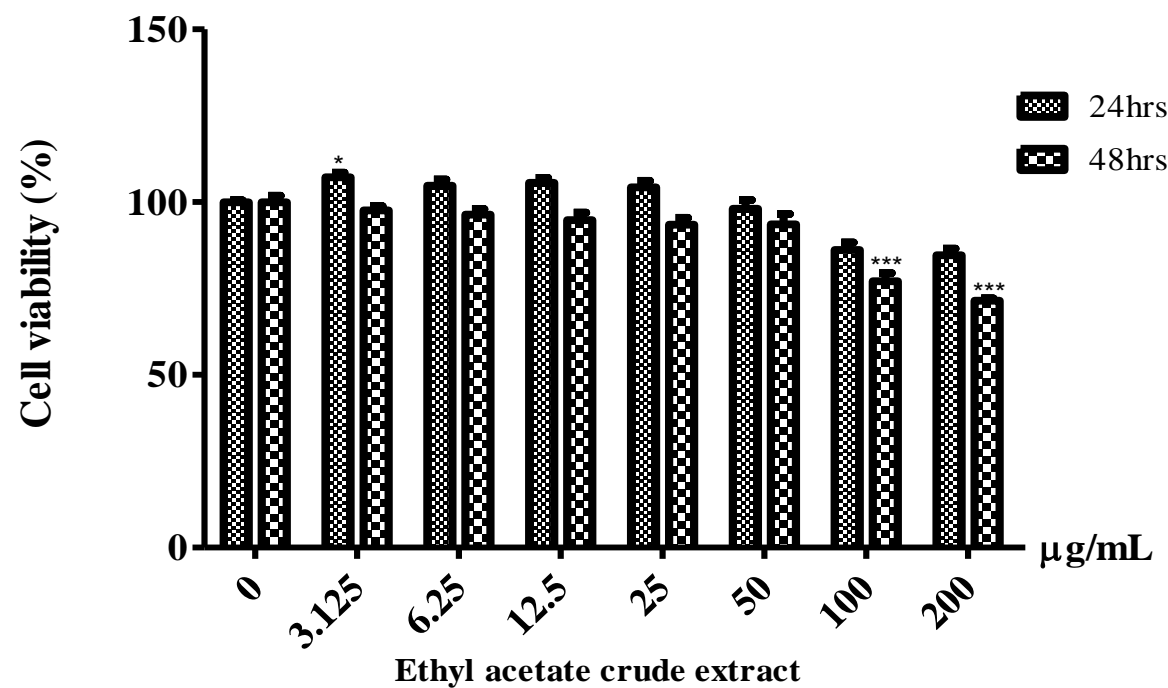


**Figure 19: Effect of ethyl acetate crude extract of bunga kantan on HK-1 cell viability. Each bar represents the mean  $\pm$  standard deviation (S.D.) from 3 independent experiments (n=3). \*\*\* $P < 0.001$  and \* $P < 0.05$  indicate the statistical significant difference with respect to untreated control group.**

#### **3.4.1.3 Effect of hexane crude extract of bunga kantan on HK-1 cell viability**

HK-1 cell line was treated with various concentrations of crude hexane extract of bunga kantan from 3.13 µg/mL to 200 µg/mL at 24 and 48 hrs and cell viability was evaluated (**Figure 20**). Control group was not treated with the crude extract. At 24 hrs, the percentage of cell viability in each concentration was high, ranging from  $74.27 \pm 2.51\%$  to  $105.3 \pm 1.42\%$ . None of the concentrations gave cell viability lower than 50%. At 48 hrs, none of the concentrations showed more than 50% cell inhibition with cell viability ranging from  $72.07 \pm 2.81\%$  to  $102.7 \pm 0.66\%$ . Extract concentrations of 50 µg/mL and above had significant ( $p < 0.001$ ) decrease in viable cells when compared to untreated control group. Thus, it can be concluded that crude hexane extract of bunga kantan has low cytotoxic activity against HK-1 cell line.

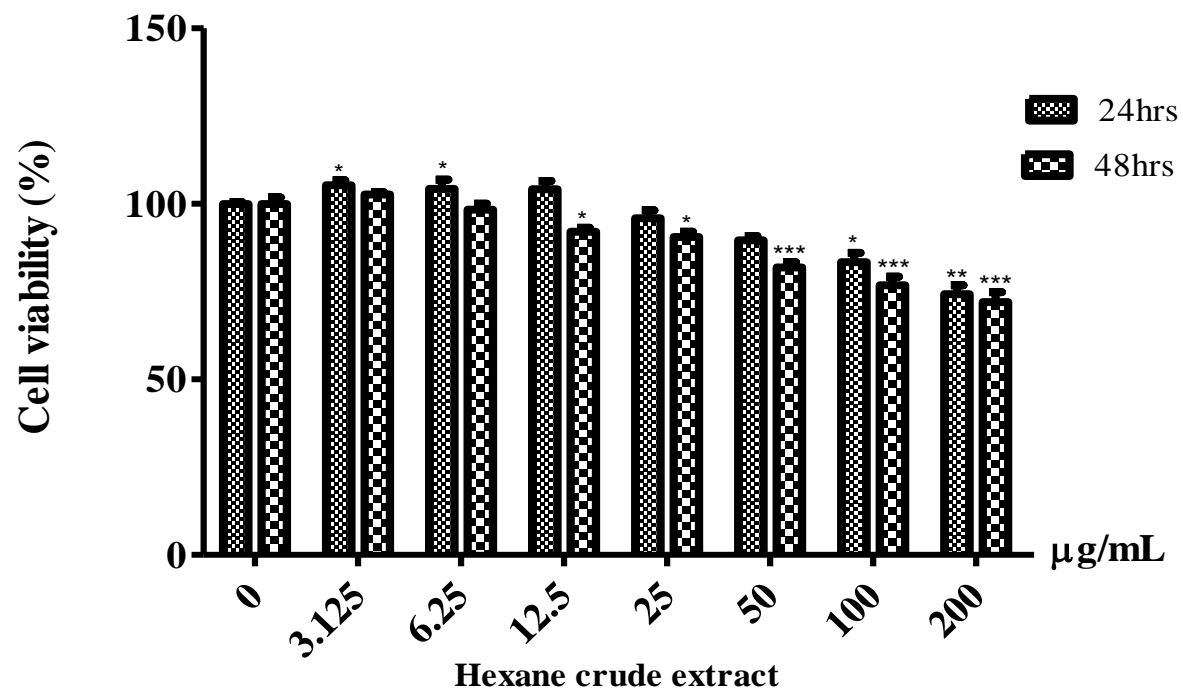


**Figure 20: Effect of hexane crude extract of bunga kantan on HK-1 cell viability. Each bar represents the mean  $\pm$  standard deviation (S.D.) from 3 independent experiments (n=3). \*\*\* $P < 0.001$ , \*\* $P < 0.01$  and \* $P < 0.05$  indicate the statistical significant difference with respect to untreated control group.**

#### **3.4.1.4 Effect of methanol solid 1 crude extract of bunga kantan on HK-1 cell viability**

HK-1 cell line was treated with various concentrations of crude methanolic solid 1 extract of bunga kantan from 3.13 µg/mL to 200 µg/mL at 24 and 48 hrs and cell viability was evaluated (**Figure 21**). Control group was not treated with the crude extract. At 24 hrs, the percentage of cell viability in each concentration was high, ranging from 90.69±1.28% to 108.4±0.78%. None of the concentrations gave cell viability lower than 50%. At 48 hrs, none of the concentrations showed more than 50% cell inhibition with cell viability ranging from 60.51±1.21% to 101.2±1.17%. Extract concentrations of 12.5 µg/mL and above had significant ( $p<0.001$ ) decrease in viable cells when compared to untreated control group. Thus, it can be concluded that crude methanolic solid 1 extract of bunga kantan has low cytotoxic activity against HK-1 cell line.



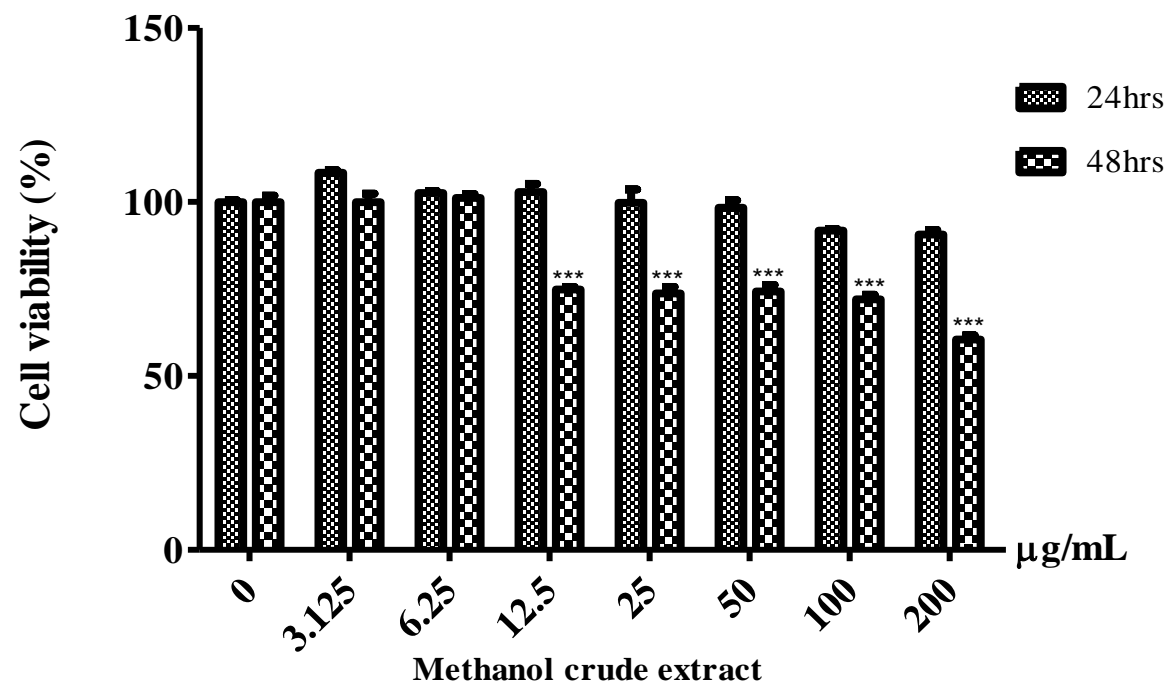


**Figure 21: Effect of methanol solid 1 crude extract of bunga kantan on HK-1 cell viability. Each bar represents the mean  $\pm$  standard deviation (S.D.) from 3 independent experiments (n=3). \*\*\* $P < 0.001$  indicates the statistical significant difference with respect to untreated control group.**

#### **3.4.1.5 Effect of methanol crude extract of curry leaf on HK-1 cell viability**

HK-1 cell line was treated with various concentrations of crude methanolic extract of curry leaf from 3.13 µg/mL to 200 µg/mL at 24 and 48 hrs and cell viability was evaluated (**Figure 22**). Control group was not treated with the crude extract. At 24 hrs, the percentage of cell viability in each concentration was moderate, ranging from 54.10±2.68% to 108.3±0.48%. Treatment with 200 µg/mL of extract showed that approximately half of the cell growth was inhibited. At 48 hrs, there was more than 50% growth inhibition with 39.65±0.78% cell viability. Extract concentrations of 100 and 200 µg/mL had significant ( $p<0.001$ ) decrease in viable cells when compared to untreated control group. Thus, it can be concluded that crude methanolic extract of curry leaf has moderate cytotoxic activity against HK-1 cell line.

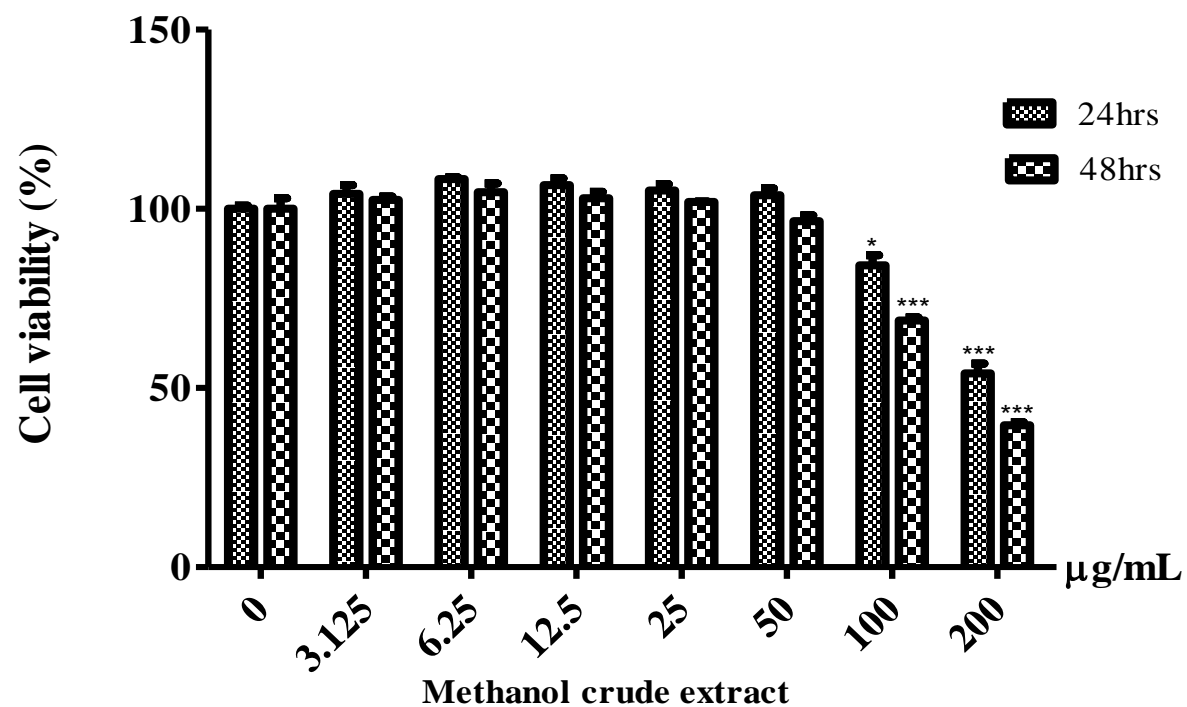


**Figure 22: Effect of methanol crude extract of curry leaf on HK-1 cell viability. Each bar represents the mean  $\pm$  standard deviation (S.D.) from 3 independent experiments (n=3). \*\*\* $P < 0.001$  and \* $P < 0.05$  indicate the statistical significant difference with respect to untreated control group.**

#### **3.4.1.6 Effect of ethyl acetate crude extract of curry leaf on HK-1 cell viability**

HK-1 cell line was treated with various concentrations of crude ethyl acetate extract of curry leaf from 3.13  $\mu\text{g/mL}$  to 200  $\mu\text{g/mL}$  at 24 and 48 hrs and cell viability was evaluated (**Figure 23**). Control group was not treated with the crude extract. At 24 hrs, the percentage of cell viability in each concentration was moderate, ranging from  $59.46 \pm 0.40\%$  to  $108.3 \pm 1.24\%$ . Treatment with 50  $\mu\text{g/mL}$  of extract and above showed that about half of the cell growth was inhibited. At 48 hrs, slightly less than 50% growth inhibition was observed at concentration 25  $\mu\text{g/mL}$  and above ranging from  $55.15 \pm 0.84\%$  to  $60.63 \pm 0.65\%$ . At 48 hrs, all concentrations had significant ( $p < 0.001$ ) decrease in viable cells when compared to untreated control group. Thus, it can be concluded that crude ethyl acetate extract of curry leaf has low cytotoxic activity against HK-1 cell line.

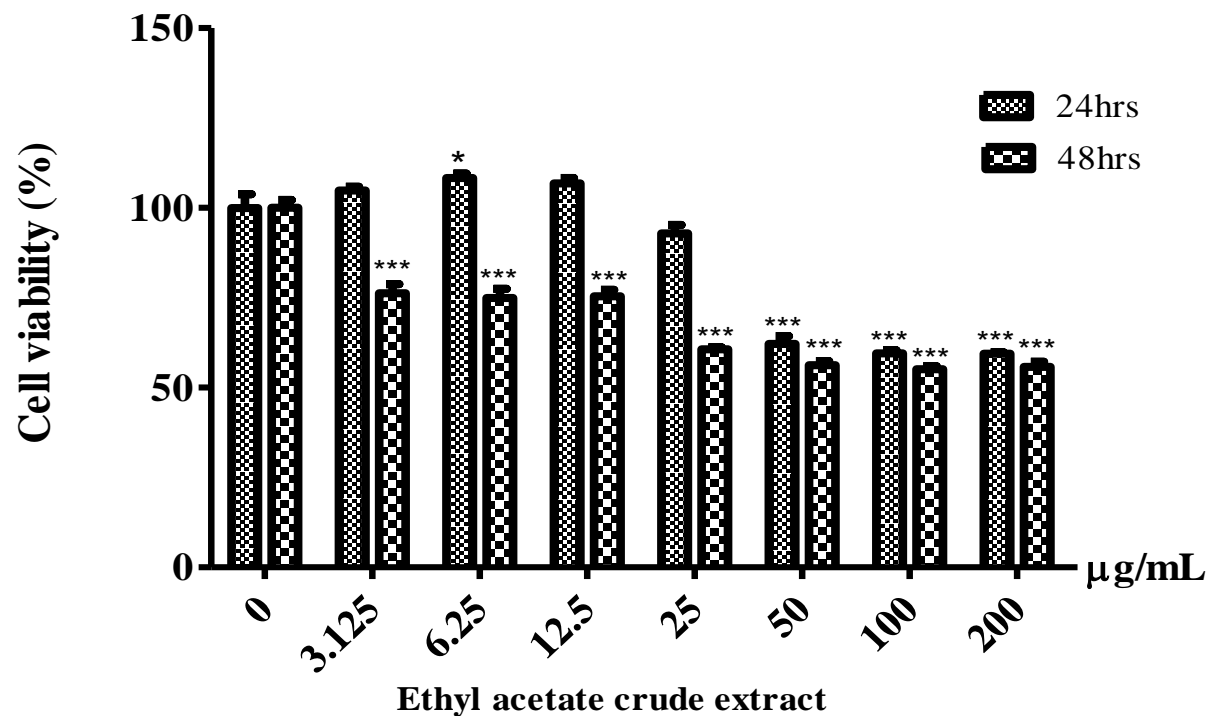


**Figure 23: Effect of ethyl acetate crude extract of curry leaf on HK-1 cell viability. Each bar represents the mean  $\pm$  standard deviation (S.D.) from 3 independent experiments (n=3). \*\*\* $P < 0.001$  and \* $P < 0.05$  indicate the statistical significant difference with respect to untreated control group.**

#### **3.4.1.7 Effect of hexane crude extract of curry leaf on HK-1 cell viability**

HK-1 cell line was treated with various concentrations of crude hexane extract of curry leaf from 3.13 µg/mL to 200 µg/mL at 24 and 48 hrs and cell viability was evaluated (**Figure 24**). Control group was not treated with the crude extract. At 24 hrs, the percentage of cell viability in each concentration was moderate, ranging from 58.41±2.06% to 108.5±1.96%. Treatment with 200 µg/mL of extract showed that about half of the cell growth was inhibited. At 48 hrs, there were more than 50% growth inhibition at concentrations 100 and 200 µg/mL with 43.49±1.62% and 37.58±2.06% cell viability respectively. At 24 and 48 hrs, extract concentrations of 50 µg/mL and above had significant ( $p<0.001$ ) decrease in viable cells when compared to untreated control group. Thus, it can be concluded that crude hexane extract of curry leaf has high cytotoxic activity against HK-1 cell line.

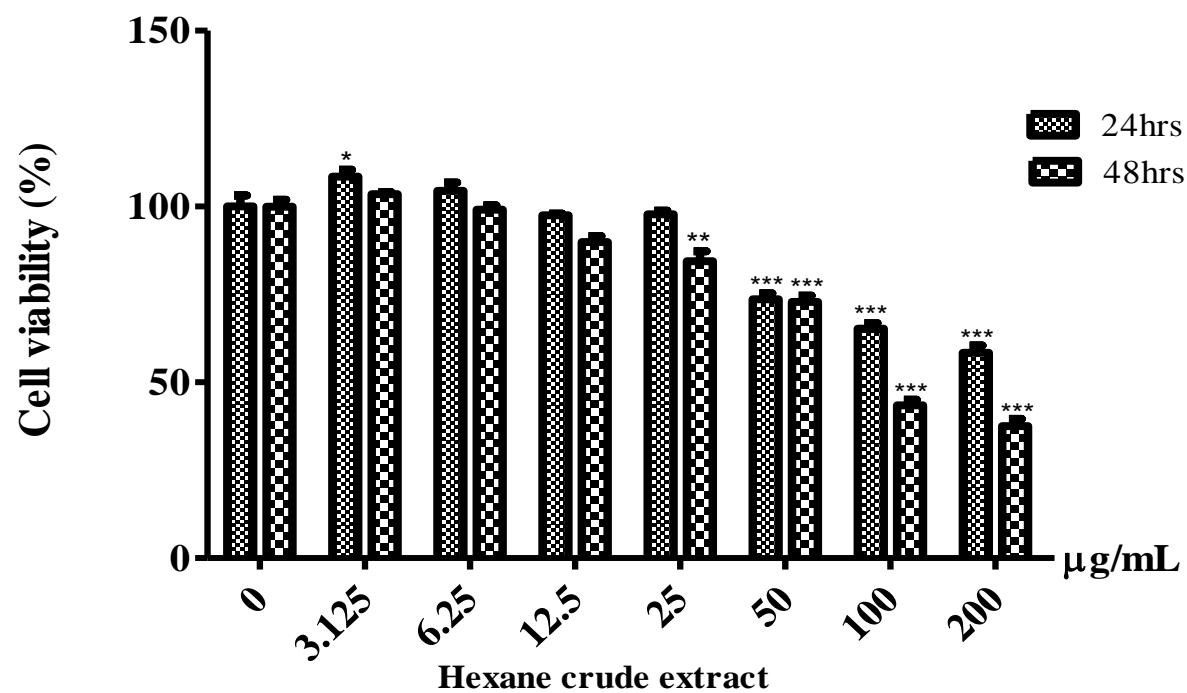


**Figure 24: Effect of hexane crude extract of curry leaf on HK-1 cell viability. Each bar represents the mean  $\pm$  standard deviation (S.D.) from 3 independent experiments (n=3). \*\*\* $P < 0.001$ , \*\* $P < 0.01$  and \* $P < 0.05$  indicate the statistical significant difference with respect to untreated control group.**

#### **3.4.1.8 Effect of methanol crude extract of temu kunci on HK-1 cell viability**

HK-1 cell line was treated with various concentrations of crude methanol extract of temu kunci from 3.13 µg/mL to 200 µg/mL at 24 and 48 hrs and cell viability was evaluated (**Figure 25**). Control group was not treated with the crude extract. At 24 hrs, the percentage of cell viability in each concentration was moderate, ranging from 53.63±1.24% to 106.3±3.93%. Treatment with 200 µg/mL of extract showed that about half of the cell growth was inhibited. At 48 hrs, there was more than 50% growth inhibition at concentrations 200 µg/mL with 38.21±1.79% cell viability. At 24 and 48 hrs, extract concentration of 200 µg/mL had significant ( $p<0.001$ ) decrease in viable cells when compared to untreated control group. Thus, it can be concluded that crude methanolic extract of temu kunci has moderate cytotoxic activity against HK-1 cell line.



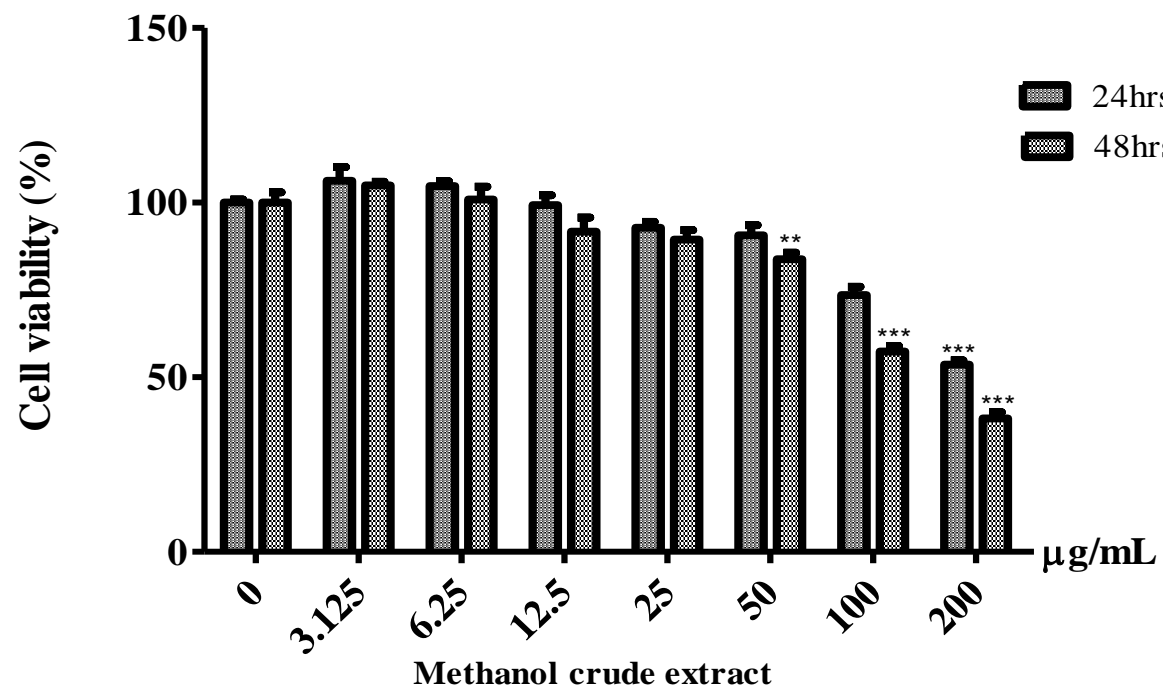


**Figure 25: Effect of methanol crude extract of temu kunci on HK-1 cell viability. Each bar represents the mean  $\pm$  standard deviation (S.D.) from 3 independent experiments (n=3). \*\*\* $P < 0.001$  and \*\* $P < 0.01$  indicate the statistical significant difference with respect to untreated control group.**

#### **3.4.1.9 Effect of ethyl acetate crude extract of temu kunci on HK-1 cell viability**

HK-1 cell line was treated with various concentrations of crude ethyl acetate extract of temu kunci from 3.13 µg/mL to 200 µg/mL at 24 and 48 hrs and cell viability was evaluated (**Figure 26**). Control group was not treated with the crude extract. At 24 hrs, the percentage of cell viability in each concentration was moderate, ranging from 53.63±1.24% to 95.55±2.20%. Treatment with 200 µg/mL of extract showed that slightly less than half of the cell growth was inhibited with 53.63±1.24% cell viability. At 48 hrs, about 50% growth inhibition was observed at concentrations 100 and 200 µg/mL with cell viability of 54.91±1.16% and 51.88±1.38% respectively. At 48 hrs, concentrations 25µg/ml and above had significant ( $p<0.001$ ) decrease in viable cells when compared to untreated control group. Thus, it can be concluded that crude ethyl acetate extract of temu kunci has low cytotoxic activity against HK-1 cell line.

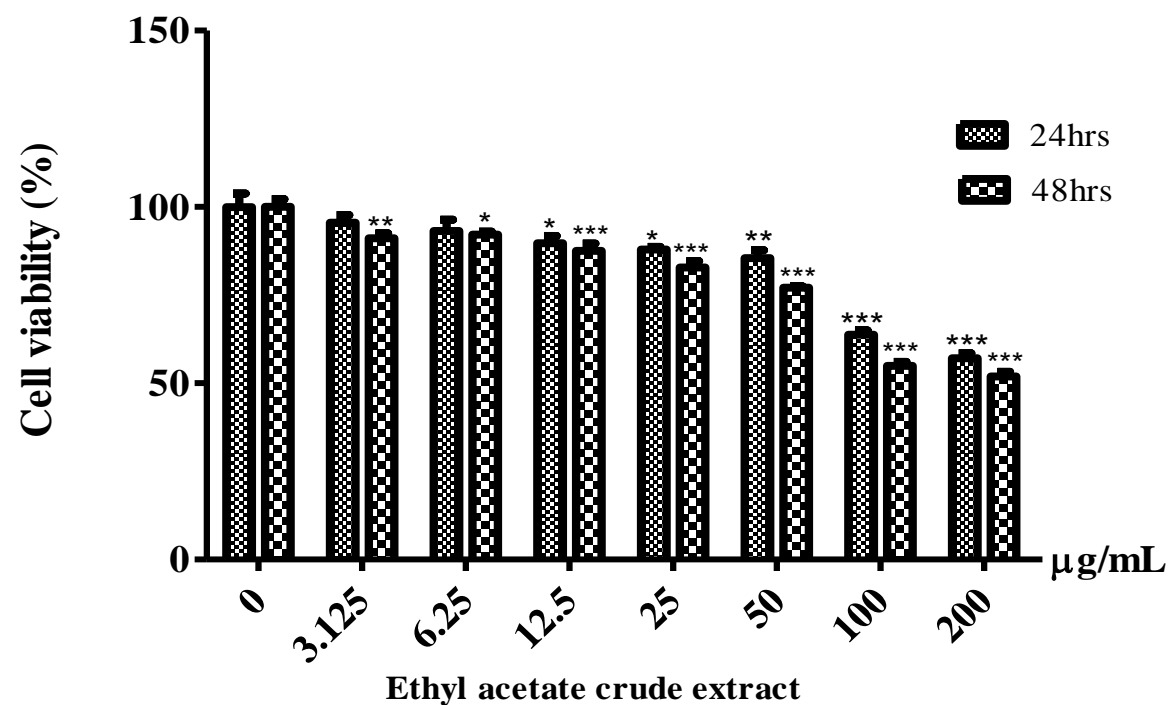


**Figure 26: Effect of ethyl acetate crude extract of temu kunci on HK-1 cell viability.** Each bar represents the mean  $\pm$  standard deviation (S.D.) from 3 independent experiments (n=3). \*\*\* $P < 0.001$ , \*\* $P < 0.01$  and \* $P < 0.05$  indicate the statistical significant difference with respect to untreated control group.

#### **3.4.1.10 Effect of hexane crude extract of temu kunci on HK-1 cell viability**

HK-1 cell line was treated with various concentrations of crude hexane extract of temu kunci from 3.13 µg/mL to 200 µg/mL at 24 and 48 hrs and cell viability was evaluated (**Figure 27**). Control group was not treated with the crude extract. At 24 hrs, the percentage of cell viability in each concentration was moderate, ranging from 59.42±1.21% to 100.9±1.76%. At 48 hrs, there was more than 50% growth inhibition at concentrations 50 and 100 µg/mL with 41.97±0.49% and 37.30±0.57% cell viability respectively. At 24 and 48 hrs, extract concentrations of 25 µg/mL and above had significant ( $p<0.001$ ) decrease in viable cells when compared to untreated control group. Thus, it can be concluded that crude hexane extract of temu kunci has high cytotoxic activity against HK-1 cell line.

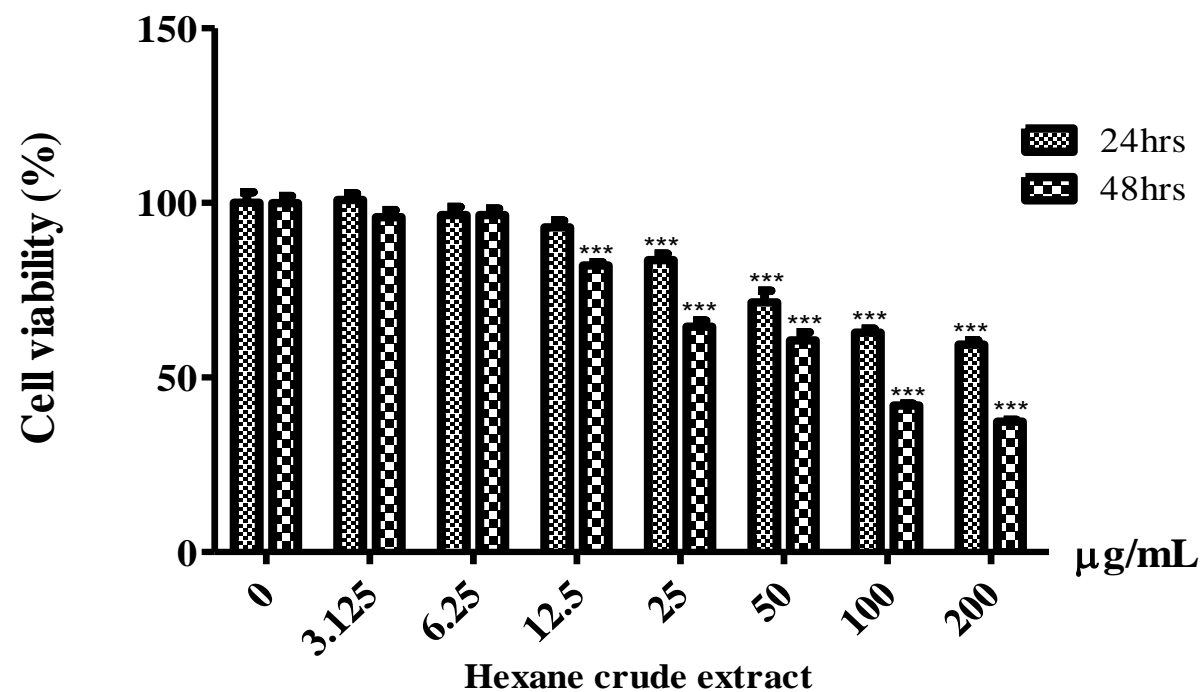


**Figure 27: Effect of hexane crude extract of temu kunci on HK-1 cell viability.** Each bar represents the mean  $\pm$  standard deviation (S.D.) from 3 independent experiments (n=3). \*\*\* $P < 0.001$  indicates the statistical significant difference with respect to untreated control group.

#### **3.4.1.11 Effect of methanol crude extract of spring onion leaf on HK-1 cell viability**

HK-1 cell line was treated with various concentrations of crude methanol extract of spring onion leaf from 3.13 µg/mL to 200 µg/mL at 24 and 48 hrs and cell viability was evaluated (**Figure 28**). Control group was not treated with the crude extract. At 24 hrs, the percentage of cell viability in each concentration was high, ranging from 85.46±1.70% to 106.0±2.07%. None of concentrations gave cell viability lower than 50%. At 48 hrs, none of the concentrations showed more than 50% cell inhibition with cell viability ranging from 79.60±2.14% to 104.7±1.77%. Extract concentration of 200 µg/mL had significant ( $p<0.001$ ) decrease in viable cells when compared to untreated control group. Thus, it can be concluded that crude methanolic extract of spring onion has low cytotoxic activity against HK-1 cell line.

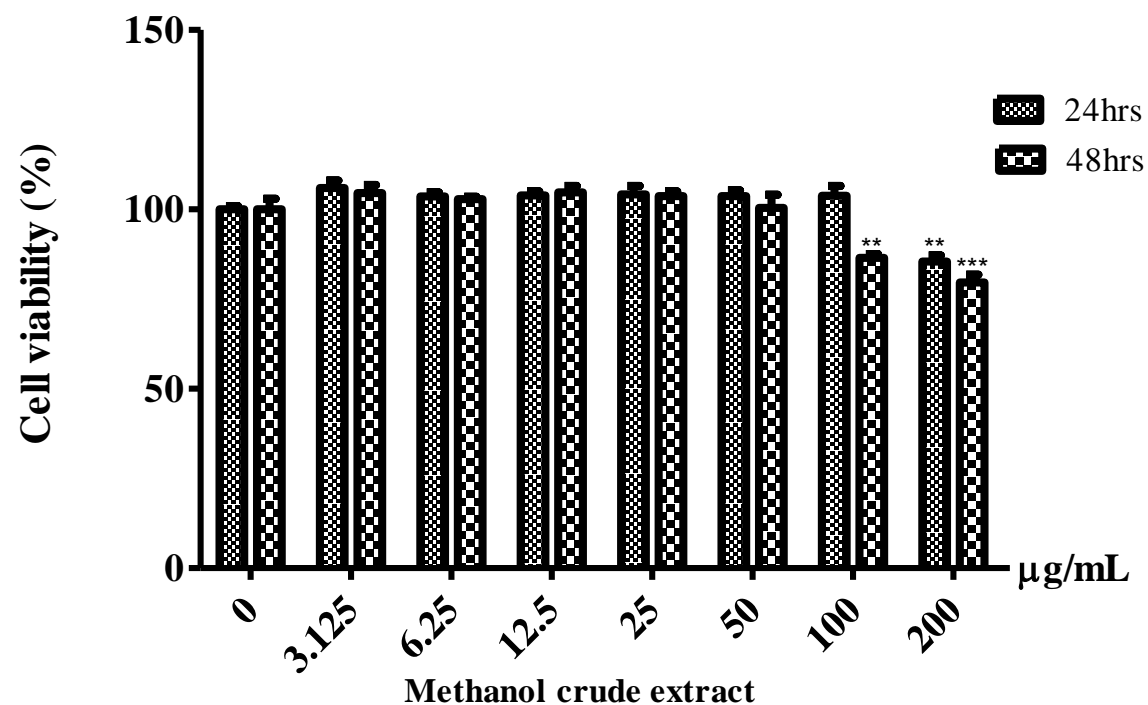


**Figure 28: Effect of methanol crude extract of spring onion on HK-1 cell viability. Each bar represents the mean  $\pm$  standard deviation (S.D.) from 3 independent experiments (n=3). \*\*\* $P < 0.001$  and \*\* $P < 0.01$  indicate the statistical significant difference with respect to untreated control group.**

#### **3.4.1.12 Effect of ethyl acetate crude extract of spring onion leaf on HK-1 cell viability**

HK-1 cell line was treated with various concentrations of crude ethyl acetate extract of spring onion from 3.13 µg/mL to 200 µg/mL at 24 and 48 hrs and cell viability was evaluated (**Figure 29**). Control group was not treated with the crude extract. At 24 hrs, the percentage of cell viability in each concentration was moderate, ranging from 67.03±3.19% to 108.30±0.55%. None of the concentrations gave cell viability lower than 50%. At 48 hrs, none of the concentrations showed more than 50% cell inhibition with cell viability ranging from 58.02±2.39% to 95.65±1.44%. At 24 and 48 hrs, extract concentrations of 50 µg/mL and above had significant ( $p<0.001$ ) decrease in viable cells when compared to untreated control group. Thus, it can be concluded that crude ethyl acetate extract of spring onion has low cytotoxic activity against HK-1 cell line.



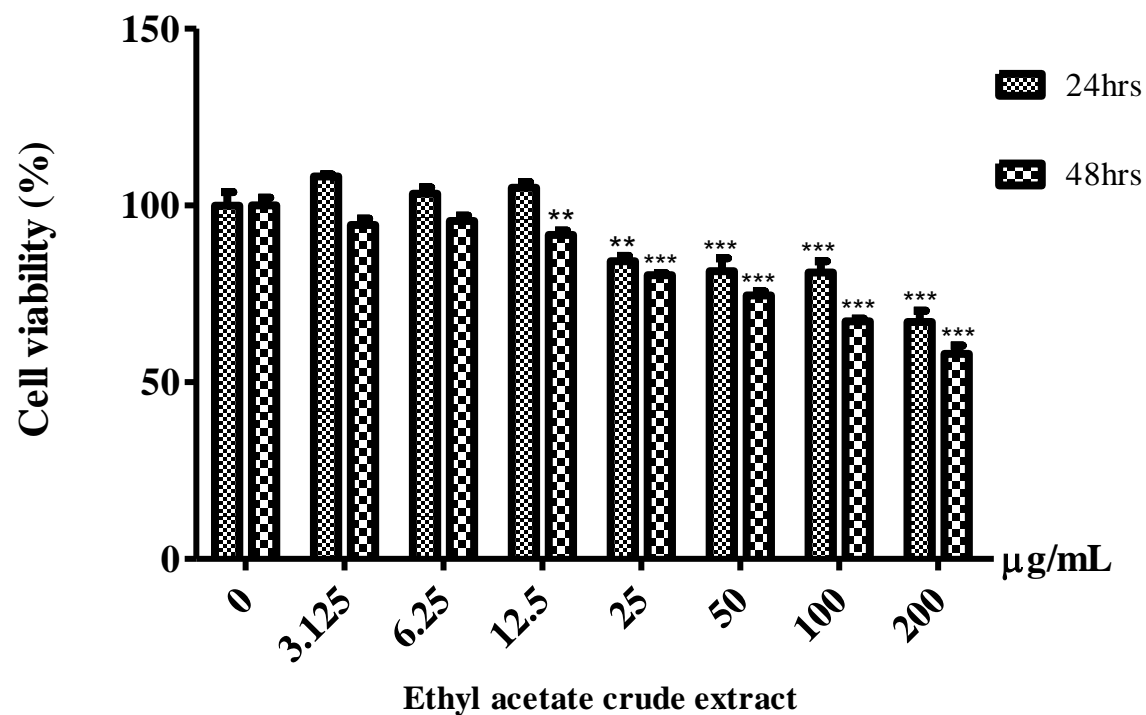


**Figure 29: Effect of ethyl acetate crude extract of spring onion on HK-1 cell viability.** Each bar represents the mean  $\pm$  standard deviation (S.D.) from 3 independent experiments (n=3). \*\*\* $P < 0.001$  and \*\* $P < 0.01$  indicate the statistical significant difference with respect to untreated control group.

#### **3.4.1.13      Effect of methanol crude extract of temu kunci on HK-1 cell viability**

HK-1 cell line was treated with various concentrations of crude hexane extract of spring onion leaf from 3.13 µg/mL to 200 µg/mL at 24 and 48 hrs and cell viability was evaluated (**Figure 30**). Control group was not treated with the crude extract. At 24 hrs, the percentage of cell viability in each concentration was high, ranging from 95.43±0.61% to 106.3±3.25%. None of the concentrations gave cell viability lower than 50%. At 48 hrs, none of the concentrations showed more than 50% cell inhibition with cell viability ranging from 78.94±1.19% to 93.37±3.02%. Extract concentration of 200 µg/mL had significant ( $p<0.001$ ) decrease in viable cells when compared to untreated control group. Thus, it can be concluded that crude hexane extract of spring onion has low cytotoxic activity against HK-1 cell line.

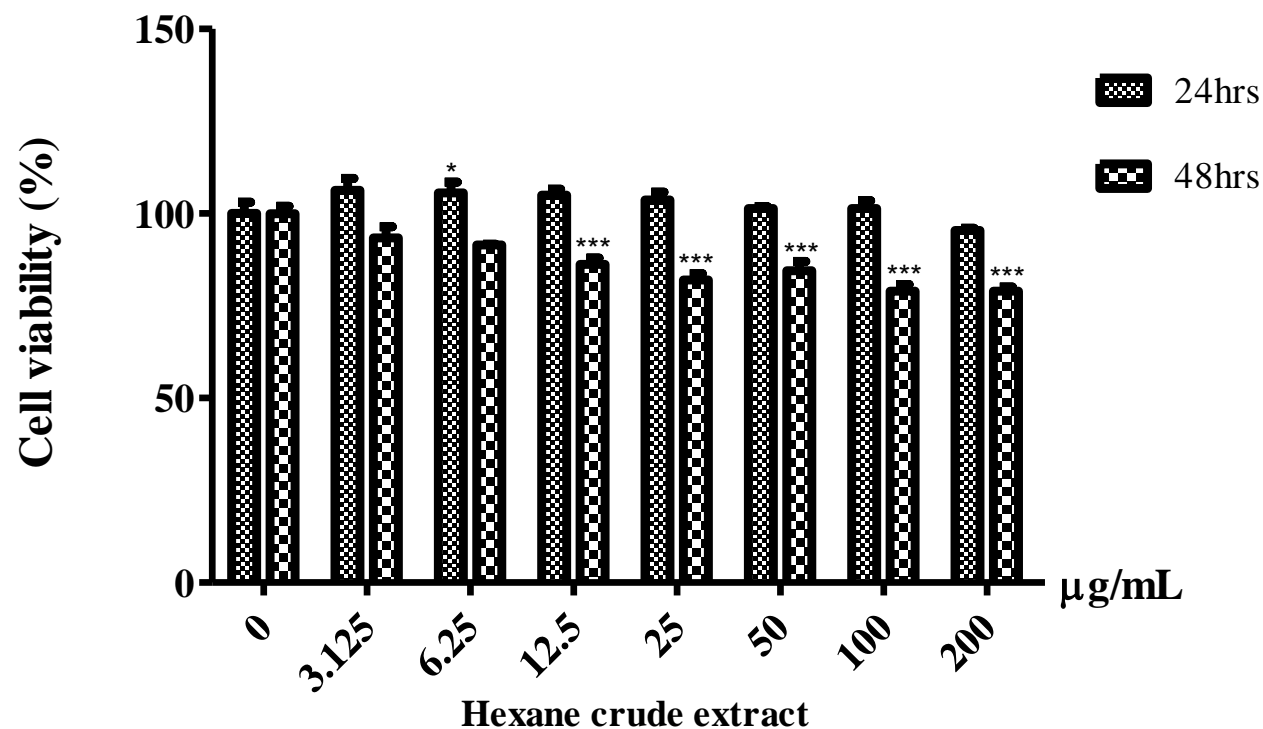


**Figure 30: Effect of hexane crude extract of spring onion on HK-1 cell viability.** Each bar represents the mean  $\pm$  standard deviation (S.D.) from 3 independent experiments (n=3). \*\*\* $P < 0.001$  and \* $P < 0.05$  indicate the statistical significant difference with respect to untreated control group.

#### **3.4.1.14 Effect of methanol crude extract of mushroom bean on HK-1 cell viability**

HK-1 cell line was treated with various concentrations of crude methanolic extract of mushroom bean from 3.13 µg/mL to 200 µg/mL at 24 and 48 hrs and cell viability was evaluated (**Figure 31**). Control group was not treated with the crude extract. At 24 hrs, the percentage of cell viability in each concentration was high, ranging from 101.9±0.39% to 104.9±1.83%. None of the concentrations gave cell viability lower than 50%. At 48 hrs, none of the concentrations showed more than 50% cell inhibition with cell viability ranging from 73.81±1.26% to 100.6±1.88%. For 48 hrs treatment, extract concentrations of 25 µg/mL and above had significant ( $p<0.001$ ) decrease in viable cells when compared to untreated control group. Thus, it can be concluded that crude methanolic extract of mushroom bean has low cytotoxic activity against HK-1 cell line.

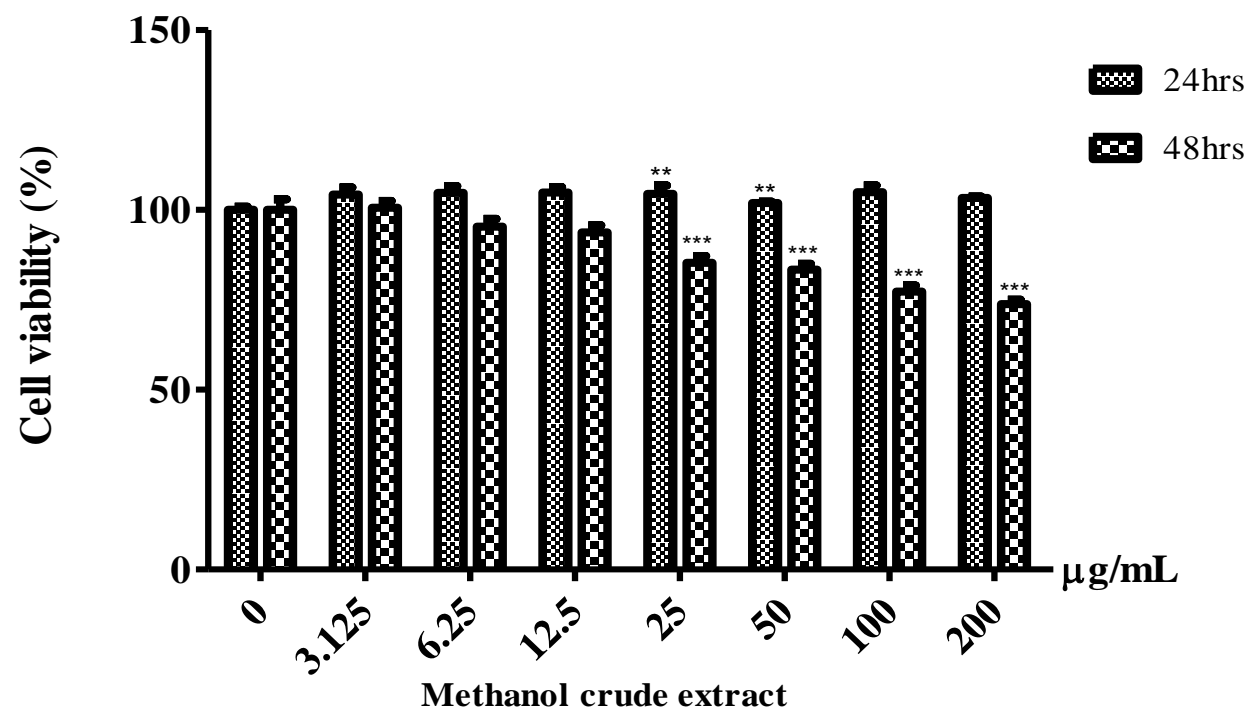


**Figure 31: Effect of methanol crude extract of mushroom bean on HK-1 cell viability. Each bar represents the mean  $\pm$  standard deviation (S.D.) from 3 independent experiments (n=3). \*\*\* $P < 0.001$  and \*\* $P < 0.01$  indicate the statistical significant difference with respect to untreated control group.**

### **3.4.1.15      Effect of ethyl acetate crude extract of mushroom bean on HK-1 cell viability**

HK-1 cell line was treated with various concentrations of crude ethyl acetate extract of mushroom bean from 3.13 µg/mL to 200 µg/mL at 24 and 48 hrs and cell viability was evaluated (**Figure 32**). Control group was not treated with the crude extract. At 24 hrs, the percentage of cell viability in each concentration was moderate, ranging from 77.69±0.02% to 93.49±1.58%. None of the concentrations gave cell viability lower than 50%. At 48 hrs, none of the concentrations showed more than 50% cell inhibition except at 200 µg/mL almost half of the cell growth was inhibited with cell viability of 52.98±1.29%. At 24 and 48 hrs, extract concentrations of 12.5 µg/ml and above had significant ( $p<0.001$ ) decrease in viable cells when compared to untreated control group. Thus, it can be concluded that crude ethyl acetate extract of mushroom bean has low cytotoxic activity against HK-1 cell line.

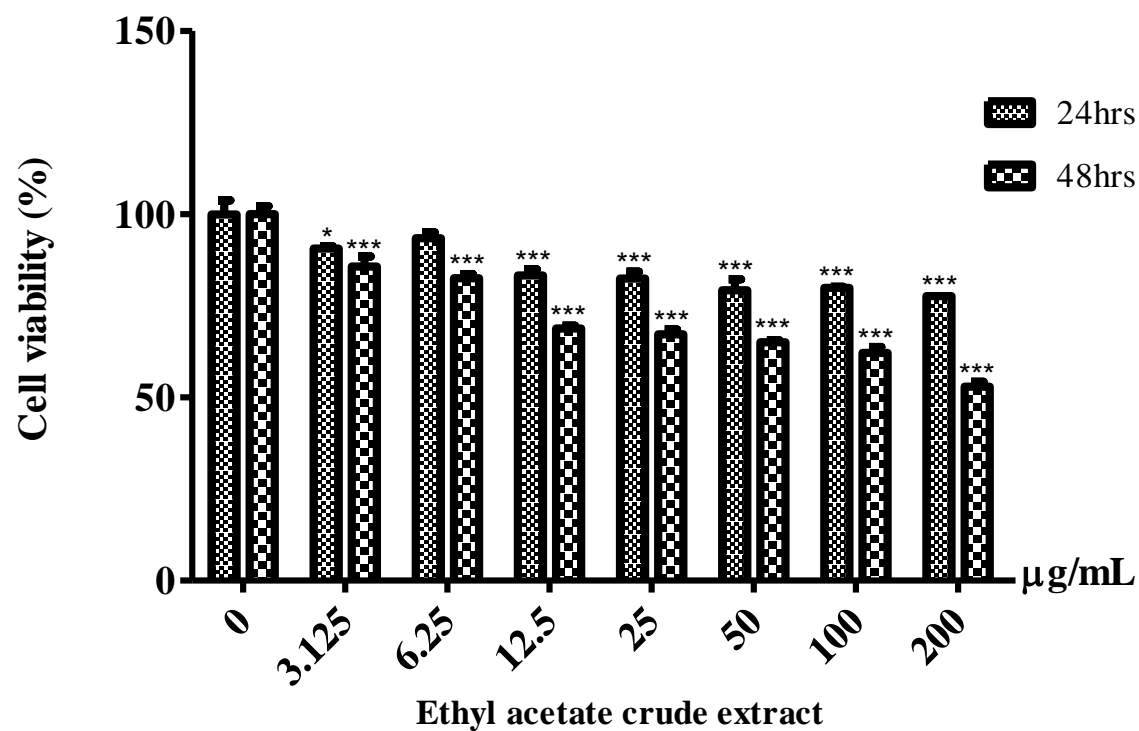


**Figure 32: Effect of ethyl acetate crude extract of mushroom bean on HK-1 cell viability. Each bar represents the mean  $\pm$  standard deviation (S.D.) from 3 independent experiments (n=3). \*\*\* $P < 0.001$  and \* $P < 0.05$  indicate the statistical significant difference with respect to untreated control group.**

#### **3.4.1.16      Effect of hexane crude extract of mushroom bean on HK-1 cell viability**

HK-1 cell line was treated with various concentrations of crude hexane extract of mushroom bean from 3.13 µg/mL to 200 µg/mL at 24 and 48 hrs and cell viability was evaluated (**Figure 33**). Control group was not treated with the crude extract. At 24 hrs, the percentage of cell viability in each concentration was moderate, ranging from 83.66±0.21% to 108.5±2.63%. None of the concentrations gave cell viability lower than 50%. At 48 hrs, none of the concentrations showed more than 50% cell inhibition with cell viability ranging from 59.51±1.69% to 87.34±2.47%. At 48 hrs, extract concentrations of 6.25 µg/mL and above had significant ( $p<0.001$ ) decrease in viable cells when compared to untreated control group. Thus, it can be concluded that crude hexane extract of mushroom bean has low cytotoxic activity against HK-1 cell line.



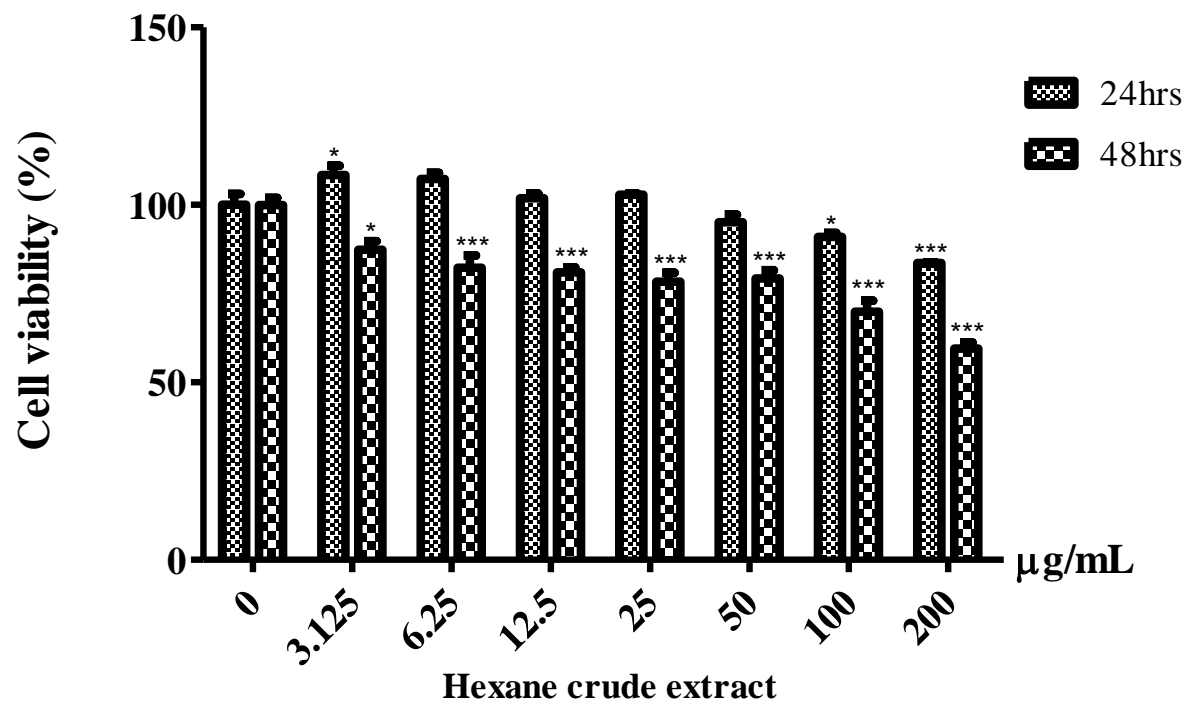


**Figure 33: Effect of hexane crude extract of mushroom bean on HK-1 cell viability.** Each bar represents the mean  $\pm$  standard deviation (S.D.) from 3 independent experiments (n=3). \*\*\* $P < 0.001$  and \* $P < 0.05$  indicate the statistical significant difference with respect to untreated control group.

#### **3.4.1.17      Effect of 5-fluorouracil on HK-1 cell viability**

HK-1 cell line was treated with various concentrations of 5-fluorouracil from 3.13 µg/mL to 200 µg/mL and cell viability was evaluated (**Figure 34**). Control group was not treated with 5-fluorouracil. At 24 hrs, the percentage of cell viability in each concentration showed a constant decrease, ranging from 41.47±1.87% to 67.24±2.86%. After 48 hrs, more than half of the cancer cells were inhibited by 5-fluorouracil at concentrations 12.5 µg/mL and more with cell viability ranging from 32.99±2.40% to 67.88±0.54%. The increase of 5-fluorouracil concentrations against HK-1 cell line had significantly ( $p<0.001$ ) decreased the cell viability when compared to untreated control group. It can be concluded chemopreventive drug 5-fluorouracil has high cytotoxic activity against HK-1 cell line.

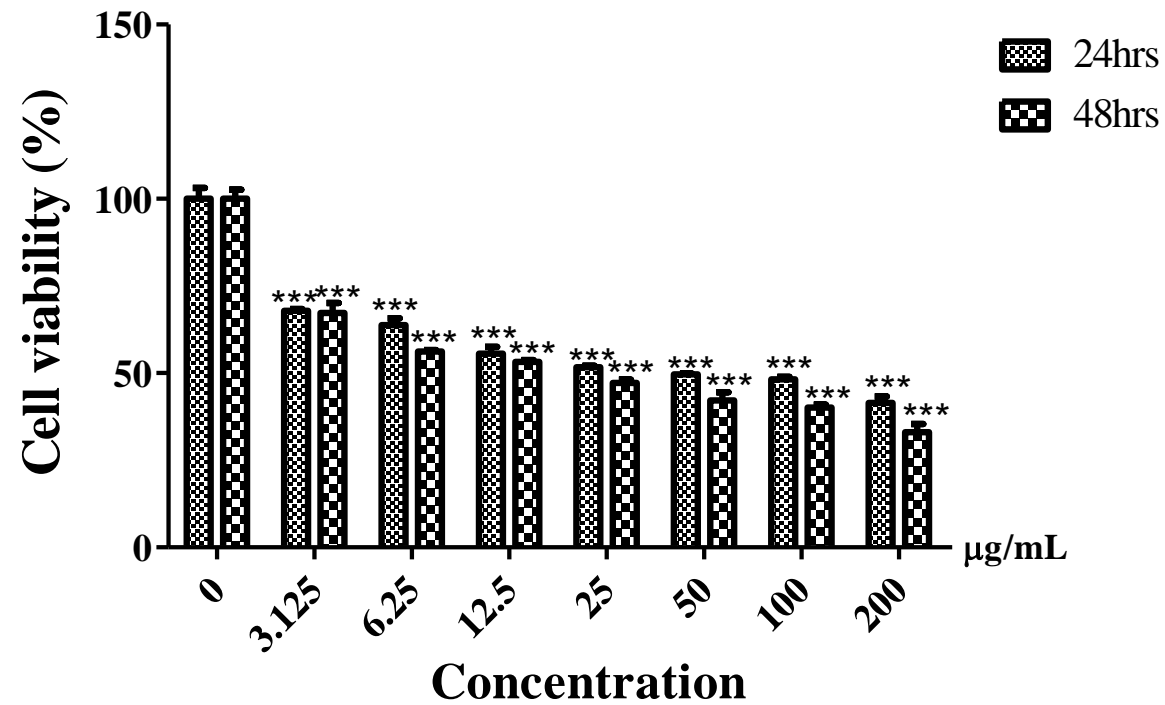


**Figure 34: Effect of 5-fluorouracil on HK-1 cell viability. Each bar represents the mean  $\pm$  standard deviation (S.D.) from 3 independent experiments (n=3). \*\*\* $P < 0.001$  indicates the statistical significant difference with respect to untreated control group.**

### **3.4.2 Effect of various crude extracts on NP-69 cell viability**

#### **3.4.2.1 Effect of methanol crude extract of bunga kantan on NP-69 cell viability**

NP-69 cell line was treated with various concentrations of crude methanol extract of bunga kantan from 3.13 µg/mL to 200 µg/mL at 24 and 48 hrs and the cell viability was evaluated (**Figure 35**). Control group was not treated with the crude extract. At 24 hrs, the percentage of cell viability in each concentration was moderate, ranging from 59.66±0.44% to 102.2±1.36%. None of the concentrations gave cell viability lower than 50%. At 48 hrs, none of the concentrations showed more than 50% cell inhibition with cell viability ranging from 65.53±1.96% to 90.48±2.10%. Extract concentrations of more than 50 µg/mL had significant ( $p<0.001$ ) decrease in viable cells when compared to untreated control group. Thus, it can be concluded that crude methanolic extract of bunga kantan has low cytotoxic activity against NP-69 cell line.

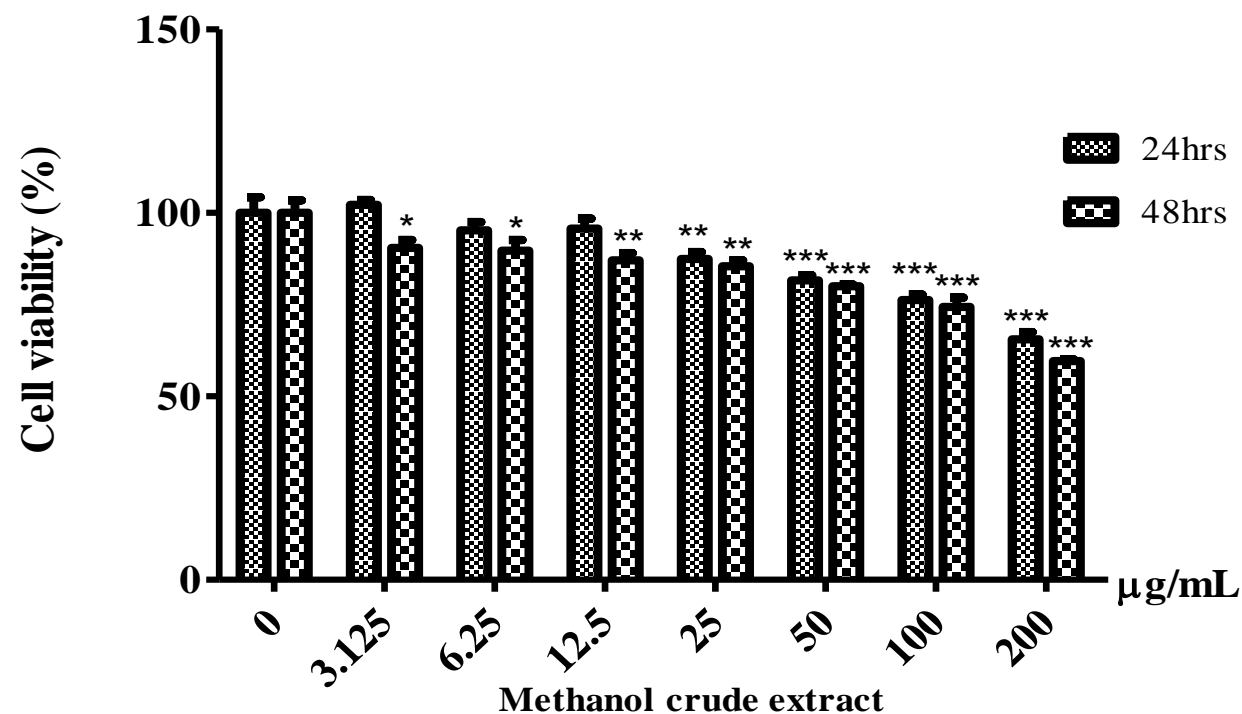


**Figure 35: Effect of methanol crude extract of bunga kantan on NP-69 cell viability.** Each bar represents the mean  $\pm$  standard deviation (S.D.) from 3 independent experiments (n=3). \*\*\* $P < 0.001$ , \*\* $P < 0.01$  and \* $P < 0.05$  indicate the statistical significant difference with respect to untreated control group.

### 3.4.2.2 Effect of ethyl acetate crude extract of bunga kantan on NP-69 cell viability

NP-69 cell line was treated with various concentrations of crude ethyl acetate extract of bunga kantan from 3.13 µg/mL to 200 µg/mL at 24 and 48 hrs and the cell viability was evaluated (**Figure 36**). Control group was not treated with the crude extract. At 24 hrs, the percentage of cell viability in each concentration was moderate, ranging from 59.98±1.19 % to 93.83±1.75%. None of the concentrations gave cell viability lower than 50%. At 48 hrs, none of the concentrations showed more than 50% cell inhibition with cell viability ranging from 55.12±1.48% to 94.92±2.51%. Extract concentrations of more than 50 µg/mL had significant ( $p<0.001$ ) decrease in viable cells when compared to untreated control group. Thus, it can be concluded that crude ethyl acetate extract of bunga kantan has low cytotoxic activity against NP-69 cell line.

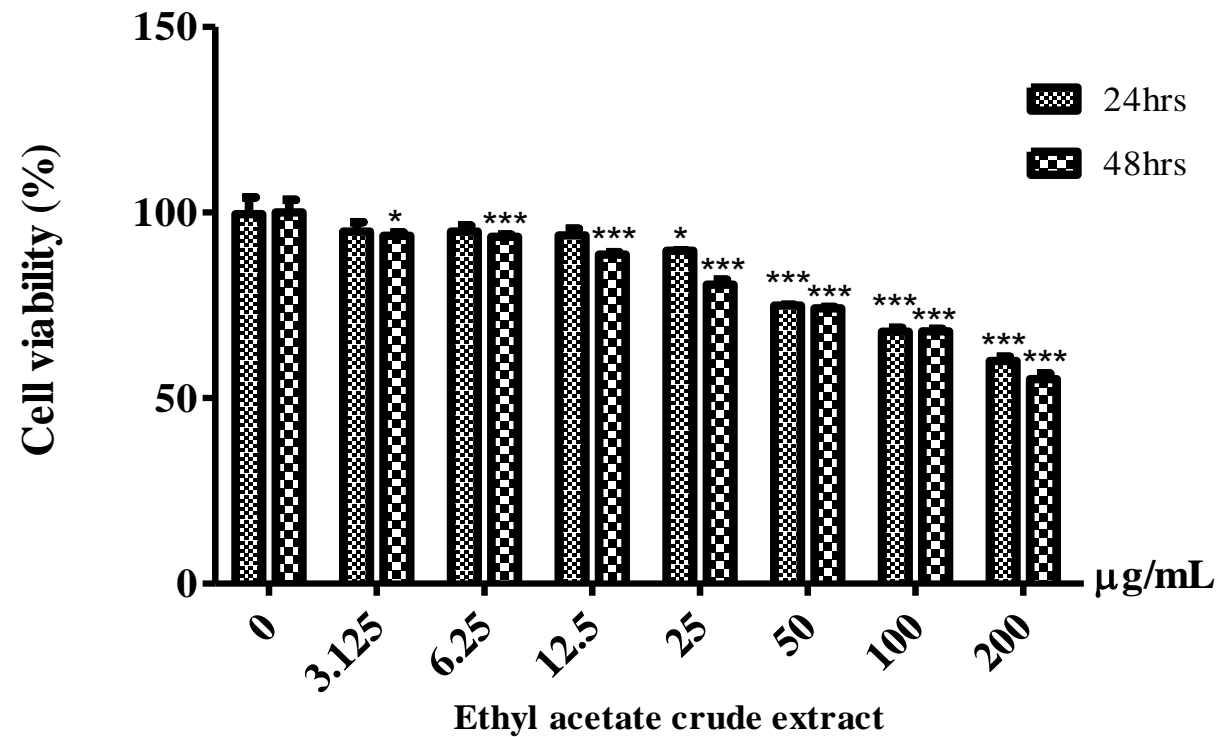


**Figure 36: Effect of ethyl acetate crude extract of bunga kantan on NP-69 cell viability. Each bar represents the mean  $\pm$  standard deviation (S.D.) from 3 independent experiments (n=3). \*\*\* $P < 0.001$  and \* $P < 0.05$  indicate the statistical significant difference with respect to untreated control group.**

### 3.4.2.3 Effect of hexane crude extract of bunga kantan on NP-69 cell viability

NP-69 cell line was treated with various concentrations of crude hexane extract of bunga kantan from 3.13  $\mu\text{g/mL}$  to 200  $\mu\text{g/mL}$  at 24 and 48 hrs and the cell viability was evaluated (**Figure 37**). Control group was not treated with the crude extract. At 24 hrs, the percentage of cell viability in each concentration was moderate, ranging from  $59.26 \pm 0.97\%$  to  $96.73 \pm 2.53\%$ . None of the concentrations gave cell viability lower than 50%. At 48 hrs, none of the concentrations showed more than 50% cell inhibition with cell viability ranging from  $52.48 \pm 0.70\%$  to  $93.37 \pm 1.83\%$ . Extract concentrations of more than 25  $\mu\text{g/mL}$  had significant ( $p < 0.001$ ) decrease in viable cells when compared to untreated control group. Thus, it can be concluded that crude hexane extract of bunga kantan has low cytotoxic activity against NP-69 cell line.



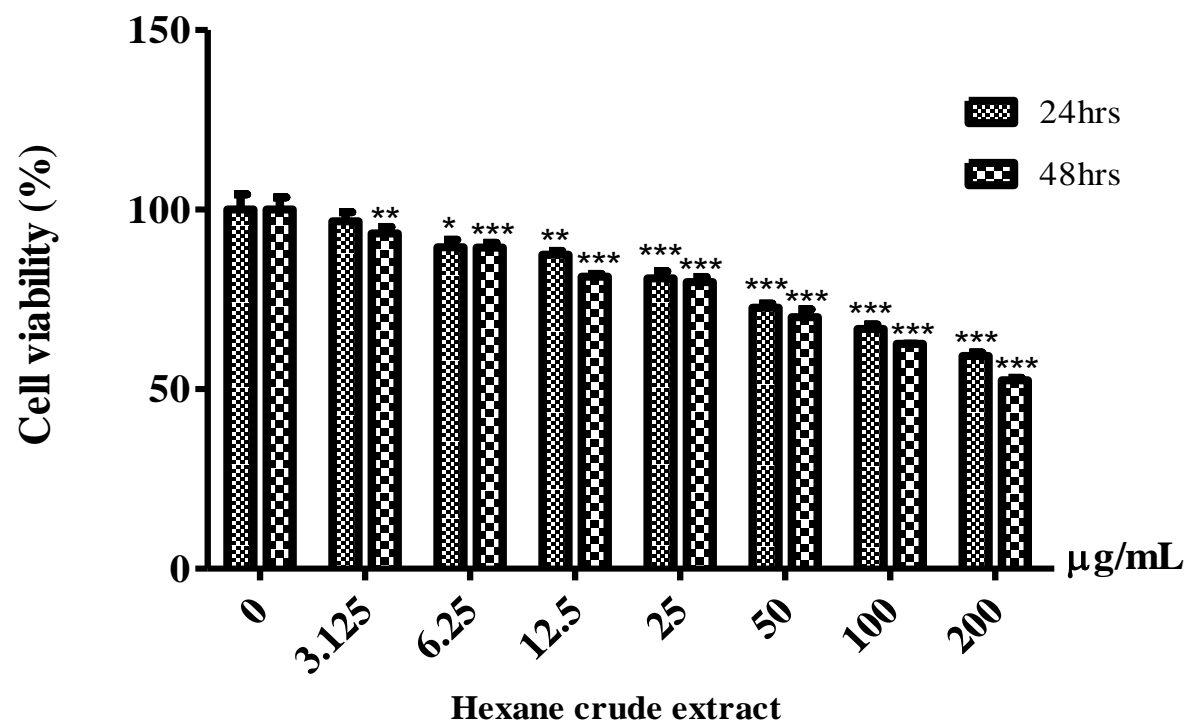


**Figure 37: Effect of hexane crude extract of bunga kantan on NP-69 cell viability.** Each bar represents the mean  $\pm$  standard deviation (S.D.) from 3 independent experiments (n=3). \*\*\* $P < 0.001$ , \*\* $P < 0.01$  and \* $P < 0.05$  indicate the statistical significant difference with respect to untreated control group.

#### **3.4.2.4 Effect of methanol solid 1 crude extract of bunga kantan on NP-69 cell viability**

NP-69 cell line was treated with various concentrations of crude methanolic solid 1 extract of bunga kantan from 3.13 µg/mL to 200 µg/mL at 24 and 48 hrs and the cell viability was evaluated (**Figure 38**). Control group was not treated with the crude extract. At 24 hrs, the percentage of cell viability in each concentration was moderate, ranging from 61.93±0.22% to 96.23±3.45%. None of the concentrations gave cell viability lower than 50%. At 48 hrs, none of the concentrations showed more than 50% cell inhibition with cell viability ranging from 55.62±1.91% to 88.89±1.99%. Extract concentrations of more than 6.25 µg/mL had significant ( $p<0.001$ ) decrease in viable cells when compared to untreated control group. Thus, it can be concluded that crude methanolic solid 1 extract of bunga kantan has low cytotoxic activity against NP-69 cell line.

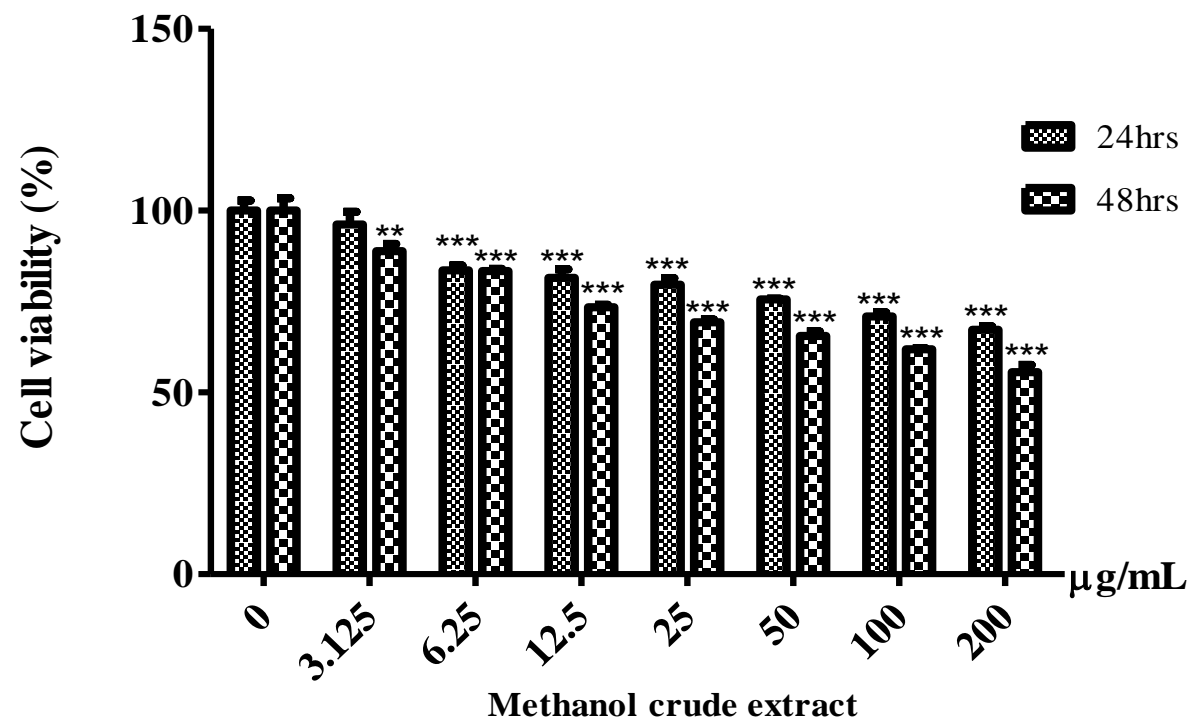


**Figure 38: Effect of methanol solid 1 crude extract of bunga kantan on NP-69 cell viability. Each bar represents the mean  $\pm$  standard deviation (S.D.) from 3 independent experiments (n=3). \*\*\* $P < 0.001$  and \*\* $P < 0.01$  indicate the statistical significant difference with respect to untreated control group.**

#### **3.4.2.5 Effect of methanol crude extract of curry leaf on NP-69 cell viability**

NP-69 cell line was treated with various concentrations of crude methanolic extract of curry leaf from 3.13 µg/mL to 200 µg/mL at 24 and 48 hrs and the cell viability was evaluated (**Figure 39**). Control group was not treated with the crude extract. At 24 hrs, the percentage of cell viability in each concentration was moderate, ranging from 75.90±1.27% to 109.2±1.49%. None of the concentrations gave cell viability lower than 50%. At 48 hrs, none of the concentrations showed more than 50% cell inhibition with cell viability ranging from 55.90±0.80% to 104.7±1.25%. At 24 hrs, extract concentrations of 25 µg/mL and more had significant ( $p<0.001$ ) decrease in viable cells when compared to untreated control group. Thus, it can be concluded that crude methanolic extract of curry leaf has low cytotoxic activity against NP-69 cell line.

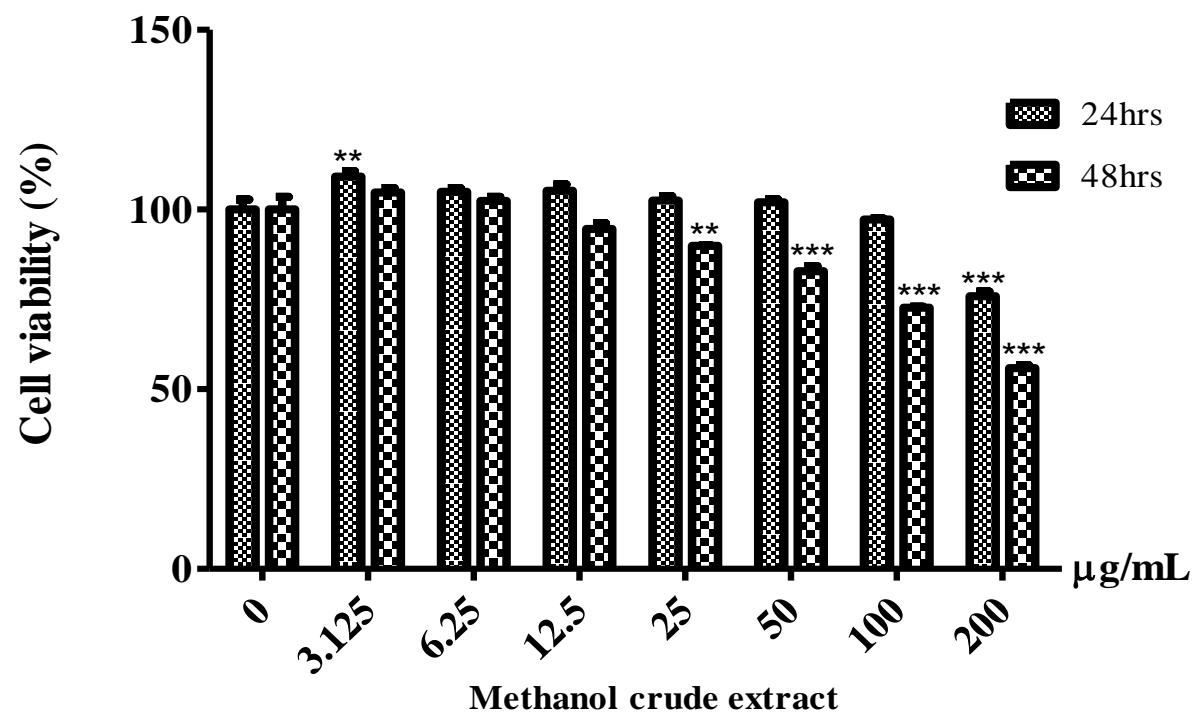


**Figure 39: Effect of methanol crude extract of curry leaf on NP-69 cell viability. Each bar represents the mean  $\pm$  standard deviation (S.D.) from 3 independent experiments (n=3). \*\*\* $P < 0.001$  and \*\* $P < 0.01$  indicate the statistical significant difference with respect to untreated control group.**

#### **3.4.2.6 Effect of ethyl acetate crude extract of curry leaf on NP-69 cell viability**

NP-69 cell line was treated with various concentrations of crude ethyl acetate extract of curry leaf from 3.13  $\mu\text{g/mL}$  to 200  $\mu\text{g/mL}$  at 24 and 48 hrs and the cell viability was evaluated (**Figure 40**). Control group was not treated with the crude extract. At 24 hrs, the percentage of cell viability in each concentration was moderate, ranging from  $72.44 \pm 0.59\%$  to  $104.8 \pm 1.49\%$ . None of the concentrations gave cell viability lower than 50%. At 48 hrs, none of the concentrations showed more than 50% cell inhibition with cell viability ranging from  $51.46 \pm 0.53\%$  to  $104.5 \pm 1.20\%$ . Extract concentrations of 25  $\mu\text{g/mL}$  and more had significant ( $p < 0.001$ ) decrease in viable cells when compared to untreated control group. Thus, it can be concluded that crude ethyl acetate extract of curry leaf has low cytotoxic activity against NP-69 cell line.

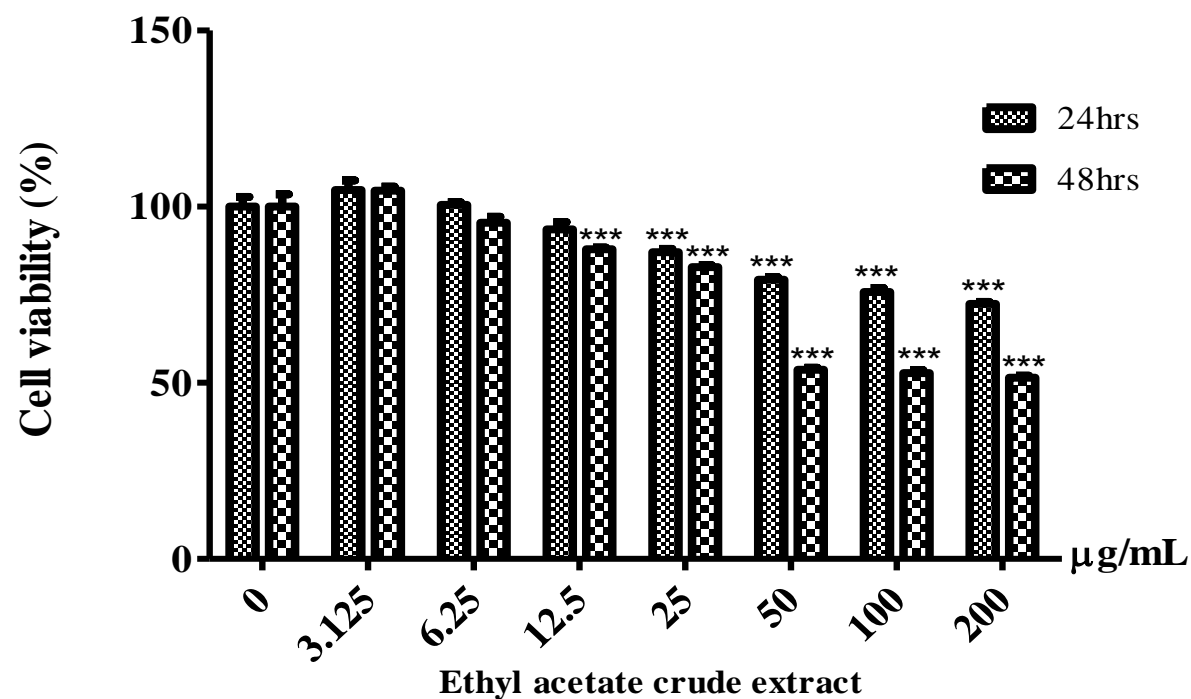


**Figure 40: Effect of ethyl acetate crude extract of curry leaf on NP-69 cell viability. Each bar represents the mean  $\pm$  standard deviation (S.D.) from 3 independent experiments (n=3). \*\*\* $P < 0.001$  indicates the statistical significant difference with respect to untreated control group.**

#### **3.4.2.7 Effect of hexane crude extract of curry leaf on NP-69 cell viability**

NP-69 cell line was treated with various concentrations of crude hexane extract of curry leaf from 3.13 µg/mL to 200 µg/mL at 24 and 48 hrs and the cell viability was evaluated (**Figure 41**). Control group was not treated with the crude extract. At 24 hrs, the percentage of cell viability in each concentration was moderate, ranging from 63.76±1.82% to 107.3±0.50%. None of the concentrations gave cell viability lower than 50%. At 48 hrs, none of the concentrations showed more than 50% cell inhibition with cell viability ranging from 63.76±1.82% to 101.1±0.52%. Extract concentrations of 100 and 200 µg/mL had significant ( $p<0.001$ ) decrease in viable cells when compared to untreated control group. Thus, it can be concluded that crude hexane extract of curry leaf has low cytotoxic activity against NP-69 cell line.



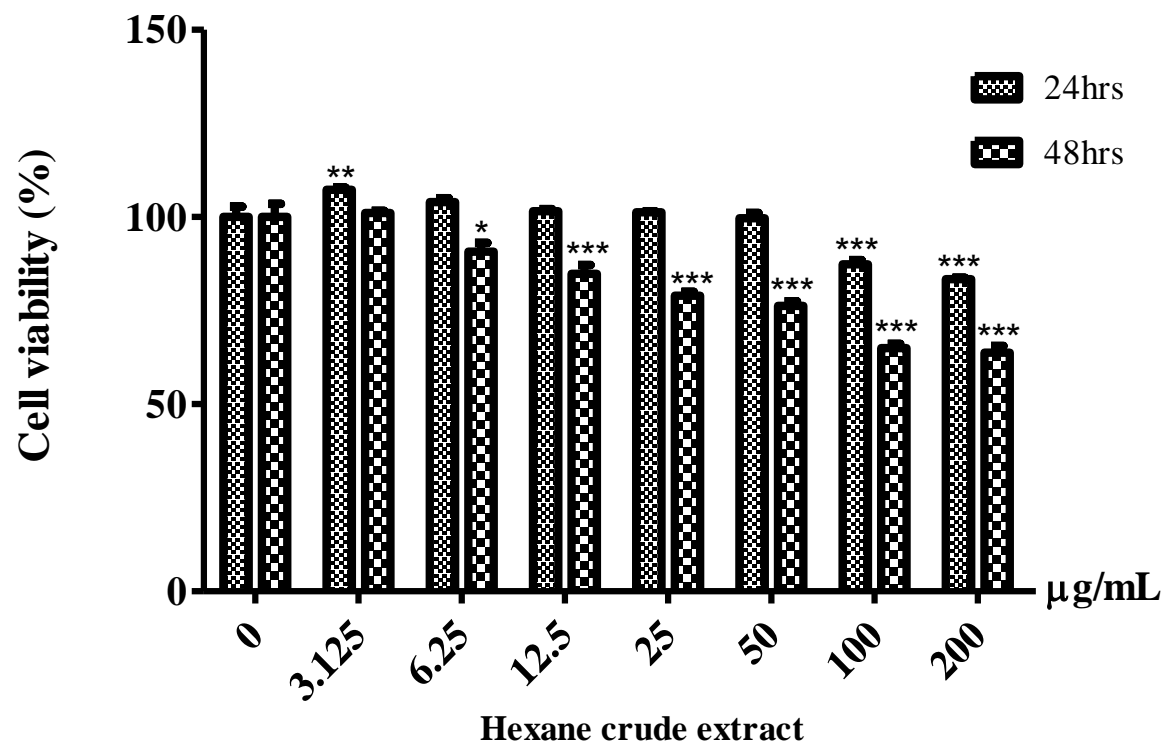


**Figure 41: Effect of hexane crude extract of curry leaf on NP-69 cell viability.** Each bar represents the mean  $\pm$  standard deviation (S.D.) from 3 independent experiments (n=3). \*\*\* $P < 0.001$  \*\* $P < 0.01$  and \* $P < 0.05$  indicate the statistical significant difference with respect to untreated control group.

#### **3.4.2.8 Effect of methanol crude extract of temu kunci on NP-69 cell viability**

NP-69 cell line was treated with various concentrations of crude methanolic extract of temu kunci from 3.13 µg/mL to 200 µg/mL at 24 and 48 hrs and the cell viability was evaluated (**Figure 42**). Control group was not treated with the crude extract. At 24 hrs, the percentage of cell viability in each concentration was moderate, ranging from 64.83±1.43% to 110.8±0.28%. None of the concentrations gave cell viability lower than 50%. At 48 hrs, none of the concentrations showed more than 50% cell inhibition with cell viability ranging from 61.37±2.16% to 100.7±1.04%. Extract concentrations of 25 µg/mL and more had significant ( $p<0.001$ ) decrease in viable cells when compared to untreated control group. Thus, it can be concluded that crude methanolic extract of curry leaf has low cytotoxic activity against NP-69 cell line.

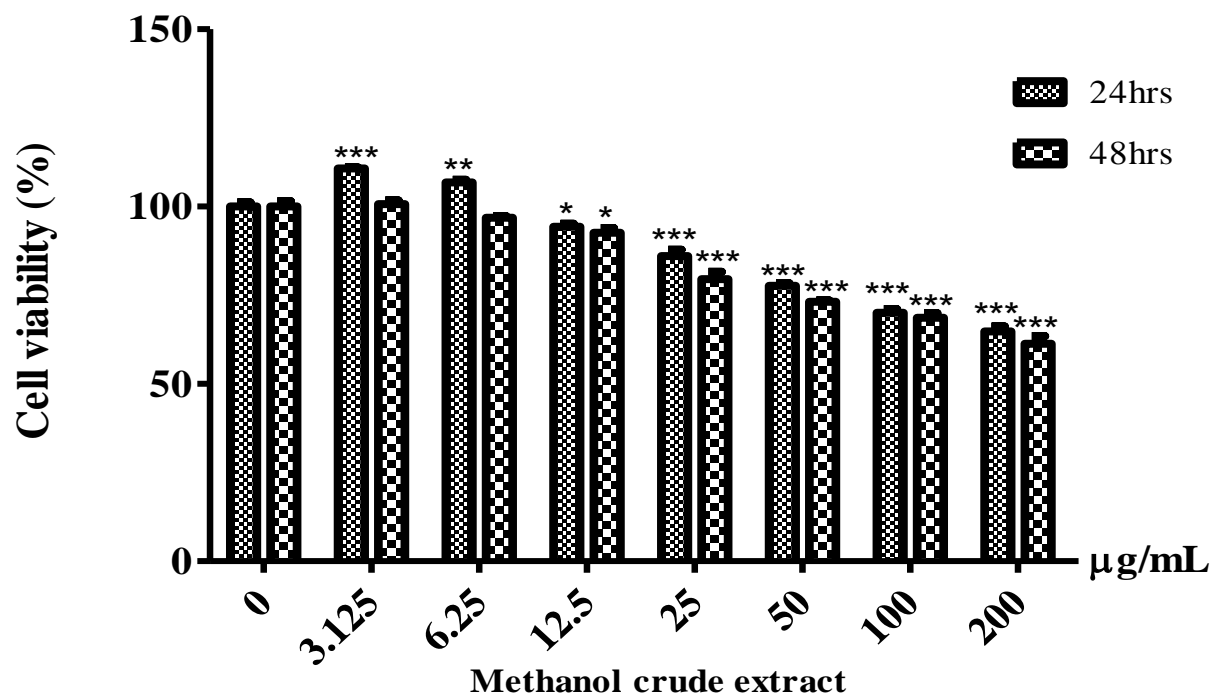


**Figure 42: Effect of methanol crude extract of temu kunci on NP-69 cell viability. Each bar represents the mean  $\pm$  standard deviation (S.D.) from 3 independent experiments (n=3). \*\*\* $P < 0.001$ , \*\* $P < 0.01$  and \* $P < 0.05$  indicate the statistical significant difference with respect to untreated control group.**

#### **3.4.2.9 Effect of ethyl acetate crude extract of temu kunci on NP-69 cell viability**

NP-69 cell line was treated with various concentrations of crude ethyl acetate extract of temu kunci from 3.13 µg/mL to 200 µg/mL at 24 and 48 hrs and the cell viability was evaluated (**Figure 43**). Control group was not treated with the crude extract. At 24 hrs, the percentage of cell viability in each concentration was moderate, ranging from 70.40±1.25% to 108.6±1.72%. None of the concentrations gave cell viability lower than 50%. At 48 hrs, none of the concentrations showed more than 50% cell inhibition with cell viability ranging from 65.44±0.80% to 103.5±1.77%. Extract concentrations of 25 µg/mL and more had significant ( $p<0.001$ ) decrease in viable cells when compared to untreated control group. Thus, it can be concluded that crude ethyl acetate extract of curry leaf has low cytotoxic activity against NP-69 cell line.

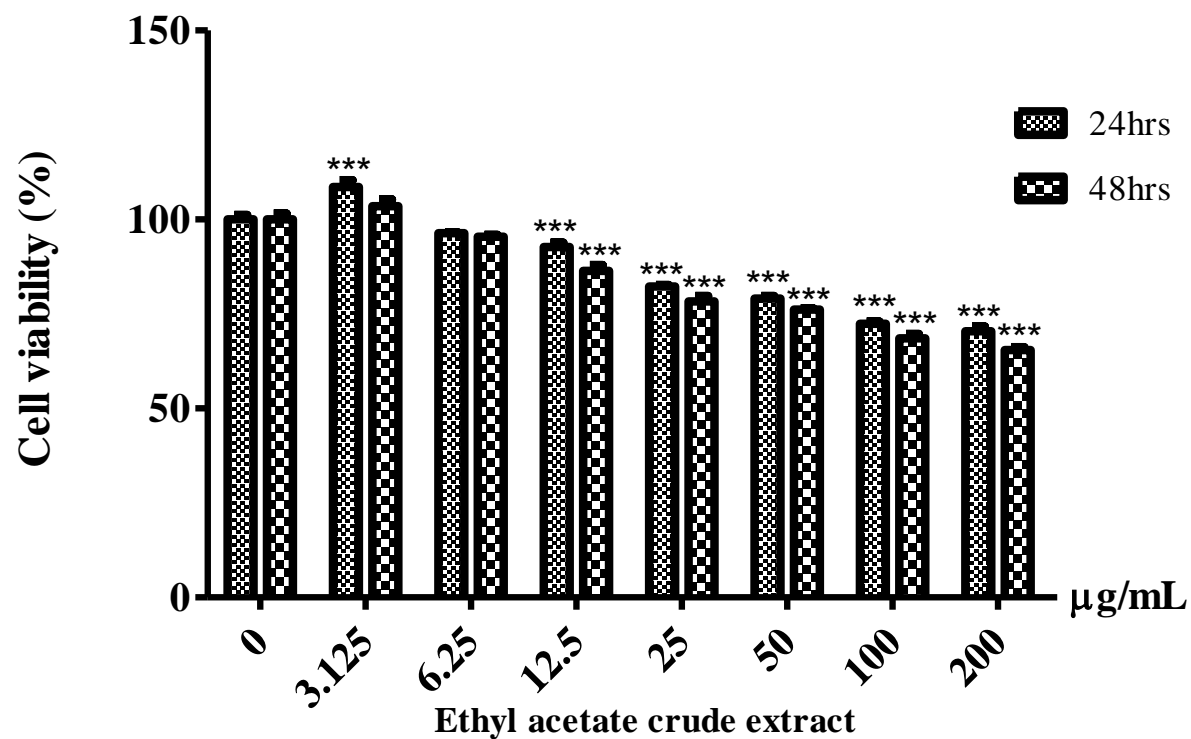


**Figure 43: Effect of ethyl acetate crude extract of temu kunci on NP-69 cell viability. Each bar represents the mean  $\pm$  standard deviation (S.D.) from 3 independent experiments (n=3). \*\*\* $P < 0.001$  indicates the statistical significant difference with respect to untreated control group.**

#### **3.4.2.10 Effect of hexane crude extract of temu kunci on NP-69 cell viability**

NP-69 cell line was treated with various concentrations of crude hexane extract of temu kunci from 3.13  $\mu\text{g/mL}$  to 200  $\mu\text{g/mL}$  at 24 and 48 hrs and the cell viability was evaluated (**Figure 44**). Control group was not treated with the crude extract. At 24 hrs, the percentage of cell viability in each concentration was moderate, ranging from  $69.19 \pm 2.50\%$  to  $105.3 \pm 0.48\%$ . None of the concentrations gave cell viability lower than 50%. At 48 hrs, none of the concentrations showed more than 50% cell inhibition with cell viability ranging from  $61.75 \pm 1.69\%$  to  $94.43 \pm 0.17\%$ . Extract concentrations of 25  $\mu\text{g/mL}$  and more had significant ( $p < 0.001$ ) decrease in viable cells when compared to untreated control group. Thus, it can be concluded that crude hexane extract of curry leaf has low cytotoxic activity against NP-69 cell line.

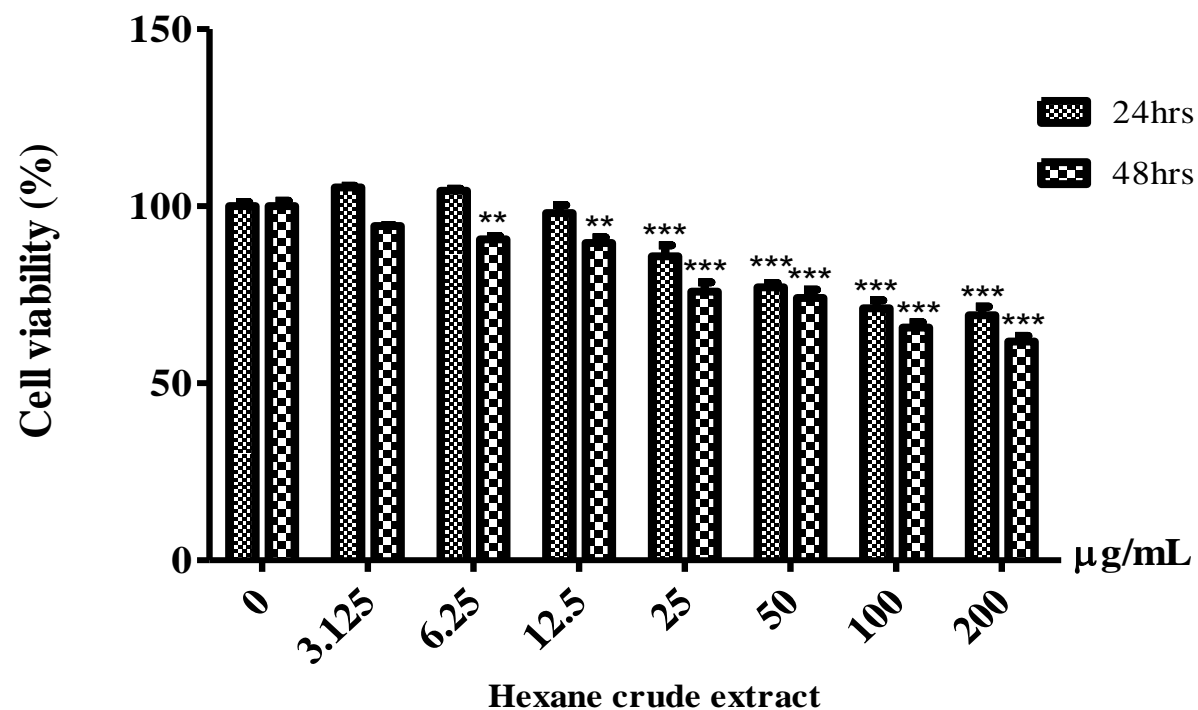


**Figure 44: Effect of hexane crude extract of temu kunci on NP-69 cell viability. Each bar represents the mean  $\pm$  standard deviation (S.D.) from 3 independent experiments (n=3). \*\*\* $P < 0.001$  and \*\* $P < 0.01$  indicate the statistical significant difference with respect to untreated control group.**

#### **3.4.2.11 Effect of methanol crude extract of spring onion on NP-69 cell viability**

NP-69 cell line was treated with various concentrations of crude methanolic extract of spring onion leaf from 3.13 µg/mL to 200 µg/mL at 24 and 48 hrs and the cell viability was evaluated (**Figure 45**). Control group was not treated with the crude extract. At 24 hrs, the percentage of cell viability in each concentration was moderate, ranging from 68.85±1.18% to 95.30±1.63%. None of the concentrations gave cell viability lower than 50%. At 48 hrs, none of the concentrations showed more than 50% cell inhibition with cell viability ranging from 68.75±2.14% to 90.44±1.47%. Extract concentrations of 6.25 µg/mL and more had significant ( $p<0.001$ ) decrease in viable cells when compared to untreated control group. Thus, it can be concluded that crude methanolic extract of spring onion leaf has low cytotoxic activity against NP-69 cell line.



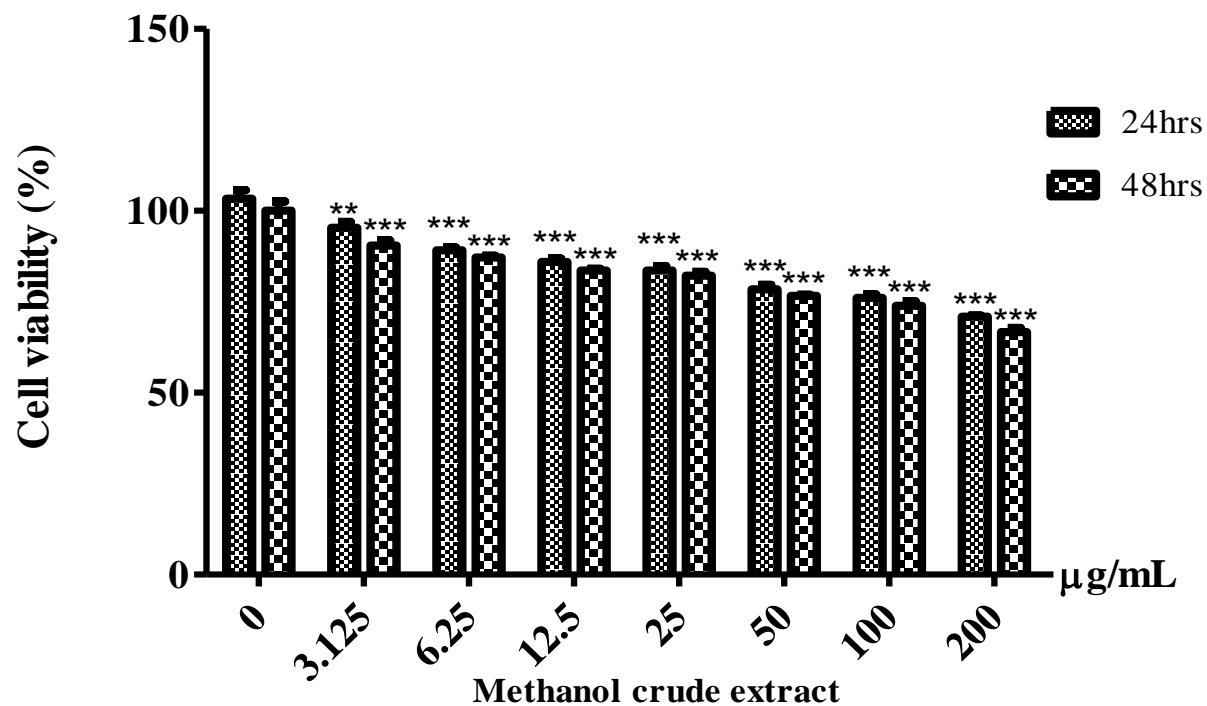


**Figure 45: Effect of methanol crude extract of spring onion on NP-69 cell viability. Each bar represents the mean  $\pm$  standard deviation (S.D.) from 3 independent experiments (n=3). \*\*\* $P < 0.001$  and \*\* $P < 0.01$  indicate the statistical significant difference with respect to untreated control group.**

#### **3.4.2.12 Effect of ethyl acetate crude extract of spring onion on NP-69 cell viability**

NP-69 cell line was treated with various concentrations of crude ethyl acetate extract of spring onion leaf from 3.13  $\mu\text{g/mL}$  to 200  $\mu\text{g/mL}$  at 24 and 48 hrs and the cell viability was evaluated (**Figure 46**). Control group was not treated with the crude extract. At 24 hrs, the percentage of cell viability in each concentration was moderate, ranging from  $60.85 \pm 2.26\%$  to  $119.2 \pm 2.49\%$ . None of the concentrations gave cell viability lower than 50%. At 48 hrs, none of the concentrations showed more than 50% cell inhibition with cell viability ranging from  $56.28 \pm 2.33\%$  to  $95.64 \pm 1.41\%$ . Extract concentrations of 25  $\mu\text{g/mL}$  and more had significant ( $p < 0.001$ ) decrease in viable cells when compared to untreated control group. Thus, it can be concluded that crude ethyl acetate extract of spring onion leaf has low cytotoxic activity against NP-69 cell line.

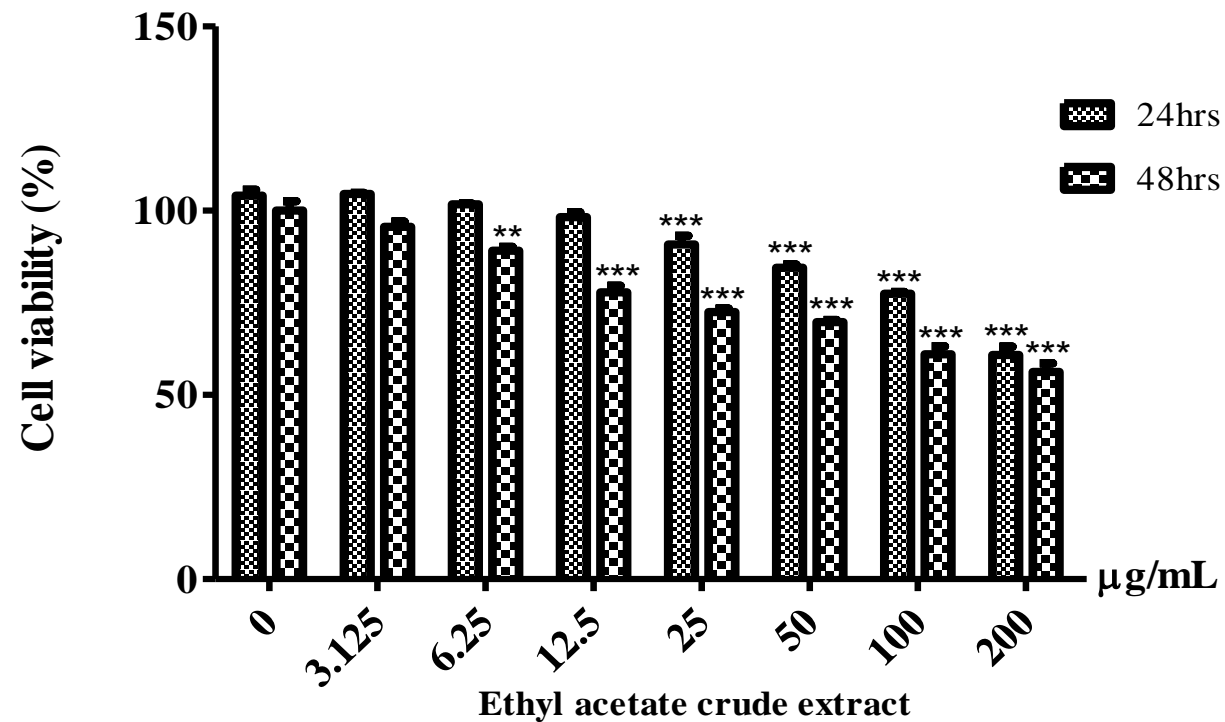


**Figure 46: Effect of ethyl acetate crude extract of spring onion on NP-69 cell viability. Each bar represents the mean  $\pm$  standard deviation (S.D.) from 3 independent experiments (n=3). \*\*\* $P < 0.001$  and \*\* $P < 0.01$  indicate the statistical significant difference with respect to untreated control group.**

### **3.4.2.13 Effect of hexane crude extract of spring onion on NP-69 cell viability**

NP-69 cell line was treated with various concentrations of crude hexane extract of spring onion leaf from 3.13 µg/mL to 200 µg/mL at 24 and 48 hrs and the cell viability was evaluated (**Figure 47**). Control group was not treated with the crude extract. At 24 hrs, the percentage of cell viability in each concentration was moderate, ranging from 54.50±0.34% to 114.4±1.68%. None of the concentrations gave cell viability lower than 50%. At 48 hrs, none of the concentrations showed more than 50% cell inhibition with cell viability ranging from 52.07±0.44% to 93.65±1.86%. Extract concentrations of 25 µg/mL and more had significant ( $p<0.001$ ) decrease in viable cells when compared to untreated control group. Thus, it can be concluded that crude hexane extract of spring onion leaf has low cytotoxic activity against NP-69 cell line.

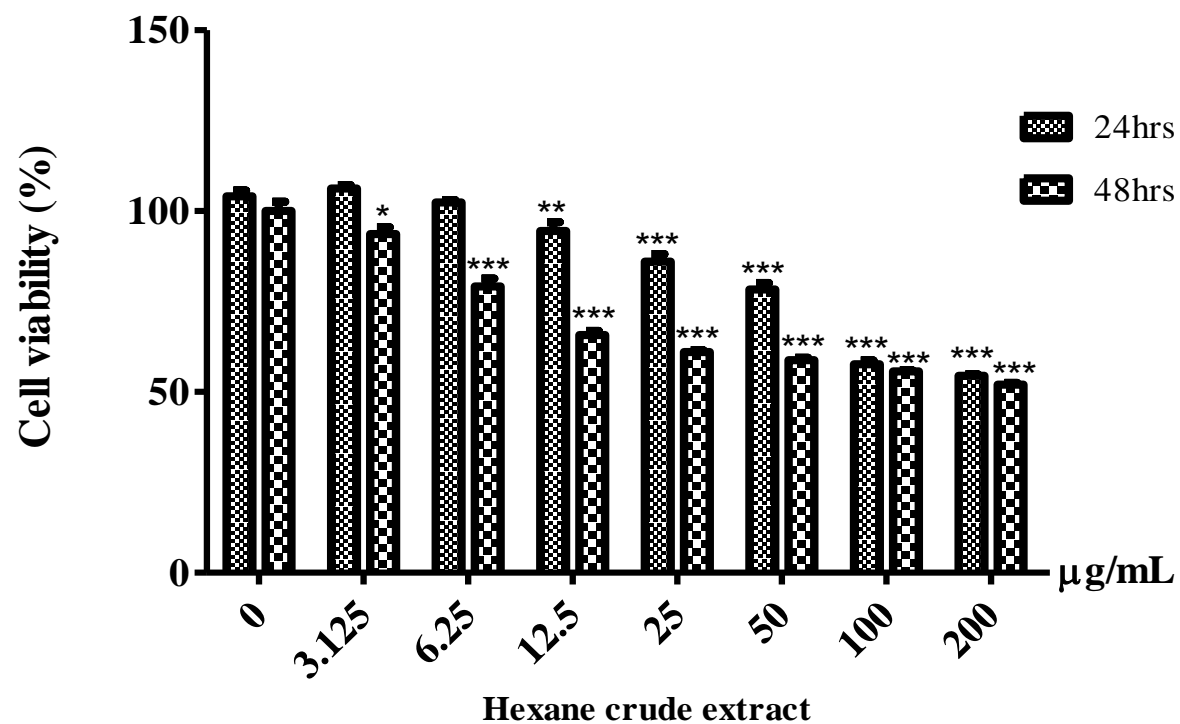


**Figure 47: Effect of hexane crude extract of spring onion on NP-69 cell viability.** Each bar represents the mean  $\pm$  standard deviation (S.D.) from 3 independent experiments (n=3). \*\*\* $P < 0.001$ , \*\* $P < 0.01$  and \* $P < 0.05$  indicate the statistical significant difference with respect to untreated control group.

#### **3.4.2.14 Effect of methanol crude extract of mushroom bean on NP-69 cell viability**

NP-69 cell line was treated with various concentrations of crude methanolic extract of mushroom bean from 3.13  $\mu\text{g/mL}$  to 200  $\mu\text{g/mL}$  at 24 and 48 hrs and the cell viability was evaluated (**Figure 48**). Control group was not treated with the crude extract. At 24 hrs, the percentage of cell viability in each concentration was high, ranging from  $82.25 \pm 2.53\%$  to  $117.0 \pm 0.75\%$ . None of the concentrations gave cell viability lower than 50%. At 48 hrs, none of the concentrations showed more than 50% cell inhibition with cell viability ranging from  $73.88 \pm 0.08\%$  to  $108.5 \pm 0.41\%$ . Extract concentration of 200  $\mu\text{g/mL}$  had significant ( $p < 0.001$ ) decrease in viable cells when compared to untreated control group. Thus, it can be concluded that crude methanolic extract of mushroom bean has low cytotoxic activity against NP-69 cell line.

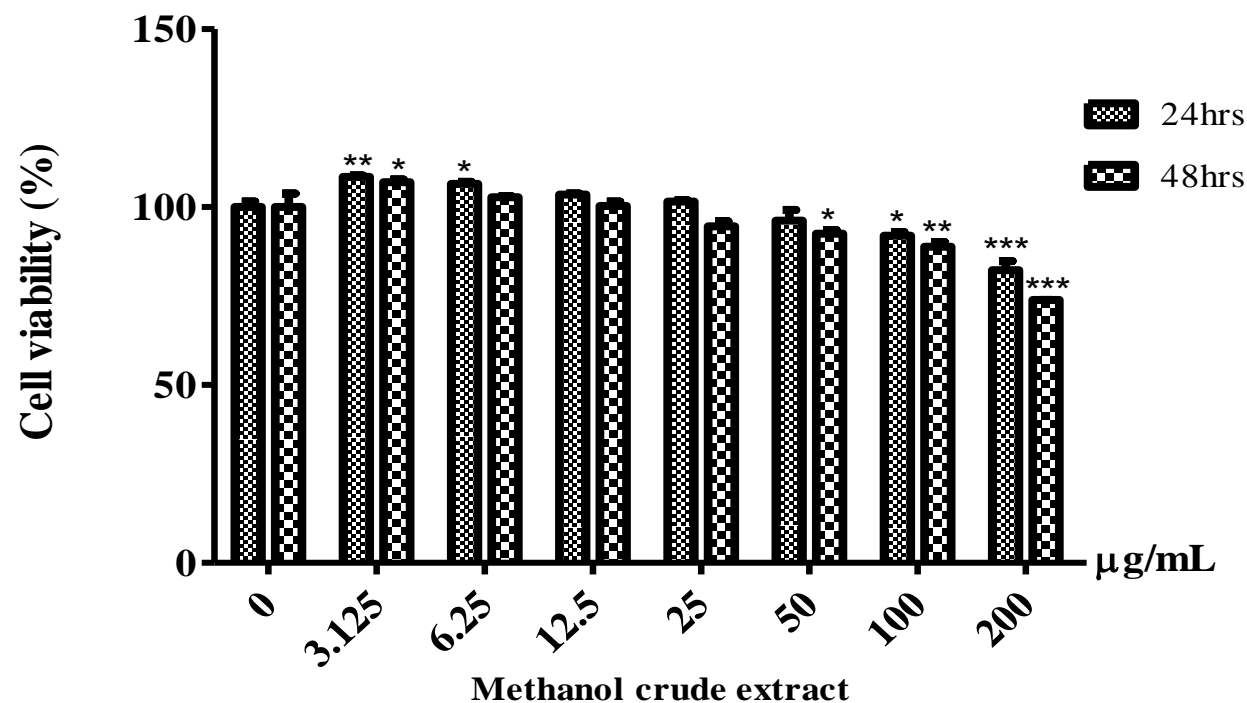


**Figure 48: Effect of methanol crude extract of mushroom bean on NP-69 cell viability. Each bar represents the mean  $\pm$  standard deviation (S.D.) from 3 independent experiments (n=3). \*\*\* $P < 0.001$ ,  $P < 0.01$  and \* $P < 0.05$  indicate the statistical significant difference with respect to untreated control group.**

#### **3.4.2.15 Effect of ethyl acetate crude extract of mushroom bean on NP-69 cell viability**

NP-69 cell line was treated with various concentrations of crude ethyl acetate extract of mushroom bean from 3.13 µg/mL to 200 µg/mL at 24 and 48 hrs and the cell viability was evaluated (**Figure 49**). Control group was not treated with the crude extract. At 24 hrs, the percentage of cell viability in each concentration was high, ranging from 82.02±1.10% to 115.6±0.82%. None of the concentrations gave cell viability lower than 50%. At 48 hrs, none of the concentrations showed more than 50% cell inhibition with cell viability ranging from 70.74±0.30% to 107.3±0.41%. Extract concentrations of 100 and 200 µg/mL had significant ( $p<0.001$ ) decrease in viable cells when compared to untreated control group. Thus, it can be concluded that crude ethyl acetate extract of mushroom bean has low cytotoxic activity against NP-69 cell line.



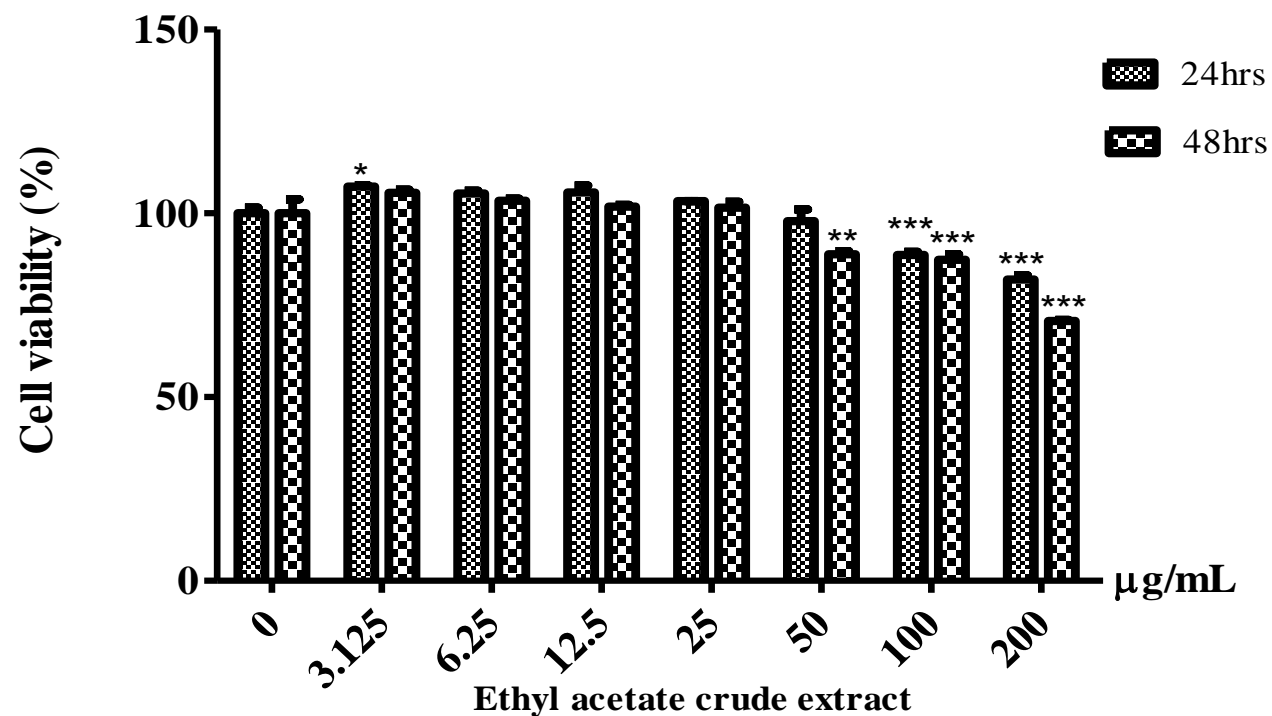


**Figure 49: Effect of ethyl acetate crude extract of mushroom bean on NP-69 cell viability.** Each bar represents the mean  $\pm$  standard deviation (S.D.) from 3 independent experiments (n=3). \*\*\* $P < 0.001$ , \*\* $P < 0.01$  and \* $P < 0.05$  indicate the statistical significant difference with respect to untreated control group.

#### **3.4.2.16 Effect of hexane crude extract of mushroom bean on NP-69 cell viability**

NP-69 cell line was treated with various concentrations of crude hexane extract of mushroom bean from 3.13 µg/mL to 200 µg/mL at 24 and 48 hrs and the cell viability was evaluated (**Figure 50**). Control group was not treated with the crude extract. At 24 hrs, the percentage of cell viability in each concentration was high, ranging from 87.02±3.66% to 115.3±1.97%. None of the concentrations gave cell viability lower than 50%. At 48 hrs, none of the concentrations showed more than 50% cell inhibition with cell viability ranging from 81.77±1.55% to 108.9±0.20%. Extract concentration of 200 µg/mL had significant ( $p<0.001$ ) decrease in viable cells when compared to untreated control group. Thus, it can be concluded that crude hexane extract of mushroom bean has low cytotoxic activity against NP-69 cell line.

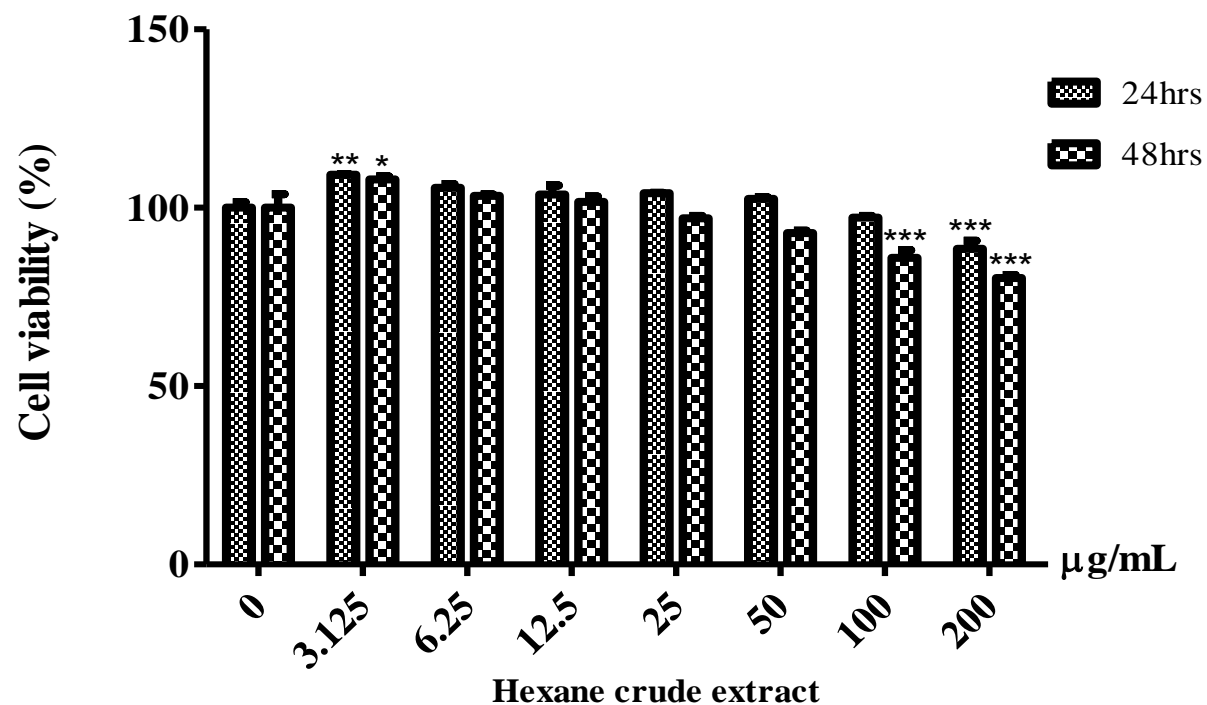


**Figure 50: Effect of hexane crude extract of mushroom bean on NP-69 cell viability. Each bar represents the mean  $\pm$  standard deviation (S.D.) from 3 independent experiments (n=3). \*\*\* $P < 0.001$ , \*\* $P < 0.01$  and \* $P < 0.05$  indicate the statistical significant difference with respect to untreated control group.**

### 3.4.3 IC<sub>50</sub> (Concentration that produces 50% growth inhibition) values of cytotoxic activity.

The results indicate IC<sub>50</sub> values of methanolic, ethyl acetate and hexane crude extracts of curry leaf (*Murraya koenigii*), temu kunci (*Boesenbergia rotunda*), spring onion leaf (*Allium cepa*), mushroom bean (*Phaseolus vulgaris*) and bunga kantan (*Phaeomeria imperialis*) in HK-1 and NP-69 cell lines (Table 2). The IC<sub>50</sub> values are inversely proportional to the cytotoxic activity which means lower IC<sub>50</sub> value indicates a higher cytotoxic activity. For HK-1 cell line, methanolic and hexane crude extracts of curry leaf (*Murraya koenigii*) showed IC<sub>50</sub> values less than 200 µg/mL with IC<sub>50</sub> values of 177.7±3.684 µg/mL and 88.92±2.602 µg/mL respectively. Methanolic and hexane crude extracts of temu kunci (*Boesenbergia rotunda*) revealed more than 50% cells inhibition at concentrations of 138.6±8.805 µg/mL and 77.86±2.839 µg/mL respectively. These crude extracts showed higher IC<sub>50</sub> values than positive control 5-fluorouracil at 19.43±1.598 µg/mL respectively after 48 hrs treatment.

As for NP-69 cell line, all crude extracts showed weak cytotoxic activity with IC<sub>50</sub> value of more than 200 µg/mL. All crude extracts did not exhibit cytotoxicity against immortalized nasopharyngeal epithelial (NP-69) cell line.

Hexane crude extract of temu kunci (*Boesenbergia rotunda*) revealed lowest IC<sub>50</sub> compared to all other extracts. Hence, hexane crude extract will be used as a reference for selection of isolated bioactive compounds published in previous literature.

**Table 2: IC<sub>50</sub> values of various crude extracts on HK-1 and NP-69 cell lines.**

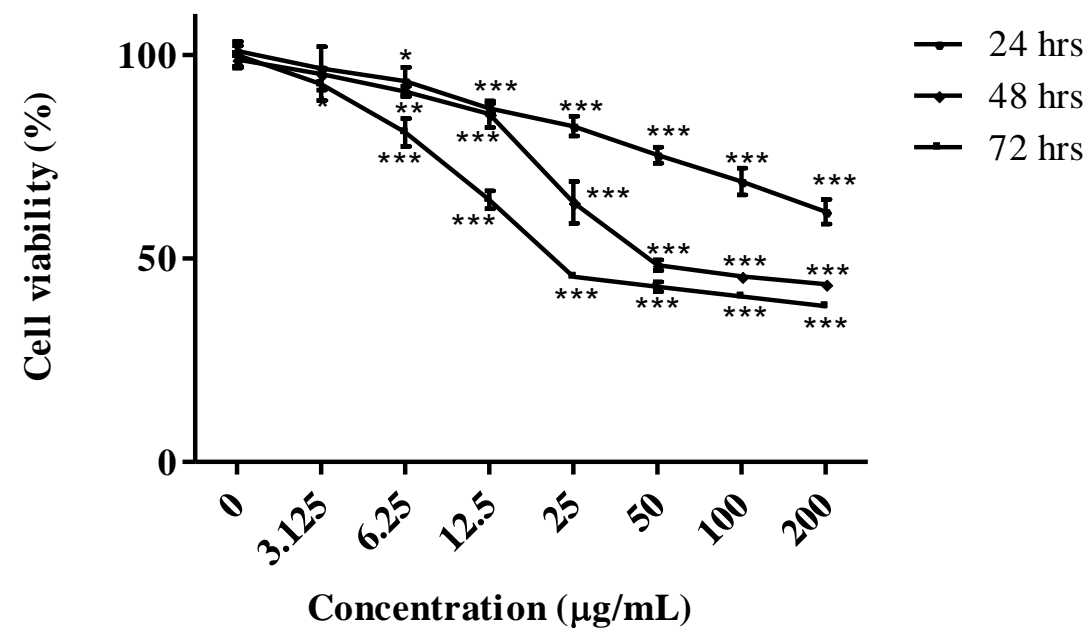
Edible plant	Crude extract	IC <sub>50</sub> value (µg/mL)			
		HK-1		NP-69	
		24 hrs	48 hrs	24 hrs	48 hrs
<b>Bunga kantan</b> ( <i>Phaeomeria imperialis</i> )	M	>200	>200	>200	>200
	EA	>200	>200	>200	>200
	H	>200	>200	>200	>200
	S1	>200	>200	>200	>200
<b>Curry leaf</b> ( <i>Murraya koenigii</i> )	M	>200	<b>177.7±3.684</b>	>200	>200
	EA	>200	>200	>200	>200
	H	>200	<b>88.92±2.602</b>	>200	>200
<b>Temu kunci</b> ( <i>Boesenbergia rotunda</i> )	M	>200	<b>138.6±8.805</b>	>200	>200
	EA	>200	>200	>200	>200
	H	>200	<b>77.86±2.839</b>	>200	>200
<b>Spring Onion</b> ( <i>Allium cepa</i> )	M	>200	>200	>200	>200
	EA	>200	>200	>200	>200
	H	>200	>200	>200	>200
<b>Mushroom bean</b> ( <i>Phaseolus vulgaris</i> )	M	>200	>200	>200	>200
	EA	>200	>200	>200	>200
	H	>200	>200	>200	>200

M represents the methanolic crude extract; EA represents ethyl acetate crude extract; H represents hexane crude extract; S1 represents methanolic solid 1

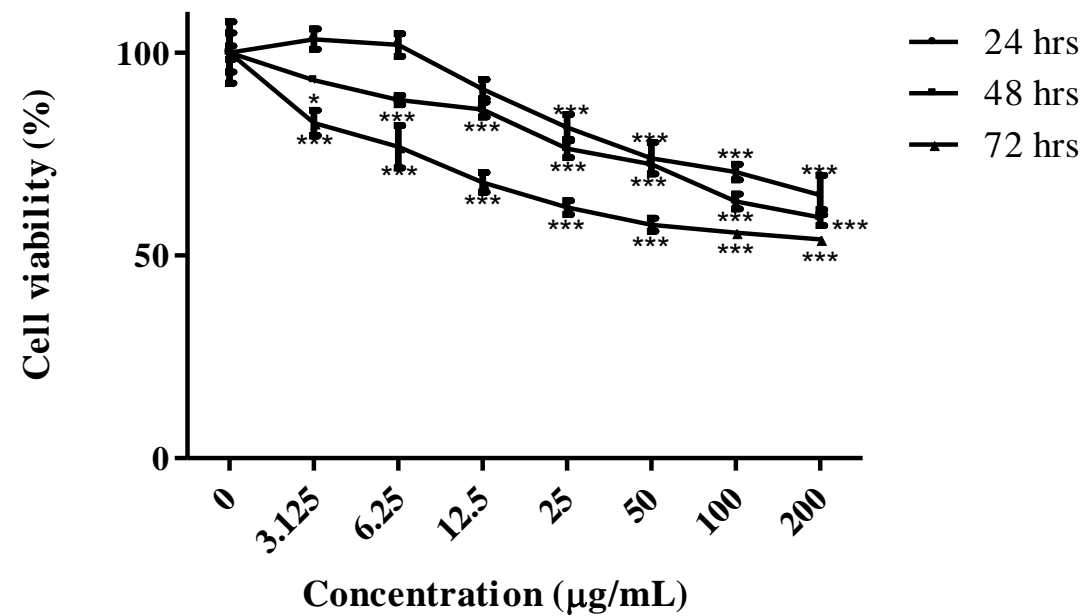
### 3.5 Cytotoxic effects of cardamonin, pinostrobin, naringin and hesperidin against HK-1 and NP-69 cell lines

With these valuable results, we then proceed to carry out the cytotoxic effects of compounds found in the crude extracts of temu kunci (*Boesenbergia rotunda*). Compounds were selected based on promising results published by previous research team as summarized in **Figure 6**.

Four commercially available flavonoids (cardamonin and pinostrobin) and polyphenols (naringin and hesperidin) were tested against nasopharyngeal carcinoma, HK-1 and immortalized epithelial nasopharyngeal, NP-69 cell lines for 24, 48 and 72 hrs to evaluate their cytotoxic effects. Cardamonin was found to be cytotoxic against HK-1 cells at  $IC_{50}$  of 47  $\mu\text{g/mL}$  after 48 hrs (**Figure 51**). After 72 hrs of exposure to cardamonin,  $IC_{50}$  was reduced to 22  $\mu\text{g/mL}$ . This 50% inhibitory concentration ( $IC_{50}$ ) will be used for all other bioassays in proposed mitochondrial-dependent cell death pathway. Hesperidin and naringin did not exhibit any cytotoxic effects against HK-1 cell line as all  $IC_{50}$  were recorded to be more than 200  $\mu\text{g/mL}$  (**Figure 52**; **Figure 53**). As for pinostrobin, cytotoxic effect was observed after 72 hrs at  $IC_{50}$  of 38  $\mu\text{g/mL}$  (**Figure 54**).  $IC_{50}$  values were recorded in **Table 3**.

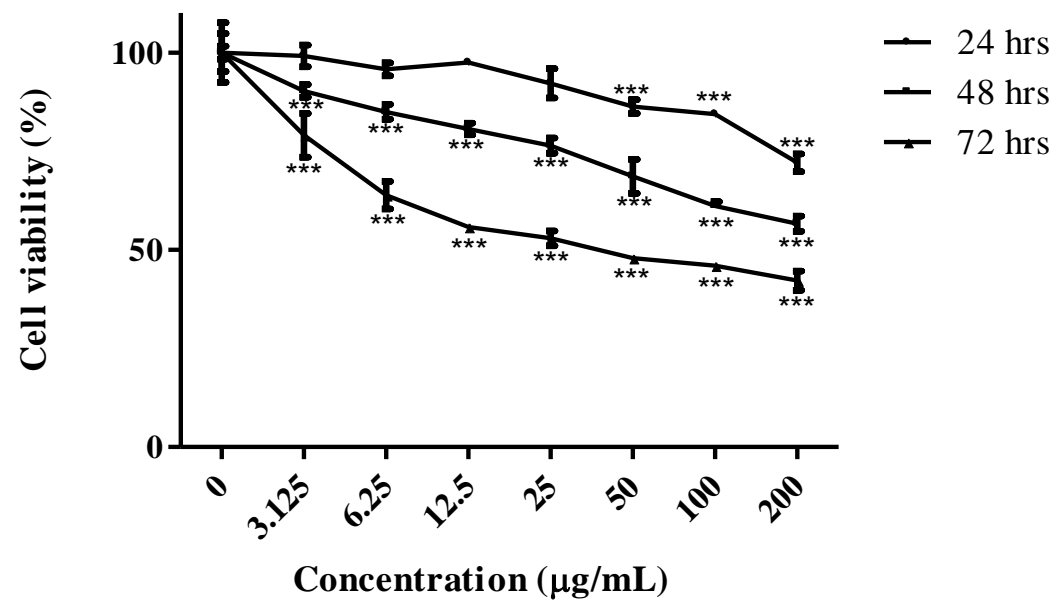


**Figure 51:** Cytotoxic effect of various concentrations of cardamomin on HK-1 cell viability at 24, 48 and 72 hrs. Each point represents the mean  $\pm$  standard deviation (S.D.) from 3 independent experiments (n=3). \*\*\*P < 0.001, \*\*P < 0.05 and \*P < 0.01 indicate the statistical significant difference with respect to untreated control group.

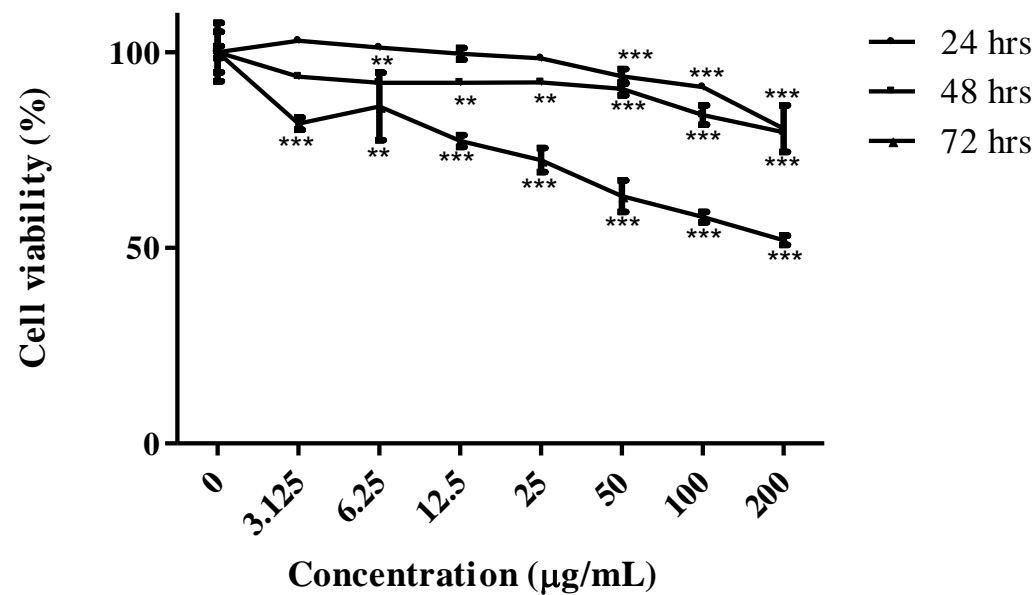


**Figure 52:** Cytotoxic effect of various concentrations of hesperidin on HK-1 cell viability at 24, 48 and 72 hrs. Each point represents the mean  $\pm$  standard deviation (S.D.) from 3 independent experiments (n=3). \*\*\*P < 0.001 and \*P < 0.01 indicate the statistical significant difference with respect to untreated control group.



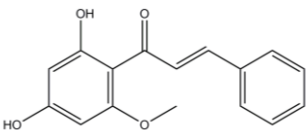
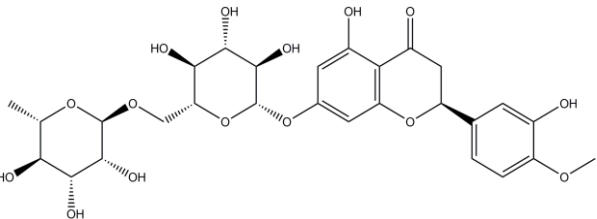
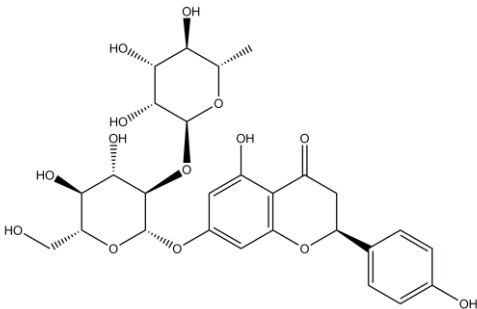
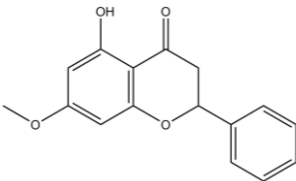


**Figure 53:** Cytotoxic effect of various concentrations of naringin on HK-1 cell viability at 24, 48 and 72 hrs. Each point represents the mean  $\pm$  standard deviation (S.D.) from 3 independent experiments (n=3). \*\*\*P < 0.001 indicates the statistical significant difference with respect to untreated control group.



**Figure 54:** Cytotoxic effect of various concentrations of pinostrobin on HK-1 cell viability at 24, 48 and 72 hrs. Each point represents the mean  $\pm$  standard deviation (S.D.) from 3 independent experiments (n=3). \*\*\*P < 0.001 and \*\*P < 0.05 indicate the statistical significant difference with respect to untreated control group.

**Table 3:** IC<sub>50</sub> values for all four commercially available flavonoids and polyphenols tested against HK-1 cells. All values were generated from three independent experiments (n=3).

Tested compound	IC <sub>50</sub> values (µg/mL)		
	Duration of treatment		
	(hrs)		
	24	48	72
<b>Cardamonin (Flavonoid)</b> 	>200	47±2.65	22±0.71
<b>Hesperidin (Polyphenol)</b> 	>200	>200	>200
<b>Naringin (Polyphenol)</b> 	>200	>200	>200
<b>Pinostrobin (Flavonoid)</b> 	>200	>200	38±6.08

### **3.6 Cardamonin induces cell death and decreases cell viability in HK-1 cells**

HK-1 and NP-69 cells were treated with various concentrations (0, 3.125, 6.25, 12.5, 25, 50, 100 and 200 µg/mL) of cardamonin. MTT assay was conducted to evaluate percentage (%) of viable cells in time- and dose-dependent manner (**Figure 51; Figure 56**). The results demonstrated that as the concentration of cardamonin increases, cell viability of HK-1 cells decreases. A time-dependent cytotoxic effect of cardamonin against HK-1 cell line was also conducted. At 72 hrs, it was found that 50% of HK-1 cell proliferation was inhibited at 22 µg/mL. Cardamonin concentrations of 12.5 µg/mL and above had significant ( $p < 0.001$ ) decrease in viable cells when compared to untreated control group for up to 72 hrs. Cardamonin-treated NP-69 cells was not affected after 24 and 48 hrs. Nevertheless, at 72 hrs, there was a moderate cytotoxic activity against NP-69 cells. To further confirm the occurrence of cell death, a simple test using trypan blue stain was employed (**Figure 55**). Unstained viable cells were counted using haemocytometer. After 24 hrs exposed to cardamonin, more than half of the cell population has decreased. More than 4-fold decrease in viable cell count was observed after 72 hrs of cardamonin treatment. At all tested time point, there was a significant decrease ( $P < 0.001$ ) in viable cell count. Hence, this concentration was used to conduct other assays.

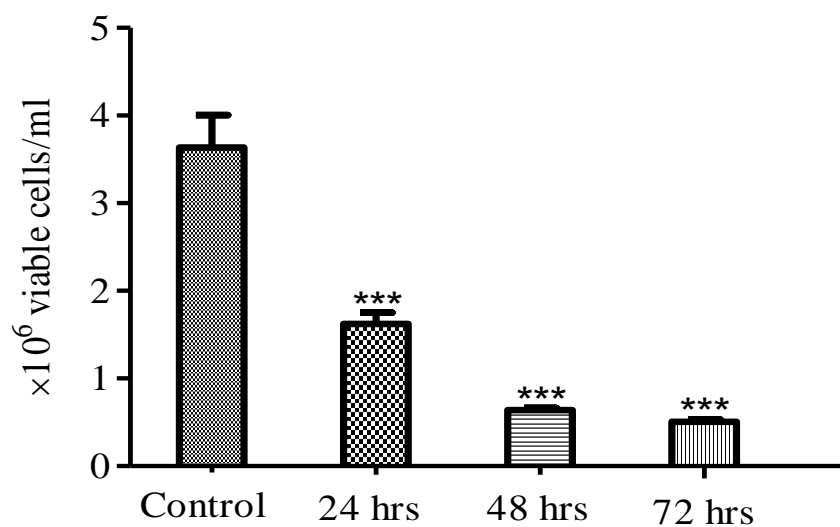


**Figure 55:** Cell viability after 24, 48 and 72 hrs treatment with 22  $\mu\text{g/mL}$  of cardamonin. Each bar represents the mean  $\pm$  standard deviation (S.D.) from three independent experiments ( $n=3$ ). \*\*\*  $P < 0.001$  indicates the statistical significant difference with respect to untreated control group.

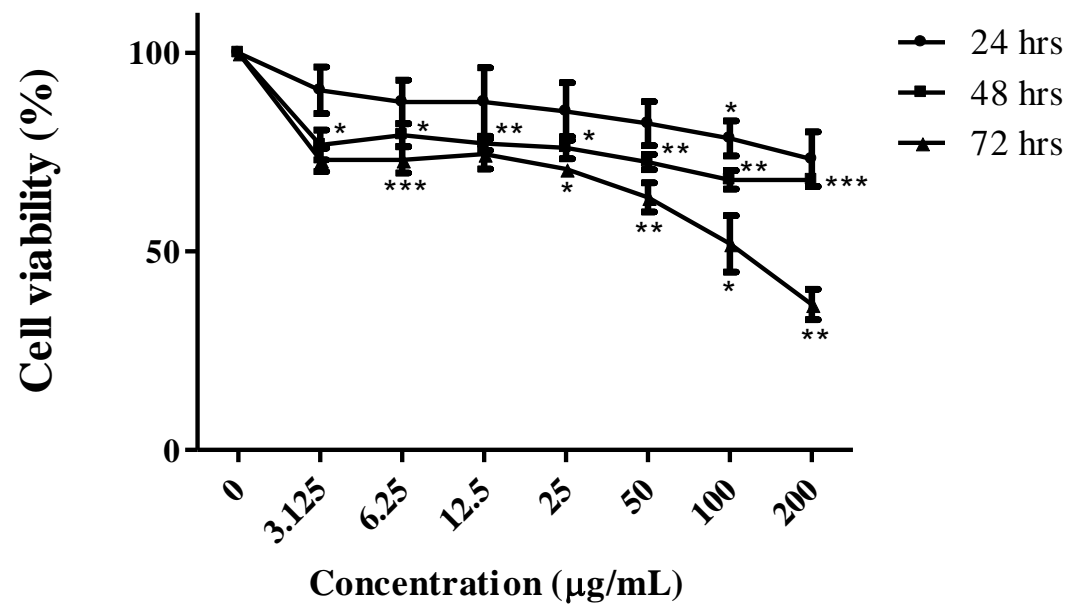


**Figure 56:** Cytotoxic effect of various concentrations of cardamonin against NP-69 cell line after 24, 48 and 72 hrs.  $IC_{50}$  at 72 hrs was found at 112.5 µg/mL of cardamonin. Each point represents the mean  $\pm$  standard deviation (S.D.) from three independent experiments (n=3). \*\*\* $P < 0.001$ , \*\* $P < 0.05$  and \* $P < 0.01$  indicate the statistical significant difference with respect to untreated control group.

### **3.7 Cardamonin induces morphological changes in HK-1 cells**

HK-1 cells were treated with increasing concentration at 72 hrs to view the morphological changes using inverted microscope ( $\times 100$ ). At cardamonin-induced concentration of 12.5  $\mu\text{g/mL}$ , HK-1 cells detached from flask and formed clumps of cells floating in medium. Also, detached cells had uneven shape and unable to maintain their intact membranes. When cells were exposed to cardamonin for more than 25  $\mu\text{g/mL}$ , large number of cells was observed in suspension which substantiates the indication of pyknosis (**Figure 57A**). Similar morphological changes were observed in HK-1 cells at 18 hrs of exposure to  $\text{IC}_{50}$  22  $\mu\text{g/mL}$  cardamonin (**Figure 57B**).

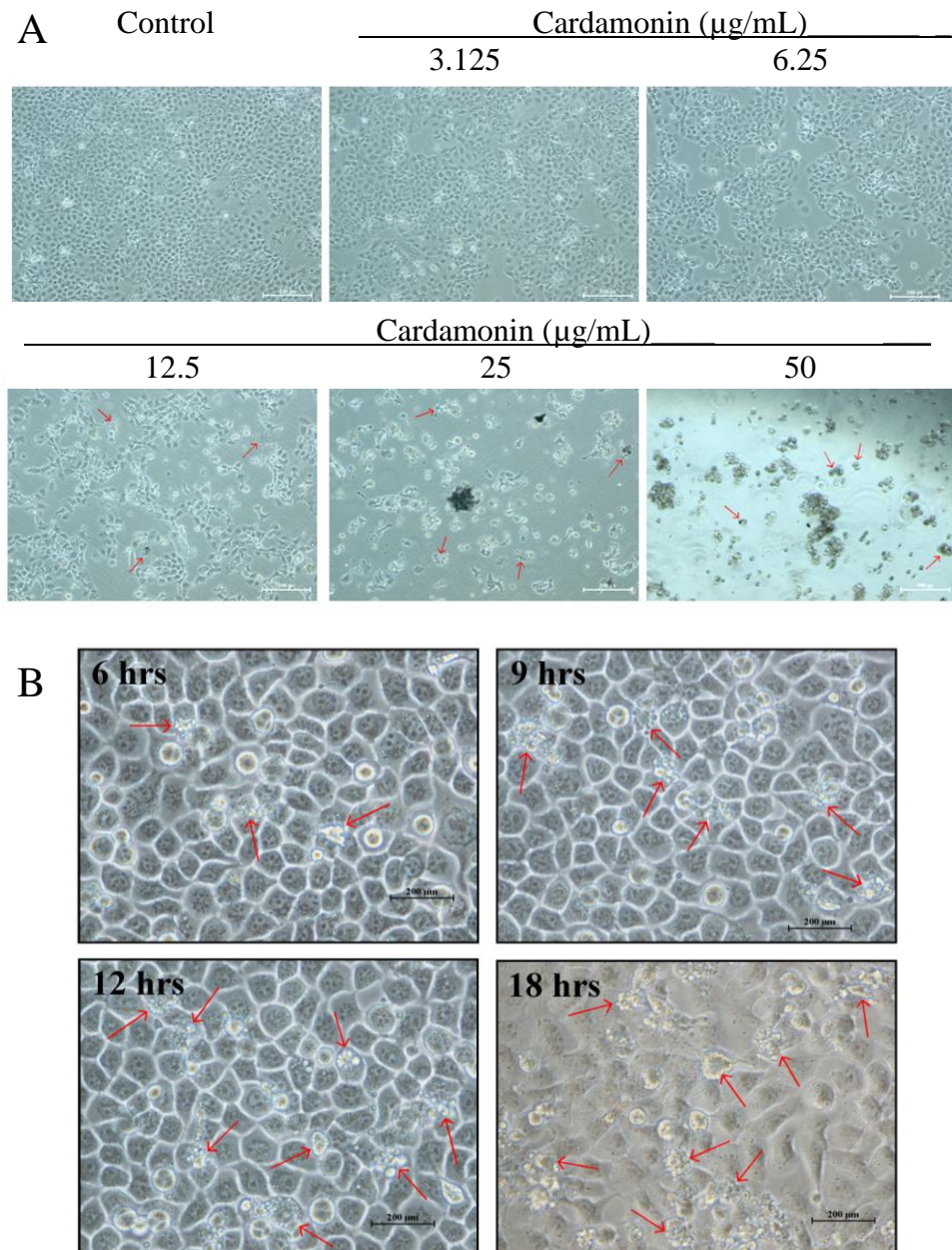


**Figure 57:** (A) Cardamonin induces HK-1 cellular apoptosis at 72 hrs in dose-dependent manner. Changes in cell morphology were examined by light inverted microscope ( $\times 100$ ). (B) HK-1 cells treated with  $\text{IC}_{50}$  of  $22 \mu\text{g/mL}$  and cell morphological changes were examined ( $\times 200$ ) in time-dependent manner. Cell shrinkage and plasma membrane blebbing (indicated by red arrows) were observed after 18 hrs of treatment.



### 3.8 Cardamonin induces apoptosis in HK-1 cells stained with fluorescence dyes

HK-1 cells treated with 22  $\mu\text{g/mL}$  of cardamonin at 24 and 48 hrs were stained with two DNA-binding dyes; acridine orange (AO) and propidium iodide (PI) to identify stages of apoptosis occurring in time-dependent manner (**Figure 58**). Acridine orange is able to pass through plasma membrane of viable cells and cells that are undergoing early apoptosis and stain DNA. Ciapetti *et al.* (2002) identified that viable cells with intact nucleus emit green fluorescence whereas cells undergoing early apoptosis appear dense green with chromatin condensation in the nucleus upon excitation of acridine orange. Cells stained with propidium iodide emit dense orange fluorescence with chromatin condensation. These cells are in their late apoptosis stage whereas secondary necrosis cells appear orange with intact nucleus when cells are stained with propidium iodide (Ciapetti *et al.*, 2002). From our results, HK-1 cells showed strong emission of green fluorescence in untreated cells but when exposed to cardamonin for 24 hrs, cells emit orange red fluorescence more densely at the centre of the cells indicating late apoptosis. More dead cells were stained with PI after 48 hrs of cardamonin treatment emitting red fluorescence as shown in **Figure 58(B)**.

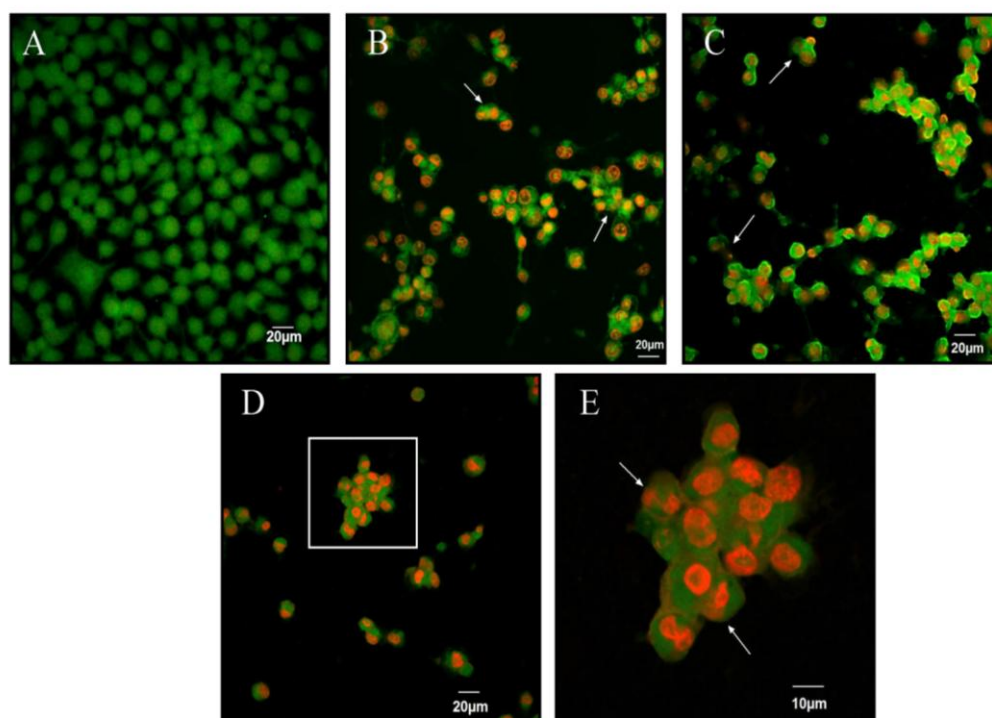


**Figure 58:** HK-1 cells stained with acridine orange and propidium iodide fluorescence dyes showed green and orange fluorescence in untreated cells and cells treated with 22  $\mu\text{g/mL}$  cardamonin at 24 and 48 hrs. Cell-permeable acridine orange stained untreated HK-1 cells and emits green fluorescence (A). After 24 hrs exposure to cardamonin, propidium iodide stained DNA to emit red fluorescence (B & C) in apoptotic cells. Dense orange areas of DNA chromatin condensation can be observed in late apoptotic cells after 48 hrs of cardamonin exposure (D). A clump of HK-1 cells undergoing late apoptosis was observed in an enlarged view (E). Arrows in white indicate cells are undergoing apoptosis with uneven shape and no intact nucleus. All cells were observed using laser confocal microscope ( $\times 400$ ).

### 3.9 Cardamonin induces apoptosis leading to DNA fragmentation

DNA from untreated and treated HK-1 cells were extracted at 24, 48 and 72 hrs and run on agarose gel for DNA separation (**Figure 59**). Nuclear fragmentation was observed in treated HK-1 cells. In untreated HK-1 cells, most DNAs were still intact with high molecular weight DNA strands being trapped on the gel. Cardamonin-treated cells showed DNA smearing with fragments mostly at 250-1000 base pairs at 48 and 72 hrs suggesting the occurrence of apoptosis. DNA sample from 5-fluorouracil-treated (positive control) showed DNA fragmentation after 24 hrs.

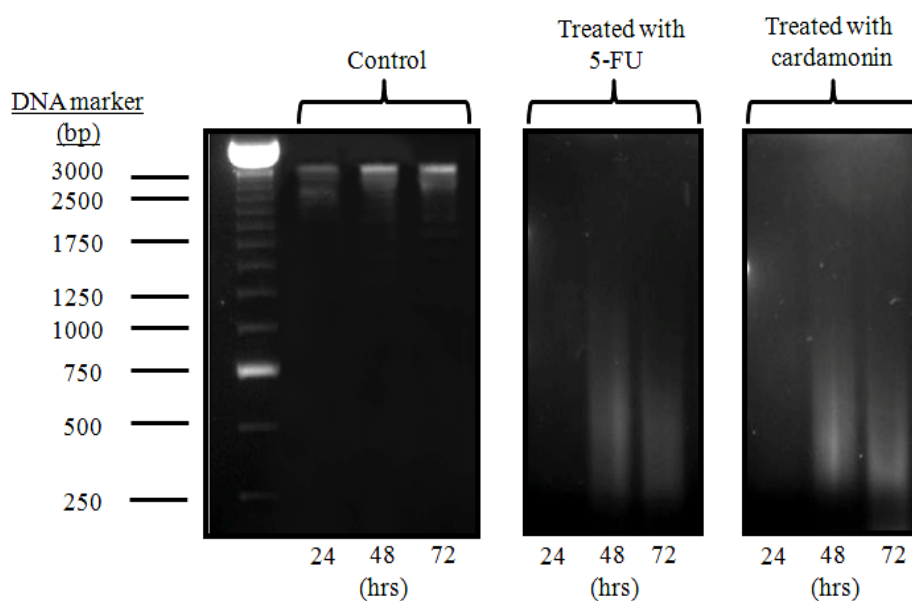


**Figure 59:** DNA fragmentation of HK-1 cells when untreated, treated with 19  $\mu\text{g/mL}$  of anticancer drug, 5-fluorouracil (5-FU) and 22  $\mu\text{g/mL}$  of cardamonin at 24, 48 and 72 hrs. DNA agarose gel electrophoresis was performed at 70V for 1-2 hrs.

### **3.10 Cell cycle analysis: Cardamonin induces cell cycle arrest at G2/M phase and Sub-G1 (apoptotic) phase**

In cell cycle, there are three checkpoints to monitor cell division. Checkpoints at different stages in cell cycle prevent complications before cell enters mitosis. Hence, cell cycle analysis examines population of cells at different phases by their DNA content; these phases are Sub-G1, G0/G1, S and G2/M. Sub-G1 represents Gap 0 resting phase (quiescent). Gap 0/Gap 1 (G0/G1) phase is when cell increase in size ready for DNA synthesis. DNA replication occurs in synthesis (S) phase. Gap 2/Mitosis (G2/M) phase prepares cell to enter mitosis and divide. Cells at G0/G1 phase are diploid, having DNA content of  $2n$  where as cells within G2/M phase contain DNA content  $4n$ . In S phase, DNA content is between  $2n$  and  $4n$  as cells are undergoing DNA replication. Apoptotic cells contain DNA content of less than  $2n$  which can be observed in Sub-G1 phase. The difference in DNA content allows propidium iodide, a DNA-binding fluorescent dye to emit different intensities which will be quantified using flow cytometry.

In current results, cardamonin induces cell cycle arrest at G2/M and Sub-G1 phase (apoptotic cells) (**Figure 60**). It was found that cardamonin-treated HK-1 cells after 12 hrs resulted in higher number of cells in G2/M phase (49.57%) compared to control group (3.58%) (**Figure 61**). Concurrently, cell population in G0/G1 phase after 12 hrs exposure to cardamonin showed a decrease (11.20%) in respect with control group (70.41%). An increase in apoptotic cells (Sub-G1 phase) was found after 12 hrs incubation with

cardamomin. More than 36% HK-1 cells were accumulated in Sub-G1 phase compared to control group (2.64%).

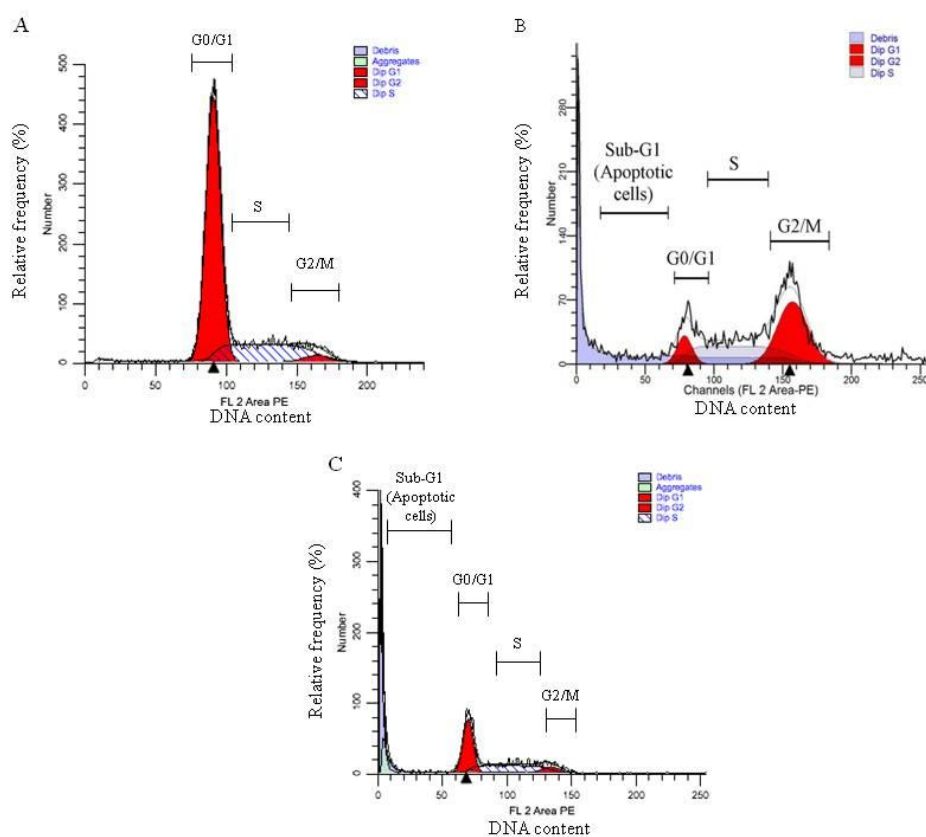


**Figure 60:** Effects of cardamomin on cell cycle phase distribution in HK-1 cells at 12 (B) and 24 (C) hrs. HK-1 cells untreated (A) and treated with cardamomin at respective hours were stained with propidium iodide (PI) prior to flow cytometry analysis. Histograms indicate HK-1 cells distribution according to DNA content at different cell cycle checkpoints.

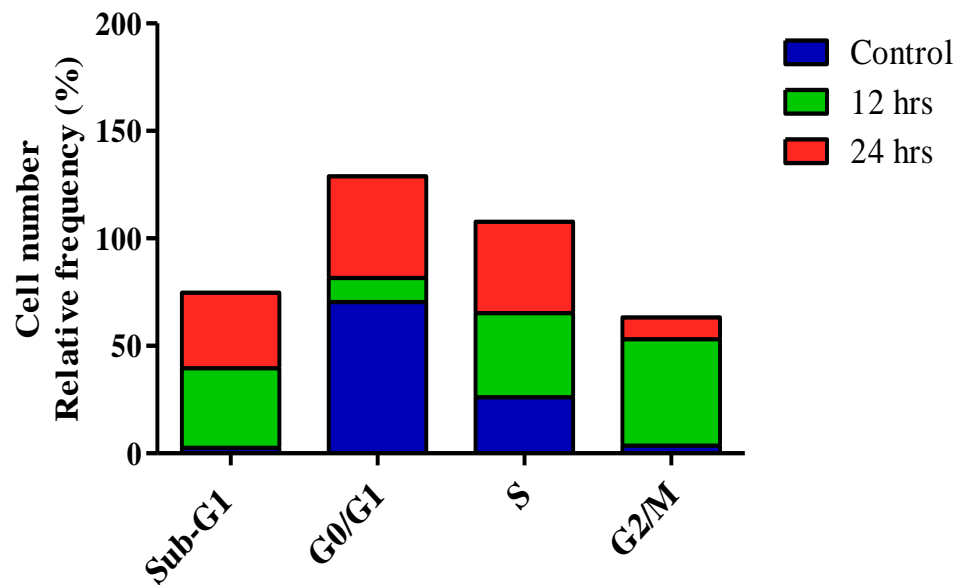


**Figure 61:** Cardamonin induces cell cycle arrest at G2/M phase and sub-G1 (apoptosis) in HK-1 cells at 12 and 24 hrs. Cell cycle distribution was examined using flow cytometry. Each stacked bar expresses percentage of total number of cells at different phase in cell cycle.

### **3.11 Cardamonin induces up-regulation of both caspase-3 and caspase-8 in HK-1 cells**

#### **3.11.1 Cardamonin induces up-regulation of caspase-3**

HK-1 cells were treated with and without 22 µg/mL of cardamonin for 24, 48 and 72 hrs. Cardamonin has significantly enhanced the activity of caspase-3 in HK-1 cells compared to untreated cells within 24 hrs (**Figure 62A**). There was a slight decrease in caspase-3 activity at 48 hrs exposure but increased in the next 24 hrs. To verify that the fluorescence signal was due to the action of caspase-3, a treated set of experiments were conducted as negative control. Cells were treated with cardamonin but a caspase-inhibitor was added to inhibit actions of caspase. Negative control was used to verify signal recorded was captured from caspase activity and not due to other fluorescence signal.

#### **3.11.2 Cardamonin induces up-regulation of caspase-8**

HK-1 cells were treated with and without 22 µg/mL of cardamonin for 24, 48 and 72 hrs. Cardamonin has significantly enhanced the activity of caspase-8 in HK-1 cells compared to untreated cells within 24 hrs (**Figure 62B**). At 24 hrs after treatment, there was relatively high caspase-8 activity detected. Caspase-8 activity decreased at 48 hrs but in the next 24hrs, there was a slight increase. To verify that the fluorescence signal was due to the action of caspase-8, a treated set of experiments were conducted as negative control.

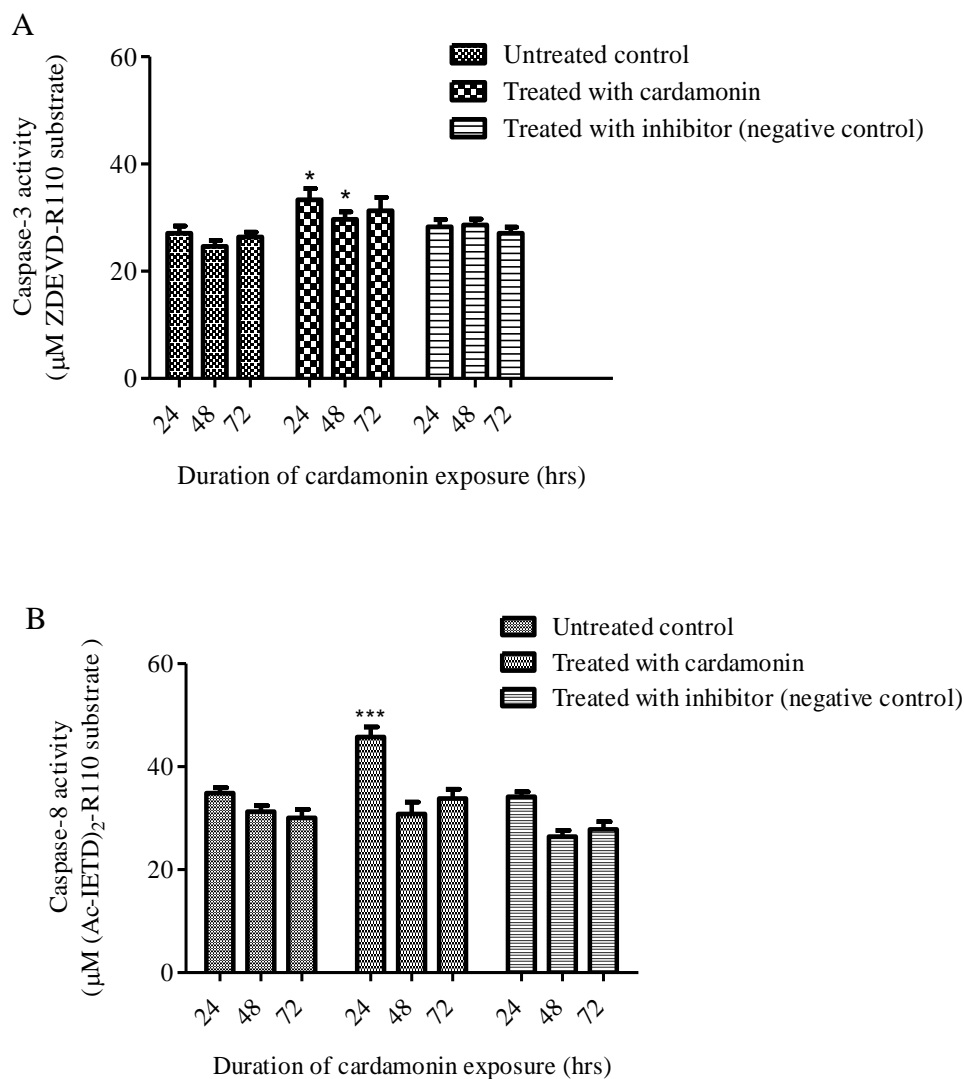


**Figure 62:** (A) Caspase-3 activity in HK-1 cells when untreated, treated with 22  $\mu\text{g/mL}$  of cardamonin and treated with 22  $\mu\text{g/mL}$  of cardamonin then caspase-3 inhibitor at 24, 48 and 72 hrs. (B) Caspase-8 activity of HK-1 cells when untreated, treated with 22  $\mu\text{g/mL}$  of cardamonin and treated with 22  $\mu\text{g/mL}$  of cardamonin then caspase-8 inhibitor at 24, 48 and 72 hrs. Each bar represents mean  $\pm$  standard deviation (S.D.) from three independent experiments ( $n=3$ ). \*\*\* $P < 0.001$  and \* $P < 0.05$  indicate the statistical significant difference with respect to untreated control group.



### **3.12 Cardamonin decreases intracellular ROS production and ROS does not contribute to HK-1 cell death**

Cardamonin decreases ROS production in HK-1 cells. HK-1 cells were exposed to cardamonin at increasing concentration of 12.5, 25, 50, 100 and 200  $\mu\text{M}$  (**Figure 63**). Increasing concentrations were chosen to observe the trend of radical scavenging activity with highest concentration at 200  $\mu\text{M}$  similar to MTT assay.  $\mu\text{g/mL}$  was converted to  $\mu\text{M}$  to calculate CAA and  $\text{EC}_{50}$ . Quercetin was used as a standard in a similar experimental set up (**Figure 64**). HK-1 cells not treated with cardamonin (at 0  $\mu\text{M}$ ) emit highest DCF fluorescence reading within one hour.

HK-1 cells exposed to higher concentrations of cardamonin displayed lower fluorescent intensity due to the action of cardamonin as a natural antioxidant agent to quench ROS within the cells. This result is substantiated by an increase in CAA as the concentration of cardamonin increases (**Figure 65**). Cardamonin was found to be effectively inhibiting radical-induced DCFH oxidation at 79.73  $\mu\text{M}$  (**Table 4**). However, the rate of CAA declines at increasing dosage of cardamonin (**Table 5**). This suggests that cardamonin at lower concentrations may act as an antioxidant to quench increasing level of ROS generated by HK-1 cells. However, as its concentration increases, CAA rate declined.

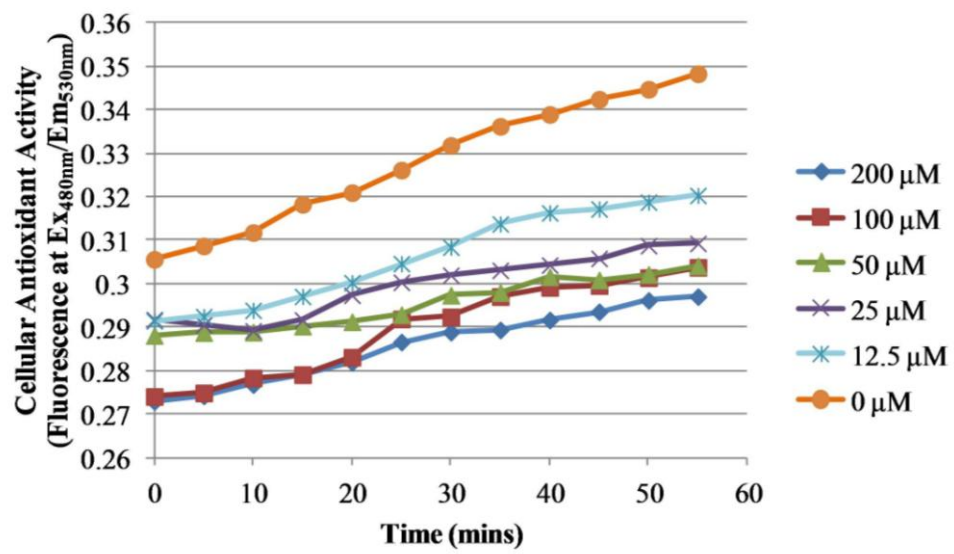


**Figure 63:** Cellular Antioxidant Activity of Cardamonin in HK-1 cells.

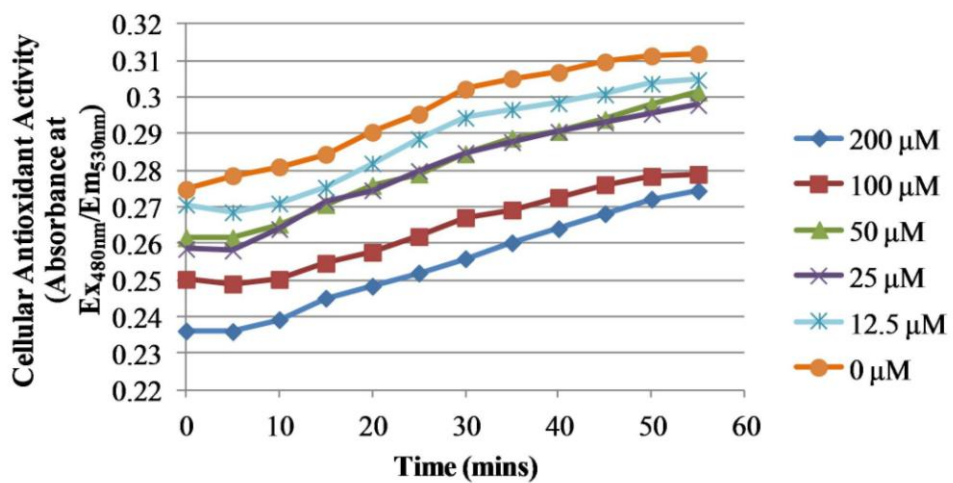


**Figure 64:** Cellular Antioxidant Activity of Quercetin in HK-1 cells.

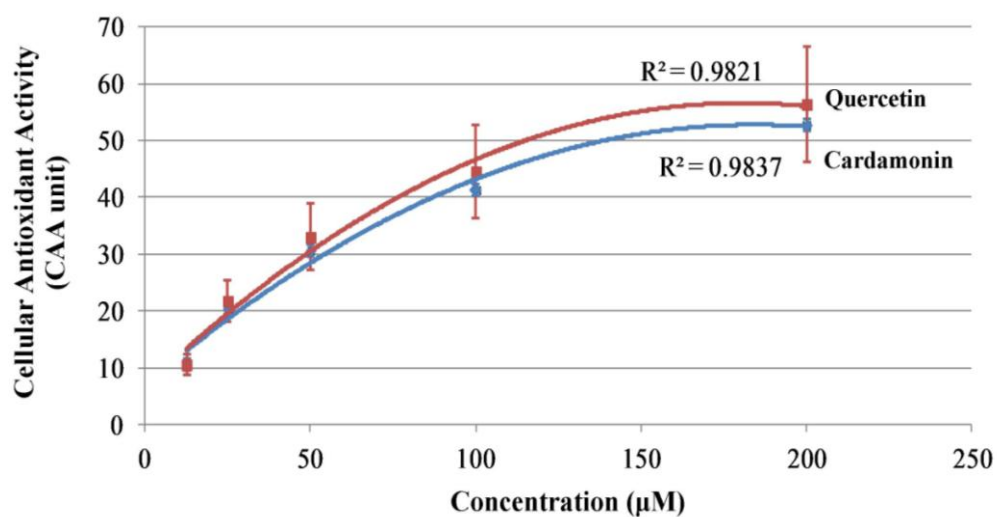


**Figure 65:** Dose-response curve of Quercetin standard and Cardamonin in HK-1 cells. Each concentration was presented as mean  $\pm$  standard deviation (S.D.).

**Table 4: EC<sub>50</sub> values from dose-response curve.**

Standard/Sample	EC <sub>50</sub> (μM)
Quercetin	89.27
Cardamonin	79.73

**Table 5: Rate of Cellular Antioxidant Activity of Quercetin and Cardamonin in HK-1 cells**

Concentration (μM)	Rate of Cellular Antioxidant Activity (CAA unit per μM)	
	Quercetin	Cardamonin
12.5	0.0000	0.0000
25	0.89466	0.7948
50	0.4504	0.4096
100	0.2311	0.2131
200	0.1185	0.1145

### 3.13 Cardamonin induces loss of mitochondrial membrane potential in HK-1 cells

It was previously reported that curcumin and aloe-emodin induce loss of mitochondrial membrane potential in nasopharyngeal carcinoma cells (Kuo *et al.*, 2011; Lin *et al.*, 2010). Hence, to examine whether cardamonin demonstrates similar activity as these natural compounds, we utilize a cytofluorimetric dye called JC-1 (5,5',6,6'-tetrachloro-1,1',3,3'-tetraethylbenzimidazolylcarbocyanine iodide) to study the behavior of mitochondria membrane potential in HK-1 cells. HK-1 cells were treated with IC<sub>50</sub> of 22 µg/mL and fluorescence readings were taken after 3 and 6 hrs (**Figure 66**). A significant increase in mitochondrial membrane potential in HK-1 cells was observed after 3 hrs. Mitochondrial membrane potential increased five-fold compared to untreated control but decreased approximately three-fold after 6 hrs exposure to cardamonin.

HK-1 cells treated and untreated with cardamonin were stained with JC-1 solution and changes in mitochondrial membrane potential after 3 and 6 hrs were visualized using Fluoview 1000 laser scanning confocal microscope (Olympus IX 81 Motorized Inverted Microscope). It was observed that untreated cells after 3 hrs (**Figure 67**) and 6 hrs (**Figure 68**) showed strong J-aggregates and emit strong red fluorescence. However, in cardamonin-treated HK-1 cells, most of the cells observed were emitting green fluorescence indicating low mitochondrial membrane potential after 3 hrs (**Figure 69**) and 6 hrs (**Figure 70**).

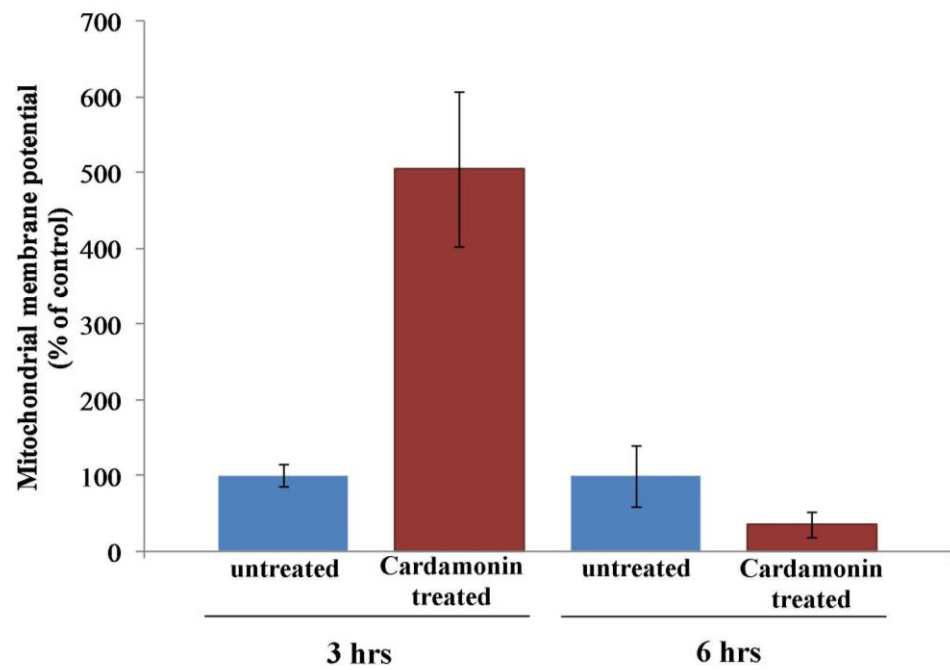


**Figure 66:** Effect of cardamonin on mitochondrial membrane potential in HK-1 cells after 3 and 6 hrs. Each bar represents mean  $\pm$  standard deviation (S.D.) from there independent experiments (n=3). \*\*\* $P < 0.001$  indicates the statistical significant difference with respect to untreated control group.

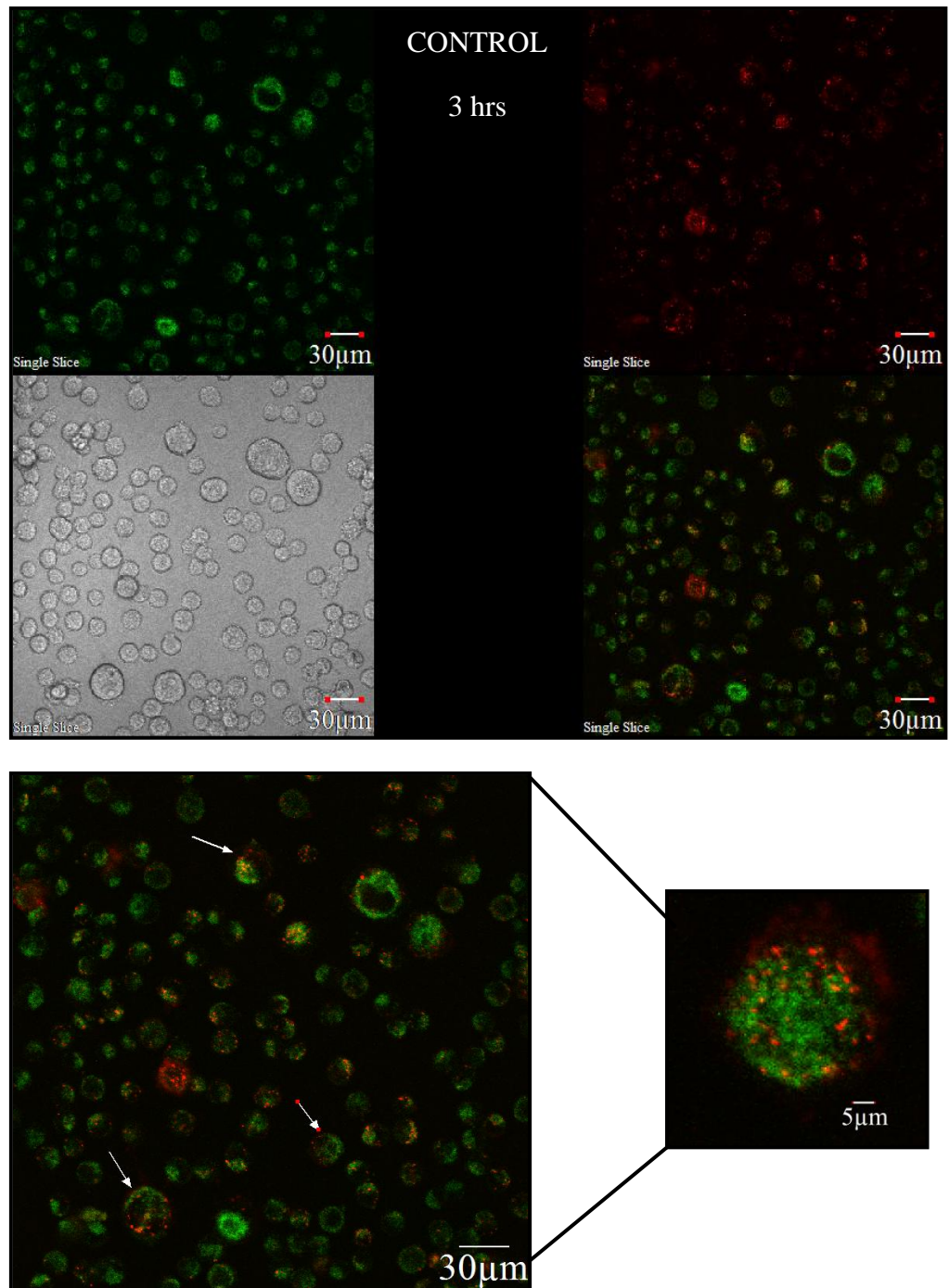


**Figure 67:** Mitochondrial membrane potential in HK-1 cells (control group) after 3 hrs (Fluoview 1000 laser scanning confocal microscope, Olympus IX 81 Motorized Inverted Microscope,  $\times 400$ ). Untreated cells showing strong J-aggregation and emits red fluorescence (indicated by white arrows). Single slices (red and green fluorescence) were stacked to obtain the final image.

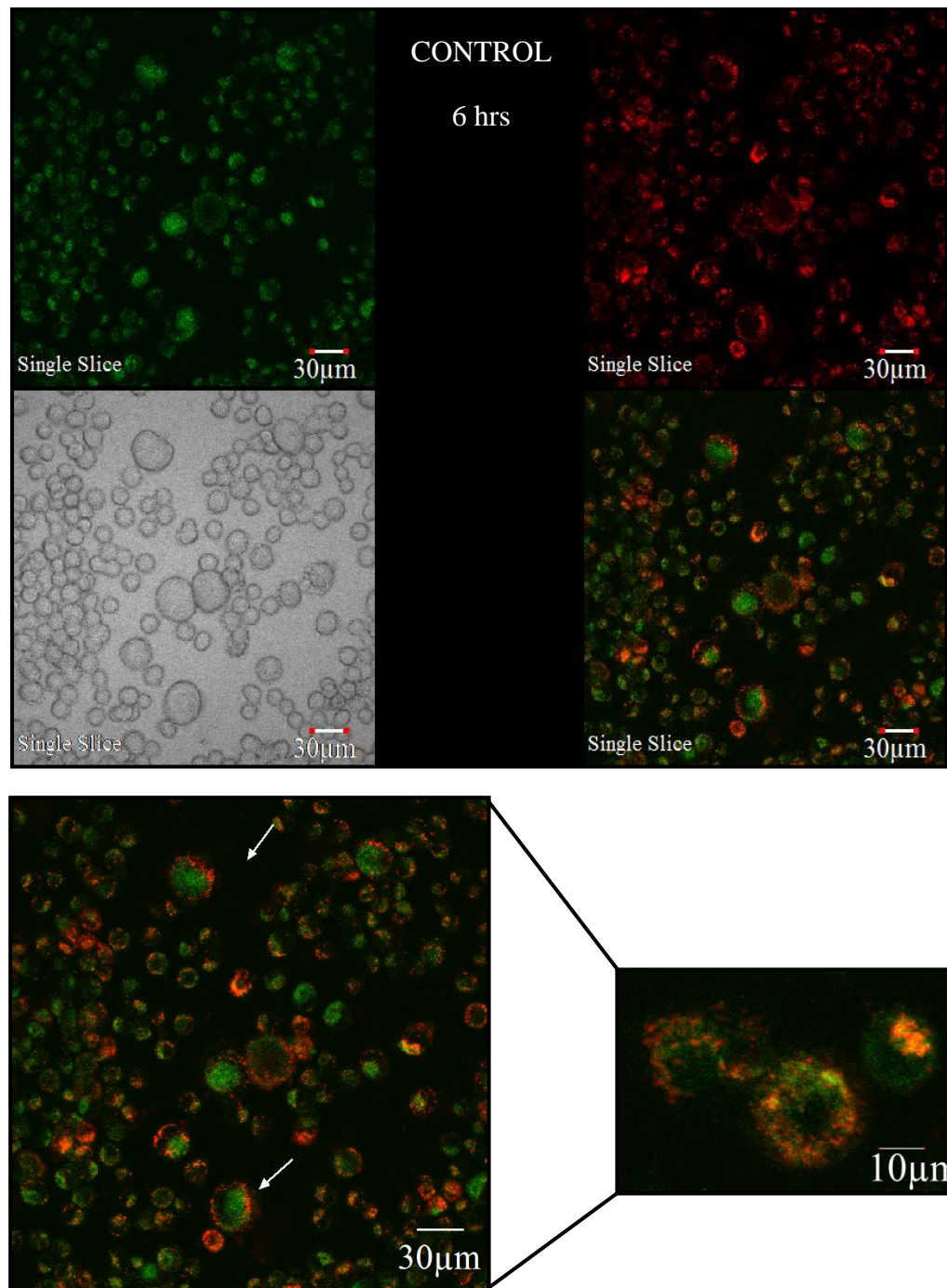


**Figure 68:** Mitochondrial membrane potential in HK-1 cells (control group) after 6 hrs (Fluoview 1000 laser scanning confocal microscope, Olympus IX 81 Motorized Inverted Microscope,  $\times 400$ ). Untreated cells showing strong J-aggregation and emits red fluorescence (indicated by white arrows). Single slices (red and green fluorescence) were stacked to obtain the final image.



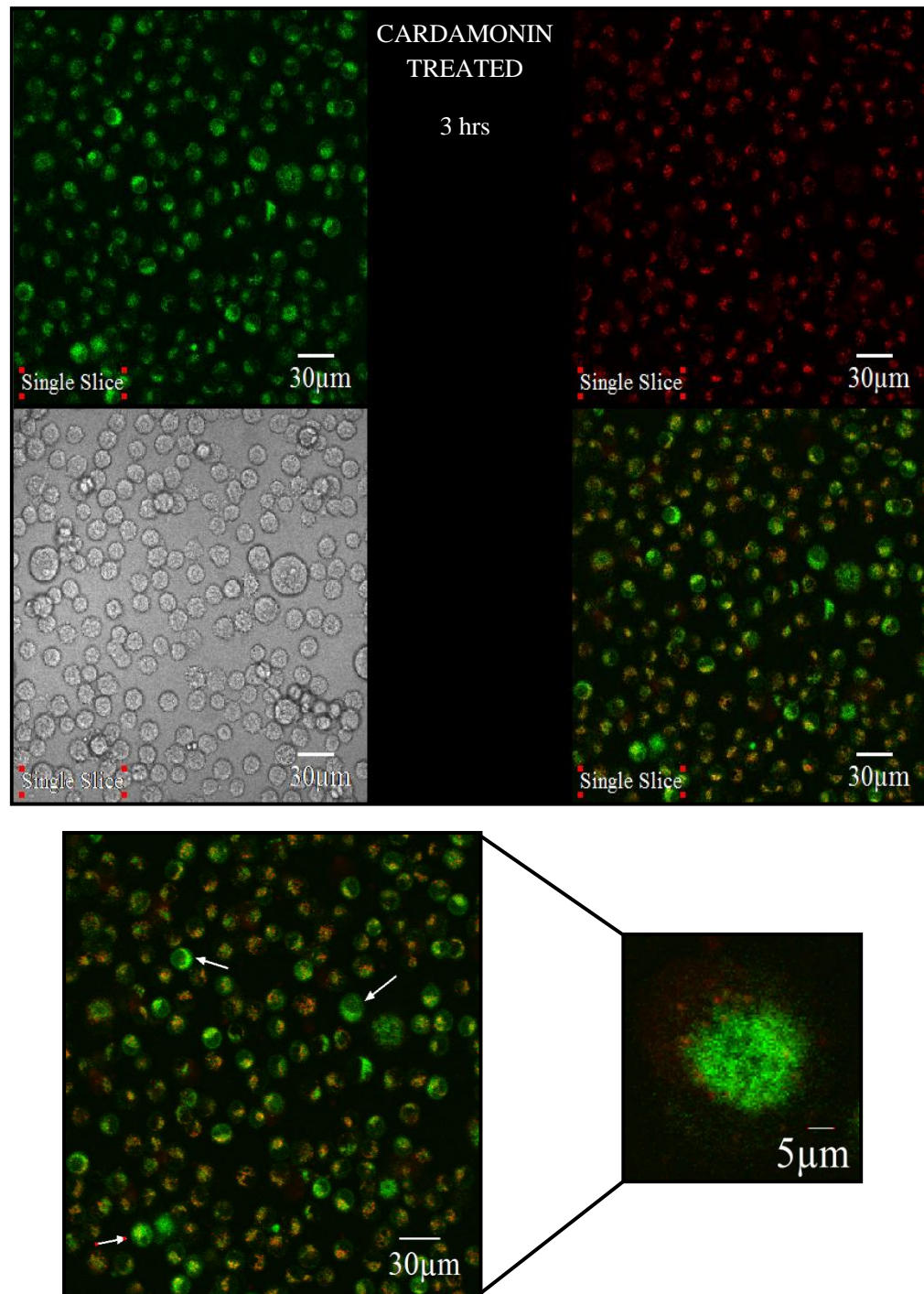


**Figure 69:** Effect of cardamonin on mitochondrial membrane potential in HK-1 cells after 3 hrs (Fluoview 1000 laser scanning confocal microscope, Olympus IX 81 Motorized Inverted Microscope,  $\times 400$ ). Untreated cells showing strong J-aggregation and emits red fluorescence (indicated by white arrows). Single slices (red and green fluorescence) were stacked to obtain the final image.

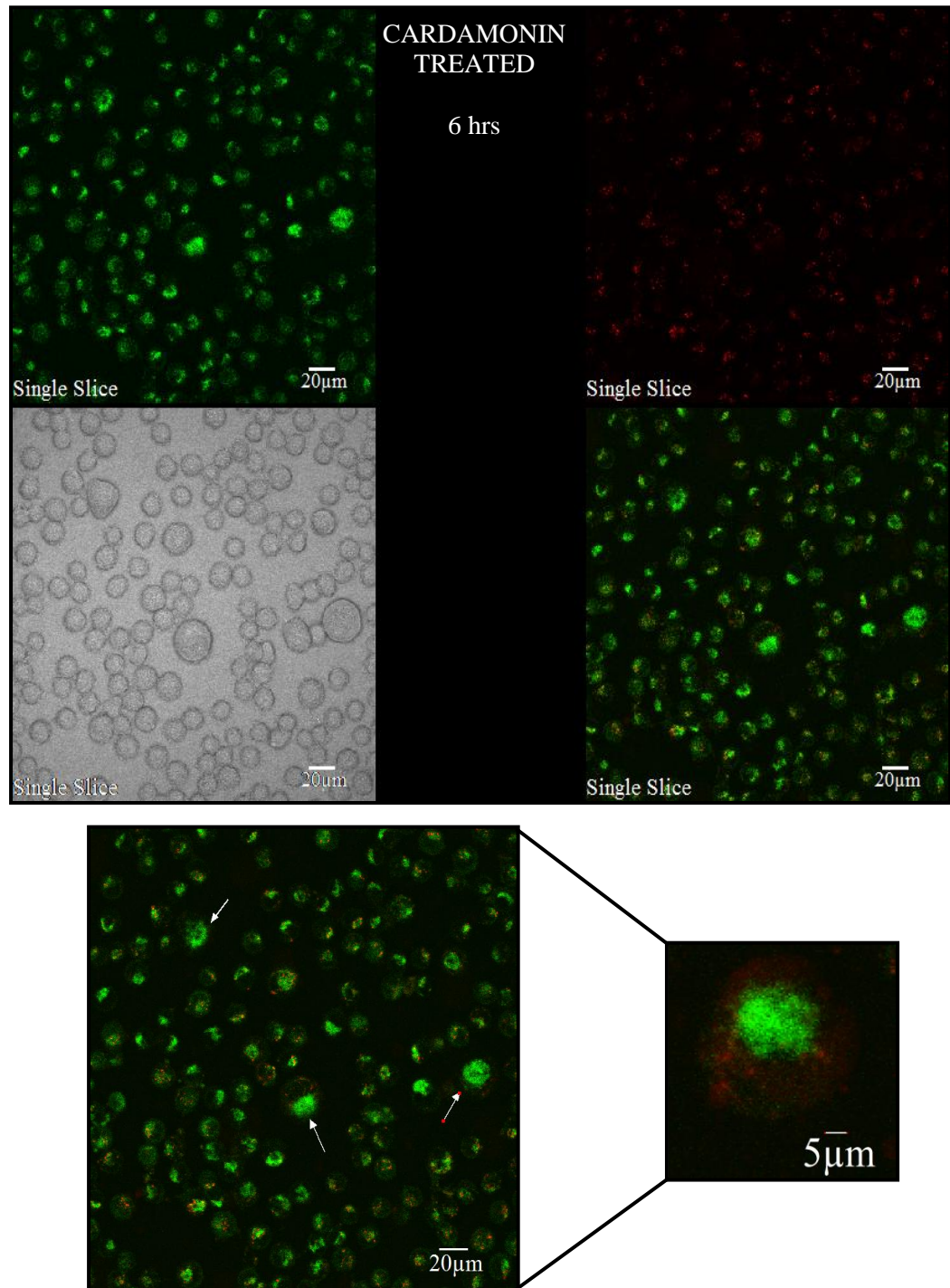


**Figure 70:** Effect of cardamonin on mitochondrial membrane potential in HK-1 cells after 6 hrs (Fluoview 1000 laser scanning confocal microscope, Olympus IX 81 Motorized Inverted Microscope,  $\times 400$ ). Untreated cells showing strong J-aggregation and emits red fluorescence (indicated by white arrows). Single slices (red and green fluorescence) were stacked to obtain the final image.

### **3.14 Cardamonin decreases intracellular ATP levels in HK-1 cells**

Cardamonin induces loss of membrane potential in our previous finding and hence we evaluate the level of intracellular ATP in HK-1 cells after treatment with cardamonin. In current research, an increase in intracellular ATP levels in control groups showed proliferating HK-1 cells. However, in cardamonin treated HK-1 cells, ATP levels decreased after 3 and 6 hrs was observed (**Figure 71A**).

Changes in intracellular ATP level was further analysed by interpretation of ADP/ATP ratio. No significant increase in ADP levels with an elevated ATP levels in cardamonin treated cells in relative to control cells signify cells proliferation (ADP=, ATP $\uparrow$ ). After 6 hrs of exposure to cardamonin, it was observed that ADP/ATP ratio increased in comparison to control HK-1 cells (**Figure 71B**).

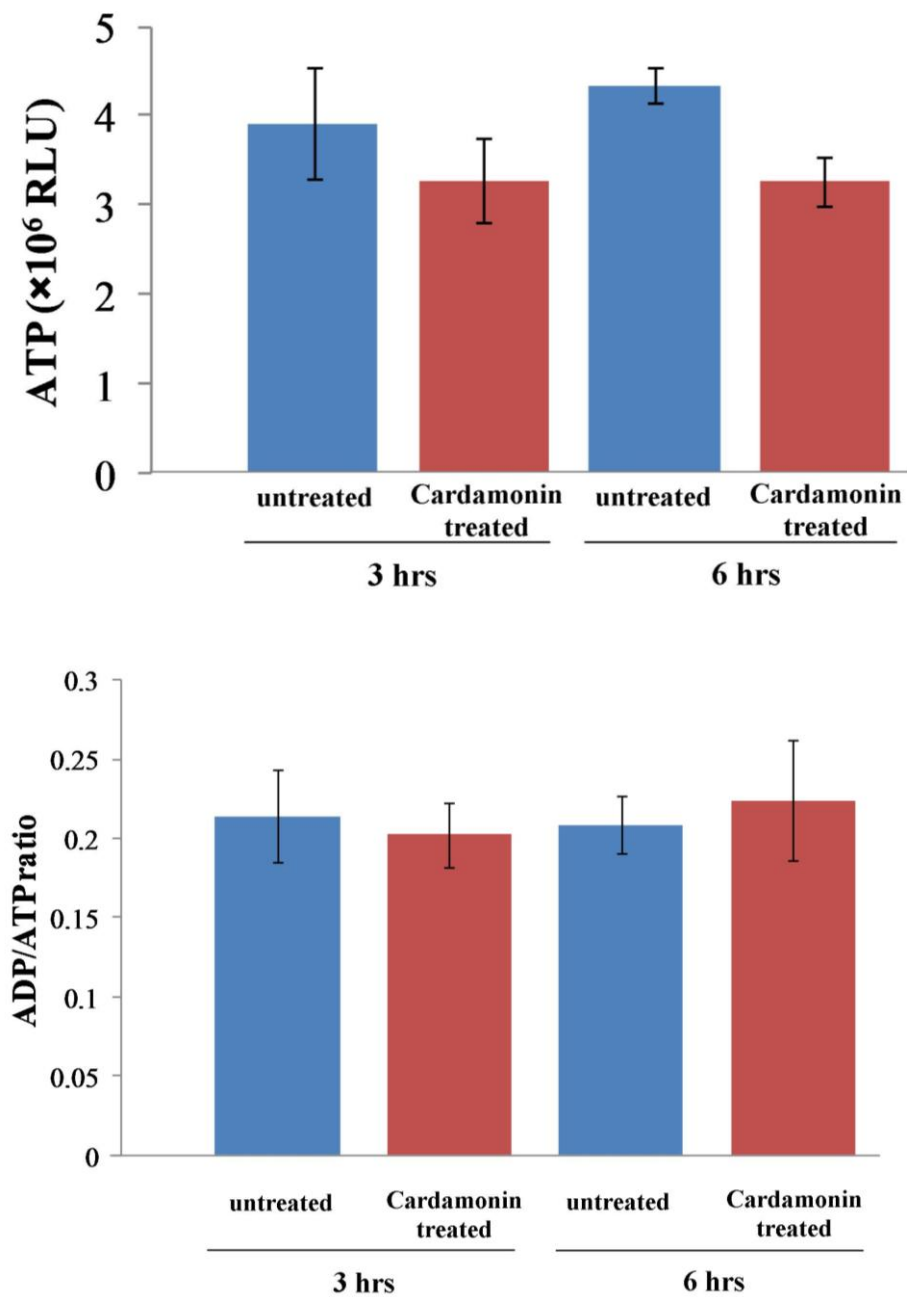


**Figure 71:** Effect of cardamonin on intracellular ATP levels (A) and ADP/ATP ratio (B) in HK-1 cells after 3 and 6 hrs. Each bar represents mean  $\pm$  standard deviation (S.D.) from there independent experiments (n=3).

### 3.15 Cardamonin induces cell death *via* activations of mitochondrial-dependent pathway associated proteins

#### 3.15.1 Protein separation using gel electrophoresis for 24, 48 and 72 hrs.

Proteins were extracted from HK-1 cells after exposure to cardamonin for 24, 48 and 72 hrs. Protein lysates from untreated control and treated HK-1 cells were separated using SDS-PAGE (**Figure 72**). Proteins were separated according to different molecular mass indicated by protein ladder. Proteins on gel were transferred to nitrocellulose membrane using electro blotting to determine expression levels of protein of interest.

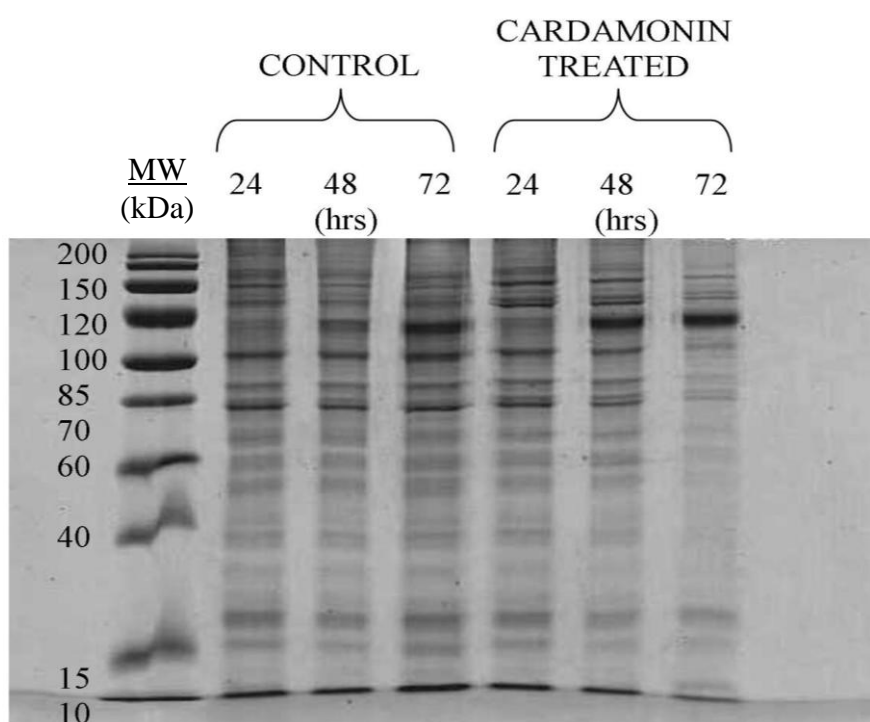


**Figure 72:** Protein lysates extracted from HK-1 cells treated with cardamonin at 24, 48 and 72 hrs were separated on 4% stacking gel and 12% resolving gel. Gel electrophoresis was run at 120V for 1 hr 15 mins.

### 3.15.2 Up-regulation of Bcl2-L1 anti-apoptotic protein level after 24 hrs cardamonin treatment

Electro blotting was initially conducted on detection of Bcl2-L1 anti-apoptotic protein using cell lysates from 24, 48 and 72 hrs cardamonin-induced HK-1 cells. Protein bands were observed at only 24 hrs (**Figure 73**). Mitochondrial dependent apoptotic pathway associated proteins will be investigated within 24 hrs as actions of Bcl2-L1 proteins were most active in the first 24 hrs of cardamonin treatment. The levels of all proteins of interest were observed in time-dependent manner at 3, 6, 9, 12, 18 and 24 hrs in cardamonin-treated HK-1 cells. Intensities of all protein bands were quantified using Quantity One 1-D Analysis Software to observe the expression of protein level with respect to control.

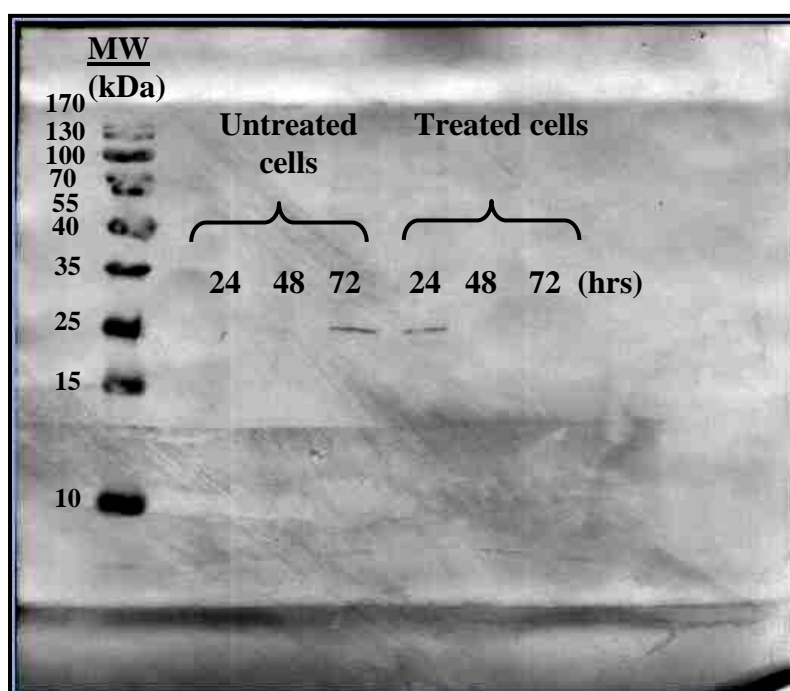


**Figure 73:** Bcl2-L1 protein expression for 24, 48 and 72 hrs in cardamonin-induced HK-1 cells. Expected molecular size: Approximately 26 kDa.



### 3.15.3 Protein separation using gel electrophoresis for untreated control and 3-24 hrs cardamomin-treated HK-1 cells

Proteins were extracted from HK-1 cells after exposure to cardamomin for 3, 6, 9, 12, 18 and 24 hrs. Protein lysates from untreated control and treated HK-1 cells were separated using SDS-PAGE (**Figure 74**). Proteins were separated according to different molecular mass indicated by protein ladder. Proteins on gel were transferred to nitrocellulose membrane using electro blotting to determine expression levels of protein of interest.

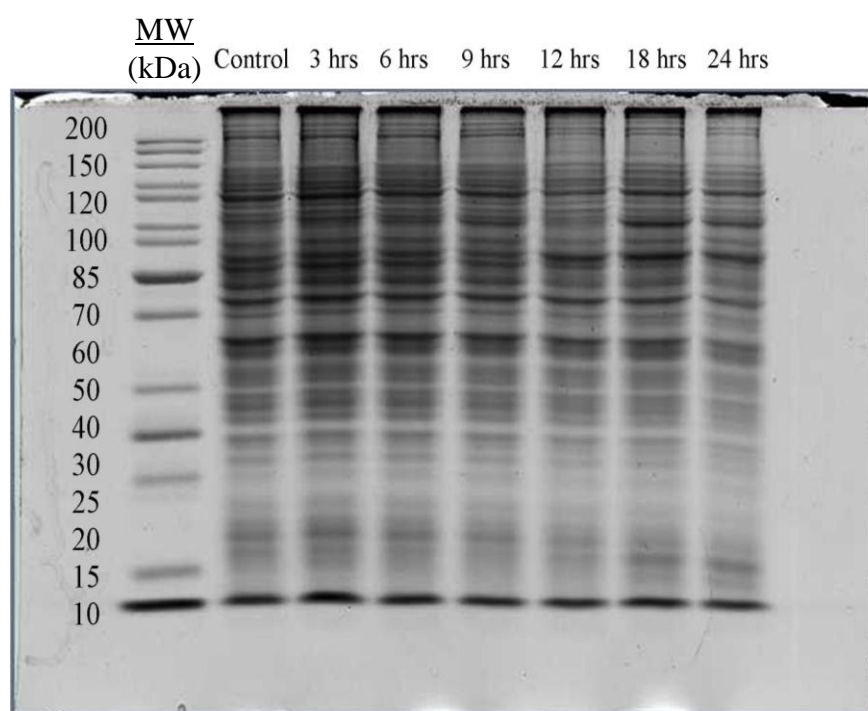


**Figure 74:** Protein lysates extracted from HK-1 cells treated with cardamomin at 3, 6, 9, 12, 18 and 24 hrs were separated on 4% stacking gel and 12% resolving gel. Gel electrophoresis was run at 120V for 1 hr 15 mins.

#### **3.15.4 Changes in mitochondrial-dependent pathway associated protein expression levels**

Proteins extracted from cardamonin-treated HK-1 cells at 3, 6, 9, 12, 18, 24 hrs and untreated control were separated on SDS-PAGE gel and blotted onto nitrocellulose membrane for detection of proteins associated with mitochondrial dependent pathway and their expression levels. Effect of mitochondrial dependent pathway associated proteins expression levels were summarized in **Figure 75 (Appendix 7.10.3)**. A significant decrease in Bcl-2 proteins was observed after 6 hrs of cardamonin exposure (**Figure 76**) where as cytochrome c level was highest at 6 hrs of cardamonin exposure (**Figure 79**). Approximately 12% decrease in Bcl-2 protein expression level was observed after 9 hrs of cardamonin exposure. Bcl-2 protein prevents the occurrence of apoptosis by inhibiting high release of cytochrome c between 3 to 6 hrs. However, as Bcl-2 proteins decreases, an increase in cytochrome c was observed at 6<sup>th</sup> hour.

Our findings showed that there was no significant change in Bcl2-L1 (also known as Bcl2-X<sub>L</sub>) anti-apoptotic protein level (**Figure 77**). Bad pro-apoptotic protein was not detected within 24 hrs of cardamonin exposure. A significant increase in Bax pro-apoptotic protein expression level was observed between 3 to 9 hrs of cardamonin exposure (**Figure 78**). More than 25% increase in Bax proteins within first 9 hrs after treatment with cardamonin.



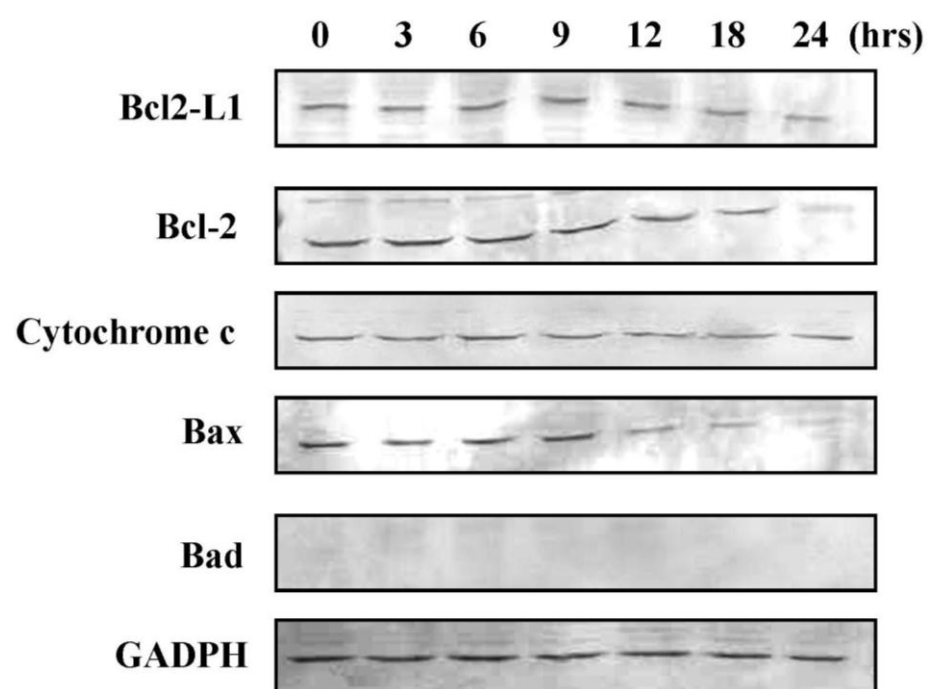


**Figure 75:** Changes in mitochondrial dependent pathway-associated protein expression levels were analyzed qualitatively by Western blotting. HK-1 cells were treated with 22  $\mu$ M of cardamomin for 3, 6, 9, 12, 18, 24 hrs and control was not treated. The levels of apoptosis-associated protein expressions; Bcl2-L1, cytochrome c, Bcl-2, Bad and Bax were analyzed using specific antibodies and GADPH was used as internal control for sample loading.

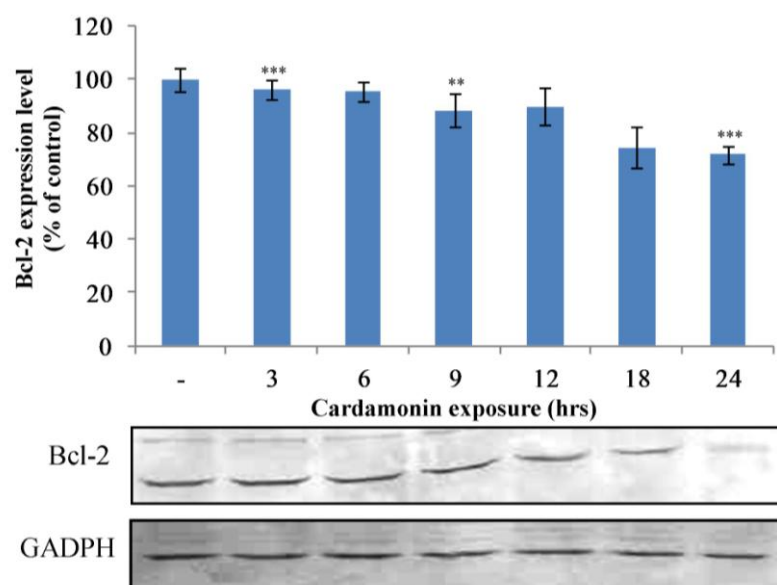


**Figure 76:** Effect of cardamonin on Bcl-2 protein expression level in time-dependent manner. Each bar represents the mean  $\pm$  standard deviation (S.D.) derived from three replicates reading. \*\*\* $P < 0.001$  and \*\* $P < 0.01$  indicate the statistical significant difference with respect to control.

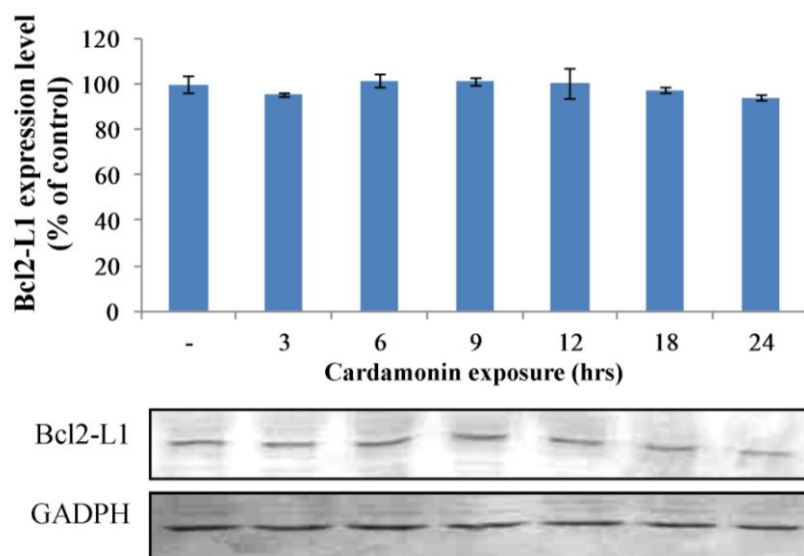


**Figure 77:** Effect of cardamonin on Bcl2-L1 protein expression level in time-dependent manner. Each bar represents the mean  $\pm$  standard deviation (S.D.) derived from three replicates reading.

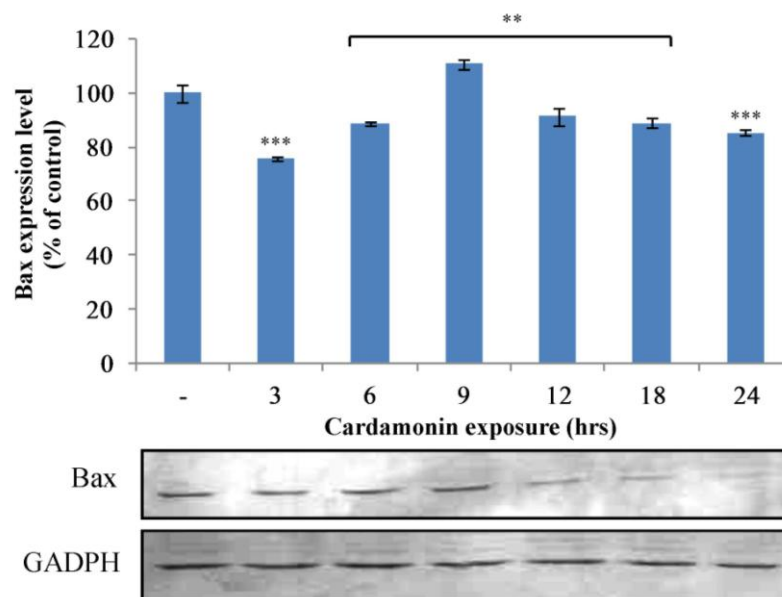


**Figure 78:** Effect of cardamomin on Bax protein expression level in time-dependent manner. Each bar represents the mean  $\pm$  standard deviation (S.D.) derived from three replicates reading. \*\*\* $P$ <0.001 and \*\* $P$ <0.01 indicate the statistical significant difference with respect to control.

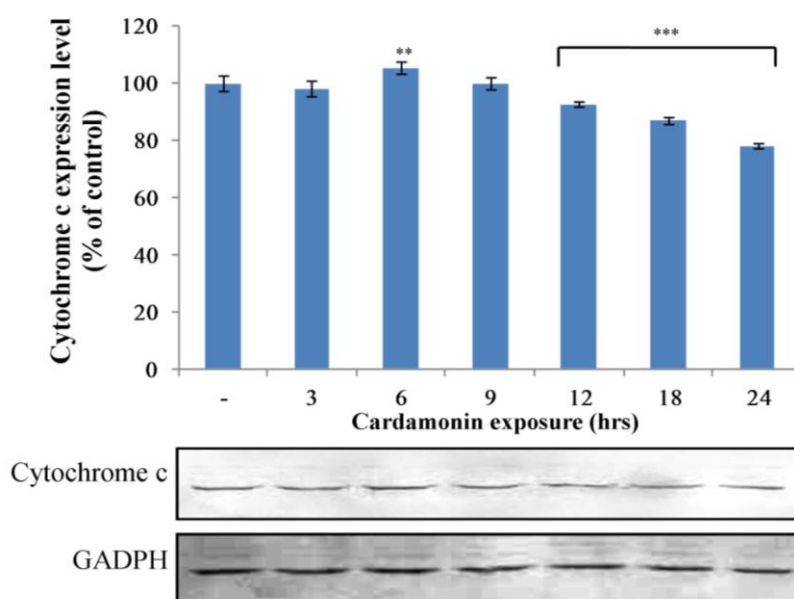


**Figure 79:** Effect of cardamomin on cytochrome c protein expression level in time-dependent manner. Each bar represents the mean  $\pm$  standard deviation (S.D.) derived from three replicates reading. \*\*\* $P$ <0.001 and \*\* $P$ <0.05 indicate the statistical significant difference with respect to control.

### **3.16 Mitochondrial-dependent apoptotic pathway occurs independent of caspase-9**

Total RNA was extracted from 24 hrs cardamonin-treated and non-treated HK-1 cells. Separation on agarose gel showed two distinct bands with detection of ribosomal RNA (more than 80% mammalian cells has ribosomal RNA) with 28S rRNA has twice the intensity and molecular mass of 18S rRNA (**Appendix 7.11.2**). RNA was quantified (**Appendix 7.11.1**) and used as starting material for relative quantification of gene expression level of caspase-9 using real time RT-PCR. Gene expression level of caspase-9 was measured in cardamonin-treated sample relative to control group. In addition, gene expression level of caspase-9 was normalized to the gene expression of a reference housekeeping gene, GAPDH based on  $C_T$  values obtained in real time RT-PCR (**Table 6**). Relative quantification (RQ) was obtained and expressed as fold difference in respective to reference gene. Livak method was employed to quantify the fold change (**Appendix 7.11.17**) and based on current results, it has been found that the normalized gene expression ratio is 1.04 (**Table 7**). There was no change in gene expression level after HK-1 cells were treated with cardamonin after 24 hrs. Caspase-9 is not involved in cardamonin-induced HK-1 cell death.

After 40 cycles of gene amplifications, melting curve analysis was run to assess the dissociation characteristics of double stranded DNA amplicons. Melting temperature of amplicons expressing caspase-9 in both control and cardamonin-treated groups was recorded at 82.9<sup>0</sup>C. As for amplified products

expressing GADPH housekeeping gene, melting temperature were 83.2<sup>0</sup>C and 82.6<sup>0</sup>C in control and cardamonin-treated group respectively (**Table 7**).

Based on the amplification plot (**Appendices 7.11.6 and 7.11.7**), in non-template control (NTC) of GADPH gene amplification, we observed an amplification primer after cycle 33. As NTC does not contain RNA template, amplification should not occur. We hypothesized that this amplification was due to primer-dimer effect. Melting curve analysis revealed that this amplification contributes to a peak with meting temperature of lower than true amplicons (**Appendices 7.11.10 and 7.11.11**) which further confirm the occurrence of primer-dimer effect.

Amplicons were separated on agarose gel electrophoresis to determine the molecular mass of amplicons. It was found that both amplicons responsible for caspase-9 and GADPH were located at approximately 125 bp and 100 bp (**Appendix 7.11.16**).

**Table 6: Threshold cycle ( $C_T$ ) values of caspase-9 and GADPH in control and cardamonin-treated groups.**

	Threshold cycle ( $C_T$ ) values	
	Gene of interest (Caspase-9)	Reference gene (GADPH)
<b>Control</b>	25.75 $\pm$ 0.15	14.33 $\pm$ 0.40
<b>Cardamonin treated</b>	26.66 $\pm$ 0.55	15.18 $\pm$ 0.57

**Table 7: Normalized gene expression ratio and melting temperature of caspase-9 and GADPH in control and cardamonin-treated groups.**

	Normalized gene expression ratio	Melting temperature ( $^{\circ}$ C)	
		Gene of interest (Caspase-9)	Reference gene (GADPH)
<b>Control</b>	-	82.9	83.2
<b>Cardamonin treated</b>	1.04	82.9	82.6

#### 4.0 DISCUSSION

Nasopharyngeal carcinoma (NPC) has long been associated with high occurrence rate in Chinese nationality and some who are of Asian ancestry. Compared to other types of cancers, NPC is considered rare but it has been affecting certain ethnic in Southern China for decades. Besides ethnic background, NPC also arises due to dietary habits such as high consumption of alcohol and salted food (Ning *et al.*, 1990). Since NPC is largely affected by dietary habits, we propose to explore the possibility of utilizing plant herbal sources as a potential approach in search for an anticancer agent. Hence, we begin with selection of several edible plants from different families that have been previously explored as potential and effective anticancer source. Five selected edible plants from different families, namely curry leaf (*Murraya koenigii*), temu kunci (*Boesenbergia rotunda*), spring onion leaf (*Allium cepa*), mushroom bean (*Phaseolus vulgaris*) and bunga kantan (*Phaeomeria imperialis*) were dried and macerated using three different solvents to extract compounds of different polarities. Various crude extracts obtained were qualitatively screened for presence of phytochemicals and evaluated for cytotoxic effect against NPC (HK-1) and normal immortalized nasopharyngeal epithelial (NP-69) cell lines.

Total phenolic contents of various crude extracts were determined using Folin-Ciocalteu's method. The Folin Ciocalteu's reagent was introduced by Otto Folin and Vintila Ciocalteu and has been used by many researchers to detect the presence of phenolic compounds. The reagent will react with phenols forming chromogens that can be detected spectrophotometrically. Colour is

developed due to the transfer of electrons at basic pH to reduce the phosphomolybdic/ phosphotungstic acid complexes. This will form the chromogen in which the metal ion in it will have a lower valence. Initially yellow in colour, the chromogen formed a blue coloured molybdenum oxide and measured at maximum absorbance 750 nm, at visible region of electromagnetic spectrum (Singleton *et al.*, 1974).

From the results, it was observed that methanolic crude extract of bunga kantan (*Phaemia imperialis*) has highest content of phenolic compounds compared to other crude extracts of bunga kantan (*Phaemia imperialis*) (**Figure 16**). Bunga kantan (*Phaemia imperialis*) inflorescence was previously extracted using 50% methanol and reported to contain high total phenols content compared to 100% acetone (Wijekoon *et al.*, 2011). Flowers of bunga kantan (*Phaemia imperialis*) have been reported to contain higher phenolic content when extracted with ethanol compared to with acetone (Chun *et al.*, 2009). In other research, ethyl acetate extract revealed very significant inhibitory effect against human T-4 lymphoblastoid (CEM-SS) and human breast cancer (MCF-7) cell lines (Habsah *et al.*, 2005). In most of the traditional Chinese medicinal plants, high phenolics content was associated with high anticancer and antioxidant activities. (Cai *et al.*, 2003). High amount of phenolic compounds were isolated from *Garcinia mangostana* fruit pericarp and positive results were obtained in anticancer testing (Yu *et al.*, 2009). Researchers discovered there was high amount of phenolic in extra virgin olive oil which resulted in high antiproliferative and anticancer activities (García-Villalba *et al.*, 2010). In recent years, research focus on the goodness and



astonishing function of food in protecting body health because food is the safest source of remedy against disease.

However, there was no significant correlation between total phenolic content of methanolic crude extract of bunga kantan (*Phaemia imperialis*) and its cytotoxic activity. Methanolic crude extract of bunga kantan (*Phaemia imperialis*) did not inhibit HK-1 cell proliferation. Total phenolic content in ethyl acetate crude extract of temu kunci (*Boesenbergia rotunda*) was reported to be highest followed by ethyl acetate crude extract of curry leaf (*Murraya koenigii*). There were no significant correlations between total phenolic content of ethyl acetate crude extracts of curry leaf (*Murraya koenigii*) and temu kunci (*Boesenbergia rotunda*) and cytotoxic activity against HK-1 cell line. It may suggest that phenolics compounds present did not contribute to inhibitory effect against HK-1 cell line.

From the phytochemical tests, it was revealed that saponins were found in all crude extracts of bunga kantan (*Phaemia imperialis*) (**Table 1**). Similarly, 80% methanol was used for extraction of flower of bunga kantan (*Phaemia imperialis*) and phytochemical screening revealed the presence of saponins (Lachumy *et al.*, 2010). Saponins are responsible for some anticancer activities using crude extracts from therapeutic plants. The increase in composition of saponins in root of *Panax notoginseng* resulted in antiproliferative effect against cancer cells when it undergoes steaming at different times and temperatures (Sun *et al.*, 2010). Overall functions of saponins include anti-inflammatory activity, antifungal activity, antibacterial activity, antiparasitic activity, antiviral activity and antitumor activity (Sparg *et*

*al.*, 2004). The main component of Chinese traditional medicine *Pari polyphylla*, the *Rhizoma Paridis Saponins* (RPS) has demonstrated the effect to induce apoptosis and inhibit metastasis in mouse lung (Man *et al.*, 2009). However, the presence of saponins has no correlation with cytotoxic activity against HK-1 cell line as all crude extracts of bunga kantan (*Phaemeria imperialis*) did not exhibit cytotoxic effect against HK-1 cell line although saponins were present in all crude extracts.

Phytochemical analyses revealed that flavonoids and alkaloids were present in all crude extracts of temu kunci (*Boesenbergia rotunda*). Total flavonoid content was determined using Dowd method (**Figure 80**). Aluminium chloride was used to form acid stable complexes with C-4 keto group and either C-3 or C-5 hydroxyl groups of flavonoids.

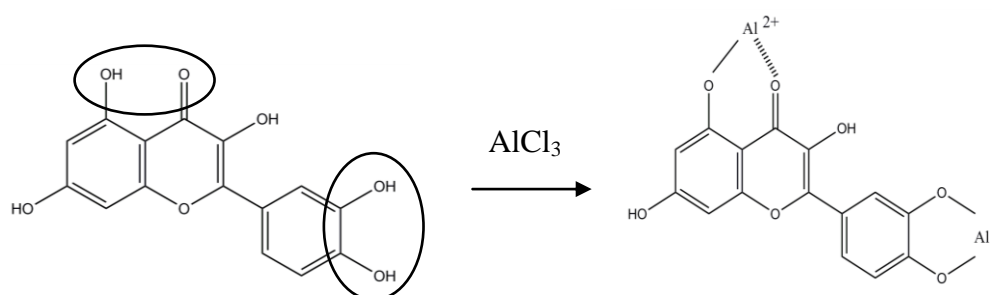


**Figure 80:** Dowd method

Quercetin was used as a standard in current research and it formed complexes with ortho-dihydroxyl groups at maximum absorbance of 415nm (Chang *et al.*, 2002). From current results, ethyl acetate crude extract of temu kunci (*Boesenbergia rotunda*) was found to contain highest amount of flavonoid with  $833.0 \pm 12.63$  mg of quercetin equivalents in 1 g of sample. However, there was no correlation between total flavonoid content and cytotoxic activity.

Methanolic and hexane crude extracts of temu kunci (*Boesenbergia rotunda*) revealed more than 50% cell growth inhibition against HK-1 cell line but ethyl acetate crude extract of temu kunci (*Boesenbergia rotunda*) was found to contain highest content of flavonoids. However, total flavonoid content of methanolic and hexane crude extracts were relatively high with  $269 \pm 6.960$  mg of quercetin equivalents in 1 g of sample and  $243.7 \pm 4.330$  mg of quercetin equivalents in 1 g of sample respectively. This suggests that cytotoxic effect against HK-1 cell line may be from the action of flavonoids present in both crude extracts.

Both methanolic crude extracts of spring onion leaf (*Allium cepa*) and mushroom bean (*Phaseolus vulgaris*) revealed the presence of tannins and phlobatannins but there were no correlations with cytotoxic effects against HK-1 cell line.

Cytotoxic activities of various crude extracts were tested using MTT assay to determine inhibitory concentration ( $IC_{50}$ ) of each crude extract against human nasopharyngeal carcinoma (HK-1) and immortalized nasopharyngeal epithelial cell line (NP-69) cell lines. MTT assay was conducted to measure cell viabilities after treated with various crude extracts at different concentrations and time point. Methanolic and hexane crude extracts of curry leaf (*Murraya koenigii*) showed  $IC_{50}$  values of  $177.7 \pm 3.684$   $\mu\text{g/mL}$  and  $88.92 \pm 2.602$   $\mu\text{g/mL}$  respectively compared to positive control 5-fluorouracil with  $IC_{50}$  value of  $42.25 \pm 2.246$   $\mu\text{g/mL}$  (**Figures 22; 24; 34**). Simultaneously, methanolic and hexane crude extracts of curry leaf (*Murraya koenigii*) showed a low cytotoxic activity against NP-69 cell line with  $IC_{50}$  value of more than

200  $\mu\text{g/mL}$  (**Figures 39; 41**). This suggests that both methanolic and hexane crude extracts of curry leaf (*Murraya koenigii*) have significantly inhibited growth of HK-1 cell line.

It has been previously reported that alkaloids isolated from curry leaf displayed anticancer effect. Koenoline (**Figure 81A**), a carbazole alkaloid isolated from root bark of curry leaf (*Murraya koenigii*) using chloroform was found to exhibit cytotoxic effect against human malignant KB cell line (Fiebig *et al.*, 1985). Methyl group introduced at various positions on the aromatic ring in koenoline is able to bind to DNA by bis-intercalation and activates DNA repair processes. The structure is similar to ditercalinium (**Figure 81B**), a synthetic nucleic acid binder which acts as an anticancer drug (Léon *et al.*, 1987).

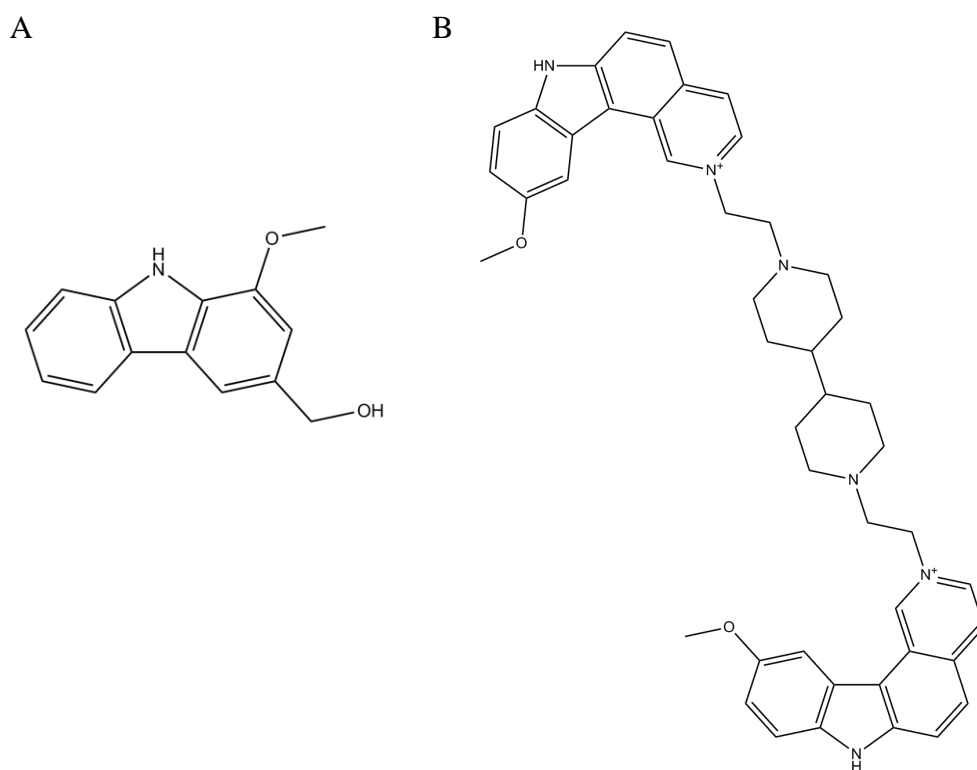
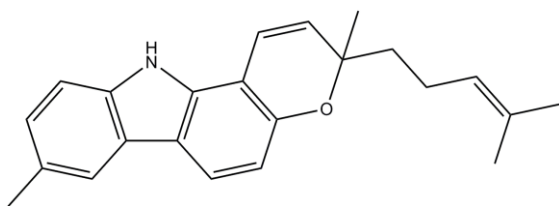


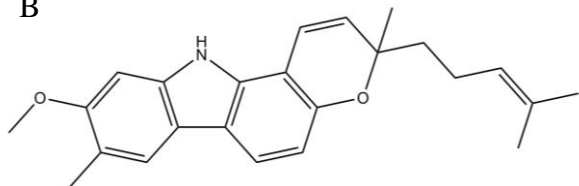
**Figure 81:** (A) Structure of koenoline. (B) Structure of ditercalinium.

In another study, isolation of curry leaf (*Murraya koenigii*) in methanolic and ethyl acetate extracts yield 2 new alkaloids and 12 existing carbazole alkaloids. Mahanimbicine (**Figure 82A**) and murrayamine-E (**Figure 82B**) have significantly exhibited cytotoxic affect against B16 melanoma 4A5 cell line. 4-hydroxycarbazole showed moderate cytotoxic activity. The presence of hydroxyl and terpenyl groups may contribute to inhibitory effect against melanogenesis. (Nakamura *et al.*, 2013). Hydro-methanolic extract of curry leaf (*Murraya koenigii*) has successfully induced cell death in two cancer cell lines, MCF-7 and MDA-MB-231. This study suggests the presence of bioactive compound in curry leaf (*Murraya koenigii*) that may be a source of proteasome inhibitor that leads to cancer cell apoptosis (Noolu *et al.*, 2013). Three out of ten carbazole alkaloids isolated from curry leaf (*Murraya koenigii*) isolated using acetone solvent were shown to induce apoptosis in human promyelocytic leukemia (HL-60) cell line through caspase-9/caspase-3 pathway. Mahanine (**Figure 82C**), pyrayafoline (**Figure 82D**) and murrayafoline (**Figure 82E**) were able to induce loss of mitochondrial membrane potential of HL-60 cells (Ito *et al.*, 2006).

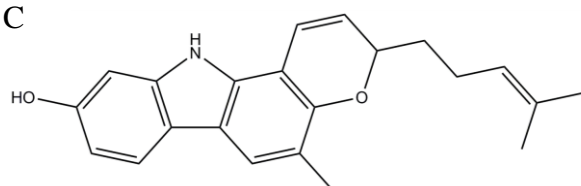
A



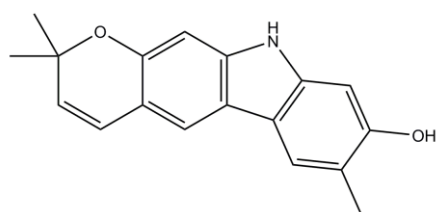
B



C



D



E

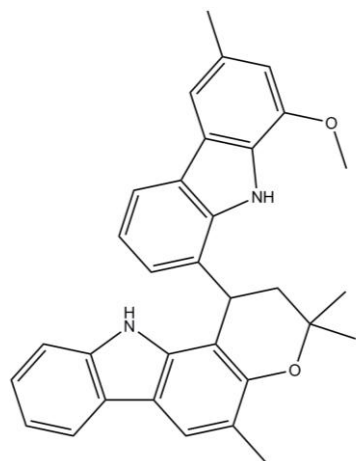


**Figure 82:** (A) Structure of mahanimbicine. (B) Structure of murrayamine. (C) Structure of mahanine. (D) Structure of pyrayafoline. (E) Structure of murrayfoline.

From these results, it was found that there was no significant correlation between the phenolic content and the cytotoxic activities of cell lines. Although ethyl acetate crude extracts of curry leaf (*Murraya koenigii*) and temu kunci (*Boesenbergia rotunda*) showed higher total phenolic compounds, they resulted in lower cytotoxic activities compared to methanolic and hexane crude extracts of curry leaf (*Murraya koenigii*) and temu kunci (*Boesenbergia rotunda*).

Few assumptions can be made from the results. First, there may be an overestimation of phenolics content in the crude extracts. The Folin-Ciocalteu assay conducted on samples may have several external effects. The colour formation during the assay was based on chemical reduction of the reagent. During the reaction, interference from other compounds present in crude extracts such as sugar might lead to a higher absorbance reading than what should be recorded (Singleton and Rossi, 1965). Besides that, Folin-Ciocalteu assay is only able to detect all compounds that have phenol as functional group. When comparing the data with a single standard, it is can be misleading as the compounds analyzed might not be the phenolic compounds that contribute to cytotoxic activity against cancerous cell line (Waterhouse, 2002).

Methanolic and hexane crude extracts of temu kunci (*Boesenbergia rotunda*) showed IC<sub>50</sub> values of 138.6±8.805 µg/mL and 77.86±2.839 µg/mL respectively compared to positive control 5-fluorouracil with IC<sub>50</sub> value of 42.25±2.246 µg/mL (**Figures 25; 27; 34**). Simultaneously, methanolic and hexane crude extracts of temu kunci (*Boesenbergia rotunda*) showed low cytotoxic activity against NP-69 cell line with IC<sub>50</sub> value of more than 200 µg/mL (**Figures 42; 44**). This suggests that both methanolic and hexane crude

extracts of temu kunci (*Boesenbergia rotunda*) too have significantly inhibited growth of HK-1 cell line although both IC<sub>50</sub> were higher than positive control 5-fluorouracil with IC<sub>50</sub> value of 42.25±2.246 µg/mL. IC<sub>50</sub> value of methanolic crude extract of temu kunci (*Boesenbergia rotunda*) was approximately three-fold higher than IC<sub>50</sub> value of hexane crude extract of temu kunci (*Boesenbergia rotunda*). Phytochemicals in hexane crude extract of temu kunci (*Boesenbergia rotunda*) may potentially exert greater cytotoxic effect against HK-1 cells compared to methanolic crude extract of temu kunci (*Boesenbergia rotunda*).

Several literatures have been previously published on the discovery of temu kunci (*Boesenbergia rotunda*) in inhibition of cancer cell growth. Rhizomes of temu kunci (*Boesenbergia rotunda*) were extracted using methanol and four new prenylcalcones and four new prenylflavanones were isolated. All eight constituents have revealed inhibitory effect against tumor necrosis factor- $\alpha$  (TNF- $\alpha$ )-induced in murine aneuploid fibrosarcoma (L929) cells (Morikawa *et al.*, 2008). Synthetic methoxy-chalcone and fluoro-chalcone derivatives such as 4-trifluoromethyl-2'-methoxychalcone and 3-trifluoromethyl-2',4'-dimethoxychalcone have been reported to induce apoptosis in human melanoma (A375) cell line. Methoxy and trifluoromethyl groups in the chalcone skeleton may contribute to the inhibitory effect (Henmi *et al.*, 2009). Synthetically derived 4'-chloroflavanone showed a significant inhibitory effect against human breast cancer cells compared to treatment with flavanone. Halogenated flavanone was proved to be more potent at causing cytotoxic effect compared to just flavanone (Choi *et al.*, 2010). Hence, we are



interested to investigate if crude extracts of temu kunci (*Boesenbergia rotunda*) will demonstrate similar cytotoxic effect against HK-1 cells.

To conclude first part of this research, phytochemical analyses revealed the presence of flavonoid and alkaloids in all crude extracts of temu kunci (*Boesenbergia rotunda*) and curry leaf (*Murraya koenigii*). Methanol and hexane crude extracts of curry leaf (*Murraya koenigii*) and temu kunci (*Boesenbergia rotunda*) showed higher IC<sub>50</sub> values (164.55 and 88.91 µg/mL respectively for curry leaf and 138.48 and 78.48 µg/ml respectively for temu kunci) relative to positive control 5-fluorouracil (42.67 µg/mL) against HK-1 cell line. All plant crude extracts showed weak cytotoxic activity with IC<sub>50</sub> value of more than 200 µg/ml against NP-69 cell line. Hence, the results of present study indicate that methanol and hexane crude extracts of temu kunci (*Boesenbergia rotunda*) and curry leaf (*Murraya koenigii*) contained potential bioactive compounds that can be further investigated for anticancer activity.

Based on preliminary cytotoxic tests using crude extracts macerated from temu kunci (*Boesenbergia rotunda*), methanol and hexane crude extracts were shown to display cytotoxic effect against HK-1 cells. Hence, four commercially available flavonoids and polyphenols were selected. Naringin and hesperidin are polyphenols that were previously isolated using methanol solvent (Jing *et al.*, 2010) similar to our current result using methanol crude extract from temu kunci (*Boesenbergia rotunda*). Cardamonin and pinostrobin are flavonoids that were previously isolated using hexane solvent (Ching *et al.*, 2007). Similarly, hexane crude extract exhibit cytotoxic effect against HK-1 cell line in current result. Hence, all four compounds were tested against HK-1 and NP-69 cell lines. Among all four tested compounds, cardamonin displayed

highest cytotoxic effect against HK-1 cells without affecting normal NP-69 cell line.

Further tests were conducted to observe and quantify HK-1 cell death. The hallmark of apoptosis is defined by Kerr *et al.* as cell morphology alteration which includes cell shrinkage, chromatin condensation, plasma membrane blebbing (irregular in shape) and eventually apoptotic body formation (Kerr *et al.*, 1972). These morphology changes differ from necrosis, which is characterized by membrane disruption and cell swelling (Edinger and Thompson, 1972). Cardamonin triggers HK-1 cell morphological change and caused uneven shape in HK-1 cells under light microscopic observation (**Figure 57**). More than half of the cells were stained with trypan blue (only stained dead cells) after 24 hrs treated with cardamonin (**Figure 55**). These non-viable cells have greater affinity to take up trypan blue dye.

Acridine Orange (AO) and propidium iodide (PI) fluorescent dyes were utilized to observe stages of apoptosis in HK-1 cells viewed under fluorescence microscope. AO is able to permeate cells and bind to their DNA forming complex. A molecule of AO intercalates three base pairs of double stranded DNA and emits green fluorescence (Zbigniew, 1990). In current observations, most HK-1 cells stained were emitting green fluorescence more densely in the centre, in the area of chromatin (**Figure 58**). This suggests that most cells were undergoing early apoptosis. In addition, cell-impermeable propidium iodide (PI) fluorescent dye stained HK-1 cells that are undergoing late apoptosis with exposed DNA due to ruptured membrane. Most cells emit red orange fluorescence and formed clumps.

Since early apoptosis was proven to occur within first 24 hrs, we further investigate cell cycle arrest within 24 hrs of cardamonin treatment. HK-1 cell cycle was arrested at G2/M phase after 12 hrs of cardamonin treatment (**Figure 61**). Number of cells in G2/M phase was recorded at least 19-fold increase compared to G2/M phase in control group. Similarly, aloe-emodin was previously reported to induce apoptosis in NPC by arresting G2/M phase in cell cycle (Lin *et al.*, 2010). Curcumin was also reported to induce apoptosis in NPC by arresting G2/M phase after 6 hrs of treatment (Kuo *et al.*, 2011).

As discussed earlier, caspases play important roles in the activation of apoptosis and hence the activity of caspase-3 and caspase-8 were studied. Caspase activity is greatly dependent on time of exposure of an apoptosis-inducing agent. A Rhodamine-linked peptide was used as a substrate to measure caspase activity upon induction of apoptosis. The rhodamine-linked peptide is a fluorogenic substrate that contains two DEVD tetrapeptides, (Ac-DEVD)<sub>2</sub>-R110. Caspase-3 present in *in vitro* experiment will cleave the first DEVD peptide at recognition site DEVD where cleavage occurs at second D, the aspartic acid. This will form an intermediate monopeptide which only emit about 10% of the fluorescence (Hug *et al.*, 1999). Successive cleavage of the monopeptide by caspase-3 releases a greater green fluorescence dye. In short, *Bis*-substituted peptide derivatives of rhodamine 110 was cleaved intracellularly by activated caspase into mono-substituted rhodamine 110 (which emits green fluorescence) and a free rhodamine 110 molecule. This green fluorescence is measured under fluorescence excitation of 470 nm (Rothe *et al.*, 1992). As for caspase-8, the fluorogenic substrate contains two IETD

tetrapeptides, (Ac-IETD)<sub>2</sub>-R110 which targets the cleavage at recognition site IETD.

Current results revealed that after 24 hrs treated with cardamonin, caspase activity was greatly amplified in HK-1 cells. More than 18% increase in caspase-3 activity was recorded for the first 24 hrs in cardamonin-treated HK-1 cells (**Figure 62**). At the same time, about 26% increase in caspase-8 activity. However, both caspase-3 and -8 activities decreased after 24 hrs of treatment. It was previously found that in Jurkat cells, caspase-8 activity was optimum only after 3 hrs of drug treatment while caspase-3 activity peaked at 7<sup>th</sup> hour (Farhan *et al.*, 2004). This aptly explained caspase-8 activity was relatively higher than caspase-3 in current findings. An increase in caspase-3 activity triggers DNA fragmentation which is an indication of apoptosis as reported by Jänicke *et al.* (Jänicke *et al.*, 1998). In current findings, DNA samples extracted from cardamonin-treated HK-1 cells were found to be fragmented. It has been previously reported that caspase-3 is indeed required for DNA fragmentation leading to morphological changes in cancer cells. DNA is being fragmented at internucleosomal linker sites because these sites are easily accessible by Caspase-Activated DNase (CAD) enzyme. CAD forms a complex with an inhibitor, the Inhibitor of Caspase-Activated DNase (ICAD) which inactivates CAD. Caspase-3 cleaves the complex and leaving CAD to be in active form and hence degrades nuclear DNA (Enari *et al.*, 1998). Therefore, caspase plays a crucial role in DNA fragmentation. To further prove that caspase-3 is essential for DNA fragmentation, deletion of 47-base pair within exon 5 of *CASP-3* gene in breast carcinoma cell line was proven to induce cell death but no DNA fragmentation and cell shrinkage were observed (Jänicke *et*

*al.*, 1998). It can be concluded that the up-regulation of caspase has greatly contributed to the distinct morphological changes in HK-1 cells i.e. DNA fragmentation.

Studies have suggested that caspase-8 mediates apoptosis in NPC which leads to activation of mitochondrial-dependent pathway through regulations of Bcl-2 family proteins (Lin *et al.*, 2010). Cardamonin has been proven to trigger apoptosis through caspase-activation in nasopharyngeal carcinoma (HK-1) cells. Thus, based on current findings, we study regulation of Bcl-2 family proteins in mitochondrial-dependent cell death pathway to discover mode of actions of cardamonin in affecting basic functions of mitochondria.

Regulation of pro-apoptotic and anti-apoptotic proteins belonging to Bcl-2 family has great influence in triggering cell death by promoting the cell's susceptibility to apoptotic stimuli (Wang and Youle, 2009). In our study, we treated nasopharyngeal carcinoma cell line, HK-1 with 22 µg/mL of cardamonin in time-dependent manner (24, 48 and 72 hrs). Cell lysates containing proteins extracted from HK-1 cells treated with cardamonin at 24, 48 and 72 hrs were separated on 4% stacking and 12% resolving Tris-HCl SDS-PAGE gel. Gel was then blotted onto a nitrocellulose membrane for Bcl2-L1 protein detection. Level of Bcl2-L1 protein expression was initially investigated in 24, 48 and 72 hrs cardamonin-treated HK-1 cells (**Figure 73**). It was found that protein bands were detected only within 24 hrs of treatment with cardamonin. It can be deduced that mode of actions of Bcl2-L1 proteins were most effective within 24 hrs after treated with cardamonin. Lin *et al.* reported an up-regulation of Bcl-2 protein in nasopharyngeal carcinoma cells

treated with aloe-emodin was observed from 0 to 24 hrs. However, after 24 hrs, a sharp decrease of Bcl-2 protein expression was observed (Lin *et al.*, 2010). Hence, expression levels of all other proteins associated with mitochondrial dependent pathway were investigated from 0 to 24 hrs in cardamonin-induced HK-1 cells.

Bcl-2 proteins showed significant decrease after 6 hrs of cardamonin exposure whereas cytochrome c level (5% increased compared to control group) was highest at 6 hrs of cardamonin exposure (**Figure 75**). Recent report showed that down-regulation of Bcl-2 proteins level permits release of cytochrome c into cytosol in curcumin-treated human nasopharyngeal carcinoma cells (Kuo *et al.*, 2011). Hence, drop in Bcl-2 proteins may assist in release of cytochrome c in HK-1 cells. Bad pro-apoptotic protein was not detected within 24 hrs of cardamonin exposure. This suggests that Bad pro-apoptotic was not involved in regulation of mitochondrial cell-death pathway. Previous literature suggested that this BH3-only member protein of Bcl-2 family may act as a sensitizer that binds to only pro-survival proteins to activate cell death (Willis and Adams, 2005). Hence, Bad protein was not entirely required for activation of mitochondrial-dependent apoptotic pathway.

Bax pro-apoptotic protein expression level increased after 9 hrs (10% increased compared to control group) treated with cardamonin (**Figure 78**). Previous study showed that when Bcl-X<sub>L</sub>, an anti-apoptotic protein expression level decreases as Bax pro-apoptotic protein expression level increases, this regulation of Bcl-2 family proteins promote the release of cytochrome c and led to an up-regulation of caspase-3 thus triggered apoptosis in nasopharyngeal

carcinoma cell lines (NPC-TW039 and NPC-TW076) treated with bioactive compound isolated from rhizomes of *Rheum palmatum* (Lin *et al.*, 2010). Kuo *et al.* reported that when NPC-TW076 was exposed to a potent anticancer agent, curcumin in time-dependent manner, cell death pathway was activated. An up-regulation of Bax protein level accompanied by down-regulation of Bcl-2 protein level led to malfunction of mitochondria and subsequently triggered an activation of caspase-3 leading to cell death (Kuo *et al.*, 2011). Bax undergoes homodimerization and translocates from cytosol to mitochondria causing a stimulated death in cell to be activated. Under circumstances where Bcl-2 is present, cells are protected by blocking the translocation of Bax pro-apoptotic proteins (Gross *et al.*, 1998). Similarly, current results increase in Bax pro-apoptotic protein showed that it greatly contributes to cellular apoptosis in HK-1 cells.

To conclude second part of the research, Bcl-2 family proteins function as regulators that work collaboratively in execution of cell death. This study demonstrates that mitochondrial cell-death pathway was triggered through an increase in Bax pro-apoptotic proteins by inhibiting Bcl-2 anti-apoptotic proteins to release death stimuli (proven by an increase in cytochrome c expression level).

We next explore changes of mitochondrial membrane potential and how it affects generation of ATP followed by gene expression level of caspase-9 in cardamonin-treated HK-1 cells. The permeability of mitochondrial membrane to allow protein translocation is greatly dependent on the activity of caspase. Caspase activation induces permeabilization of mitochondrial

membrane to allow protein BID cleavage to an active fragment, tBID and thus being translocated to OMM. The initial signal triggered from caspase activation will be transmitted to release apoptogenic factors such as cytochrome c (Luo *et al.*, 1998). These factors bind to apoptosis activating factor to form complex in order to activate the release of caspase-9 and hence stimulates apoptosis.

Earlier results suggest that caspase-8 activity was significantly amplified in HK-1 cells within first 24 hrs after treated with cardamonin. Caspase-8 cleavage leads to translocation of Bid (pro-apoptotic protein) to membrane of mitochondria. This causes recruitment of another pro-apoptotic protein, Bax to stimulate opening of mitochondrial PTP. Hence, we evaluate mitochondrial membrane potential ( $\Delta\Psi_m$ ) after exposure to cardamonin in time-dependent manner. Cardamonin induces loss of mitochondrial membrane potential in HK-1 cells after 6 hrs of treatment (**Figure 66**). Loss of mitochondrial membrane potential is an initial requirement for cellular apoptosis.

Gottlieb *et al.*, proposed that ROS scavengers may delay mitochondrial depolarization and cell death. Hence, we hypothesize that cardamonin acts as an antioxidant (as proven earlier) which delayed cell death. This may explain the initial increase of MMP at 3 hrs (Gottlieb *et al.*, 2000). Since cardamonin induces loss in mitochondrial membrane potential within first 6 hrs (approximately three-fold compared to control group), we decided to look into changes in intracellular ATP and ADP levels within the same duration.



It was found that intracellular ATP levels decreased approximately 10% after 3 hrs and 20% after 6 hrs of exposure to cardamonin (**Figure 71**). Increase in intracellular ADP/ATP ratio was detected after 6 hrs of treatment with cardamonin. These suggest that intracellular ATP level decreases concurrently as mitochondrial membrane potential drops. ADP/ATP level increase was only observed at 6 hrs and not at 3 hrs. This situation may be similar to MMP drop. At initial stage (first 3 hrs), MMP was found to increase hence ADP/ATP level did not show any significant changes. ADP/ATP ratio only increase at 6 hrs where concurrently MMP decreased.

These results showed that cardamonin induces cellular apoptosis in HK-1 cells by disruption of mitochondrial membrane potential which is a preliminary condition of cell death *via* mitochondrial-dependent apoptotic pathway. Loss in mitochondrial membrane potential within the few hours of cardamonin exposure was further justified by decline in intracellular ATP levels in HK-1 cells. Recent study reported that capsaicin isolated from chilli pepper causes disruption in mitochondrial membrane potential which leads to inhibition of ATP synthesis in tumor cells (Skrzypski *et al.*, 2014).

ROS has long been associated with cancer because cancer cells are transformed cells and tend to generate more ROS for cell proliferation (Schumacker, 2006). Cancer cells normally overproduce ROS compared to normal cells (Szatrowski and Nathan, 1991). In current research, Cellular Antioxidant Activity (CAA) assay was conducted to determine antioxidant properties of cardamonin against HK-1 cells. Fluorescence intensity measured is directly proportional to ROS levels within the cell cytosol. A decrease in

fluorescence intensity in all cardamonin concentrations showed an inhibition of ROS production within 1 hr in HK-1 cells (**Figure 63**). This may be due to the action of cardamonin as an antioxidant to scavenge and quench ROS. This shows that cardamonin reduces ROS production and does not contribute to HK-1 cell death. In fact, it demonstrates an antioxidant property that protect HK-1 cells against overproduction of ROS and hence apoptosis. Similarly, Skrzypski *et al.* proposed that capsaicin from chili pepper reduces ROS generation and was not responsible to induce cytotoxicity in tumor cells (Skrzypski *et al.*, 2014). Hence, cardamonin did not contribute to cell death pathway in HK-1 cells.

It is also important to note that in untreated HK-1 cells (control group) ROS production level is relatively high. Mitochondrion is extensively studied and proven to be a major intracellular source of ROS. ROS production is due to partial inhibition of mitochondrial respiratory chain which leads to cell death (Fleury *et al.*, 2002). Mutation of genes encoding components in mitochondrial electron transport chain (ETC) increase ROS generation. Impairment in ETC causes an accumulation of electrons which will be captured by oxygen and hence formation of superoxide, a type of radical. It has been previously demonstrated that mitochondria play important roles in induction of apoptosis (Wallace, 2005). In fact, ROS play important role in oxidation of mitochondrial pores and disrupts its membrane potential to aid the release of apoptotic signal, cytochrome c (Zorov *et al.*, 2006). There is a crucial relationship between ROS and mitochondria in activation of cellular apoptosis. However, cardamonin did not induce overproduction of ROS to trigger apoptosis in HK-1 cells; instead it reduces ROS level in HK-1 cells (antioxidant properties). Decrease in ROS

level did not lead to any significant difference in activation of cellular apoptosis in HK-1 cells.

Gene expression level of caspase-9, a final protein required before cleavage of apoptotic substrates, which is necessary to trigger apoptotic signal for permanent cell death was relatively quantified using real-time PCR. Based on current finding, there was no fold change of caspase-9 gene expression level relative to control group (**Table 7**). Despite recent evidences that prove caspase-9 is an important initiator to activate caspase-3 to trigger cell death (Yu *et al.*, 2010; Jen *et al.*, 2008; Bretnall *et al.*, 2013), our results proved otherwise. Upon release of cytochrome c, caspase-9 form an apoptosome with apoptotic peptidase activating factor (Apaf-1) to activate caspase-3. However, it was found that after 24 hrs of treatment with cardamonin, gene expression level of caspase-9 did not show an increase compared to control group. Although apoptotic-inducing factor, cytochrome c was shown to release from mitochondria in previous result, it did not function to induce caspase-9 to form apoptosome. Hence, caspase-9 was not involved in triggering HK-1 cell death. Instead, HK-1 cellular apoptosis was induced by the actions of caspase-3 and caspase-8.

Several literatures reported that caspase-9 was not required in some cellular apoptosis. Apoptotic death of platelets and megakaryocytes were shown to be independent of caspase-9. Caspase-9 deficient fetal liver cells in mice revealed that platelets and megakaryocytes still possess apoptotic functions (White *et al.*, 2012). Ekert *et al.*, reported that Apaf-1 and caspase-9 are not required for apoptosis in drug-treated cells (Ekert *et al.*, 2004). In

hydrogen peroxide (H<sub>2</sub>O<sub>2</sub>)-induced apoptosis HeLa cells, caspase-3 was found to be activated by caspase-8 instead of caspase-9 in mitochondrial-dependent pathway (Wu *et al.*, 2011). Similarly, cardamonin triggers apoptosis in HK-1 cells mediated by caspase-8 that activates caspase-3 directly. A summary of how cardamonin triggers apoptosis *via* activation of mitochondrial-dependent pathway mediated by caspase-8 ( — — — ➡ ) that directly activates caspase-3 is illustrated in **Figure 83**. Time frame of caspase and mitochondrial activities are summarized in **Figure 84**.

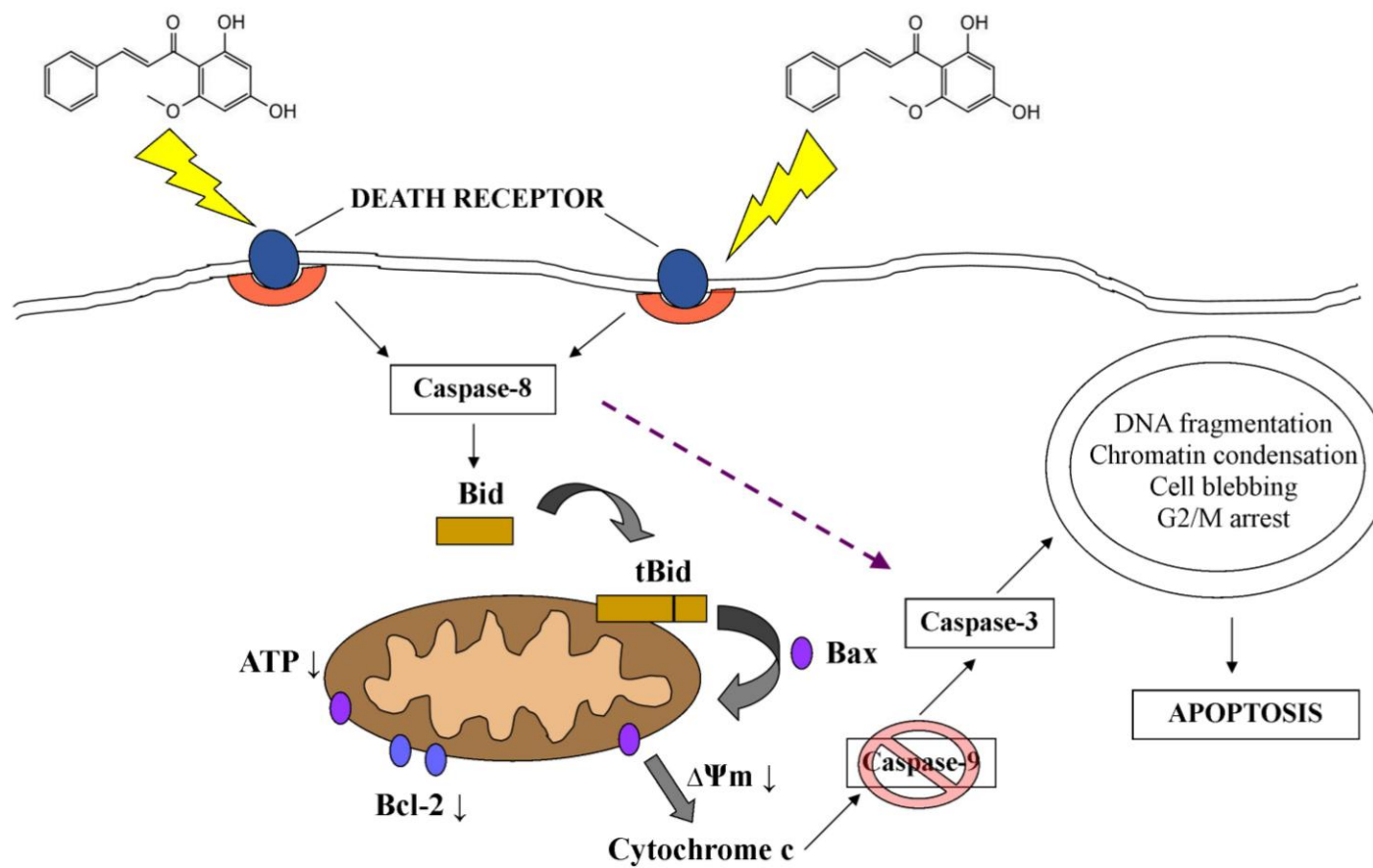


**Figure 83:** This diagram illustrates mode of actions of cardamomin in activation of mitochondrial-dependent pathway mediated by caspase-8 against nasopharyngeal carcinoma (HK-1) cells.

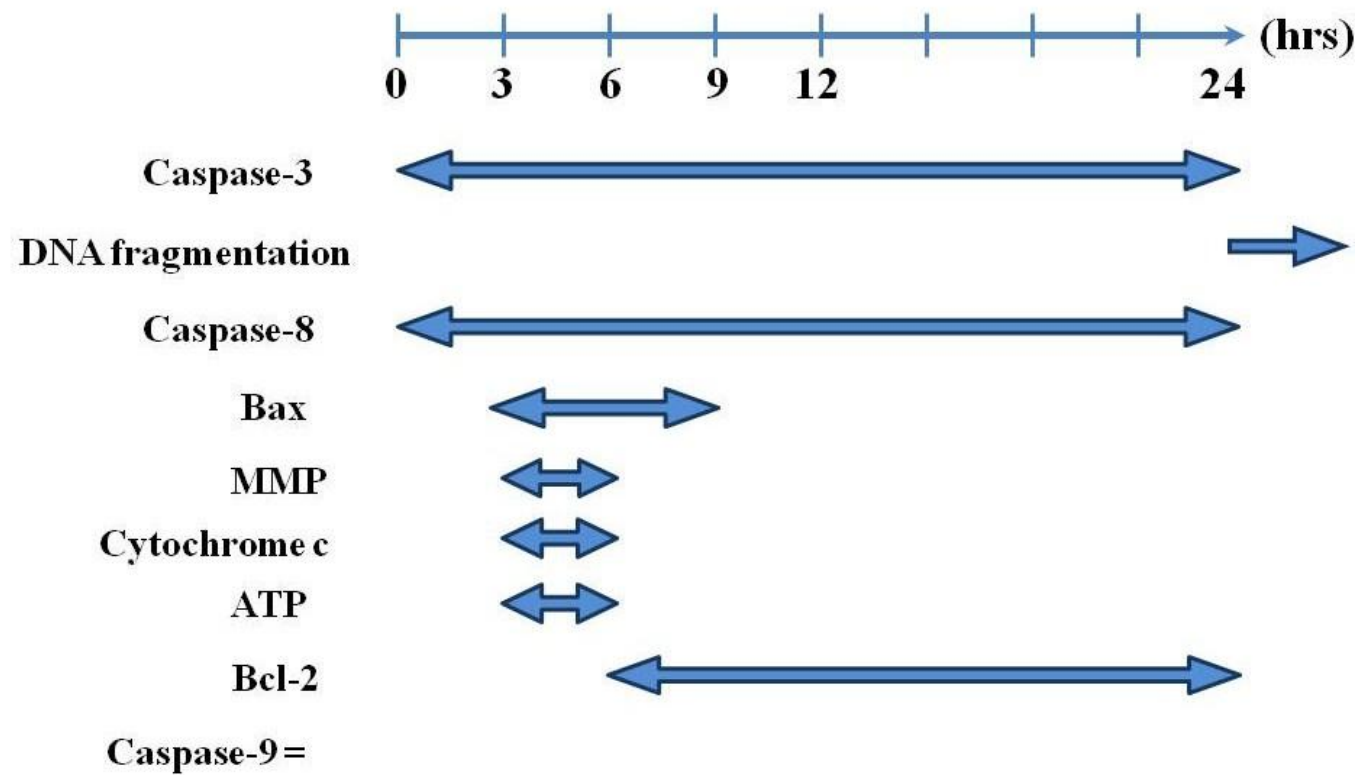


**Figure 84:** Time Frame of HK-1 cell death.

It is interesting to note that cardamonin belonging to the flavonoid family, or more precisely chalcone (class classification in flavonoid family) contributes to the anticancer effect in NPC. As mentioned earlier, cardamonin contains two aromatic rings connected by an  $\alpha,\beta$ -unsaturated carbonyl group (**Figure 7**). It was proven that this carbonyl group in chalcone plays an important role in various biological activities (Sahu *et al.*, 2012). Chalcone derivatives such as boronic chalcone exhibits potent anticancer activity which was associated with accumulation of p53 proteins, a tumor suppressor protein (Achanta *et al.*, 2006). Synthesis of methoxychalcone through Claisen-Schmidt condensation reaction revealed promising results as an anticancer agent (Babasaheb *et al.*, 2009). Chun and the team substituted both electron withdrawing and electron-donating groups to structure of chalcones which showed selective anticancer activities against TRAIL resistant cancer cells. Among the synthesized compounds, chalcone containing an amino group ( $-\text{NH}_2$ ) on the aromatic ring was found to be most potent against cancer cells (Chun *et al.*, 2014). Hence, we are interested to further explore the effects of addition of functional groups to cardamonin and how it affects and further enhance cellular death in NPC. We have so far concluded the effect of cardamonin against NPC through mitochondrial-dependent pathway where cardamonin affects cell death within the cell. The actions of cellular apoptotic pathway occur in cytoplasm whereby initial apoptotic signal is triggered through cell surface receptor. For future work, we would propose the study of cell surface receptor as a target for cardamonin and its synthesized compounds to induce cell death. Future work will be further explained in next chapter.

## 5.0 CONCLUSION AND PROPOSED FUTURE STUDIES

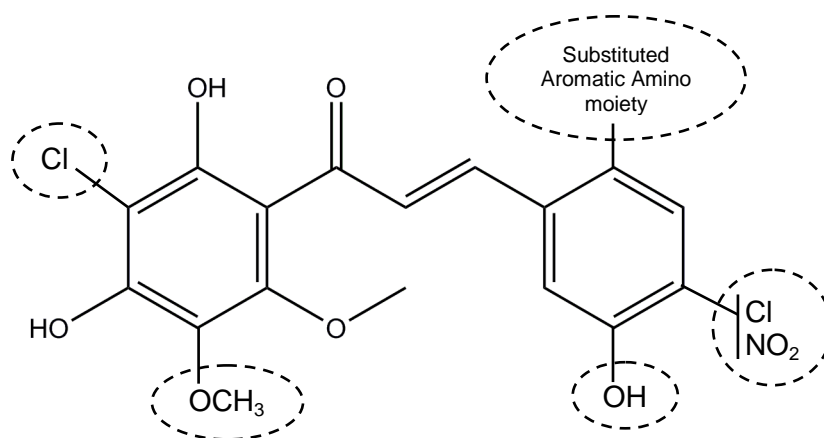
In conclusion, these studies demonstrate mode of actions of cardamonin-induced apoptosis in HK-1 cells mediated by caspase-8 activation and subsequently leads to cell death *via* mitochondrial-dependent apoptotic pathway *in vitro*. Cardamonin triggers nasopharyngeal carcinoma (NPC HK-1) cell death characterized by cell morphological changes, DNA fragmentation, activation of caspase-3 activity and G2/M phase arrest. In addition, cardamonin-induced apoptosis causes loss of mitochondrial membrane potential within 6 hrs and concurrently, intracellular ATP was reported to be low. Regulation of mitochondrial-dependent apoptotic pathway associated protein levels were detected using immunoblotting. Pro-apoptotic protein, Bax was up-regulated and anti-apoptotic protein, Bcl-2 was down-regulated leading to release of apoptotic signalling factor, cytochrome c. Real-time polymerase chain reaction (qPCR) of gene expression level of caspase-9 showed no fold change. Caspase-3 was activated by caspase-8 and did not require caspase-9 to induce HK-1 cell death. Taken together, these results indicate that cardamonin plays a critical role as a potential anticancer agent against NPC cells.

Future studies are required to test effect of cardamonin *in vivo*. We proposed further investigation on animal testing to observe the overall effects of cardamonin on living organism as a whole. NPC-induced animals can be tested based on oral intake of cardamonin and its effect on NPC tumor size. As cardamonin is originally isolated from edible plant *Boesenbergia rotunda*, it is safe



for animal consumption. Furthermore, current results obtained can be validated using animal testing. We hypothesized that deletion of pro-apoptotic genes such as caspase-3 and caspase-8 will lead to normal proliferation of NPC cells in animal and hence tumor formation. Other cell death pathways can be studied on larger biological organism before it is suitable to be tested for clinical trials and develop into an anticancer drug. Development of an anticancer drug may take more than a decade because drug development serves purpose to alleviate risk of death and promote recovery and thus clinical trials must be done comprehensively. Tests and trials on biological organisms are conducted to a greater extent to ensure efficiency and efficacy of a tested anticancer drug. Current preliminary findings represent initial breakthrough that may contribute to the wellbeing of mankind in future.

Concurrently, we propose the addition of functional groups to cardamonin to enhance the anticancer effect against NPC. A few novel derivatives of flavones with substitution of chloro, isopropyl, nitro and methoxy groups were found to be effective against gastric cancer cells (Liu *et al.*, 2010). Addition of aromatic amino moiety and imidazole ring enhance cytotoxicities in breast cancer cells (Singh *et al.*, 2014). Hence, it is worth to note that modifications on cardamonin at different positions may contribute to greater anticancer effects against NPC (**Figure 85**). Cardamonin acts as an important scaffold which may lead to a significant discovery of a potent compound to induce apoptosis in NPC. **Table 8** proposed addition of functional groups on cardamonin to study the structure activity relationship in anticancer activity. These additions of functional groups have been previously proven to be effective against NPC.

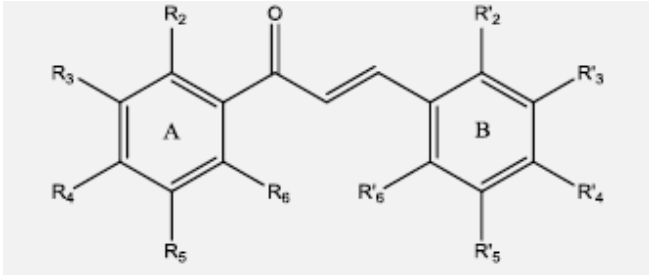


**Figure 85:** Addition of functional groups on chalcone enhances anticancer activities.

Furthermore, cardamonin contains a  $\alpha,\beta$ -unsaturated carbonyl group which allow the alkene group to be substituted . It is known as Michael acceptor which readily acts as an electrophile for substitution. Michael reaction provides a platform for synthesis of Pan-Assay Interference Compounds (PAINS) which can be tested for a range of bioassays targeting different diseases.

**Table 8:** Proposed addition of functional groups on cardamonin.

Addition of functional group	Justifications
Pyrimidinyl group	<div data-bbox="609 472 1364 1071"> <p> <math>\text{1} + \text{2} \xrightarrow[\text{DMF}]{\text{K}_2\text{CO}_3} \text{3}</math> </p> <p> <math>\text{2a R}^1 = \text{H}</math>  <math>\text{2b R}^1 = \text{OMe}</math>  <math>\text{2c R}^1 = \text{Cl}</math> </p> <p> <math>\text{3} + \text{4} \xrightarrow[\text{EtOH}]{\text{KOH}} \text{5}</math> </p> <p> <math>\text{5a R}^1 = \text{H}; \text{R}^2 = \text{H}</math>      <math>\text{5b R}^1 = \text{H}; \text{R}^2 = 4\text{-Me}</math>  <math>\text{5c R}^1 = \text{H}; \text{R}^2 = 4\text{-OMe}</math>      <math>\text{5d R}^1 = \text{H}; \text{R}^2 = 4\text{-NO}_2</math>  <math>\text{5e R}^1 = \text{H}; \text{R}^2 = 2\text{-OH}</math>      <math>\text{5f R}^1 = \text{OMe}; \text{R}^2 = \text{H}</math>  <math>\text{5g R}^1 = \text{OMe}; \text{R}^2 = 4\text{-OMe}</math>      <math>\text{5h R}^1 = \text{OMe}; \text{R}^2 = 2\text{-OH}</math>  <math>\text{5i R}^1 = \text{Cl}; \text{R}^2 = \text{H}</math>      <math>\text{5j R}^1 = \text{Cl}; \text{R}^2 = 4\text{-OMe}</math>  <math>\text{5k R}^1 = \text{Cl}; \text{R}^2 = 2\text{-OH}</math> </p> </div> <p style="text-align: right;">(Jin <i>et al.</i>, 2013)</p> <p>Compound <b>3</b> (pyrimidinyl group) is synthesized from 4,6-dimethoxy-2-(methylsulfonyl)pyrimidine (<b>1</b>) and starting material 3-substituted-4-hydroxybenzaldehyde (<b>2</b>) in the presence of potassium carbonate, K<sub>2</sub>CO<sub>3</sub> in DMF. Then, chalcone derivatives (<b>5a-5k</b>) are prepared from substituted acetophenone (<b>4</b>) and compound <b>3</b> using a catalytic amount of potassium hydroxide, KOH in ethanol. Jin <i>et al.</i> has proven compound <b>5g</b> is most effective against NPC (CNE-2) cells at IC<sub>50</sub> of 14.0μM.</p>

Methoxy group (electron donating)	<p>Mai <i>et al.</i> (2014) has proven high cytotoxicity against NPC (CNE-1) cells with 2 methoxy groups added to ring A of chalcone (positions R<sub>4</sub> and R<sub>6</sub> below). We propose the addition of methoxy group to Ring B, position 3. The reaction uses 2,4-dihydroxyacetophenone as starting material to react with dimethyl sulphate (methylation) to produce cardamonin with an addition of methoxy group at Ring B, position 3.</p>  <p>(Mai <i>et al.</i>, 2014)</p>
-----------------------------------	---

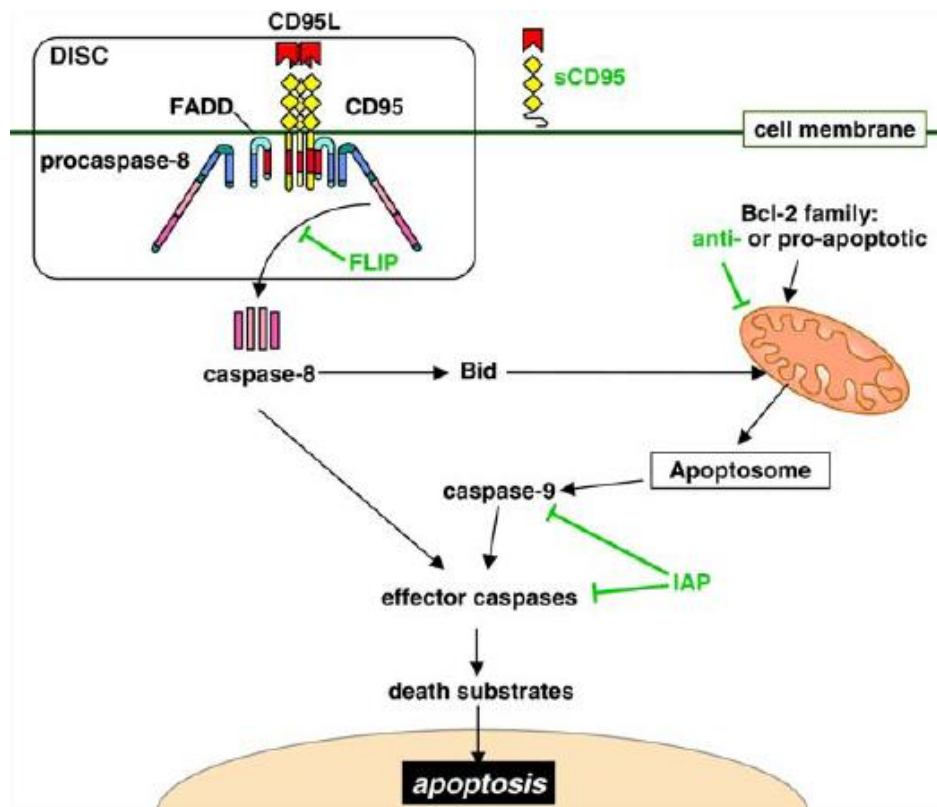
Furthermore, we believe the first target of cardamonin on NPC is on cell surface receptor. In fact, mitochondrial-dependent pathway is a death receptor signalling pathway. By understanding the molecular events that occurs in mitochondria and cytoplasm which we have proven in this research, we hypothesize the action was triggered by a receptor called Fas. The Fas receptor/ligand system is the regulator of mitochondrial cell death pathway.

For decades, cell surface receptors have been a target for cancer cells. Anticancer drugs going through clinical trials targeting receptors overexpressing in cancer cells have been showing positive results. There are a few examples of drugs targeting NPC. Xie and team investigated the expression of folate receptor on head and neck squamous carcinoma tissue samples and found that folate receptor mediates endocytosis through folate-conjugated anticancer nanomedicines. This

discovery was proven to reduce the severe side effects in patients undergoing chemotherapy because this study provide targeted drug delivery with the help of this cell surface receptor (Xie *et al.*, 2013). It was found tha epidermal growth factor receptor (EGFR) was overexpressed in NPC. The overexpression of EGFR was shown to be the main cause that leads to tumor formation. Nimotuzumab, a genetically engineered humanized monoclonal antibody that recognizes epitope in EGFR was proven to promote anticancer effect in patients undergoing radiotherapy (Gondhowiardjo *et al.*, 2009). Vascular endothelial growth factor (VEGF)/VEGF receptor is a potential target as VEGF is overexpressed on NPC. Sorafenib combined with cisplatin and 5-fluorouracil was tested in Phase II study showed positive results with tolerable recurrent rate of metastatic NPC (Xue *et al.*, 2012). Other anticancer drug such as AKT inhibitor MK-2206 has downregulated the overexpression of AKT (protein kinase B) on NPC cell surface and hence inhibits AKT signalling in NPC cell lines. PI3K/AKT/mTOR intracellular signalling pathway is important to regulate cell cycle. Hence, the disruption of this pathway is an important target for cellular apoptosis in NPC (Ma *et al.*, 2012).

In 1999, Tsai and team conducted a biopsy on NPC patients and found that there is an overexpression of Fas ligand proteins detected exclusively on the cell surface of NPC (Tsai *et al.*, 1999). Overexpression of Fas ligand in tumor triggers apoptosis of lymphocytes (because Fas ligand binds to Fas receptor on lymphocytes) and hence tumor may escape the naturally occurring immune response termed “tumor counterattack” (Igney and Krammer, 2005).

Fas (CD95/APO-1) receptor is a cell surface protein belonging to the family of tumor necrosis factor (TNF) receptor (**Figure 86**). Fas ligand (Fas L/CD178) is a membrane protein that binds to Fas receptor to induce apoptosis. When Fas L binds to Fas receptor, a death-inducing signalling complex (DISC) is formed and this receptor complex is internalized into cell. This receptor complex consists of a death domain. This death domain will then bind to another death domain of Fas-associated death domain (FADD). On FADD, there is a death effector domain (DED) at its amino terminus which will bind to DED of initiator, caspase-8. Caspase-8 is responsible to initiate a series of apoptotic cascade reactions. The activity of caspase-8 and other caspases were investigated in this research. The results showed an increase in caspase-8 activity which further substantiates our study on how cardamomin signal the Fas/Fas L system to initiate apoptosis.



(Igney and Krammer, 2005)

**Figure 86:** Apoptosis signalling *via* Fas/Fas L system

Hence, we hypothesize that cardamonin induces the activation of Fas/Fas L system on NPC cell surface thus triggering apoptosis of NPC.

## 6.0 REFERENCES

- Achanta, G., Modzelewska, A., Feng, L., Khan, S.R. & Huang, P. (2006). A Boronic-Chalcone Derivative Exhibits Potent Anticancer Activity through Inhibition of the Proteasome. *Molecular Pharmacology*, **70**(1): 426-433.
- American Cancer Society. (2012). Cancer Facts & Figures. *American Cancer Society*. Atlanta, United States of America.
- Allan, L.A. & Clarke, P.R. (2009). Apoptosis and autophagy: Regulation of caspase-9 by phosphorylation. *The FEBS Journal*, **276**(21): 6063-6073.
- Babasaheb, P.B., Gawande, S.S., Bodade, R.G., Totre, J.V. & Khobragade, C.N. (2010). Synthesis and biological evaluation of simple methoxylated chalcones as anticancer, anti-inflammatory and antioxidant agents. *Bioorganic & Medicinal Chemistry*, **18**(3): 1364-1370.
- Beninger, C.W. & Hosfield, G.L. (2003). Antioxidant activity of extracts, condensed tannin fractions and pure flavonoids from *Phaseolus vulgaris* L. seed coat colour genotypes. *Journal of Agricultural and Food Chemistry*, **51**(27): 7879-7883.
- Breckenridge, D.G. & Xue, D. (2004). Regulation of mitochondrial membrane permeabilization by BCL-2 family proteins and caspases. *Current opinion in cell biology*, **16**(6): 647-652.
- Bretnall, M., Rodriguez-Menocal, L., De Guevara, R.L., Cepero, E. & Boise, L.H. (2013). Caspase-9, caspase-3 and caspase-7 have distinct roles during intrinsic apoptosis. *BMC Cell Biology*, **14**: 32.
- Burt, J. (2007). Growing spring onions. In *Farmnote 30/99*. Agriculture Western Australia: Perth.
- Bustin, S.A. (2005). Real-Time PCR (pp.1117-1125). In *Encyclopedia of Diagnostic Genomics and Proteomics*. New York, USA: Marcel Dekker Inc.
- Cai, Y. Z., Luo, Q., Sun, M., & Harold, C. (2003). Antioxidant activity and phenolic compounds of 112 traditional Chinese medicinal plants associated with anticancer. *Life Sciences*, **74**: 2157-2184.
- Carmichael, J., DeGraff, W. G., Gazdar, A. F., Minna, J.D. & Mitchell, J. B. (1987). Evaluation of a tetrazolium-based semiautomated colorimetric assay: Assessment of chemosensitivity testing. *Cancer Research*, **47**: 936-942.



- Carvalho, A.M., Gonçalves, L.M., Valente, I.M., Rodrigues, J.A. & Barros, A.A. (2011). Analysis of Cardamonin by Square Wave Voltammetry. *Phytochemical Analysis*, **23**(4): 396-399.
- Castillo, M.H., Perkins, E., Campbell, J.H., *et al.* (1989). The effects of the bioflavonoid quercetin on squamous cell carcinoma of head and neck region. *The American Journal of Surgery*, **158**: 351-355.
- Chan, E.W.C., Lim, Y.Y. & Omar, M. (2007). Antioxidant and antibacterial activity of leaves of *Etlingera* species (Zingiberaceae) in Peninsular Malaysia. *Food Chemistry*, **104**: 1586-1593.
- Chang, C.C., Yang, H.M., Wen, H.M. & Chern, J.C. (2002). Estimation of total flavonoid content in propolis by two complementary colorimetric methods. *Journal of Food and Drug Analysis*, **10**: 178-182.
- Chaudhury, R. & Rafei, U.M. (2001). In *Traditional Medicine in Asia* (pp135-158). New Delhi: World Health Organization.
- Ching, A.Y.L., Wah, T.S., Sukari, A., Lian, G.E.C., Rahmani, M. & Khalid, K. (2007). Characterization of flavonoid derivatives of *Boesenbergia rotunda* (L.). *The Malaysian Journal of Analytical Sciences*, **11**(1): 154-159.
- Choi, E.J., Lee, J.I. & Kim, G-H. (2010). Anti-carcinogenic effect of a new analogue 4'-chloroflavanone from flavanone in human breast cancer cells. *International Journal of Molecular Medicine*, **25**: 293-298.
- Chow, Y., Lee, K., Vidyadaran, S., Lajis, N.H., Akhtar, M.N., Israf, D.A. & Syahida, A. (2012). Cardamonin from *Alpinia rafflesiana* inhibits inflammatory responses in IFN- $\gamma$ /LPS-stimulated BV2 microglia via NF- $\kappa$ B signaling pathway. *International Immunopharmacology* **12**(4): 657-665.
- Chowdhury, J.U., Bhuiyan, M.N.I. & Yusuf M. (2008). Chemical composition of the leaf essential oils of *Murraya koenigii* (L.) Spreng and *Murraya paniculata* (L.) Jack. *Journal of Bangladesh Pharmacological Society*, **3**:59-63.
- Chun, W.M., Wong, S.Y., Tan, E.L., Balijepalli, M.K. & Pichika, M.R. (2009). Antiproliferative and apoptotic studies of the standardized extracts of *Etlingera elatior* on Human Colorectal Carcinoma cells. *Malaysian Journal of Chemistry*, **11**(1):136-142.
- Chun, W.M., Yaeghoobi, M., Abd-Rahman, N., Kang, Y.B. & Pichika, M.R. (2014). Chalcones with electron-withdrawing and electron-donating substituents: Anticancer activity against TRAIL resistant cancer cells, structure-activity relationship analysis and regulation of apoptotic proteins. *European Journal of Medicinal Chemistry*, **77**: 378-387.

- Ciapetti, G., Granchi, D., Savarino, L., Cenni, E., Magrini, E., Baldini, N. & Giunt, A. (2002). *In vitro* testing of the potential for orthopaedic bone cements to cause apoptosis of osteoblast-like cells. *Biomaterials*, **23**: 617-627.
- Circu, M.L. & Aw, T.Y. (2010). Reactive oxygen species, cellular redox systems, and apoptosis. *Free Radical Biology & Medicine*, **48**: 749-762.
- Crompton, M. (1999). The mitochondrial permeability transition pore and its role in cell death. *Biochemical Journal*, **341**: 233-249.
- Dalziel, J.M. (1937). *The Useful Plants of West-Tropical Africa* (pp. 70-71). London: Crown Agents for the Colonies.
- Dinelli, G., Bonetti, A., Minelli, M., Catizone, P. & Mazzanti, A. (2006). Content of flavonols in Italian bean (*Phaseolus vulgaris* L.) ecotypes. *Food chemistry*, **99**(1): 105-114.
- Dollinger, M., Ko, A. H., Rosenbaum, E. H. & Foster, D. A. (2002). Diagnosis and Treatment: Understanding Cancer. In Authors (Eds.), *Everyone's guide to Cancer Therapy* (pp. 3-12). United States of America (USA): Andrews McMeel Publishing.
- Duchen, M.R. (2004). Section III: Mitochondria,  $\beta$ -cell Function, and Type 2 Diabetes. Role of Mitochondria in Health and Disease. *Diabetes*, **53**: 96-102.
- Duncan, K., Harris, S. & Murray Ardies, C. (1997). Running exercise may reduce risk for lung and liver cancer by inducing activity of antioxidant and phase II enzymes. *Cancer Letters*, **116**: 151-158.
- Edinger, A.L. & Thompson, C.B. (2004). Death by design: apoptosis, necrosis and autophagy. *Current Opinion in Cell Biology*, **16**(6): 663-669.
- Ekert, P.G., Read, S.H., Silke, J., Marsden, V.S., Kaufmann, H., Hawkins, C.J., Gerl, R., Kumar, S. & Vaux, D.L. (2004). Apaf-1 and caspase-9 accelerate apoptosis, but do not determine whether factor-deprived or drug-treated cells die. *The Journal of Cell Biology*, **165**(6): 835-842.
- Elhefian, E.A., Jacknoon, A.A., Mohammed, A.M., Abdalla, O., Hamdi, A. & Yahaya, A.H. (2012). A preliminary qualitative study of two common *Acacia* species in Sudan. *E-Journal of Chemistry*, **9**(2): 851-856.
- Enari, M., Sakahira, H., Yokoyama, H., Okawa, K., Iwamatsu, A. & Nagata, S. (1998). A caspase-activated DNase that degrades DNA during apoptosis, and its inhibitor ICAD. *Nature*, **391**: 43-50.

- Farhan, A., Yeager, T., Moravec, R. & Niles, A. (2004). Multiplexing Homogenous Cell-based Assays. *Cell Notes*, **10**: 15-18.
- Fauzi, A.N., Norazmi, M.N. & Yaacob, N.S. (2011). Tualang honey induces apoptosis and disrupts the mitochondrial membrane potential of human breast and cervical cancer cell lines. *Food and Chemical Toxicology*, **49**: 871-878.
- Fiebig, M., Pezzuto, J.M., Soejarto, D.D. & Kinghorn, A.D. (1985). Koenoline, a further cytotoxic carbazole alkaloid from *Murraya koenigii*. *Phytochemistry*, **24(12)**: 3041-3043.
- Fleury, C., Mignotte, B. & Vayssière, J. (2002). Mitochondrial reactive oxygen species in cell death signaling. *Biochimie*, **84**: 131-141.
- Fraga, D., Meulia, T. & Fenster, S. (2008). Real-Time PCR. *Current Protocols Essential Laboratory Techniques*, **10(3)**: 1-33.
- García-Villalba, R., Carrasco-Pancorbo, A., Oliveras-Ferraro, C., Vázquez-Martín, A., Menéndez, J. A., Segura-Carretero, A. & Fernández-Gutiérrez, A. (2010). Characterization and quantification of phenolic compounds of extra-virgin olive oils with anticancer properties by a rapid and resolute LC-ESI-TOF MS method. *Journal of Pharmaceutical and Biomedical Analysis*, **51**:416–429.
- Gondhowiardjo, S., Muthalib, A., Khotimah, S. & Rachman, A. (2009). Nimotuzumab combined with radiotherapy reduces primary tumor and nodal volume in advanced undifferentiated nasopharyngeal carcinoma. *Asia-Pacific Journal of Clinical Oncology*, **5**: 175-180.
- Gogvadze, V., Orrenius, S., Zhivotovsky, B. (2008). Mitochondria in cancer cells: what is so special about them?. *Trends in Cell Biology*, **18**: 165-173.
- Gottlieb, E., Vander Heiden, M.G., Thompson, C.B. (2000). Bcl-xL prevents the initial decrease in mitochondrial membrane potential and subsequent reactive oxygen species production during Tumor Necrosis Factor Alpha-Induced Apoptosis. *Molecular and Cellular Biology*, **20**: 5680-5689.
- Gray, R., Bhattacharya, S., Bowden, C., Miller, K., Comis, R. L. (2009). Independent review of E2100: a phase III trial of bevacizumab plus paclitaxel in women with metastatic breast cancer. *Journal of Clinical Oncology*, **27**:4966-4972.
- Gross, A., Jockel, J., Wei, M.C. & Korsmeyer, S.J. (1998). Enforced dimerization of BAX results in its translocation, mitochondrial dysfunction and apoptosis. *The EMBO Journal*, **17(14)**: 3878-3885.

- Habsah, M., Lim, Y.M., Amran, M., Jasril, K., Lajis, M.N., Ali, A.M., Kikuzaki, H., Nakatani, N., Rahman, A.A., Ghafar. (2000). Antioxidant and antitumor promoting activities of Zingiberaceae species from Malaysia. In Chang Y.S., Mastura M, Subramaniam, V., Zainon A.S., eds. Towards Bridging Science and Herbal Industry: proceedings of the seminar on Medicinal and Aromatic Plants, Kuala Lumpur: FRIM, 183-188.
- Habsah, M., Ali, A.M., Lajis, N.H., Sukari, M.A., Yap, Y.H., Kikuzaki, H. & Nakatani, N. (2005). Antitumor-promoting and cytotoxic constituents of *Etilingera elatior*. *Malaysian Journal of Medical Sciences*, **12(1)**: 6-12.
- Hangen, L. & Bennick, M.R. (2002). Consumption of black beans and navy beans (*Phaseolus vulgaris*) reduced azoxymethane-induced colon cancer in rats. *Nutrition and Cancer*, **44**: 60-65.
- Harbeck, N., Salem, M., Nitz, U., Gluz, O. & Liedtke, C. (2010). Personalized treatment of early-stage breast cancer: Present concepts and future directions. *Cancer Treatment Reviews*, **36**: 584–594.
- Heinrich, E.L., Welty, L.A.Y., Banner, L.R. & Oppenheimer, S.B. (2005). Direct targeting of cancer cells: A multiparameter approach. *Acta Histochemica*, **107**: 335-344.
- Hengartner, M.O. (1997). Cell death. In: "C. elegans II", Riddle, D.L., Blumenthal T, Meyer ,B.J., Priess JR (eds.). Cold Spring Harbour Laboratory, Plainview: New York; pp. 383-496.
- Henmi, K., Hiwatashi, Y., Hikita, E., Toyama, N. & Hirano, T. (2009). Methoxy- and fluoro-chalcone derivatives arrest cell cycle progression and induce apoptosis in human melanoma cell A375. *Biology and Pharmaceutical Bulletin*, **32(6)**: 1109-1113.
- Hockenbery, D., Nunez, G., Milliman, C., Schreiber, R. & Korsmeyer, S.J. (1990). Bcl-2 is an inner mitochondrial membrane protein that blocks programmed cell death. *Nature*, **348**: 334-336.
- Hu, S., Snipas, S.J., Vincenz, C., Salvesen, G. & Dixit, V.M. (1998). Caspase-14 is a novel developmentally regulated protease. *The Journal of Biological Chemistry*, **273**: 29648-53.
- Huang, D.P., Ho, J.H., Poon, Y.F., Chew, E.C., Saw, D., Lui, M., Li, C.L., Mak, L.S., Lai, S.H. & Lau, W.H. (1980). Establishment of a cell line (NPC/HK1) from a differentiated squamous carcinoma of the nasopharynx. *International Journal of Cancer*, **26(2)**: 127-132.

- Huang, R-P., Wu, J-X., Fan, Y. & Adamson, E.D. (1996). UV Activates Growth Factor Receptors *via* Reactive Oxygen Intermediates. *The Journal of Cell Biology*, **133**: 211-220.
- Hug, H., Los, M., Hirt, W. & Debatin, K. (1999). Rhodamine 110-Linked Amino Acids and Peptides as Substrates To Measure Caspase Activity upon Apoptosis Induction in Intact Cells. *Biochemistry*, **38**: 13906-13911.
- Ito, C., Itoigawa, M., Nakao, K., Murata, T., Tsuboi, M. & Kaneda, N. (2006). Induction of apoptosis by carbazole alkaloid isolated from *Murraya koenigii*. *Phytomedicine*, **13**: 359-365.
- Igney, F.H. & Krammer, P.H. (2005). Tumor counterattack: fact or fiction?. *Cancer Immunology, Immunotherapy*, **54**: 1127-1136.
- Jacobson, M.D., Burne, J.F. & Raff, M.C. (1994). Programmed cell death and Bcl-2 protection in the absence of a nucleus. *The EMBO Journal*, **13**: 1899-1910.
- Jänicke, R.U., Sprengart, M.L., Wati, M.R., & Porter, A.G. (1998). Caspase-3 is required for DNA fragmentation and morphological changes associated with apoptosis. *Journal of Biological Chemistry*, **273**(16): 9357-9360.
- Jen, C., Lin, C., Huang, B. & Leu, S. (2008). Cordycepin Induced MA-10 Mouse Leydig Tumor Cell Apoptosis through caspase-9 Pathway. *Evidence-Based Complementary and Alternative Medicine*, **2011**: 11.
- Jin, C., Liang, Y-J., He, H. & Fu, L. (2013). Synthesis and antitumor activity of novel chalcone derivatives. *Biomedicine & Pharmacotherapy*, **67**: 215-217.
- Jing, L.J., Mohamed, M., Rahmat, A. & Abu Bakar, M.F. (2010). Phytochemicals, antioxidant properties and anticancer investigations of the different parts of several gingers species (*Boesenbergia rotunda*, *Boesenbergia pulchella* var *attenuata* and *Boesenbergia armeniaca*). *Journal of Medicinal Plants Research*, **4**(1): 27-32.
- Jones, W. P. & Kinghorn, A. D. (2005). Methods in Biotechnology: Natural Products Isolation. In Sarker S. D., Latif Z. & Gray A. I. (Eds.), *Extraction of Plant Secondary Metabolites* (pp. 323-351). Totowa, New Jersey: Humana Press.
- Kerr, J.F., Wyllie, A.H. & Currie, A.R. (1972). Apoptosis: a basic biological phenomenon with wide-ranging implications in tissue kinetics. *British Journal of Cancer*, **26**(4): 239-257.

- Kim, K., Yu, S., Lee, S., Chun, S., Choi, Y., Park, Y., Song, C.S., Chatterjee, B. & Ahn, S. (2011). Salinomycin-induced apoptosis of human prostate cancer cells due to accumulated reactive oxygen species and mitochondrial membrane depolarization. *Biochemical and Biophysical Research Communication*, **413**: 80-86.
- Kirana, C., Jones, G.P., Record, I. R. & McIntosh, H. (2007). Anticancer properties of panduratin A isolated from *Boesenbergia pandurata* (Zingiberaceae). *Journal of Natural Medicines*, **61**: 131-137.
- Koppikar, S.J., Choudhari, A.S., Suryavanshi, S.A., Kumari, S., Chattopadhyay, S. & Kaul-Ghanekar, R. (2010). Aqueous Cinnamon Extract (ACE-c) from the bark of *Cinnamomum cassia* causes apoptosis in human cervical cancer cell line (SiHa) through loss of mitochondrial membrane potential. *BMC Cancer*, **10**: 210.
- Krippner, A., Mastuno-Yagi, A., Gottlieb, R.A. & Babior, B.M. (1996). Loss of Function of Cytochrome *c* in Jurkat Cells Undergoing Fas-mediated Apoptosis. *Journal of Biological Chemistry*, **271**: 21629-21636.
- Kumi-Diaka, J., Sanderson, N. & Hall, A. (2000). The mediating role of caspase-3 protease in the intracellular mechanism of genistein-induced apoptosis in human prostatic carcinoma cell lines, DU145 and LNCaP. *Biology of the Cell*, **92**: 595-604.
- Kuntz, S., Wenzel, U. & Daniel, H. (1999). Comparative analysis of the effects of flavonoids on proliferation, cytotoxicity and apoptosis in human colon cancer cell lines. *European Journal of Nutrition*, **38**: 133-142.
- Kuo, C., Wu, S.Y., Ip, S., Wu, P., Yu, C., Yang, J., Chen, P., Wu, S.H. & Chung, J. (2011). Apoptotic death in curcumin-treated NPC-TW 076 human nasopharyngeal carcinoma cells is mediated through ROS, mitochondrial depolarization and caspase-3-dependent signalling responses. *International Journal of Oncology*, **39**: 319-328.
- Kureel, S.P., Kapil, R.S. & Popli, S.P. (1969). Two novel alkaloids from *Murraya koenigii* Spreng: Mahanimbicine and bicyclomahanimbicine. *Chemistry and Industry*, **29**:958.
- Kurien, B.T. & Scofield, R.H. (2006). Western blotting. *Methods for Analyzing Cytokines*, **38(4)**: 283–293.
- Kuwana, T., Mackey, M.R., Perkins, G., Ellisman, M.H., Latterich, M., Schneider, R., Green, D.R. & Newmeyer, D.D. (2002). Bid, Bax, and lipids cooperate to form supramolecular openings in the outer mitochondrial membrane. *Cell*, **111(3)**: 331-342.

- Lachumy, S.J.T., Sasidharan, S., Sumathy, V. & Zuraini Z. (2010). Pharmacological activity, phytochemical analysis and toxicity of methanol extract of *Etlingera elatior* (torch ginger) flowers. *Asian Pacific Journal of Tropical Medicine*, 769-774.
- Lazarus, C.L., Logemann, J.A., Pauloski, B.R., Colangelo, L.A., Kahrilas, P.J., Mittal, B.B., Pierce, M. (2009). Swallowing Disorders in Head and Neck Cancer Patients Treated With Radiotherapy and Adjuvant Chemotherapy. *The Laryngoscope*, **106**: 1157-1166.
- Lee, J.S., Jung, W., Jeong, M.H., Yoon, T.R. & Kim, H.K. (2012). Sanguinarine Induces Apoptosis of HT-29 Human Colon Cancer Cells *via* the Regulation of Bax/Bcl-2 Ratio and Caspase-9-Dependent Pathway. *International Journal of Toxicology*, **31(1)**: 70-77.
- Lee, Y.S., Nam, D.H. & Kim, J-A. (2000). Induction of apoptosis by capsaicin in A172 human glioblastoma cells. *Cancer Letters*, **161**: 121-130.
- Léon, P., Garbay-Jaureguiberry, C., Barsi, M.C., Le Pecq, J.B. & Roques, B. P. (1987). Modulation of the antitumor activity by methyl substitution in the series of 7*H*-Pyridocarbazole monomers and dimers. *Journal of Medicinal Chemistry*, **30**: 2074-2080.
- Li, H., Zhu, H., Xu, C.J. & Yuan, J. (1998). Cleavage of BID by caspase 8 mediates the mitochondrial damage in the Fas pathway of apoptosis. *Cell*, **94(4)**: 491-501.
- Lin, M., Chen, S., Lu, Y., Liang, R., Ho, Y., Yang, C. & Chung, J. (2007). Rhein induces apoptosis through induction of endoplasmic reticulum stress and Ca<sup>2+</sup>-dependent mitochondrial death pathway in human nasopharyngeal carcinoma cells. *Anticancer research*, **27**: 3313-3322.
- Lin, M., Lu, Y., Chung, J., Li, Y., Wang, S., Ng, S., Wu, C., Su, H. & Chen, S. (2010). Aloe-emodin induces apoptosis of human nasopharyngeal carcinoma cells via caspase-8-mediated activation of the mitochondrial death pathway. *Cancer Letters*, **291(1)**: 46–58.
- Liu, H., Dong, A., Gao, C., Tan, C., Xie, Z., Zu, X., Qu, L. & Jiang, Y. (2010). New synthetic flavone derivatives induce apoptosis of hepatocarcinoma cells. *Bioorganic & Medicinal Chemistry*, **18(17)**: 6322-6328.
- Livak, K.J. & Schmittgen, T.D. (2001). Analysis of Relative Gene Expression Data Using Real-Time Quantitative PCR and the 2<sup>- $\Delta\Delta C_T$</sup>  Method. *Methods*, **25**: 402-408.

- Lui, V.W.Y., Yau, D.M.S., Wong, E.Y.L., Ng, Y-K., Lau, C.P.K., Ho, Y., Chan, J.P.L., Hong, B., Ho, K., Cheung, C.S., Tsang, C-M., Tsao, S-W. & Chau, A.T.C. (2009). Cucurbitacin I elicits anoikis sensitization, inhibits cellular invasion and *in vivo* tumor formation ability of nasopharyngeal carcinoma cells. *Carcinogenesis*, **30**: 2085-2094.
- Lundin, A. (2000). Use of Firefly Luciferase in ATP-Related Assays of Biomass, Enzymes, and Metabolites. *Methods in Enzymology*, **305**: 346-370.
- Luo, X., Budihardjo, I., Zou, H., Slaughter, C. & Wang, X. (1998). Bid, a Bcl2 Interacting Protein, Mediates Cytochrome c Release from Mitochondria in Response to Activation of Cell Surface Death Receptors, *Cell*, **94**(4): 481–490.
- Lutter, M., Fang, M., Luo, X., Nishijima, M., Xie, X. & Wang, X. (2000). Cardiopilin provides specificity for targeting of tBid to mitochondria. *Nature Cell Biology*, **2**: 754-761.
- Ly, J.D., Grubb, D.R. & Lawen, A. (2003). The mitochondrial membrane potential ( $\Delta\Psi$ m) in apoptosis; an update. *Apoptosis*, **8**: 115-128.
- Ma, B.B.Y., Lui, V.W.Y., Hui, C.W.C., Lau, C.P.Y., Wong, C-H., Hui, E.P., Ng, M.H., Tsao, S.W., Li, Y., Chan, A.T.C. (2013). Preclinical evaluation of the AKT inhibitor MK-2206 in nasopharyngeal carcinoma cell lines. *Invest New Drugs*, **31**: 567-575.
- Mai, C.W., Yaeghoobi, M., Abd-Rahman, N., Kang, Y.B. & Pichika, M.R. (2014). Chalcones with electron-withdrawing and electron-donating substituents: Anticancer activity against TRAIL resistant cancer cells, structure-activity relationship analysis and regulation of apoptotic proteins. *European Journal of Medicinal Chemistry*, **77**: 378-387.
- Mackeen, M.M., Ali, A.M., El-Sharkawy, S.H., Manap, M.Y., Salleh, K.M., Lajis, N.H. & Kawazu, K. (1997). Antimicrobial and cytotoxic properties of some Malaysian Traditional Vegetables (Ulam). *Pharmaceutical Biology*, **35**(3): 174-178.
- Madhuri, S. & Govind, P. (2009). Some anticancer medicinal plants of foreign origin. *Current Science*, **96**(6): 779-783.
- Mahmood, A.A., Mariod, A.A., Abdelwahab, S.I., Ismail S. & Al-Bayat, F. (2010). Potential activity of ethanolic extract of *Boesenbergia rotunda* (L.) rhizomes extract in accelerating wound healing in rats. *Journal of Medicinal Plants Research*, **4**(15): 1570-1576.



- Mahmood, T. & Yang, P. (2012). Western blot: Technique, Theory and Trouble Shooting. *North American Journal of Medical Sciences*, **4**(9): 429-434.
- Man, S. L., Gao, W.Y., Zhang, Y. J., Yan, L., Ma, C. Y., Liu, C. X. & Huang, L. Q. (2009). Antitumor and antimetastatic activities of Rhizoma Paridis saponins, *Steroids*, **74**:1051–1056.
- Marsden, V.S., O'Connor, L., O'Reilly, L.A., Silke, J., Metcalf, D., Ekert, P.G., Huang, D.C.S., Cecconi, F., Kuida, K., Tomaselli, K.J., Roy, S., Nicholson, D.W., Vaux, D.L., Bouillet, P., Adams, J.M. & Strasser, A. (2002). Apoptosis initiated by Bcl-2-regulated caspase activation independently of the cytochrome c/Apaf-1/caspase-9 apoptosome. *Letters to Nature*, **419**: 634-637.
- Mol, J. N. M., De Lange, P., Oostdam, A. & Van der Plas, L.H.W. (1990). Progress in Plant Cellular and Molecular Biology. In Nijkamp, H. J. J., Van der Plas, L. H. W. & Van Aartrijk J. (Eds.), *Plant Cell Reports* (pp. 712-716). Netherlands: Kluwer Academic Publications.
- Morikawa, T., Funakoshi, K., Ninomiya, K., Yasuda, D., Miyagawa, K., Matsuda, H. & Yoshikawa, M. (2008). Medicinal Foodstuffs. XXXIV: Structures of New Prenylchalcones and Prenylflavanones with TNF- $\alpha$  and aminopeptidase N inhibitory activities from *Boesenbergia rotunda*. *Chemical & Pharmaceutical Bulletin*, **56**(7): 956-962.
- Mosmann, T. (1983). Rapid colorimetric assay for cellular growth and survival: application to proliferation and cytotoxicity assays. *Journal of Immunology Methods*, **65**: 55-63.
- Mullis, K.B. & Faloona, F.A. (1987). Specific Synthesis of DNA *in vitro* via a Polymerase-Catalyzed Chain Reaction. *Methods in Enzymology*, **155**: 335-350.
- Murakami, A., Ali, A.M., Mat-Salleh, K., Koshimizu, K. & Ohigashi, H. (2000). Screening for *in vitro* antitumor promoting activities of edible plants from Malaysia. *Bioscience, Biotechnology and Biochemistry*, **64**: 9-16.
- Nakamura, S., Nakashima, S., Oda, Y., Yokota, N., Fujimoto, K., Matsumoto, T., Ohta, T., Ogawa, K., Maeda, S., Nishida, S., Matsuda, H. & Yoshikawa, M. (2013). Alkaloids from Sri Lankan curry-leaf (*Murraya koenigii*) display melanogenesis inhibitory activity: Structures of karapinchamines A and B. *Bioorganic & Medicinal Chemistry*, **21**(2013): 1043-1049.
- Niki, E. (1990). Free radical initiators as source of water- or lipid-soluble peroxy radicals. *Methods in Enzymology*, **186**: 100-108.

- Ning, J.P., Yu, M.C., Wang, Q.S. & Henderson, B.E. (1990). Consumption of salted fish and other risk factors for nasopharyngeal carcinoma (NPC) in Tianjin, a low-risk region for NPC in the People's Republic of China. *Journal of the National Cancer Institute*, **82**(4): 291-296.
- Noolu, B., Ajumeera, R., Chauhan, A., Nagalla, B., Manchala, R. & Ismail, A. (2013). *Murraya koenigii* leaf extract inhibits proteasome activity and induces cell death in breast cancer cells. *BMC Complementary & Alternative Medicine*, **13**:7.
- Ochatt, S.J. (2006). Flow cytometry (ploidy determination, cell cycle analysis, DNA content per nucleus). *Medicago truncatula* handbook, version November 2006. Dijon, France.
- Ormerod, M.G. (2008). Flow Cytometry- A Basic Introduction. Online printer version, DeNovo software: [www.flowbook.denovosoftware.com](http://www.flowbook.denovosoftware.com).
- Oteiza, P.I., Erlejtman, A.G., Verstraeten, S.V., Keen, C.L. & Fraga, C.G. (2005). Flavonoid-membrane interactions: a protective role of flavonoids at the membrane surface. *Clinical and Developmental Immunology*, **12**(1): 19-25.
- Park, E.J. & Pezzuto, J.M. (2002). Botanicals in cancer chemoprevention. *Cancer Metastasis Reviews*, **21**: 221-255.
- Park, S., Gwak, J., Han, S.J. & Oh, S. (2013). Cardamonin suppresses the proliferation of colon cancer cells by promoting  $\beta$ -catenin degradation. *Biology and Pharmaceutical Bulletin*, **36**(6): 1040-1044.
- Park, M.K., Jo, S.H., Lee, H.J., Kang, J.H., Kim, Y.R., Kim, H.J., Lee, E.J., Koh, J.Y., Ahn, K.O., Jung, K.C., Oh, S.H., Kim, S.Y. & Lee, C.H. (2013). Novel suppressive effects of cardamonin on the activity and expression of transglutaminase-2 lead to blocking the migration and invasion of cancer cells. *Life Sciences*, **92**: 154-160.
- Parul, S., Javed, A., Neha, B., Honey, J., Anuj, B. (2012). Curry leaves-A medicinal herb. *Asian Journal of Pharmaceutical Research*, **2**: 51-53.
- Petit, P.X., Lecoeur, H., Zorn, E., Dauquet, C., Mignotte, B. & Gougeon, M.L. (1995). Alterations in mitochondrial structure and function are early events of dexamethasone-induced thymocyte apoptosis. *The Journal of Cell Biology*, **130**(1): 157-167.
- Porter, A.G. & Jänicke, R.U. (1999). Emerging roles of caspase-3 in apoptosis. *Cell Death and Differentiation*, **6**: 99-104.

- Qin, L., Zhang, X., Zhang, L., Feng, Y., Weng, G-X., Li, M-Z., Kong, Q-L., Qian, C-N., Zeng, Y-X., Zeng, M-S., Liao, D-F. & Song, L-B. (2008). Downregulation of *BMI-1* enhances 5-fluorouracil-induced apoptosis in nasopharyngeal carcinoma cells. *Biochemical and Biophysical Research Communications*, **371**: 531-535.
- Qin, Y., Sun, C., Lu, F., Shu, X., Yang, D., Chen, L., She, X., Gregg, N.M., Guo, T. & Hu, Y. (2012). Cardamonin exerts potent activity against multiple myeloma through blockade of NF- $\kappa$ B pathway *in vitro*. *Leukemia Research*, **36**: 514-520.
- Ravindran, J., Prasad, S. & Aggarwal, B.B. (2009). Curcumin and Cancer cells: How many ways can curry kill tumor cells selectively? *American Association of Pharmaceutical Scientists*, **11(3)**: 495-510.
- Richmond, S. (2010). History. In *Malaysia, Singapore and Brunei* (pp. 82-83). China: Lonely Planet.
- Ririe, K.M., Rasmussen, R.P. & Wittwer, C.T. (1997). Product Differentiation by Analysis of DNA Melting Curves during Polymerase Chain Reaction. *Analytical Biochemistry*, **245**: 154-160.
- Robinson, J.P. (2006). Introduction to flow cytometry. Flow cytometry talks, Purdue University Cytometry Laboratories. Accessible at [www.cyto.purdue.edu](http://www.cyto.purdue.edu).
- Rong, Y. & Distelhorst, C.W. (2008). Bcl-2 protein family members: versatile regulators of calcium signaling in cell survival and apoptosis. *Annual review of physiology*, **70**: 73–91.
- Rothe, G., Klingel, S., Assfalg-Machleidt, I., Machleidt, W., Zirkelbach, C., Banati, R.B., Mangel, W.F. & Valet, G. (1992). Flow cytometric analysis of protease activities in vital cells. *Biological Chemistry Hoppe-Seyler*, **373**: 547-554.
- Sahu, N.K., Balbhadra, S.S., Choudhary, J. & Kohli, D.V. (2012). Exploring pharmacological significance of chalcone scaffold: a review. *Current Medicinal Chemistry*, **19**: 209-225.
- Schumacker, P.T. (2006). Reactive oxygen species in cancer cells: Live by the sword die by the sword. *Cancer Cell*, **10(3)**: 175-176.
- Schwartsmann, G., Winograd, B. & Pinedo, H. M. (1988). The main steps in the development of anticancer agents. *Radiotherapy and Oncology*, **12(4)**: 301-313.

- Shelton, S.N., Dillard, C.D. & Robertson, J.D. (2010). Activation of Caspase-9, but Not Caspase-2 or Caspase-8, Is Essential for Heat-induced Apoptosis in Jurkat Cells. *The Journal of Biological Chemistry*, **285**(52): 40525-40533.
- Shindo, K., Kato, M., Kinoshita, A., Kobayashi, A. & Koike, Y. (2006). Analysis of antioxidant activities contained in *Boesenbergia pandurata* Schult. rhizome. *Bioscience, Biotechnology and Biochemistry*, **70**(9): 2281-2284.
- Simon, H-U., Haj-Yehia, A. & Levi-Schaffer, F. (2000). Role of reactive oxygen species (ROS) in apoptosis induction. *Apoptosis*, **5**: 415-418.
- Singh, A. & Shukla, Y. (1998). Antitumor activity of diallyl sulfide in two-stage mouse skin model of carcinogenesis. *Biomedical and Environmental Sciences*, **11**: 258-263.
- Singh, M., Kaur, M. & Silakari, O. (2014). Flavones: An important scaffold for medicinal chemistry. *European Journal of Medicinal Chemistry*, **84**: 206-239.
- Singleton, V. L., Orthofer, R. & Lamuela-Raventos, R. M. (1974). Analysis of total phenols and other oxidation substrates and antioxidants by means of Folin-Ciocalteu reagent. In Parker L. (Ed.), *Methods in Enzymology, Polyphenol and Flavonoids* (pp. 152-178). United States of America(USA): Academic Press.
- Singleton, V. L. & Rossi, J. A. (1965). Colorimetry of total phenolics with phosphomolybdic-phosphotungstic acid reagents. *American Journal of Enology and Viticulture*, **16**:144-158.
- Siriruga, P. (1992). A revision of the genus *Boesenbergia kuntze* (Zingiberaceae) in Thailand. *Natural History Bulletin of the Siam Society*, **40**: 67-90.
- Skrzypski, M., Sassek, M., Abdelmessih, S., Mergler, S., Grötzinger, C., Metzke, D., Wojciechowicz, T., Nowak, K.W. & Strowski, M.Z. (2014). Capsaicin induces cytotoxicity in pancreatic neuroendocrine tumor cells via mitochondrial action. *Cellular Signalling*, **26**: 41-48.
- Slater, T.F., Sawyer, B. & Sträuli, U. (1963). Studies on succinate-tetrazolium reductase systems: III. Point of coupling of four different tetrazolium salts. *Biochimia et Biophysica Acta*, **77**: 383-393.
- Sparg, S.G., Light, M.E. & Van Staden, J. (2004). Biological activities and distribution of plant saponins. *Journal of Ethnopharmacology*, **94**: 219–243.
- Stajner, D. & Varga, I.S. (2003). An evaluation of the antioxidant abilities of *Allium* species. *Acta Biologica Szegediensis*, **47**(1-4):103-106.

- Stennicke, H.R. & Salvesen, G.S. (1998). Properties of the caspases. *Biochimica et Biophysica Acta*, **1387**: 17-31.
- Sukari, M.A., Sharif, N.W.M., Ching, A.Y.L., Lian, G.E.C., Rahmani, M. & Khalid, K. (2008). Chemical constituents variations of essential oils from rhizomes of four Zingiberaceae species. *The Malaysian Journal of Analytical Sciences*, **12(3)**: 638-644.
- Sumiyoshi, H. & Wargovich M.J. (1990). Chemopreventive of 1,2-dimethylhydrazine-induced colon cancer in mice by naturally occurring organosulfur compounds. *Cancer Research*, **50**: 5084-5087.
- Sun S., Wang W. Z., Tong, R., Li, X. L., Fishbein, A., Wan, Q., He, T. C., Du, W. & Yuan, C.S. (2010). Effects of steaming the root of *Panax notoginseng* on chemical composition and anticancer activities. *Food Chemistry*, **118**: 307–314.
- Sun, Y., Xun, K., Wang, Y. & Chen, X. (2009). A systematic review of the anticancer properties of berberine. a natural product from Chinese herbs. *Anticancer Drugs*, **20**: 757-769.
- Sung, F.L., Poon, T.C.W., Hui, E.P., Ma, B.B.Y., Liong E., To, K.F., Huang, D.P.W.S. & Chan, A.T.C. (2005). Antitumor effect and enhancement of cytotoxic drug activity by Cetuximab in nasopharyngeal carcinoma cells. *In vivo*, **19**: 237-246.
- Szatrowski, T.P. & Nathan, C.F. (1991). Production of Large Amounts of Hydrogen Peroxide by Human Tumor Cells. *Cancer Research*, **51**: 794-798.
- Tait, S.W.G. & Green, D.R. (2010). Mitochondria and cell death: outer membrane permeabilization and beyond. *Molecular Cell Biology*, **11**: 621-632.
- Tan, E-C., Lee, Y-K., Chee C-F., Heh, C-H., Wong, S-M., Thio, C.L-P., Foo, G-T., Khalid, N., Abd Rahman, N., Karsani, S.A., Othman, S., Othman, R. & Yusof, R. (2012). *Boesenbergia rotunda*: From Ethnomedicine to Drug Discovery. *Evidence-Based Complementary and Alternative Medicine*, **2012**: 25.
- Tan, S.K. (2005). Flavonoids from *Boesenbergia rotunda* (L.) Mansf.: Chemistry, Bioactivity and accumulation. *PhD dissertation*, Faculty of Science, University of Malaya, Kuala Lumpur, Malaysia.
- Tewtrakul, S., Subhadhirasakul, S., Puripattanavong, J. & Panphadung, T. (2003). HIV-1 protease inhibitory substances from the rhizomes of *Boesenbergia pandurata* Holtt. *Songklanakarin Journal Science and Technology*, **25(4)**: 503-508.

- Thomas, E., Shanmugham, J., Raf & M.M. (1999). *In-vitro* antibacterial activity of certain medicinal plants. *Biomedicine*, **19**(3): 185-190.
- Tip-pyang, S., Sathanasaowapak, S., Kokpol, U. & Phuwapraisirisan, P. (2000). Antibacterial flavonoids from *Boesenbergia pandurata*. *ACGC Chemical Research Communications*, **10**: 21-26.
- Trakoontivakorn, G., Nakahara, K., Shinmoto, H., Takenaka, M., Onishi-Kameyama, M., Ono, H., Yoshida, M., Nagata, T. & Tsushida, T. (2001). Structural analysis of a novel antimutagenic compound, 4-hydroxypanduratin A, and the antimutagenic activity of flavonoids in a Thai spice, fingerroot (*Boesenbergia pandurata* Schult.) against mutagenic heterocyclic amines. *Journal of Agriculture and Food Chemistry*, **49**(6): 3046-3050.
- Tsai, S.T., Fang, S.Y., Jin, Y.T., Su, I.J. & Yang, B.C. (1999). Analysis of the expression of Fas-L in nasopharyngeal carcinoma tissues. *Oral Oncology*, **35**(4): 421-424.
- Tsao, S.W., Tsang, C.M., Pang, P.S., Zhang, G., Chen, H. & Lo, K.W. (2012). The biology of EBV infection in human epithelial cells. *Seminars in Cell Biology*, **22**(2): 137-143.
- Tuntiwachwutiikul, P., Pancharoen, O., Reutrakul, U. & Bryne, L.T. (1984). “(1’RS, 2’SR, 6’RS)-(2,6-dihydroxy-4-methoxy-phenyl)-[3’-methyl-2’-(3’’-methylene-2’’-enyl)-6’phenyl-cyclohex-3’-enyl] methanone (panduratin A) a constituent of the red rhizomes of a variety of *Boesenbergia pandurata*. *Australian Journal of Chemistry*, **37**: 449-453.
- Velde, C.V., Cizeau, J., Dubik, D., Alimonti, J., Brown, T., Israels, S., Hakem, R. & Greenberg, A.H. (2000). BNIP3 and Genetic Control of Necrosis-Like Cell Death through the Mitochondrial Permeability Transition Pore. *Molecular and Cellular Biology*, **20**(15): 5454-5468.
- Wall, M. E., Wani, M. C. & Brown, D. M. (1996). Effect of tannins on screening of plant extracts for enzyme inhibitory activity and techniques for their removal. *Phytomedicine*, **3**: 281–285.
- Wallace, D.C. (2005). A Mitochondrial Paradigm of Metabolic and Degenerative Disease, Aging, and Cancer: A Dawn of Evolutionary Medicine. *Annual Review of Genetics*, **39**: 359-407.
- Wang, C.X. & Youle, R.J. (2009). The Role of Mitochondria in Apoptosis. *Annual Review of Genetics*, **43**: 95-118.

- Wangkangwan, W., Boonkerd, S., Chavasiri, W., Sukapirom, K., Pattanapanyasat, K., Kongkathip, N., Miyakawa, T. & Yompakdee, C. (2009). Pinostrobin from *Boesenbergia pandurata* is an inhibitor of  $\text{Ca}^{2+}$ -signal-mediated cell-cycle regulation in the yeast *Saccharomyces cerevisiae*. *Bioscience, Biotechnology and Biochemistry*, **73**(7): 1679-1682.
- Wardley, A. (2008). The need for advanced breast cancer treatment guidelines: Results of an internet-based survey, Department of Medical Oncology, Christie Hospital NHS Trust. *The Breast*, **17**: 275–281.
- Waterhouse, A. L. (2002). Determination of Total Phenolics. In Wrolstad, R. E. (Ed.), *Current Protocols in Food Analytical Chemistry* (Section II.1.1-II.1.8). New York: John Wiley and Sons.
- White, M.J., Schoenwaelder, S.M., Josefsson, E.C., Jarman, K.E., Henley, K.J., James, C., Debrincat, M.A., Jackson, S.P., Huang, D.C.S. & Kile, B.T. (2012). Caspase-9 mediates the apoptotic death of megakaryocytes and platelets, but is dispensable for their generation and function. *Platelets and Thrombopoiesis*, **119**(18): 4283-4290.
- Wijekoon, M.M.J.O., Bhat, R. & Karim, A.A. (2011). Effect of extraction solvents on the phenolic compounds and antioxidant activities of bunga kantan (*Etlintera elatior* Jack.) inflorescence. *Journal of Food Composition and Analysis*, **24**: 615-619.
- Willis, S.N. & Adams, J.M. (2005). Life in the balance: how BH3-only proteins induce apoptosis. *Current Opinion in Cell Biology*, **17**(6): 617-625.
- Win, N.N., Awale, S., Esumi, H., Tezuka, Y. & Kadota, S. (2007). Bioactive secondary metabolites from *Boesenbergia pandurata* of Myanmar and their preferential cytotoxicity against human pancreatic cancer PANC-1 cell line in nutrient-deprived medium. *Journal of Natural Products*, **70**(10): 1582-1587.
- Wolfe, K.L. & Liu, R.H. (2007). Cellular Antioxidant Activity (CAA) Assay for Assessing Antioxidants, Foods, and Dietary Supplements. *Journal of Agricultural and Food Chemistry*, **56**: 8896-8907.
- Woo, M., Hakem, R., Soengas, M.S., Duncan, G.S., Shahinian, A., Kägi, D., Hakem, A., McCurrach, M., Khoo, W., Kaufman, S.A., Senaldi, G., Howard, T., Lowe, S.W. & Mak, T.W. (1998). Essential contribution of caspase-3/CCP32 to apoptosis and its associated nuclear changes. *Genes and Development*, **12**: 806-819.

- World Health Organization. (2014). World Cancer Report. Stewart, B.W. & Wild, C.P. (Eds.), *International Agency for Research on Cancer (IARC)*. Lyon, France: IARC Press.
- World Health Organization. (2003). World Cancer Report. In Kleihues, P. & Stewart, B. W. (Eds.), *International Agency for Research on Cancer (IARC)*. Lyon, France: IARC Press.
- Wu, Y., Wang, D., Wang, X., Wang, Y., Ren, F., Chang, D., Chang, Z. & Jia, B. (2011). Caspase 3 is Activated through Caspase 8 instead of Caspase-9 during H<sub>2</sub>O<sub>2</sub>-induced Apoptosis in HeLa cells. *Cellular Physiology and Biochemistry*, **27**: 539-546.
- Xie, J-T., Chang, W-T., Wang, C-Z., Mehendale, S.R., Li, J., Ambihapahar, R., Ambihapahar, U., Fong, H.H. & Yuan, C-S. (2006). Curry leaf (*Murraya koenigii* Spreng.) reduces blood cholesterol and glucose levels in *ob/ob* mice. *American Journal of Chinese Medicine*, **34**(2): 279-284.
- Xie, M., Zhang, H., Xu, Y., Liu, T., Chen, S., Wang, J. & Zhang, T. (2013). Expression of folate receptors in nasopharyngeal and laryngeal carcinoma and folate receptor-mediated endocytosis by molecular targeted nanomedicine. *International Journal of Nanomedicine*, **8**: 2443-2451.
- Xue, C., Huang, Y., Huang, P.Y., Yu, Q.T., Pan, J.J., Liu, L.Z., Song, X.Q., Lin, S.J., Wu, J.X., Zhang, J.W., Zhao, H.Y., Xu, F., Liu, F.X., Hu, Z.H., Zhao, L.P., Zhao, Y.Y., Wu, X., Zhang, J., Ma, Y.X. & Zhang, L. (2012). Phase II study of sorafenib in combination with cisplatin and 5-fluorouracil to treat recurrent or metastatic nasopharyngeal carcinoma. *Annals of Oncology*, **00**:1-8.
- Yu, F., Huang, A., Yang, J., Yu, C., Lu, C., Chiang, J., Chiu, C. & Chung, J. (2010). Safrole Induces Cell Death in Human Tongue Squamous Cancer SCC-4 Cells through Mitochondria-Dependent Caspase Activation Cascade Apoptotic Signaling Pathways. *Environmental Toxicology*, **27**(7): 433-444.
- Yu, F., Yang, J., Yu, C., Lu, C., Chiang, J., Lin, C. & Chung, J. (2010). Safrole Induces Apoptosis in Human Oral Cancer HSC-3 Cells. *Journal of Dental Research*, **90**(2): 168-174.
- Yu, L. M., Zhao, M. M., Yang, B. & Bai, W.D. (2009). Immunomodulatory and anticancer activities of phenolics from *Garcinia mangostana* fruit pericarp. *Food Chemistry*, **116**: 969–973.
- Yun, J.M., Kwon, H. & Hwang, J-K. (2003). *In vitro* anti-inflammatory activity of panduratin A isolated from *Kaempferia pandurata* in RAW264.7 cells. *Planta Medica*, **69**: 1102-1108.



- Zbigniew, D. (1990). Differential staining of DNA and RNA in intact cells and isolated cell nuclei with acridine orange. *Methods in Cell Biology*, **33**: 285.
- Zhang, L., Zhang, Y., Zhang, L., Yang, X. & Lv, Z. (2009). Lupeol, a dietary triterpene, inhibited growth, and induced apoptosis through down-regulation of DR3 in SMMC7721 cells. *Cancer Invest*, **27**: 163-170.
- Zhang, R., Humphreys, I. & Sahu, R.P. (2008). *In vitro* and *in vivo* induction of apoptosis by capsaicin in pancreatic cancer cells is mediated through ROS generation and mitochondrial death pathway. *Apoptosis*, **13**: 1465-1478.
- Zorov, D.B., Juhaszova, M. & Sollott, S.J. (2006). Mitochondrial ROS-induced ROS release: An update and review. *Biochimica et Biophysica Acta*, **1757**: 509-517.

## 7.0 APPENDICES

### 7.1 Total phenolic content of various crude extracts determined by Folin-Ciocalteu's assay

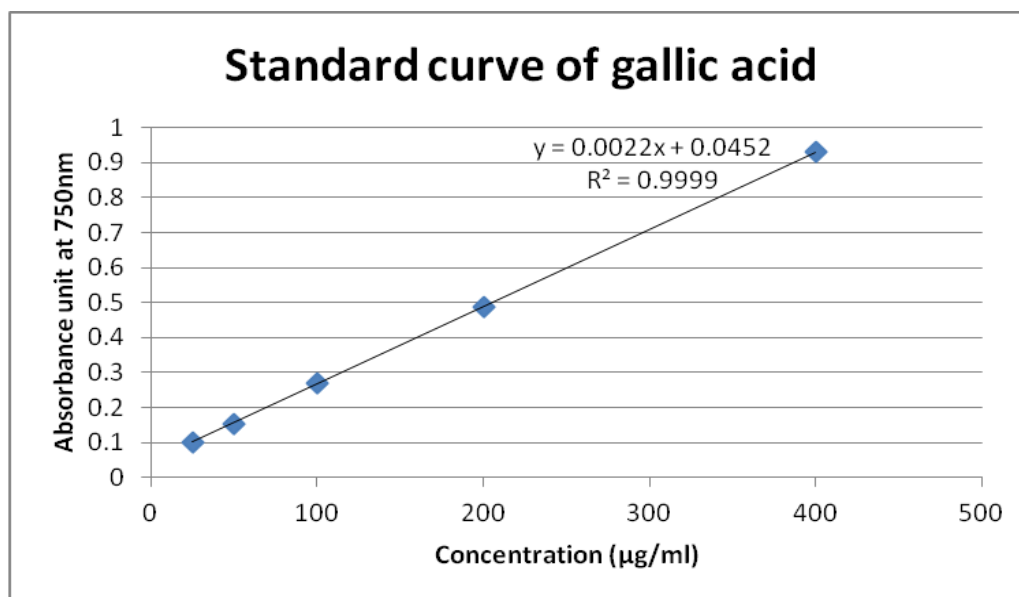
Crude extract of inflorescence of bunga kantan	Total phenolic content (mg gallic acid equivalents/g of sample)				
	Independent experiment			Average	Standard deviation
	1	2	3		
Methanolic	69.01	69.58	65.18	<b>67.92</b>	2.39
Ethyl acetate	11.21	8.43	8.28	9.31	1.65
Hexane	9.42	11.11	10.51	10.35	0.86
Methanolic solid 1	17.96	16.38	17.52	17.29	0.81
Methanolic solid 2	17.96	16.38	17.52	21.53	1.73

Crude extract of curry leaf	Total phenolic content (mg gallic acid equivalents/g of sample)				
	Independent experiment			Average	Standard deviation
	1	2	3		
Methanolic	63.93	63.00	68.17	65.03	2.75
Ethyl acetate	87.74	88.82	81.88	<b>86.15</b>	3.73
Hexane	49.24	46.09	42.80	46.04	3.22

Crude extract of temu kunci	Total phenolic content (mg gallic acid equivalents/g of sample)				
	Independent experiment			Average	Standard deviation
	1	2	3		
Methanolic	98.43	99.12	99.10	98.88	0.40
Ethyl acetate	115.06	112.56	114.17	<b>113.90</b>	1.27
Hexane	48.35	48.33	43.90	46.86	2.57

Crude extract of mushroom bean	Total phenolic content (mg gallic acid equivalents/g of sample)				
	Independent experiment			Average	Standard deviation
	1	2	3		
Methanolic	13.96	14.39	12.95	13.77	0.74
Ethyl acetate	20.06	19.36	18.87	<b>19.43</b>	0.60
Hexane	11.70	11.66	10.35	11.24	0.76

Crude extract of spring onion leaf	Total phenolic content (mg gallic acid equivalents/g of sample)				
	Independent experiment			Average	Standard deviation
	1	2	3		
Methanolic	28.30	29.92	29.65	<b>29.29</b>	0.87
Ethyl acetate	20.44	20.24	21.35	20.68	0.59
Hexane	11.75	10.32	13.78	11.95	1.74



## 7.2 Total flavonoid content of various crude extracts using Dowd method

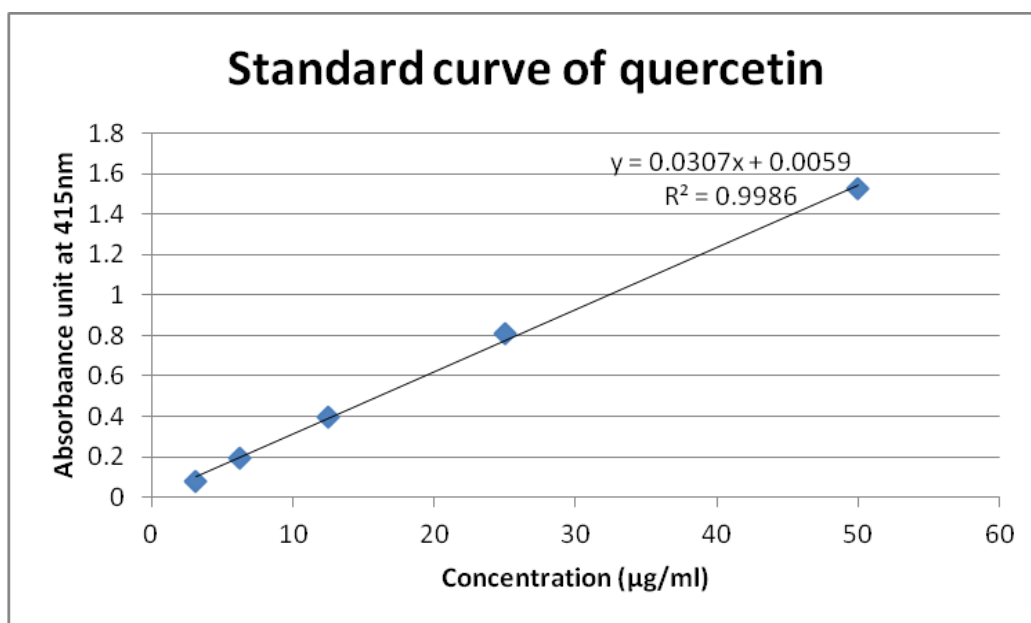
Crude extract of inflorescence of bunga kantan	Total flavonoid content (mg quercetin equivalents/g of sample)				
	Independent experiment			Average	Standard deviation
	1	2	3		
Methanolic	66.74	67.71	69.06	<b>67.84</b>	1.16
Ethyl acetate	33.34	37.97	36.86	36.06	2.41
Hexane	34.16	36.32	38.13	36.20	1.99
Methanolic solid 1	34.71	35.93	38.64	36.43	2.01
Methanolic solid 2	35.87	38.42	36.29	36.86	1.37

Crude extract of curry leaf	Total flavonoid content (mg quercetin equivalents/g of sample)				
	Independent experiment			Average	Standard deviation
	1	2	3		
Methanolic	164.73	163.81	177.16	168.60	7.46
Ethyl acetate	211.56	229.29	230.72	<b>223.90</b>	10.68
Hexane	78.43	78.22	68.44	75.03	5.71

Crude extract of temu kunci	Total flavonoid content (mg quercetin equivalents/g of sample)				
	Independent experiment			Average	Standard deviation
	1	2	3		
Methanolic	262.50	276.42	269.75	269.60	6.96
Ethyl acetate	807.80	847.21	843.93	<b>833.00</b>	21.87
Hexane	246.81	245.55	238.76	243.70	4.33

Crude extract of mushroom bean	Total flavonoid content (mg quercetin equivalents/g of sample)				
	Independent experiment			Average	Standard deviation
	1	2	3		
Methanolic	29.81	30.79	30.23	30.28	0.49
Ethyl acetate	33.90	33.95	34.64	<b>34.17</b>	0.42
Hexane	29.40	29.24	29.55	29.40	0.15

Crude extract of spring onion leaf	Total flavonoid content (mg quercetin equivalents/g of sample)				
	Independent experiment			Average	Standard deviation
	1	2	3		
Methanolic	202.31	206.34	206.78	205.10	2.46
Ethyl acetate	349.92	346.72	334.18	<b>343.60</b>	8.32
Hexane	139.98	139.31	134.39	137.90	3.06



### 7.3 Cell viability of HK-1 and NP-69 cell lines

#### 7.3.1 Template for cell treatment

Well/Row	1	2	3	4	5	6	7	8	9	10	11	12
A	crude methanolic extract (200 µg/ml)			crude ethyl acetate extract (200 µg/ml)			crude hexane extract (200 µg/ml)			Positive control 5-fluorouracil (200 µg/ml)		
B	100 µg/ml			100 µg/ml			100 µg/ml			100 µg/ml		
C	50 µg/ml			50 µg/ml			50 µg/ml			50 µg/ml		
D	25 µg/ml			25 µg/ml			25 µg/ml			25 µg/ml		
E	12.5 µg/ml			12.5 µg/ml			12.5 µg/ml			12.5 µg/ml		
F	6.25 µg/ml			6.25 µg/ml			6.25 µg/ml			6.25 µg/ml		
G	3.13 µg/ml			3.13 µg/ml			3.13 µg/ml			3.13 µg/ml		
H	Control: growth media only											

#### 7.3.2 Data of percentage of cell viability of HK-1 cells treated with crude methanolic extract of bunga kantan after 24 hrs treatment

Concentration of extract (µg/ml)	Percentage (%) of cell viability				
	Independent experiment			Average	Standard deviation
	1	2	3		
0	100.698100	100.354500	98.947360	98.16	0.9276
3.125	107.080700	109.728600	104.815500	100.9	2.459
6.25	101.783400	106.270900	101.203400	99.94	2.773
12.5	105.133100	106.654200	109.652800	107.1	2.300
25	94.120740	93.556430	97.612390	95.10	2.197
50	95.124900	95.564020	96.336700	95.68	0.6135
100	87.738600	88.625690	89.496470	88.62	0.8789
200	88.119080	87.567920	92.070100	89.25	2.456

**7.3.3 Data of percentage of cell viability of HK-1 cells treated with crude ethyl acetate extract of bunga kantan after 24 hrs treatment**

Concentration of extract (µg/ml)	Percentage (%) of cell viability				
	Independent experiment			Average	Standard deviation
	1	2	3		
0	100.6981	100.3545	98.9474	100.0	0.9276
3.125	125.1331	126.6545	119.6528	123.8	3.683
6.25	116.6174	120.2757	106.3825	114.4	7.201
12.5	105.4944	113.0437	138.1140	118.9	17.08
25	127.5234	111.1021	104.3285	114.3	11.93
50	98.7717	102.0805	93.2561	98.04	4.458
100	81.8966	107.0691	89.3223	92.76	12.93
200	98.1219	91.5692	84.0721	91.25	7.030

**7.3.4 Data of percentage of cell viability of HK-1 cells treated with crude hexane extract of bunga kantan after 24 hrs treatment**

Concentration of extract (µg/ml)	Percentage (%) of cell viability				
	Independent experiment			Average	Standard deviation
	1	2	3		
0	100.698100	100.354500	98.947360	100.0	0.9276
3.125	106.729500	102.512300	106.798200	105.3	2.455
6.25	101.221800	109.568000	102.024100	104.0	4.605
12.5	101.646100	108.810700	102.146900	104.2	4.000
25	95.552600	99.915720	92.237620	95.90	3.851
50	90.976780	90.719420	87.149870	89.62	2.139
100	87.844690	83.570880	78.881200	83.43	4.483
200	76.358610	77.191090	69.268280	74.27	4.354

**7.3.5 Data of percentage of cell viability of HK-1 cells treated with crude methanolic solid 1 extract of bunga kantan after 24 hrs treatment**

Concentration of extract (µg/ml)	Percentage (%) of cell viability				
	Independent experiment			Average	Standard deviation
	1	2	3		
0	100.698100	100.354500	98.947360	100.0	0.9276
3.125	108.906200	106.855100	109.398300	108.4	1.349
6.25	101.770800	102.541100	103.532500	102.6	0.8832
12.5	107.478400	101.656300	99.432880	102.9	4.155
25	96.754240	95.269500	107.382300	99.80	6.607
50	94.527650	102.141500	98.426410	98.37	3.807
100	92.593610	91.841140	90.880910	91.77	0.8584
200	91.182970	88.265010	92.608920	90.69	2.214

**7.3.6 Data of percentage of cell viability of HK-1 cells treated with crude methanolic extract of bunga kantan after 48 hrs treatment**

Concentration of extract (µg/ml)	Percentage (%) of cell viability				
	Independent experiment			Average	Standard deviation
	1	2	3		
0	103.418800	97.062830	99.518340	100.0	3.205
3.125	99.209830	95.166890	96.334050	96.90	2.081
6.25	92.169980	95.403790	93.983210	93.85	1.621
12.5	90.495900	92.723970	95.805950	93.01	2.666
25	88.067930	89.367310	94.612820	90.68	3.465
50	77.849140	74.190030	87.808220	79.95	7.048
100	66.122890	73.713880	74.927310	71.59	4.772
200	55.623760	65.357670	64.573870	61.85	5.408

**7.3.7 Data of percentage of cell viability of HK-1 cells treated with crude ethyl acetate extract of bunga kantan after 48 hrs treatment**

Concentration of extract (µg/ml)	Percentage (%) of cell viability				
	Independent experiment			Average	Standard deviation
	1	2	3		
0	103.418800	97.062830	99.518340	100.0	3.205
3.125	99.840470	95.680030	97.358040	97.63	2.093
6.25	96.333260	99.131990	93.654780	96.37	2.739
12.5	94.823750	98.479400	90.982280	94.76	3.749
25	95.490360	95.421100	89.480640	93.46	3.450
50	98.006470	87.841270	94.926850	93.59	5.212
100	79.642850	72.508870	79.320880	77.16	4.029
200	70.310480	71.716660	72.393340	71.47	1.063

**7.3.8 Data of percentage of cell viability of HK-1 cells treated with crude hexane extract of bunga kantan after 48 hrs treatment**

Concentration of extract (µg/ml)	Percentage (%) of cell viability				
	Independent experiment			Average	Standard deviation
	1	2	3		
0	103.418800	97.062830	99.518340	100.0	3.205
3.125	101.346600	103.463800	103.151800	102.7	1.143
6.25	100.115700	94.853650	99.990720	98.32	3.003
12.5	94.049320	89.934440	92.089710	92.02	2.058
25	92.932530	90.907520	87.934140	90.59	2.514
50	81.296520	84.797470	79.651990	81.92	2.628
100	75.843890	73.240570	81.471890	76.85	4.207
200	70.330310	77.575650	68.306400	72.07	4.874



**7.3.9 Data of percentage of cell viability of HK-1 cells treated with crude methanolic solid 1 extract of bunga kantan after 48 hrs treatment**

Concentration of extract (µg/ml)	Percentage (%) of cell viability				
	Independent experiment			Average	Standard deviation
	1	2	3		
0	103.418800	97.062830	99.518340	100.0	3.205
3.125	101.533400	103.115800	95.243000	99.96	4.164
6.25	98.842290	102.479900	102.195800	101.2	2.023
12.5	73.711500	74.567280	76.310940	74.86	1.325
25	74.566310	76.426050	70.204940	73.73	3.193
50	74.578710	70.785450	77.392200	74.25	3.315
100	70.765850	74.680900	70.667320	72.04	2.289
200	58.474830	60.382810	62.662270	60.51	2.096

**7.3.10 Data of percentage of cell viability of HK-1 cells treated with crude methanolic extract of curry leaf after 24 hrs treatment**

Concentration of extract (µg/ml)	Percentage (%) of cell viability				
	Independent experiment			Average	Standard deviation
	1	2	3		
0	100.203400	101.433400	98.363250	100.0	1.545
3.125	101.051400	108.945600	102.509600	104.2	4.201
6.25	107.450800	109.113500	108.386700	108.3	0.8335
12.5	103.327900	106.885800	109.688100	106.6	3.188
25	105.095200	108.234900	102.147100	105.2	3.044
50	104.338000	106.741900	100.376600	103.8	3.214
100	78.720830	86.772250	87.283360	84.26	4.803
200	48.835800	57.592390	55.875800	54.10	4.640

**7.3.11 Data of percentage of cell viability of HK-1 cells treated with crude ethyl acetate extract of curry leaf after 24 hrs treatment**

Concentration of extract (µg/ml)	Percentage (%) of cell viability				
	Independent experiment			Average	Standard deviation
	1	2	3		
0	103.265300	92.500730	104.233900	100.0	6.513
3.125	105.424700	102.856800	106.218700	104.8	1.757
6.25	109.623600	109.523200	105.859900	108.3	2.145
12.5	108.704100	107.859300	103.979000	106.8	2.520
25	92.290510	89.188000	97.282630	92.92	4.084
50	61.216550	59.140950	66.209430	62.19	3.633
100	60.213580	60.488510	57.988810	59.56	1.371
200	59.047640	59.085820	60.256470	59.46	0.6872

**7.3.12 Data of percentage of cell viability of HK-1 cells treated with crude hexane extract of curry leaf after 24 hrs treatment**

Concentration of extract (µg/ml)	Percentage (%) of cell viability				
	Independent experiment			Average	Standard deviation
	1	2	3		
0	95.657310	98.329020	106.013700	100.0	5.377
3.125	104.741100	109.466100	111.307200	108.5	3.387
6.25	106.814800	106.830800	99.866590	104.5	4.016
12.5	98.148330	97.707940	96.688200	97.51	0.7490
25	99.815430	96.900830	96.781990	97.83	1.718
50	76.174260	70.293200	74.386100	73.62	3.015
100	66.891380	62.005260	66.924950	65.27	2.831
200	60.718290	54.306270	60.200900	58.41	3.562

**7.3.13 Data of percentage of cell viability of HK-1 cells treated with crude methanolic extract of curry leaf after 48 hrs treatment**

Concentration of extract (µg/ml)	Percentage (%) of cell viability				
	Independent experiment			Average	Standard deviation
	1	2	3		
0	99.337080	105.371500	95.291430	100.0	5.073
3.125	101.364700	104.326100	101.871800	102.5	1.584
6.25	108.786000	104.759500	100.387500	104.6	4.200
12.5	106.214100	102.458500	100.218100	103.0	3.030
25	102.021700	101.995300	101.666500	101.9	0.1979
50	93.833700	99.556510	96.199710	96.53	2.876
100	69.427860	69.967080	67.108100	68.83	1.519
200	38.103710	40.526710	40.325230	39.65	1.345

**7.3.14 Data of percentage of cell viability of HK-1 cells treated with crude ethyl acetate extract of curry leaf after 48 hrs treatment**

Concentration of extract (µg/ml)	Percentage (%) of cell viability				
	Independent experiment			Average	Standard deviation
	1	2	3		
0	97.212650	104.409800	98.377550	100.0	3.863
3.125	80.505110	71.650540	76.683800	76.28	4.441
6.25	79.509930	74.537740	70.946810	75.00	4.300
12.5	71.945990	76.117200	78.167470	75.41	3.170
25	61.315880	61.237590	59.336270	60.63	1.121
50	58.362790	55.616910	54.844470	56.27	1.849
100	55.157630	53.701610	56.603580	55.15	1.451
200	53.116540	57.153370	57.199790	55.82	2.344

**7.3.15 Data of percentage of cell viability of HK-1 cells treated with crude hexane extract of curry leaf after 48 hrs treatment**

Concentration of extract (µg/ml)	Percentage (%) of cell viability				
	Independent experiment			Average	Standard deviation
	1	2	3		
0	96.688740	99.959010	103.352200	100.0	3.332
3.125	102.714400	103.193800	104.565300	103.5	0.9606
6.25	97.060590	99.259650	101.118800	99.15	2.031
12.5	86.585790	90.310180	92.653410	89.85	3.060
25	89.598050	83.831140	79.878990	84.44	4.888
50	69.707030	72.709210	76.141730	72.85	3.220
100	43.034620	40.946610	46.492460	43.49	2.801
200	41.540180	36.628090	34.585640	37.58	3.575

**7.3.16 Data of percentage of cell viability of HK-1 cells treated with crude methanolic extract of temu kunci after 24 hrs treatment**

Concentration of extract (µg/ml)	Percentage (%) of cell viability				
	Independent experiment			Average	Standard deviation
	1	2	3		
0	100.203400	101.433400	98.363250	100.0	1.545
3.125	111.313500	98.541310	108.985000	106.3	6.802
6.25	107.526200	103.421700	103.415500	104.8	2.372
12.5	98.306900	94.991700	104.660400	99.32	4.913
25	92.367040	90.063320	95.990500	92.81	2.988
50	85.570850	90.691570	95.646320	90.64	5.038
100	70.821880	71.573000	78.250460	73.55	4.089
200	56.105050	52.224860	52.560390	53.63	2.150

**7.3.17 Data of percentage of cell viability of HK-1 cells treated with crude ethyl acetate extract of temu kunci after 24 hrs treatment**

Concentration of extract (µg/ml)	Percentage (%) of cell viability				
	Independent experiment			Average	Standard deviation
	1	2	3		
0	103.265300	92.500730	104.233900	100.0	6.513
3.125	96.780800	98.579860	91.274700	95.55	3.806
6.25	87.167900	94.931300	97.557750	93.22	5.402
12.5	86.092230	89.822100	93.202200	89.71	3.556
25	86.938500	89.422440	87.361900	87.91	1.329
50	81.173360	86.421840	88.794270	85.40	3.900
100	61.679650	65.956390	63.535390	63.72	2.145
200	55.939460	59.929790	55.281590	53.63	2.150

**7.3.18 Data of percentage of cell viability of HK-1 cells treated with crude hexane extract of temu kunci after 24 hrs treatment**

Concentration of extract (µg/ml)	Percentage (%) of cell viability				
	Independent experiment			Average	Standard deviation
	1	2	3		
0	95.657310	98.329020	106.013700	100.0	5.377
3.125	97.858060	100.866700	103.961200	100.9	3.052
6.25	93.466380	94.946630	101.164000	96.53	4.085
12.5	90.607840	96.753110	91.686380	93.02	3.281
25	85.454570	85.314610	80.237050	83.67	2.973
50	64.691290	74.313230	75.415530	71.47	5.899
100	62.449550	64.940300	61.056450	62.82	1.968
200	59.641330	61.404830	57.220490	59.42	2.101

**7.3.19 Data of percentage of cell viability of HK-1 cells treated with crude methanolic extract of temu kunci after 48 hrs treatment**

Concentration of extract (µg/ml)	Percentage (%) of cell viability				
	Independent experiment			Average	Standard deviation
	1	2	3		
0	99.337080	105.371500	95.291430	100.0	5.073
3.125	103.938600	103.704100	107.070300	104.9	1.879
6.25	93.404010	104.748500	104.387500	100.8	6.448
12.5	89.829960	85.866320	99.412770	91.70	6.965
25	91.949390	84.016400	92.376800	89.45	4.708
50	85.397510	79.980070	85.876930	83.75	3.275
100	58.403580	59.528240	54.163700	57.37	2.829
200	39.212990	40.689170	34.734150	38.21	3.101

**7.3.20 Data of percentage of cell viability of HK-1 cells treated with crude ethyl acetate extract of temu kunci after 48 hrs treatment**

Concentration of extract (µg/ml)	Percentage (%) of cell viability				
	Independent experiment			Average	Standard deviation
	1	2	3		
0	97.212650	104.409800	98.377550	100.0	3.863
3.125	93.953920	90.293000	88.967370	91.07	2.583
6.25	91.091430	91.697420	93.784940	92.19	1.413
12.5	90.524450	83.762070	88.490510	87.59	3.470
25	82.262160	86.119010	80.167450	82.85	3.019
50	76.340690	77.764810	77.223680	77.11	0.7189
100	56.778240	52.771330	55.174540	54.91	2.017
200	52.665380	53.784690	49.194560	51.88	2.393

**7.3.21 Data of percentage of cell viability of HK-1 cells treated with crude hexane extract of temu kunci after 48 hrs treatment**

Concentration of extract (µg/ml)	Percentage (%) of cell viability				
	Independent experiment			Average	Standard deviation
	1	2	3		
0	96.688740	99.959010	103.352200	100.0	3.332
3.125	92.857320	99.769870	95.121090	95.92	3.524
6.25	93.359890	99.636360	96.671420	96.56	3.140
12.5	83.401470	80.548810	82.479620	82.14	1.456
25	65.692040	61.177890	66.763920	64.54	2.965
50	65.042880	59.555130	57.251920	60.62	4.002
100	42.572090	40.993650	42.356800	41.97	0.856
200	36.158800	37.941650	37.807300	37.30	0.9928

**7.3.22 Data of percentage of cell viability of HK-1 cells treated with crude methanolic extract of spring onion leaf after 24 hrs treatment**

Concentration of extract (µg/ml)	Percentage (%) of cell viability				
	Independent experiment			Average	Standard deviation
	1	2	3		
0	100.203400	101.433400	98.363250	100.0	1.545
3.125	106.579700	102.163700	109.277500	106.0	3.591
6.25	105.840800	101.699300	103.176500	103.6	2.099
12.5	104.160000	105.683500	101.963900	103.9	1.870
25	101.140600	108.735800	102.648500	104.2	4.021
50	106.423600	100.688300	103.935800	103.7	2.876
100	109.197900	101.468200	100.707000	103.8	4.698
200	82.259040	88.062810	86.049610	85.46	2.947

**7.3.23 Data of percentage of cell viability of HK-1 cells treated with crude ethyl acetate extract of spring onion leaf after 24 hrs treatment**

Concentration of extract (µg/ml)	Percentage (%) of cell viability				
	Independent experiment			Average	Standard deviation
	1	2	3		
0	103.265300	92.500730	104.233900	100.0	6.513
3.125	108.021400	109.305900	107.433900	108.3	0.9574
6.25	103.739900	100.013600	106.276200	103.3	3.150
12.5	107.323700	105.689700	102.027300	105.0	2.712
25	82.462600	83.034260	87.263700	84.25	2.623
50	74.156850	86.240250	83.820720	81.41	6.393
100	75.601730	86.554770	81.141000	81.10	5.477
200	65.969150	62.115190	73.001480	67.03	5.520

**7.3.24 Data of percentage of cell viability of HK-1 cells treated with crude hexane extract of spring onion leaf after 24 hrs treatment**

Concentration of extract (µg/ml)	Percentage (%) of cell viability				
	Independent experiment			Average	Standard deviation
	1	2	3		
0	95.657310	98.329020	106.013700	100.0	5.377
3.125	112.762800	102.378500	103.815400	106.3	5.627
6.25	110.152700	100.235500	106.489700	105.6	5.015
12.5	101.825600	105.552200	107.471000	104.9	2.871
25	103.068400	100.535000	107.519100	103.7	3.536
50	100.930500	102.286900	100.876600	101.4	0.7991
100	99.470500	105.660300	98.846640	101.3	3.767
200	95.874280	94.213970	96.199200	95.43	1.065

**7.3.25 Data of percentage of cell viability of HK-1 cells treated with crude methanolic extract of spring onion leaf after 48 hrs treatment**

Concentration of extract (µg/ml)	Percentage (%) of cell viability				
	Independent experiment			Average	Standard deviation
	1	2	3		
0	99.337080	105.371500	95.291430	100.0	5.073
3.125	102.138300	108.971700	102.653100	104.6	3.805
6.25	101.899600	102.698000	104.085300	102.9	1.106
12.5	105.793000	107.144300	101.279900	104.7	3.071
25	105.832900	101.471600	103.958500	103.8	2.188
50	93.031580	104.963300	103.186100	100.4	6.437
100	87.039970	84.596370	88.034760	86.56	1.769
200	81.458780	75.398410	82.130790	79.60	3.708

**7.3.26 Data of percentage of cell viability of HK-1 cells treated with crude ethyl acetate extract of spring onion leaf after 48 hrs treatment**

Concentration of extract (µg/ml)	Percentage (%) of cell viability				
	Independent experiment			Average	Standard deviation
	1	2	3		
0	97.212650	104.409800	98.377550	100.0	3.863
3.125	94.309130	97.734110	91.388850	94.48	3.176
6.25	93.189990	95.582660	98.180950	95.65	2.496
12.5	92.793170	93.035480	89.107520	91.65	2.201
25	79.121030	80.771200	81.012970	80.30	1.030
50	72.729570	76.685950	74.238660	74.55	1.997
100	67.800700	65.746190	68.250310	67.27	1.335
200	59.074310	61.533410	53.445950	58.02	4.146

**7.3.27 Data of percentage of cell viability of HK-1 cells treated with crude hexane extract of spring onion leaf after 48 hrs treatment**

Concentration of extract (µg/ml)	Percentage (%) of cell viability				
	Independent experiment			Average	Standard deviation
	1	2	3		
0	96.688740	99.959010	103.352200	100.0	3.332
3.125	98.364700	87.933250	93.823900	93.37	5.230
6.25	91.182980	91.502960	91.739620	91.48	0.2794
12.5	89.647000	85.262470	83.823440	86.24	3.033
25	81.433280	85.217770	79.239430	81.96	3.024
50	80.139940	84.763390	88.781230	84.56	4.324
100	81.675250	79.658640	75.654590	79.00	3.065
200	77.058840	78.625690	81.126560	78.94	2.052

**7.3.28 Data of percentage of cell viability of HK-1 cells treated with crude methanolic extract of pink/mushroom bean after 24 hrs treatment**

Concentration of extract (µg/ml)	Percentage (%) of cell viability				
	Independent experiment			Average	Standard deviation
	1	2	3		
0	100.203400	101.433400	98.363250	100.0	1.545
3.125	108.181200	103.029500	101.493300	104.2	3.503
6.25	101.414700	107.976500	104.809800	104.7	3.282
12.5	107.296900	105.030400	102.062300	104.8	2.625
25	101.568300	102.645000	109.201900	104.5	4.132
50	101.392500	102.672000	101.687900	101.9	0.6699
100	101.819800	104.864600	108.156000	104.9	3.169
200	104.174000	102.972600	102.769000	103.3	0.7593

**7.3.29 Data of percentage of cell viability of HK-1 cells treated with crude ethyl acetate extract of pink/mushroom bean after 24 hrs treatment**

Concentration of extract (µg/ml)	Percentage (%) of cell viability				
	Independent experiment			Average	Standard deviation
	1	2	3		
0	103.265300	92.500730	104.233900	100.0	6.513
3.125	91.404000	91.191400	89.306900	90.63	1.154
6.25	95.718030	94.296990	90.442920	93.49	2.729
12.5	83.481980	80.330000	86.167250	83.33	2.922
25	85.592830	82.868880	78.948010	82.47	3.340
50	83.155600	73.431530	81.239040	79.28	5.151
100	79.752960	79.544480	80.503240	79.93	0.5043
200	77.681820	77.733030	77.668910	77.69	0.03391

**7.3.30 Data of percentage of cell viability of HK-1 cells treated with crude hexane extract of pink/mushroom bean after 24 hrs treatment**

Concentration of extract (µg/ml)	Percentage (%) of cell viability				
	Independent experiment			Average	Standard deviation
	1	2	3		
0	95.657310	98.329020	106.013700	100.0	5.377
3.125	103.952200	113.050800	108.365200	108.5	4.550
6.25	109.714100	108.154100	103.972000	107.3	2.969
12.5	103.964500	99.306280	102.189000	101.8	2.351
25	103.299400	102.984100	102.442900	102.9	0.4332
50	99.299680	92.465370	93.708340	95.16	3.640
100	88.682650	92.056070	92.070100	90.94	1.952
200	83.458380	84.070760	83.452120	83.66	0.3554

**7.3.31 Data of percentage of cell viability of HK-1 cells treated with crude methanolic extract of pink/mushroom bean after 48 hrs treatment**

Concentration of extract (µg/ml)	Percentage (%) of cell viability				
	Independent experiment			Average	Standard deviation
	1	2	3		
0	99.337080	105.371500	95.291430	100.0	5.073
3.125	102.958400	96.884960	101.984300	100.6	3.262
6.25	97.617570	97.484330	91.021330	95.37	3.770
12.5	97.302310	93.520810	90.349560	93.72	3.481
25	83.647230	88.982990	83.382770	85.34	3.160
50	85.604140	84.276940	80.333400	83.40	2.741
100	79.542380	78.302730	74.079210	77.31	2.864
200	72.146150	76.268390	73.004460	73.81	2.175

**7.3.32 Data of percentage of cell viability of HK-1 cells treated with crude ethyl acetate extract of pink/mushroom bean after 48 hrs treatment**

Concentration of extract (µg/ml)	Percentage (%) of cell viability				
	Independent experiment			Average	Standard deviation
	1	2	3		
0	97.212650	104.409800	98.377550	100.0	3.863
3.125	84.824690	90.832920	81.682280	85.78	4.650
6.25	81.334040	81.675240	84.762520	82.59	1.889
12.5	70.273290	68.282100	67.903030	68.82	1.273
25	68.831250	64.577050	68.325930	67.24	2.324
50	65.695870	64.047830	65.576040	65.11	0.9189
100	65.248410	60.239840	61.163850	62.22	2.665
200	50.523030	54.867250	53.543650	52.98	2.227



**7.3.33 Data of percentage of cell viability of HK-1 cells treated with crude hexane extract of pink/mushroom bean after 48 hrs treatment**

Concentration of extract (µg/ml)	Percentage (%) of cell viability				
	Independent experiment			Average	Standard deviation
	1	2	3		
0	96.688740	99.959010	103.352200	100.0	3.332
3.125	86.500760	91.966090	83.542230	87.34	4.274
6.25	88.268890	76.617460	82.155890	82.35	5.828
12.5	79.956070	83.859950	79.201320	81.01	2.500
25	73.338550	81.723180	79.997990	78.35	4.428
50	78.924610	83.459580	75.500180	79.29	3.993
100	76.085620	66.399470	67.215610	69.90	5.372
200	60.093520	62.108880	56.337180	59.51	2.929

**7.3.34 Data of percentage of cell viability of HK-1 cells treated with 5-fluorouracil after 24 hrs treatment**

Concentration of extract (µg/ml)	Percentage (%) of cell viability				
	Independent experiment			Average	Standard deviation
	1	2	3		
0	100.668100	100.257100	99.074760	100.0	0.8272
3.125	87.280600	84.193740	85.310190	85.59	1.563
6.25	81.037860	80.218400	80.143840	80.47	0.4960
12.5	79.328080	75.430370	80.914020	78.56	2.822
25	69.443340	69.179630	72.899890	70.51	2.076
50	66.296710	64.373120	63.416250	64.70	1.467
100	59.164820	62.994810	63.442130	61.87	2.351
200	55.890710	56.495950	55.660580	56.02	0.4315

**7.3.35 Data of percentage of cell viability of HK-1 cells treated with 5-fluorouracil after 48 hrs treatment**

Concentration of extract (µg/ml)	Percentage (%) of cell viability				
	Independent experiment			Average	Standard deviation
	1	2	3		
0	97.844130	100.877100	101.278800	100.0	1.878
3.125	67.026180	73.597990	63.359720	67.99	5.187
6.25	64.465180	61.917730	61.844270	62.74	1.492
12.5	53.380890	60.754960	57.986630	57.37	3.725
25	54.665040	53.804950	51.944520	53.47	1.391
50	48.406370	49.110650	48.161470	48.56	0.4928
100	47.707780	48.765880	47.645580	48.04	0.6296
200	47.706730	44.444120	46.150030	46.10	1.632

**7.3.36 Data of percentage of cell viability of NP-69 cells treated with crude methanolic extract of bunga kantan after 24 hrs treatment**

Concentration of extract (µg/ml)	Percentage (%) of cell viability				
	Independent experiment			Average	Standard deviation
	1	2	3		
0	95.035110	108.562900	96.402000	100.0	7.447
3.125	103.957600	103.100800	99.517200	102.2	2.356
6.25	91.256160	95.769710	98.807720	95.28	3.800
12.5	98.757450	98.031930	90.371290	95.72	4.646
25	89.797930	88.794690	83.781900	87.46	3.223
50	83.225070	78.779820	82.837500	81.61	2.462
100	73.650860	78.746540	76.467600	76.29	2.553
200	64.566910	62.709100	69.306680	65.53	3.402

**7.3.37 Data of percentage of cell viability of NP-69 cells treated with crude ethyl acetate extract of bunga kantan after 24 hrs treatment**

Concentration of extract (µg/ml)	Percentage (%) of cell viability				
	Independent experiment			Average	Standard deviation
	1	2	3		
0	96.747740	106.814400	96.437870	100.0	5.903
3.125	94.432530	87.292400	89.717090	90.48	3.631
6.25	85.439060	88.333510	95.317570	89.70	5.078
12.5	88.521110	89.545240	83.138120	87.07	3.442
25	86.724160	82.313280	87.346460	85.46	2.744
50	79.323360	80.025340	80.861100	80.07	0.7698
100	72.608510	79.421350	71.142360	74.39	4.418
200	59.835510	60.310670	58.834700	59.66	0.7534

**7.3.38 Data of percentage of cell viability of NP-69 cells treated with crude hexane extract of bunga kantan after 24 hrs treatment**

Concentration of extract (µg/ml)	Percentage (%) of cell viability				
	Independent experiment			Average	Standard deviation
	1	2	3		
0	95.035110	108.562900	95.035110	99.54	7.810
3.125	92.519580	93.648670	95.198040	93.79	1.345
6.25	93.066840	92.857890	94.491230	93.47	0.8889
12.5	91.400090	92.857890	97.236820	93.83	3.038
25	89.756540	89.717150	89.756540	89.74	0.02274
50	75.133230	74.491230	75.133230	74.92	0.3707
100	66.949390	69.910410	66.949390	67.94	1.710
200	60.401640	61.794860	57.746010	59.98	2.057

**7.3.39 Data of percentage of cell viability of NP-69 cells treated with crude methanolic extract of bunga kantan after 48 hrs treatment**

Concentration of extract (µg/ml)	Percentage (%) of cell viability				
	Independent experiment			Average	Standard deviation
	1	2	3		
0	96.747740	106.814400	96.437870	100.0	5.903
3.125	92.229270	99.939820	92.586940	94.92	4.352
6.25	96.640150	91.591610	96.329060	94.85	2.829
12.5	87.498200	89.917190	88.591350	88.67	1.211
25	81.656880	82.168870	77.832440	80.55	2.370
50	73.712670	74.125770	74.832030	74.22	0.566
100	67.149730	67.670010	69.244320	68.02	1.091
200	53.643940	58.084850	53.643940	55.12	2.564

**7.3.40 Data of percentage of cell viability of NP-69 cells treated with crude ethyl acetate extract of bunga kantan after 48 hrs treatment**

Concentration of extract (µg/ml)	Percentage (%) of cell viability				
	Independent experiment			Average	Standard deviation
	1	2	3		
0	95.035110	108.562900	96.402000	100.0	7.447
3.125	92.432880	96.578550	101.176900	96.73	4.374
6.25	89.750940	91.520250	87.016620	89.43	2.269
12.5	80.738720	82.813190	80.553300	81.37	1.255
25	78.962860	78.059520	82.512570	79.84	2.354
50	66.797970	69.195020	74.241080	70.08	3.799
100	62.725050	62.611540	62.564550	62.63	0.08252
200	60.945970	59.251980	57.576740	59.26	1.685

**7.3.41 Data of percentage of cell viability of NP-69 cells treated with crude hexane extract of bunga kantan after 48 hrs treatment**

Concentration of extract (µg/ml)	Percentage (%) of cell viability				
	Independent experiment			Average	Standard deviation
	1	2	3		
0	96.747740	106.814400	96.437870	100.0	5.903
3.125	95.395000	89.714370	95.003220	93.37	3.173
6.25	92.740590	85.515410	90.172040	89.48	3.663
12.5	85.842190	89.340530	87.245800	87.48	1.761
25	79.895100	84.727230	78.137950	80.92	3.412
50	72.694650	74.631880	70.838050	72.72	1.897
100	69.034580	65.119130	56.297490	63.48	6.524
200	51.852040	51.712270	53.873440	52.48	1.209

**7.3.42 Data of percentage of cell viability of NP-69 cells treated with crude methanolic solid 1 extract of bunga kantan after 24 hrs treatment**

Concentration of extract (µg/ml)	Percentage (%) of cell viability				
	Independent experiment			Average	Standard deviation
	1	2	3		
0	105.175300	95.524960	99.299740	100.0	4.863
3.125	97.057740	89.880200	101.752800	96.23	5.979
6.25	81.442050	83.299180	85.954030	83.57	2.268
12.5	72.531380	72.906940	74.834560	73.42	1.236
25	69.259670	68.009020	70.650250	69.31	1.321
50	65.503970	68.386330	67.910600	67.27	1.545
100	67.248250	66.312190	63.227240	65.60	2.104
200	61.821120	61.611100	62.363940	61.93	0.3885

**7.3.43 Data of percentage of cell viability of NP-69 cells treated with crude methanolic solid 1 extract of bunga kantan after 48 hrs treatment**

Concentration of extract (µg/ml)	Percentage (%) of cell viability				
	Independent experiment			Average	Standard deviation
	1	2	3		
0	96.747740	106.814400	96.437870	100.0	5.903
3.125	92.367150	88.832880	85.468130	88.89	3.450
6.25	84.158450	82.492450	83.684490	83.45	0.8584
12.5	85.285420	77.349100	81.982220	81.54	3.987
25	75.930060	81.519530	81.443460	79.63	3.205
50	75.820570	75.768140	75.384780	75.66	0.2379
100	69.436950	70.256230	73.040640	70.91	1.889
200	56.585240	58.336390	51.932800	55.62	3.310

**7.3.44 Data of percentage of cell viability of NP-69 cells treated with crude methanolic extract of curry leaf after 24 hrs treatment**

Concentration of extract (µg/ml)	Percentage (%) of cell viability				
	Independent experiment			Average	Standard deviation
	1	2	3		
0	105.175300	95.524960	99.299740	100.0	4.863
3.125	106.173600	110.783200	110.493900	109.2	2.582
6.25	106.920200	104.675600	103.178100	104.9	1.883
12.5	102.459700	108.650000	104.433700	105.2	3.162
25	100.359900	102.290000	104.695000	102.4	2.172
50	103.795000	101.306100	100.929900	102.0	1.557
100	96.685870	97.126080	97.784320	97.20	0.5528
200	75.629020	73.841500	78.223560	75.90	2.203

**7.3.45 Data of percentage of cell viability of NP-69 cells treated with crude methanolic extract of curry leaf after 48 hrs treatment**

Concentration of extract (µg/ml)	Percentage (%) of cell viability				
	Independent experiment			Average	Standard deviation
	1	2	3		
0	98.234020	106.717500	95.048530	100.0	6.032
3.125	104.076400	102.977100	107.142800	104.7	2.159
6.25	102.105500	104.512000	100.524700	102.4	2.008
12.5	96.591530	95.760580	91.393910	94.58	2.792
25	89.952100	89.740810	90.009750	89.90	0.1416
50	84.278210	84.215630	80.074940	82.86	2.409
100	72.374510	73.290860	72.493450	72.72	0.4983
200	54.476640	57.261150	55.973100	55.90	1.394

**7.3.46 Data of percentage of cell viability of NP-69 cells treated with crude ethyl acetate extract of curry leaf after 24 hrs treatment**

Concentration of extract (µg/ml)	Percentage (%) of cell viability				
	Independent experiment			Average	Standard deviation
	1	2	3		
0	105.175300	95.524960	99.299740	100.0	4.863
3.125	104.484800	100.247400	109.621700	104.8	4.694
6.25	102.008500	100.169100	99.510220	100.6	1.295
12.5	96.546280	94.643450	89.544730	93.58	3.620
25	85.517170	88.609760	87.236290	87.12	1.550
50	77.830040	80.042630	80.075840	79.32	1.287
100	74.266240	77.986500	75.141490	75.80	1.945
200	72.705220	71.313200	73.289220	72.44	1.015

**7.3.47 Data of percentage of cell viability of NP-69 cells treated with crude ethyl acetate extract of curry leaf after 48 hrs treatment**

Concentration of extract (µg/ml)	Percentage (%) of cell viability				
	Independent experiment			Average	Standard deviation
	1	2	3		
0	98.234020	106.717500	95.048530	100.0	6.032
3.125	102.496500	104.422300	106.645000	104.5	2.076
6.25	93.565300	94.101200	98.751240	95.47	2.852
12.5	87.021450	87.900080	88.732850	87.88	0.8558
25	83.590740	83.166160	81.880210	82.88	0.8907
50	54.782880	53.164920	53.318360	53.76	0.8931
100	52.894900	54.167090	51.155650	52.74	1.512
200	50.956450	52.529730	50.896450	51.46	0.9261

**7.3.48 Data of percentage of cell viability of NP-69 cells treated with crude hexane extract of curry leaf after 24 hrs treatment**

Concentration of extract (µg/ml)	Percentage (%) of cell viability				
	Independent experiment			Average	Standard deviation
	1	2	3		
0	105.175300	95.524960	99.299740	100.0	6.032
3.125	107.625900	108.003900	106.351600	107.3	0.8657
6.25	105.999800	102.517400	103.450200	104.0	1.803
12.5	102.752200	100.786500	101.114400	101.6	1.053
25	101.001000	101.740700	101.093100	101.3	0.4031
50	102.402000	98.917630	97.713950	99.68	2.435
100	86.548570	89.497640	86.059750	87.37	1.860
200	83.020600	83.284450	84.044720	63.76	3.146

**7.3.49 Data of percentage of cell viability of NP-69 cells treated with crude hexane extract of curry leaf after 48 hrs treatment**

Concentration of extract (µg/ml)	Percentage (%) of cell viability				
	Independent experiment			Average	Standard deviation
	1	2	3		
0	98.234020	106.717500	95.048530	100.0	6.032
3.125	101.093900	101.992600	100.177500	101.1	0.9076
6.25	86.119350	94.119580	91.952800	90.73	4.138
12.5	88.479120	85.556610	80.288700	84.77	4.151
25	80.705410	77.334580	79.000010	79.01	1.685
50	75.671620	78.695200	74.347140	76.24	2.229
100	66.736080	62.786750	65.326200	64.95	2.001
200	67.083990	63.374470	60.828100	63.76	3.146

**7.3.50 Data of percentage of cell viability of NP-69 cells treated with crude methanolic extract of temu kunci after 24 hrs treatment**

Concentration of extract (µg/ml)	Percentage (%) of cell viability				
	Independent experiment			Average	Standard deviation
	1	2	3		
0	99.089240	102.390200	98.520550	100.0	2.089
3.125	110.557900	111.307200	110.411500	110.8	0.4805
6.25	105.656300	106.680200	108.157300	106.8	1.257
12.5	95.981610	93.043890	93.962630	94.33	1.503
25	83.630200	89.616550	84.869680	86.04	3.160
50	78.745230	76.302410	78.124790	77.72	1.270
100	68.756040	69.348200	72.094300	70.07	1.781
200	62.181360	65.242080	67.068230	64.83	2.469

**7.3.51 Data of percentage of cell viability of NP-69 cells treated with crude methanolic extract of temu kunci after 48 hrs treatment**

Concentration of extract (µg/ml)	Percentage (%) of cell viability				
	Independent experiment			Average	Standard deviation
	1	2	3		
0	102.818100	99.647240	97.534680	100.0	2.659
3.125	102.766800	99.413530	99.921480	100.7	1.807
6.25	96.431850	97.759370	96.384170	96.86	0.7806
12.5	92.820510	90.104050	94.817930	92.58	2.366
25	82.578910	80.495570	75.692320	79.59	3.532
50	73.238790	73.740590	72.619860	73.20	0.5614
100	69.926900	69.997150	66.110730	68.68	2.224
200	63.974670	57.075380	63.052250	61.37	3.746

**7.3.52 Data of percentage of cell viability of NP-69 cells treated with crude ethyl acetate extract of temu kunci after 24 hrs treatment**

Concentration of extract (µg/ml)	Percentage (%) of cell viability				
	Independent experiment			Average	Standard deviation
	1	2	3		
0	99.089240	102.390200	98.520550	100.0	2.089
3.125	105.200200	110.456500	110.252500	108.6	2.978
6.25	96.742890	96.160770	96.112790	96.34	0.3508
12.5	94.671600	92.702700	90.664250	92.68	2.004
25	81.643060	82.789580	82.410940	82.28	0.5842
50	77.819630	79.134120	80.227910	79.06	1.206
100	73.031000	72.936630	71.385290	72.45	0.9241
200	72.811610	69.737140	68.640190	70.40	2.162

**7.3.53 Data of percentage of cell viability of NP-69 cells treated with crude ethyl acetate extract of temu kunci after 48 hrs treatment**

Concentration of extract (µg/ml)	Percentage (%) of cell viability				
	Independent experiment			Average	Standard deviation
	1	2	3		
0	102.818100	99.647240	97.534680	100.0	2.659
3.125	104.569200	100.062100	105.899000	103.5	3.059
6.25	96.161060	94.758570	95.481530	95.47	0.7014
12.5	83.564020	87.447740	88.284490	86.43	2.5190
25	77.486960	81.021840	76.476520	78.33	2.387
50	75.742020	75.861970	76.848560	76.15	0.6072
100	70.330180	68.845310	66.487870	68.55	1.938
200	66.310740	63.853080	66.163970	65.44	1.379

**7.3.54 Data of percentage of cell viability of NP-69 cells treated with crude hexane extract of temu kunci after 24 hrs treatment**

Concentration of extract (µg/ml)	Percentage (%) of cell viability				
	Independent experiment			Average	Standard deviation
	1	2	3		
0	99.089240	102.390200	98.520550	100.0	2.089
3.125	105.005100	104.609800	106.216000	105.3	0.8369
6.25	105.098400	104.842500	103.105100	104.3	1.085
12.5	95.461110	102.516400	96.132320	98.04	3.894
25	85.299240	80.861410	91.408310	85.86	5.295
50	77.708310	74.913000	78.843390	77.15	2.023
100	74.268870	72.429970	66.770220	71.16	3.908
200	72.685740	64.360220	70.528210	69.19	4.321

**7.3.55 Data of percentage of cell viability of NP-69 cells treated with crude hexane extract of temu kunci after 48 hrs treatment**

Concentration of extract (µg/ml)	Percentage (%) of cell viability				
	Independent experiment			Average	Standard deviation
	1	2	3		
0	102.818100	99.647240	97.534680	100.0	2.659
3.125	94.290370	94.766240	94.232660	94.43	0.2928
6.25	92.286100	88.980470	90.568470	90.61	1.653
12.5	91.209170	91.199710	86.372990	89.59	2.789
25	81.128960	73.566730	73.094300	75.93	4.509
50	73.741580	70.140980	78.298370	74.06	4.088
100	64.496120	64.234720	68.621350	65.78	2.461
200	58.370030	63.385540	63.491060	61.75	2.927

**7.3.56 Data of percentage of cell viability of NP-69 cells treated with crude methanolic extract of spring onion leaf after 24 hrs treatment**

Concentration of extract (µg/ml)	Percentage (%) of cell viability				
	Independent experiment			Average	Standard deviation
	1	2	3		
0	106.901100	98.959910	104.139000	103.3	4.031
3.125	95.717800	92.298260	97.896680	95.30	2.822
6.25	87.884820	90.535290	88.975500	89.13	1.332
12.5	84.138380	86.620170	87.213640	85.99	1.631
25	81.894400	85.953770	83.069920	83.64	2.089
50	78.956770	80.309810	76.144000	78.47	2.125
100	72.145640	73.463450	76.192490	73.93	2.064
200	68.437510	67.048370	71.077180	68.85	2.046



**7.3.57 Data of percentage of cell viability of NP-69 cells treated with crude methanolic extract of spring onion leaf after 48 hrs treatment**

Concentration of extract (µg/ml)	Percentage (%) of cell viability				
	Independent experiment			Average	Standard deviation
	1	2	3		
0	95.345170	104.102600	100.552300	100.0	4.405
3.125	93.362340	89.226640	88.722430	90.44	2.546
6.25	88.037050	86.543170	86.834140	87.14	0.792
12.5	84.369350	83.613490	82.848440	83.61	0.7605
25	83.945960	80.407710	82.328460	82.23	1.771
50	76.300960	77.198560	76.451880	76.65	0.4806
100	77.856140	74.745800	75.514980	76.04	1.620
200	71.236110	70.521510	64.504620	68.75	3.697

**7.3.58 Data of percentage of cell viability of NP-69 cells treated with crude ethyl acetate extract of spring onion leaf after 24 hrs treatment**

Concentration of extract (µg/ml)	Percentage (%) of cell viability				
	Independent experiment			Average	Standard deviation
	1	2	3		
0	106.901100	101.236900	104.139000	104.1	2.832
3.125	114.216200	121.635300	121.734000	119.2	4.312
6.25	114.581300	114.963200	101.977900	110.5	7.389
12.5	96.607350	100.791500	97.349240	98.25	2.233
25	95.472470	87.526330	89.432820	90.81	4.148
50	83.164210	84.584160	85.917920	84.56	1.377
100	78.208850	76.476210	77.692860	77.46	0.8896
200	60.999270	64.676340	56.868200	60.85	3.906

**7.3.59 Data of percentage of cell viability of NP-69 cells treated with crude ethyl acetate extract of spring onion leaf after 48 hrs treatment**

Concentration of extract (µg/ml)	Percentage (%) of cell viability				
	Independent experiment			Average	Standard deviation
	1	2	3		
0	95.345170	104.102600	100.552300	100.0	4.405
3.125	96.482900	92.886590	97.561160	95.64	2.448
6.25	88.226630	91.330510	87.742460	89.10	1.947
12.5	79.843490	79.486960	74.391720	77.91	3.050
25	74.400510	71.303750	71.822830	72.51	1.659
50	68.708080	69.999840	70.631420	69.78	0.9804
100	59.587710	65.374150	58.098490	61.02	3.844
200	60.170150	56.566590	52.115230	56.28	4.035

**7.3.60 Data of percentage of cell viability of NP-69 cells treated with crude hexane extract of spring onion leaf after 24 hrs treatment**

Concentration of extract (µg/ml)	Percentage (%) of cell viability				
	Independent experiment			Average	Standard deviation
	1	2	3		
0	106.901100	101.236900	104.139000	104.1	2.832
3.125	117.630000	111.956900	113.645400	114.4	2.913
6.25	106.725500	104.529800	101.575200	104.3	2.584
12.5	90.095410	98.473560	94.875190	94.48	4.203
25	86.000180	82.585220	89.636860	86.07	3.526
50	76.245830	76.978580	81.856960	78.36	3.050
100	56.088240	59.611360	57.395130	57.70	1.781
200	54.999650	54.668170	53.840950	54.50	0.5968

**7.3.61 Data of percentage of cell viability of NP-69 cells treated with crude hexane extract of spring onion leaf after 48 hrs treatment**

Concentration of extract (µg/ml)	Percentage (%) of cell viability				
	Independent experiment			Average	Standard deviation
	1	2	3		
0	95.345170	104.102600	100.552300	100.0	4.405
3.125	94.160490	90.201180	96.578610	93.65	3.220
6.25	75.863230	78.411690	83.241440	79.17	3.747
12.5	63.447060	67.467030	66.220540	65.71	2.058
25	62.026120	60.390380	60.688720	61.04	0.8711
50	59.938940	58.852150	57.622860	58.80	1.159
100	55.378560	55.393680	56.259330	55.68	0.5042
200	51.414710	52.905740	51.877540	52.07	0.7632

**7.3.62 Data of percentage of cell viability of NP-69 cells treated with crude methanolic extract of mushroom bean after 24 hrs treatment**

Concentration of extract (µg/ml)	Percentage (%) of cell viability				
	Independent experiment			Average	Standard deviation
	1	2	3		
0	96.868310	101.235000	101.896700	100.0	2.732
3.125	115.597900	117.304900	118.153600	117.0	1.302
6.25	113.346600	112.588800	112.960900	113.0	0.3789
12.5	107.644900	106.328700	105.578100	106.5	1.046
25	101.217100	101.010200	102.296200	101.5	0.6905
50	102.001100	92.205440	94.429340	96.21	5.135
100	90.164960	90.149730	86.221240	88.85	2.273
200	85.863140	83.505400	77.387840	82.25	4.374

**7.3.63 Data of percentage of cell viability of NP-69 cells treated with crude methanolic extract of mushroom bean after 48 hrs treatment**

Concentration of extract (µg/ml)	Percentage (%) of cell viability				
	Independent experiment			Average	Standard deviation
	1	2	3		
0	94.696970	107.489700	97.813320	100.0	6.671
3.125	107.695200	109.086300	108.598000	108.5	0.7058
6.25	104.125000	102.475100	103.379500	103.3	0.8262
12.5	100.609700	102.222100	98.086200	100.3	2.085
25	94.103750	90.568830	92.921150	92.53	1.799
50	96.589260	95.206620	92.076360	94.62	2.312
100	91.485190	93.897340	90.400820	91.93	1.790
200	73.876300	74.015800	73.741590	73.88	0.1371

**7.3.64 Data of percentage of cell viability of NP-69 cells treated with crude ethyl acetate extract of mushroom bean after 24 hrs treatment**

Concentration of extract (µg/ml)	Percentage (%) of cell viability				
	Independent experiment			Average	Standard deviation
	1	2	3		
0	96.868310	101.235000	101.896700	100.0	2.732
3.125	115.597900	117.304900	118.153600	115.6	1.425
6.25	113.346600	112.588800	112.960900	113.4	0.9787
12.5	107.644900	106.328700	105.578100	105.6	3.354
25	101.217100	101.010200	102.296200	103.3	0.1183
50	102.001100	92.205440	94.429340	97.85	5.646
100	90.164960	90.149730	86.221240	88.68	1.464
200	85.863140	83.505400	77.387840	82.02	1.896

**7.3.65 Data of percentage of cell viability of NP-69 cells treated with crude ethyl acetate extract of mushroom bean after 48 hrs treatment**

Concentration of extract (µg/ml)	Percentage (%) of cell viability				
	Independent experiment			Average	Standard deviation
	1	2	3		
0	94.696970	107.489700	97.813320	100.0	6.671
3.125	107.701800	107.708000	106.480200	107.3	0.7071
6.25	107.019900	104.644500	104.431600	105.4	1.437
12.5	102.809200	101.374100	101.306700	101.8	0.8487
25	99.397260	100.643000	104.716800	101.6	2.782
50	87.528260	90.274270	88.847880	88.88	1.373
100	85.040080	87.196240	89.953420	87.40	2.463
200	70.149650	71.113010	70.969560	70.74	0.5198

**7.3.66 Data of percentage of cell viability of NP-69 cells treated with crude hexane extract of mushroom bean after 24 hrs treatment**

Concentration of extract (µg/ml)	Percentage (%) of cell viability				
	Independent experiment			Average	Standard deviation
	1	2	3		
0	96.868310	101.235000	101.896700	100.0	2.732
3.125	114.068900	112.647000	119.133800	115.3	3.410
6.25	106.244500	113.239800	109.496300	109.7	3.501
12.5	106.210400	106.364900	98.514440	103.7	4.489
25	102.141200	104.203100	103.951700	103.4	1.125
50	103.300500	102.161100	104.207300	103.2	1.025
100	97.261470	96.220650	98.107470	97.20	0.9451
200	80.031800	92.402740	88.624180	87.02	6.340

**7.3.67 Data of percentage of cell viability of NP-69 cells treated with crude hexane extract of mushroom bean after 48 hrs treatment**

Concentration of extract (µg/ml)	Percentage (%) of cell viability				
	Independent experiment			Average	Standard deviation
	1	2	3		
0	94.696970	107.489700	97.813320	100.0	6.671
3.125	108.972000	109.166300	108.504200	108.9	0.3403
6.25	104.607400	104.278100	107.757500	105.5	1.921
12.5	101.633100	104.186300	99.210880	101.7	2.488
25	97.157590	95.716020	98.132250	97.00	1.216
50	91.839710	92.630670	94.207600	92.89	1.205
100	89.616760	86.026470	82.275450	85.97	3.671
200	79.021710	84.388050	81.896680	81.77	2.685

#### 7.4 Cytotoxic effects of cardamonin, pinostrobin, naringin and hesperidin against HK-1 and NP-69 cell lines

##### 7.4.1 Data of percentage of cell viability of HK-1 cells treated with cardamonin after 24 hrs

Concentration of extract (µg/ml)	Percentage (%) of cell viability				
	Independent experiment			Average	Standard deviation
	1	2	3		
0	101.465400	101.949200	99.605630	100.00	7.595
3.125	99.439900	99.999220	90.560840	99.39	5.676
6.25	95.750010	95.297180	89.577260	95.48	1.222
12.5	88.250750	86.283570	85.909470	83.45	4.482
25	83.954770	83.780960	79.695420	74.48	0.9431
50	77.013940	75.858340	73.201960	71.08	0.7886
100	71.590880	69.890340	65.212850	69.30	1.192
200	60.201160	59.247430	64.935000	62.45	1.695

##### 7.4.2 Data of percentage of cell viability of HK-1 cells treated with cardamonin after 48 hrs

Concentration of extract (µg/ml)	Percentage (%) of cell viability				
	Independent experiment			Average	Standard deviation
	1	2	3		
0	101.792400	103.619700	94.587920	100.00	4.775
3.125	101.361700	100.269400	97.466150	99.700	2.009
6.25	82.112770	89.626990	81.650430	84.46	4.478
12.5	76.219860	75.729800	75.366100	75.77	0.4284
25	74.798780	71.936570	70.802510	72.51	2.059
50	69.888160	67.274980	67.911680	68.36	1.363
100	66.311650	65.151400	61.324350	64.26	2.610
200	61.311030	53.478550	56.400180	57.06	3.958

**7.4.3 Data of percentage of cell viability of HK-1 cells treated with cardamonin after 72 hrs**

Concentration of extract (µg/ml)	Percentage (%) of cell viability				
	Independent experiment			Average	Standard deviation
	1	2	3		
0	102.435000	101.243500	96.321530	100.00	3.241
3.125	97.328320	91.187230	89.792300	92.77	4.009
6.25	84.774260	78.232330	79.851680	80.95	3.407
12.5	66.494430	62.121980	64.578940	64.40	2.192
25	46.458730	45.063420	45.150290	45.56	0.7817
50	41.685870	43.894750	43.537760	43.04	1.186
100	40.722510	40.760480	40.583290	40.69	0.09329
200	38.539410	37.348720	38.962270	38.28	0.8367

**7.4.4 Data of percentage of cell viability of HK-1 cells treated with hesperidin after 24 hrs**

Concentration of extract (µg/ml)	Percentage (%) of cell viability				
	Independent experiment			Average	Standard deviation
	1	2	3		
0	91.383580	102.892000	105.724400	100.00	7.595
3.125	104.075700	105.348800	100.466300	103.30	2.533
6.25	101.499100	99.241220	104.804000	101.80	2.798
12.5	93.696500	89.564350	89.599430	90.95	2.376
25	77.862990	82.666820	83.988530	81.51	3.224
50	70.183870	73.724370	77.943610	73.95	3.885
100	71.777130	71.479950	68.317020	70.52	1.918
200	59.279470	66.972360	68.299720	64.85	4.870

**7.4.5 Data of percentage of cell viability of HK-1 cells treated with hesperidin after 48 hrs**

Concentration of extract (µg/ml)	Percentage (%) of cell viability				
	Independent experiment			Average	Standard deviation
	1	2	3		
0	101.792400	103.619700	94.587920	100.00	4.775
3.125	92.297520	93.925590	93.369380	93.20	0.8275
6.25	88.638530	89.221150	87.017990	88.29	1.142
12.5	87.939630	84.408050	85.342540	85.90	1.830
25	78.096990	77.193920	73.778300	76.36	2.278
50	72.622770	73.011510	71.680740	72.44	0.6843
100	65.198430	63.260640	61.489400	63.32	1.855
200	60.665060	57.087960	60.284800	59.35	1.965

**7.4.6 Data of percentage of cell viability of HK-1 cells treated with hesperidin after 72 hrs**

Concentration of extract (µg/ml)	Percentage (%) of cell viability				
	Independent experiment			Average	Standard deviation
	1	2	3		
0	99.927760	101.691700	98.380540	100.00	1.657
3.125	86.164940	81.377610	80.373010	82.64	3.095
6.25	79.363820	80.183430	70.787350	76.78	5.204
12.5	70.541390	67.697440	65.744890	67.99	2.412
25	61.605410	60.230390	63.585290	61.81	1.687
50	59.382590	56.718010	56.488480	57.53	1.609
100	55.333740	55.950370	55.520550	55.60	0.3162
200	54.323350	54.774100	52.853810	53.98	1.004

**7.4.7 Data of percentage of cell viability of HK-1 cells treated with naringin after 24 hrs**

Concentration of extract (µg/ml)	Percentage (%) of cell viability				
	Independent experiment			Average	Standard deviation
	1	2	3		
0	91.3836	102.8920	105.7244	100.0000	7.5950
3.125	102.0131	98.9054	96.5334	99.1500	2.7480
6.25	97.5746	94.3390	95.4128	95.7800	1.6480
12.5	97.8711	96.9546	97.6168	97.4800	0.4731
25	92.9589	88.1631	95.4692	92.2000	3.7120
50	86.5817	87.8366	84.4347	86.2800	1.7200
100	84.0827	84.9274	84.0664	84.3600	0.4925
200	74.5799	71.4571	70.1332	72.0600	2.2830

**7.4.8 Data of percentage of cell viability of HK-1 cells treated with naringin after 48 hrs**

Concentration of extract (µg/ml)	Percentage (%) of cell viability				
	Independent experiment			Average	Standard deviation
	1	2	3		
0	101.792400	103.619700	94.587920	100.00	4.775
3.125	92.052660	89.847530	88.904010	90.27	1.616
6.25	82.922560	85.483050	86.499540	84.97	1.843
12.5	81.679160	81.171020	78.923080	80.59	1.467
25	78.542430	75.811450	74.861110	76.40	1.911
50	70.555210	71.624180	63.712590	68.63	4.293
100	62.321850	60.787250	60.307270	61.14	1.052
200	55.013370	58.771980	56.001730	56.60	1.948

**7.4.9 Data of percentage of cell viability of HK-1 cells treated with naringin after 72 hrs**

Concentration of extract (µg/ml)	Percentage (%) of cell viability				
	Independent experiment			Average	Standard deviation
	1	2	3		
0	99.927760	101.691700	98.380540	100.00	1.657
3.125	79.704400	73.201900	84.165510	79.02	5.513
6.25	59.827980	66.049320	65.663250	63.85	3.486
12.5	56.050180	56.357460	54.827120	55.74	0.8095
25	53.448730	54.456790	50.791590	52.90	1.893
50	48.292370	47.738870	47.556470	47.86	0.3832
100	47.001160	45.358300	45.636520	46.00	0.8793
200	42.958890	44.140870	39.486540	42.20	2.419

**7.4.10 Data of percentage of cell viability of HK-1 cells treated with pinostrobin after 24 hrs**

Concentration of extract (µg/ml)	Percentage (%) of cell viability				
	Independent experiment			Average	Standard deviation
	1	2	3		
0	99.725450	98.666210	101.608300	100.00	1.490
3.125	102.608700	103.720200	102.474100	102.90	0.6839
6.25	102.029000	100.661300	100.646600	101.10	0.7939
12.5	101.311000	98.951290	98.469720	99.58	1.521
25	98.509330	97.898860	98.679760	98.36	0.4106
50	95.904210	93.121670	92.355640	93.79	1.867
100	91.428710	91.266060	90.625950	91.11	0.4244
200	77.667700	87.233380	76.386350	80.43	5.927

**7.4.11 Data of percentage of cell viability of HK-1 cells treated with pinostrobin after 48 hrs**

Concentration of extract (µg/ml)	Percentage (%) of cell viability				
	Independent experiment			Average	Standard deviation
	1	2	3		
0	107.217600	92.236280	100.546200	100.00	7.506
3.125	94.591670	93.583430	93.008070	93.73	0.8016
6.25	92.099700	92.047020	92.274580	92.14	0.1191
12.5	92.085690	92.265430	92.124080	92.16	0.09465
25	92.264570	92.174290	92.268880	92.24	0.05341
50	89.723520	92.549500	89.677390	90.65	1.645
100	81.124150	85.079900	85.618620	83.94	2.454
200	78.726420	79.191580	80.674780	79.53	1.018



**7.4.12 Data of percentage of cell viability of HK-1 cells treated with pinostrobin after 72 hrs**

Concentration of extract (µg/ml)	Percentage (%) of cell viability				
	Independent experiment			Average	Standard deviation
	1	2	3		
0	94.806620	105.152700	100.040700	100.00	5.173
3.125	82.442460	79.916760	82.780560	81.71	1.565
6.25	80.874240	81.368290	96.054600	86.10	8.625
12.5	79.057850	76.430810	76.337260	77.28	1.544
25	73.426040	74.826380	68.987290	72.41	3.048
50	62.990520	67.360470	59.231660	63.19	4.068
100	59.333210	56.857120	57.364950	57.85	1.308
200	51.125180	53.340410	51.363650	51.94	1.216

**7.4.13 Data of percentage of cell viability of NP-69 cells treated with cardamonin after 24 hrs**

Concentration of extract (µg/ml)	Percentage (%) of cell viability				
	Independent experiment			Average	Standard deviation
	1	2	3		
0	100	100	100	100	0
3.125	97.02695	85.65822	88.84946	90.51	5.863781
6.25	92.71696	81.86715	88.22995	87.60	5.451867
12.5	97.02237	80.09089	85.58076	87.56	8.638324
25	93.5197	80.5188	81.55192	85.20	7.226322
50	87.99029	76.95765	81.51631	82.15	5.54396
100	82.91548	74.04356	78.29587	78.42	4.437228
200	80.87916	67.59474	71.07999	73.18	6.887749

**7.4.14 Data of percentage of cell viability of NP-69 cells treated with cardamonin after 48 hrs**

Concentration of extract (µg/ml)	Percentage (%) of cell viability				
	Independent experiment			Average	Standard deviation
	1	2	3		
0	100	100	100	100	0
3.125	73.22404	70	75.86207	73.03	2.935912
6.25	91.25683	70.95238	76.84729	79.69	10.44554
12.5	66.66667	59.52381	64.53202	63.57	3.666499
25	75.40984	67.61905	80.29557	74.44	6.393498
50	79.78142	79.52381	79.80296	79.70	0.155322
100	59.01639	51.90476	44.82759	51.92	7.094411
200	40.98361	33.80952	34.97537	36.59	3.849796

**7.4.15 Data of percentage of cell viability of NP-69 cells treated with cardamonin after 72 hrs**

Concentration of extract (µg/ml)	Percentage (%) of cell viability				
	Independent experiment			Average	Standard deviation
	1	2	3		
0	100	100	100	100	0
3.125	76.8575	72.94142	80.53206	76.78	3.795962
6.25	80.38062	76.03499	81.35333	79.26	2.831825
12.5	77.52697	75.19774	78.78075	77.17	1.818209
25	76.86992	72.99239	78.3463	76.07	2.765238
50	73.96692	73.08547	70.28442	72.45	1.922828
100	66.20424	67.12157	70.61863	67.98	2.329441
200	68.29393	67.25746	68.40048	67.98	0.631416

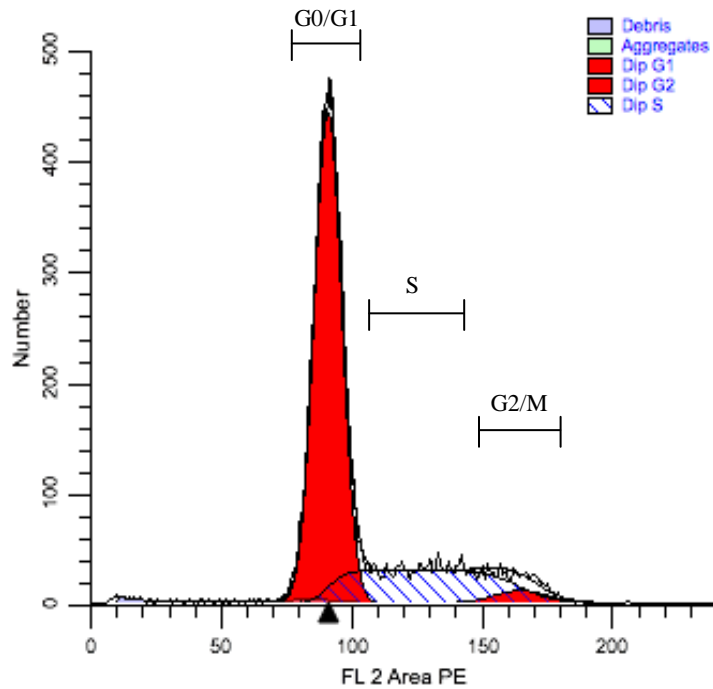
**7.4.16 Trypan blue cell counting**

Duration of cardamonin exposure (hrs)	Average cell counting (cells)	Standard deviation (cells)
Control	3637500	735590
24	1622500	256207
48	640600	52482
72	498572	56769

**7.5 Cell cycle analysis**

Cell cycle phase	Control	12 hrs	24 hrs
Sub-G1	2.64	36.91	35.16
G0/G1	70.41	11.20	47.35
S	26.01	39.23	42.56
G2/M	3.58	49.57	10.09

### 7.5.1 Histogram and forward scatter (FS) and side scatter (SS) dot plot of control group



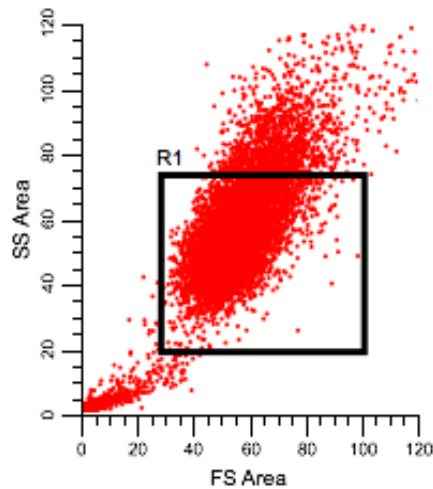
File analyzed: control 24h 1.fcs  
 Date analyzed: 21-Feb-2016  
 Model: 1DA0n DSF  
 Analysis type: Manual analysis  
 Auto Linearity: Yes

Ploidy Mode: First cycle is diploid

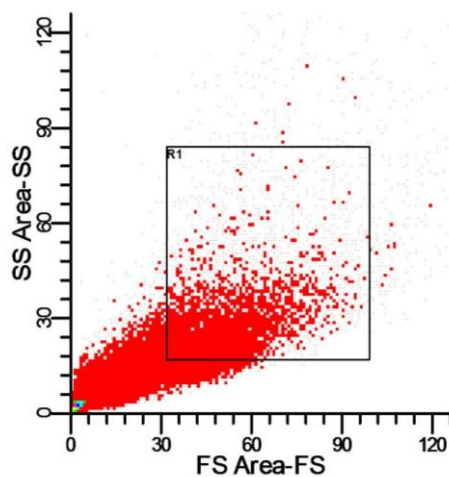
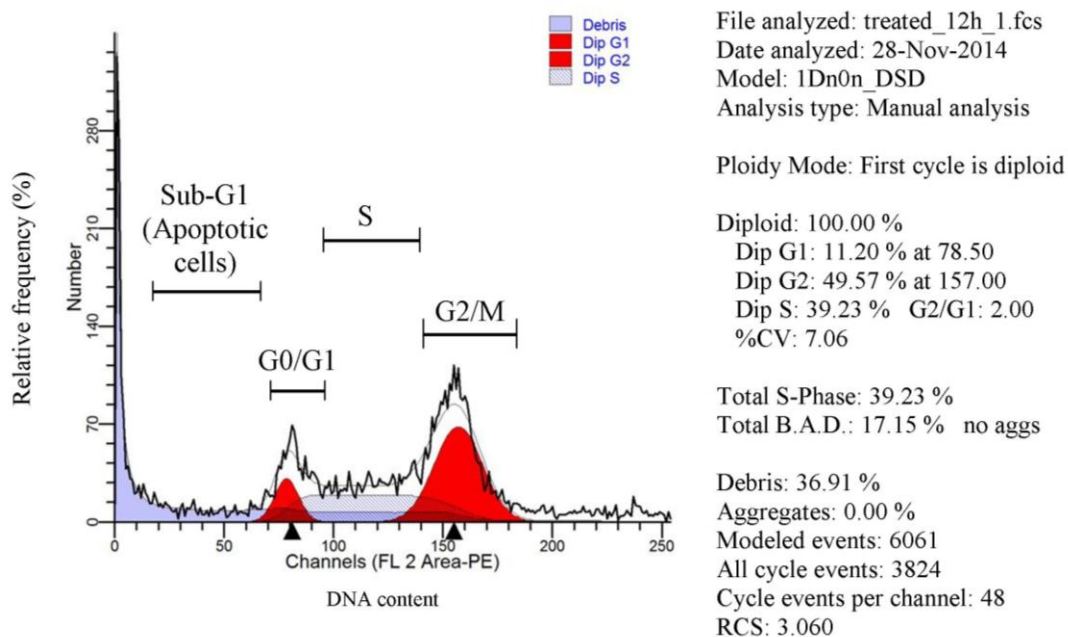
Diploid: 100.00 %  
 Dip G1: 70.41 % at 90.41  
 Dip G2: 3.58 % at 164.73  
 Dip S: 26.01 % G2/G1: 1.82  
 %CV: 5.79

Total S-Phase: 26.01 %  
 Total B.A.D.: 0.36 %

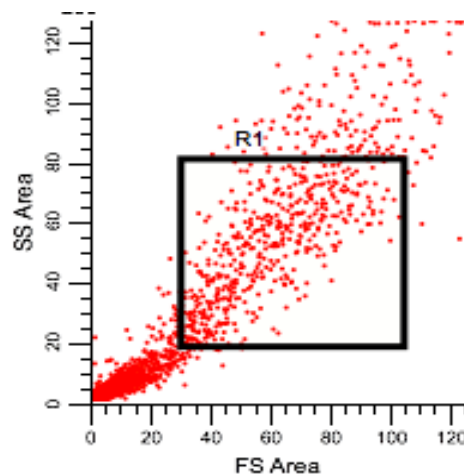
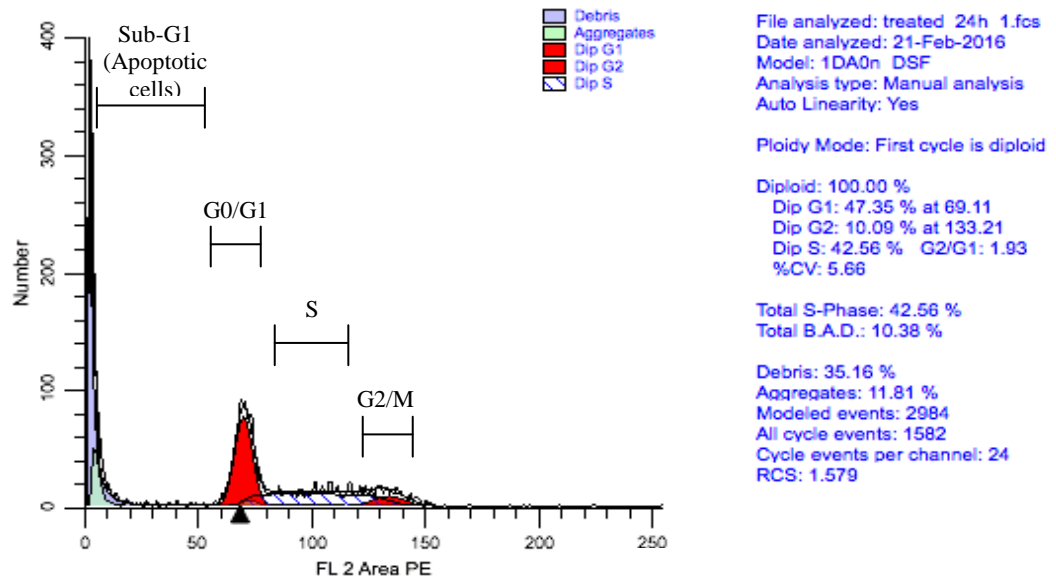
Debris: 2.64 %  
 Aggregates: 0.00 %  
 Modeled events: 8548  
 All cycle events: 8322  
 Cycle events per channel: 110  
 RCS: 1.055



### 7.5.2 Histogram and forward scatter (FS) and side scatter (SS) dot plot of cardamonin treated at 12 hrs

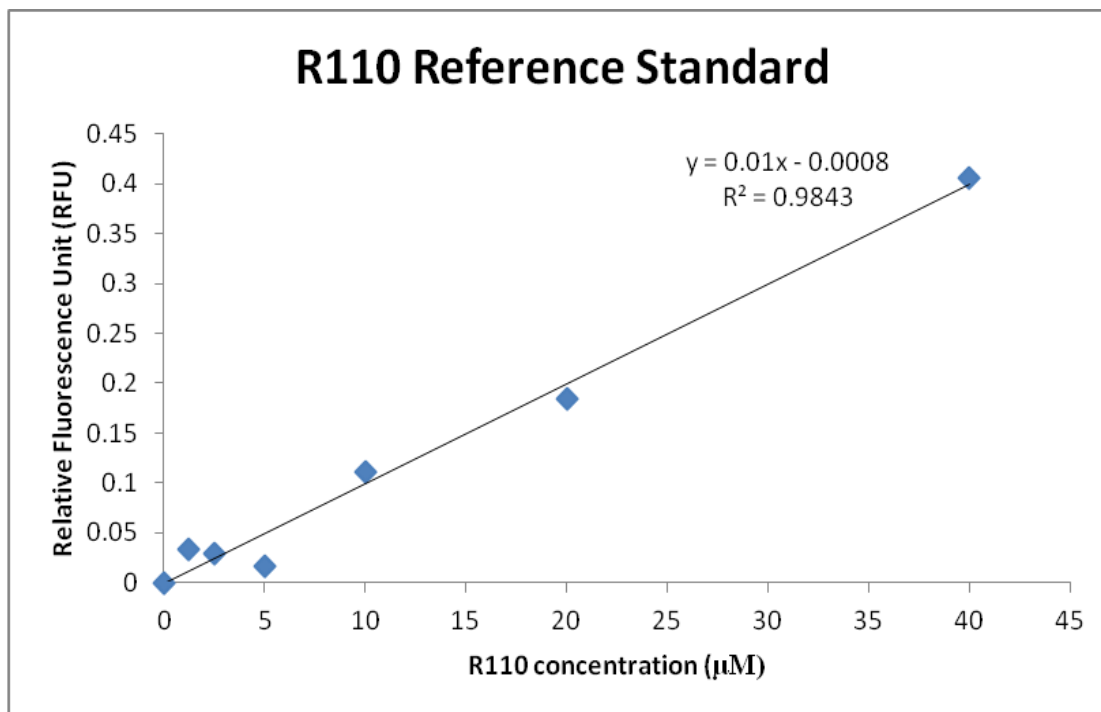


### 7.5.3 Histogram and forward scatter (FS) and side scatter (SS) dot plot of cardamomin treated at 24 hrs



## 7.6 Caspase-3, -8 assays

### 7.6.1 R110 standard curve



### 7.6.2 Caspase-3 assay

#### 7.6.2.1 Cardamonin-treated HK-1 cells at 24, 48 and 72 hrs

Time of cardamonin exposure (hrs)	Absorbance at 520 nm						Average	Standard deviation
	1	2	3	4	5	6		
24	0.386	0.341	0.320	0.330	0.394	0.398	0.361	0.035
48	0.263	0.289	0.267	0.256	0.245	0.268	0.265	0.015
72	0.244	0.227	0.321	0.317	0.184	0.291	0.264	0.055

### 7.6.2.2 Untreated HK-1 cells at 24, 48 and 72 hrs

Time of cardamonin exposure (hrs)	Absorbance at 520 nm						Average	Standard deviation
	1	2	3	4	5	6		
24	0.311	0.274	0.298	0.283	0.257	0.292	0.286	0.019
48	0.345	0.299	0.329	0.327	0.291	0.696	0.381	0.156
72	0.293	0.271	0.275	0.290	0.254	0.250	0.272	0.018

### 7.6.2.3 Cardamonin treated HK-cells with inhibitor at 24, 48 and 72 hrs

Time of cardamonin exposure (hrs)	Absorbance at 520 nm						Average	Standard deviation
	1	2	3	4	5	6		
24	0.328	0.296	0.436	0.353	0.317	0.331	0.343	0.049
48	0.306	0.295	0.282	0.293	0.263	0.258	0.283	0.019
72	0.320	0.272	0.266	0.244	0.276	0.262	0.273	0.025

## 7.6.3 Caspase-8 assay

### 7.6.3.1 Cardamonin treated HK-1 cells at 24, 48 and 72 hrs

Time of cardamonin exposure (hrs)	Absorbance at 520 nm						Average	Standard deviation
	1	2	3	4	5	6		
24	0.311	0.315	0.310	0.568	0.549	0.541	0.432	0.121
48	0.347	0.285	0.326	0.361	0.572	0.341	0.372	0.093
72	0.353	0.358	0.369	0.419	0.341	0.340	0.363	0.027

### 7.6.3.2 Untreated HK-1 cells at 24, 48 and 72 hrs

Time of cardamonin exposure (hrs)	Absorbance at 520 nm						Average	Standard deviation
	1	2	3	4	5	6		
24	0.336	0.329	0.316	0.350	0.543	0.596	0.412	0.113
48	0.336	0.336	0.327	0.360	0.287	0.312	0.326	0.023
72	0.333	0.349	0.357	0.342	0.331	0.333	0.341	0.010

### 7.6.3.3 Cardamonin treated HK-cells with inhibitor at 24, 48 and 72 hrs

Time of cardamonin exposure (hrs)	Absorbance at 520 nm						Average	Standard deviation
	1	2	3	4	5	6		
24	0.434	0.320	0.381	0.399	0.363	0.370	0.378	0.035
48	0.433	0.298	0.399	0.537	0.300	0.630	0.433	0.120
72	0.391	0.465	0.405	0.417	0.427	0.339	0.407	0.038

## 7.7 Cellular Antioxidant Activity (CAA) assay

### 7.7.1 Preparation of quercetin standard from 200 $\mu$ M stock

Standard tubes	Quercetin ( $\mu$ L)	Media ( $\mu$ L)	Total volume ( $\mu$ L)	Quercetin ( $\mu$ M)
1	0.8	199.2	200	200
2	100 from (1)	100	100	100
3	100 from (2)	100	100	50
4	100 from (3)	100	100	25
5	100 from (4)	100	100	12.5
6	0	100	100	0



### 7.7.2 Preparation of cardamonin from 200 $\mu$ M stock

Standard tubes	Cardamonin ( $\mu$ L)	Media ( $\mu$ L)	Total volume ( $\mu$ L)	Quercetin ( $\mu$ M)
1	100 from stock of 200 $\mu$ g/mL	100	200	200
2	100 from (1)	100	100	100
3	100 from (2)	100	100	50
4	100 from (3)	100	100	25
5	100 from (4)	100	100	12.5
6	0	100	100	0

### 7.7.3 CAA assay at various concentrations of cardamonin-treated HK-1 cells

Concentration	Time (mins)				Standard deviation	Average	Area Under Curve (AUC)
200 $\mu$ M	0	0.194	0.249	0.266	0.038	0.236	1.180
	5	0.197	0.248	0.263	0.034	0.236	1.188
	10	0.200	0.252	0.265	0.034	0.239	1.211
	15	0.204	0.260	0.271	0.036	0.245	1.234
	20	0.209	0.263	0.273	0.035	0.248	1.251
	25	0.209	0.268	0.278	0.037	0.252	1.270
	30	0.211	0.274	0.283	0.039	0.256	1.290
	35	0.216	0.278	0.286	0.038	0.260	1.311
	40	0.219	0.283	0.291	0.039	0.264	1.331
	45	0.222	0.289	0.294	0.040	0.268	1.351
	50	0.226	0.293	0.297	0.040	0.272	1.366
	55	0.227	0.294	0.302	0.041	0.274	
						SUM	13.981

Concentration	Time (mins)				Standard deviation	Average	Area Under Curve (AUC)
100 $\mu$ M	0	0.307	0.286	0.282	0.014	0.291	1.460
	5	0.308	0.285	0.284	0.013	0.292	1.466
	10	0.308	0.286	0.287	0.013	0.294	1.478
	15	0.312	0.290	0.289	0.013	0.297	1.493
	20	0.314	0.292	0.295	0.012	0.300	1.512
	25	0.318	0.297	0.299	0.011	0.305	1.533
	30	0.323	0.300	0.303	0.012	0.308	1.556
	35	0.327	0.306	0.308	0.012	0.314	1.575
	40	0.330	0.309	0.310	0.012	0.316	1.584
	45	0.330	0.310	0.312	0.011	0.317	1.590
	50	0.331	0.312	0.314	0.010	0.319	1.598
	55	0.332	0.313	0.316	0.010	0.320	
						SUM	16.844

Concentration	Time (mins)				Standard deviation	Average	Area Under Curve (AUC)
50 $\mu$ M	0	0.323	0.255	0.286	0.034	0.288	1.442
	5	0.325	0.255	0.287	0.035	0.289	1.444
	10	0.324	0.256	0.287	0.034	0.289	1.448
	15	0.324	0.257	0.290	0.034	0.290	1.454
	20	0.326	0.258	0.290	0.034	0.291	1.460
	25	0.326	0.259	0.294	0.034	0.293	1.476
	30	0.331	0.262	0.299	0.035	0.297	1.488
	35	0.329	0.265	0.300	0.032	0.298	1.499
	40	0.334	0.269	0.303	0.033	0.302	1.506
	45	0.331	0.270	0.302	0.031	0.301	1.508
	50	0.332	0.271	0.303	0.030	0.302	1.516
	55	0.333	0.274	0.305	0.029	0.304	
						SUM	16.241

Concentration	Time (mins)				Standard deviation	Average	Area Under Curve (AUC)
25 $\mu$ M	0	0.290	0.257	0.273	0.017	0.273	1.368
	5	0.290	0.257	0.275	0.017	0.274	1.378
	10	0.292	0.260	0.278	0.017	0.277	1.390
	15	0.295	0.262	0.280	0.017	0.279	1.403
	20	0.299	0.264	0.283	0.018	0.282	1.421
	25	0.302	0.270	0.288	0.016	0.287	1.439
	30	0.304	0.273	0.290	0.016	0.289	1.446
	35	0.302	0.275	0.291	0.014	0.289	1.453
	40	0.306	0.276	0.293	0.015	0.292	1.463
	45	0.306	0.280	0.295	0.013	0.294	1.474
	50	0.308	0.281	0.299	0.014	0.296	1.483
	55	0.310	0.283	0.298	0.013	0.297	
						SUM	15.717

Concentration	Time (mins)				Standard deviation	Average	Area Under Curve (AUC)
12.5 $\mu$ M	0	0.320	0.281	0.274	0.025	0.292	1.456
	5	0.321	0.278	0.273	0.027	0.291	1.449
	10	0.320	0.274	0.274	0.026	0.289	1.452
	15	0.323	0.275	0.277	0.027	0.292	1.473
	20	0.330	0.276	0.287	0.029	0.297	1.494
	25	0.332	0.281	0.288	0.028	0.300	1.506
	30	0.336	0.284	0.286	0.029	0.302	1.513
	35	0.335	0.287	0.287	0.027	0.303	1.519
	40	0.336	0.287	0.290	0.027	0.304	1.525
	45	0.338	0.288	0.292	0.028	0.306	1.537
	50	0.338	0.293	0.295	0.025	0.309	1.545
	55	0.341	0.292	0.295	0.027	0.309	
						SUM	16.47

Concentration	Time (mins)				Standard deviation	Average	Area Under Curve (AUC)
0 $\mu$ M	0	0.279	0.270	0.273	0.005	0.274	1.372
	5	0.280	0.272	0.272	0.005	0.275	1.383
	10	0.286	0.274	0.275	0.007	0.278	1.394
	15	0.285	0.276	0.277	0.005	0.279	1.406
	20	0.290	0.279	0.281	0.006	0.283	1.438
	25	0.302	0.284	0.289	0.010	0.292	1.461
	30	0.302	0.285	0.290	0.009	0.292	1.474
	35	0.307	0.290	0.294	0.009	0.297	1.491
	40	0.312	0.291	0.294	0.011	0.299	1.497
	45	0.311	0.294	0.293	0.010	0.300	1.503
	50	0.311	0.297	0.297	0.008	0.301	1.513
	55	0.313	0.298	0.301	0.008	0.304	
						SUM	15.93

#### 7.7.4 CAA assay at various concentrations of quercetin in HK-1 cells

Concentration	Time (mins)				Standard deviation	Average	Area Under Curve (AUC)
200 $\mu$ M	0	0.1938	0.2489	0.2656	0.0376	0.2361	1.1800
	5	0.1972	0.2479	0.2627	0.0344	0.2359	1.1878
	10	0.2004	0.2517	0.2654	0.0343	0.2392	1.2106
	15	0.2045	0.2598	0.2709	0.0356	0.2451	1.2335
	20	0.2087	0.2630	0.2733	0.0348	0.2483	1.2507
	25	0.2095	0.2679	0.2784	0.0372	0.2520	1.2696
	30	0.2108	0.2740	0.2828	0.0393	0.2559	1.2902
	35	0.2163	0.2780	0.2864	0.0383	0.2602	1.3108
	40	0.2187	0.2830	0.2906	0.0395	0.2641	1.3307
	45	0.2217	0.2886	0.2942	0.0403	0.2682	1.3508
	50	0.2262	0.2929	0.2974	0.0399	0.2722	1.3665
	55	0.2275	0.2941	0.3017	0.0409	0.2744	
						SUM	13.981

Concentration	Time (mins)				Standard deviation	Average	Area Under Curve (AUC)
100 $\mu$ M	0	0.2207	0.2415	0.2886	0.0348	0.2502	1.2480
	5	0.2185	0.2429	0.2854	0.0338	0.2490	1.2479
	10	0.2218	0.2429	0.2859	0.0326	0.2502	1.2620
	15	0.2286	0.2468	0.2884	0.0306	0.2546	1.2806
	20	0.2303	0.2518	0.2907	0.0306	0.2576	1.2989
	25	0.2366	0.2547	0.2944	0.0296	0.2619	1.3226
	30	0.2415	0.2603	0.2996	0.0296	0.2671	1.3408
	35	0.2436	0.2616	0.3024	0.0301	0.2692	1.3545
	40	0.2485	0.2648	0.3046	0.0288	0.2726	1.3719
	45	0.2525	0.2681	0.3078	0.0285	0.2761	1.3863
	50	0.2535	0.2711	0.3105	0.0292	0.2784	1.3934
	55	0.2535	0.2723	0.3111	0.0294	0.2789	1.2480
						SUM	13.981

Concentration	Time (mins)				Standard deviation	Average	Area Under Curve (AUC)
50 $\mu$ M	0	0.230	0.270	0.285	0.029	0.262	1.308
	5	0.232	0.270	0.283	0.026	0.262	1.317
	10	0.239	0.273	0.284	0.023	0.265	1.340
	15	0.247	0.275	0.290	0.022	0.271	1.366
	20	0.252	0.282	0.293	0.021	0.276	1.387
	25	0.259	0.282	0.295	0.018	0.279	1.409
	30	0.265	0.287	0.302	0.019	0.285	1.433
	35	0.271	0.291	0.305	0.017	0.289	1.449
	40	0.271	0.294	0.307	0.018	0.291	1.462
	45	0.277	0.296	0.309	0.016	0.294	1.480
	50	0.282	0.298	0.313	0.016	0.298	1.498
	55	0.287	0.303	0.315	0.014	0.301	
						SUM	15.45

Concentration	Time (mins)				Standard deviation	Average	Area Under Curve (AUC)
25 $\mu$ M	0	0.229	0.258	0.288	0.029	0.259	1.292
	5	0.230	0.260	0.284	0.027	0.258	1.305
	10	0.241	0.263	0.287	0.023	0.264	1.338
	15	0.253	0.269	0.292	0.020	0.271	1.365
	20	0.257	0.273	0.293	0.018	0.275	1.386
	25	0.267	0.276	0.296	0.015	0.280	1.412
	30	0.271	0.283	0.301	0.015	0.285	1.431
	35	0.274	0.285	0.304	0.015	0.288	1.446
	40	0.279	0.288	0.305	0.013	0.291	1.459
	45	0.282	0.290	0.308	0.013	0.293	1.472
	50	0.283	0.292	0.311	0.014	0.296	1.484
	55	0.288	0.292	0.313	0.013	0.298	
						SUM	15.390

Concentration	Time (mins)				Standard deviation	Average	Area Under Curve (AUC)
12.5 $\mu$ M	0	0.235	0.303	0.274	0.034	0.271	1.348
	5	0.236	0.297	0.273	0.031	0.269	1.349
	10	0.240	0.296	0.277	0.029	0.271	1.366
	15	0.250	0.296	0.280	0.023	0.275	1.393
	20	0.262	0.298	0.286	0.018	0.282	1.426
	25	0.272	0.300	0.294	0.015	0.289	1.458
	30	0.279	0.305	0.299	0.014	0.294	1.478
	35	0.283	0.304	0.302	0.011	0.297	1.488
	40	0.284	0.307	0.304	0.013	0.298	1.498
	45	0.286	0.307	0.309	0.013	0.301	1.511
	50	0.293	0.308	0.310	0.009	0.304	1.521
	55	0.292	0.311	0.311	0.011	0.305	
						SUM	15.835

Concentration	Time (mins)				Standard deviation	Average	Area Under Curve (AUC)
0 $\mu$ M	0	0.254	0.280	0.290	0.019	0.275	1.384
	5	0.258	0.282	0.296	0.019	0.279	1.399
	10	0.265	0.285	0.294	0.015	0.281	1.414
	15	0.271	0.289	0.293	0.012	0.284	1.437
	20	0.276	0.295	0.300	0.012	0.290	1.465
	25	0.283	0.299	0.304	0.011	0.295	1.494
	30	0.293	0.302	0.311	0.009	0.302	1.519
	35	0.297	0.304	0.315	0.009	0.305	1.530
	40	0.299	0.307	0.315	0.008	0.307	1.541
	45	0.300	0.310	0.319	0.010	0.310	1.553
	50	0.300	0.314	0.320	0.010	0.311	1.558
	55	0.303	0.314	0.318	0.008	0.312	
						SUM	16.293

**7.8 Effect of cardamonin on mitochondrial membrane potential in HK-1 cells after 3 and 6 hrs**

Samples	Duration of cardamonin exposure (hrs)	Flourescence reading at 485 nm	Flourescence reading at 560 nm	Ratio 560 nm /485 nm	% of control
Untreated control	3	0.059227±0.005389	0.278195±0.081025	1.10682±0.148342	100
	6	0.050754±0.013586	0.059836±0.027081	1.14916±0.402461	100
Cardamonin treated	3	0.067426±0.003797	0.364667±0.064949	5.609259±0.941652	504.9223
	6	0.171128±0.048942	0.060081±0.008766	0.36979±0.095027	35.96097

**7.9 Effect of cardamonin on intracellular ATP levels in HK-1 cells after 3 and 6 hrs.**

Samples	Duration of cardamonin exposure (hrs)	Luminescence reading, RLU A (ATP)	Luminescence reading, RLU B	Luminescence reading, RLU C
Untreated control	3	3919046±631267	2404952±230937	3231680±309107
	6	3275975±208919	2781937±171596	3507114±261535
Cardamonin treated	3	4346178±467888	2339151±278621	3174060±359681
	6	3268287±259727	2839610±248247	3601191±289253

**7.9.1 ADP/ATP ratio**

Samples	Duration of cardamonin exposure (hrs)	RLU C- RLU B (ADP)	ADP/ATP ratio
Untreated control	3	826728±93944.3	0.21403±0.02923
	6	696522±82482.5	0.20894±0.01813
Cardamonin treated	3	834909±91360.5	0.20264±0.0202
	6	729024±105944	0.22412±0.03811

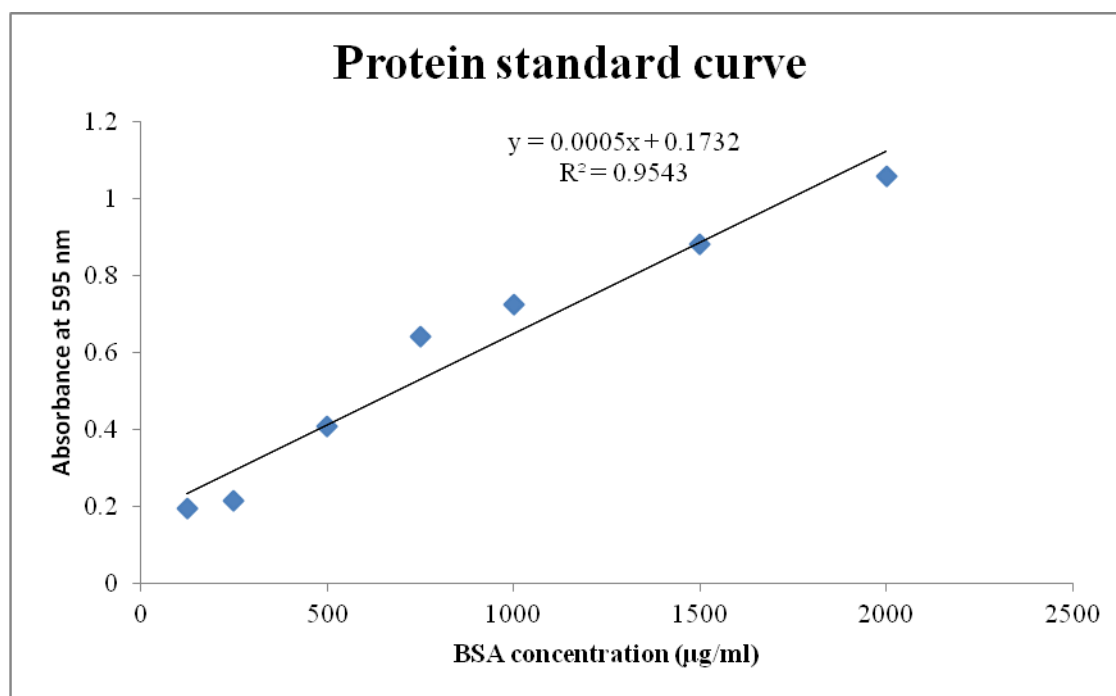


## 7.10 Western blotting

### 7.10.1 Protein quantification

#### 7.10.1.1 BSA standard curve

Tube #	Concentration of BSA (µg/mL)	Volume of diluent (dH <sub>2</sub> O) (µL)	Volume of standard (µL)	Source of standard
1	2000	0	20	2 mg/ml stock
2	1500	10	30	2 mg/ml stock
3	1000	20	20	2 mg/ml stock
4	750	20	20	Tube 2
5	500	20	20	Tube 3
6	250	20	20	Tube 5
7	125	20	20	Tube 6
8 (blank)	0	20	0	-



### 7.10.2 Gel electrophoresis (SDS-PAGE)

#### 7.10.2.1 Preparing gels at different resolving gel percentage

Constituents	4% stacking gel (make 5mL)	8% resolving gel (make 6 mL)	12% resolving gel (make 6 mL)
30% Bis acrylamide	0.66 mL	1.5	2.4 mL
0.5M Tris-HCl pH 8.8	1.26 mL	-	-
1.5M Tris-HCl pH 6.8	-	1.4 mL	1.4 mL
10% SDS	50 $\mu$ L	150 $\mu$ L	150 $\mu$ L
dH <sub>2</sub> O	3 mL	1.4 mL	2.0 mL
TEMED	5 $\mu$ L	7.5 $\mu$ L	7.5 $\mu$ L
10% APS	25 $\mu$ L	75 $\mu$ L	75 $\mu$ L

Constituents	4% stacking gel (make 5mL)	10% resolving gel (make 6 mL)	15% resolving gel (make 6 mL)
30% Bis acrylamide	0.66 mL	1.98	3.0 mL
0.5M Tris-HCl pH 8.8	1.26 mL	-	-
1.5M Tris-HCl pH 6.8	-	1.4 mL	1.4 mL
10% SDS	50 $\mu$ L	150 $\mu$ L	150 $\mu$ L
dH <sub>2</sub> O	3 mL	2.5 mL	1.4 mL
TEMED	5 $\mu$ L	7.5 $\mu$ L	7.5 $\mu$ L
10% APS	25 $\mu$ L	75 $\mu$ L	75 $\mu$ L

#### 7.10.2.2 Separation of proteins on gel electrophoresis for 24, 48 and 72 hrs.

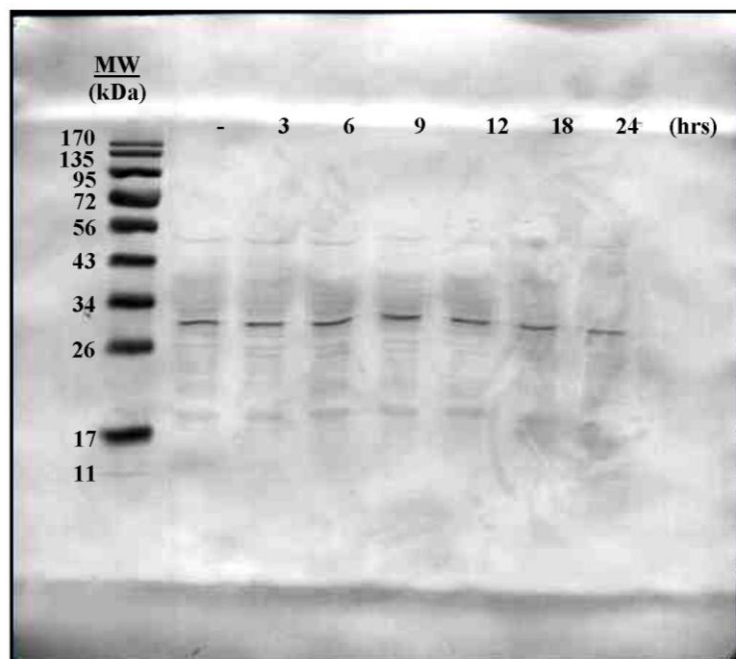
Tubes	Amount of protein (mg/ml)	Volume for 11.9 $\mu$ g ( $\mu$ L)	Top up volume ( $\mu$ L)	Volume of 7X loading dye ( $\mu$ L)	Total volume ( $\mu$ L)
Control (24 hrs)	774.8	15.4	2.6	3	18
Treated (24 hrs)	754.3	15.8	2.2	3	18
Control (48 hrs)	1787.6	6.7	11.3	3	18
Treated (48 hrs)	1540.6	7.7	10.3	3	18
Control (72 hrs)	668.3	17.8	0.2	3	18
Treated (72 hrs)	1449.6	8.2	9.8	3	18

### 7.10.2.3 Separation of proteins on gel electrophoresis 0-24 hrs

Duration of exposure (hrs)	Amount of protein (mg/ml)	Volume for 30 µg (µL)	Top up volume (µL)	Volume of 5X loading dye (µL)	Total volume (µL)
0	2855.7	10.5	1.5	3	15
3	2901.5	10.3	1.7	3	15
6	2970.3	10.1	1.9	3	15
9	2754.0	10.9	1.1	3	15
12	2326.6	12.9	0	3	15
18	2413.2	12.4	0	3	15
24	2389.2	12.6	0	3	15

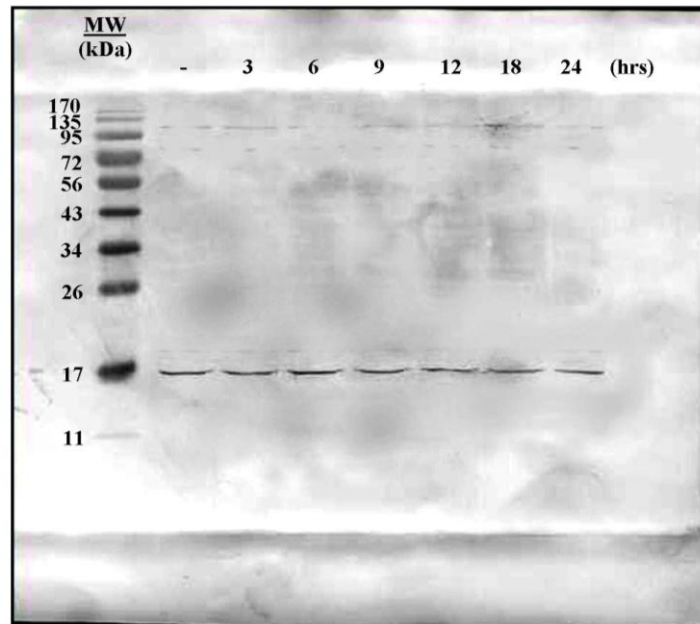
### 7.10.3 Electro blotting

#### 7.10.3.1 Bcl2-L1 protein expression in 0-24hrs cardamonin-induced HK-1 cells



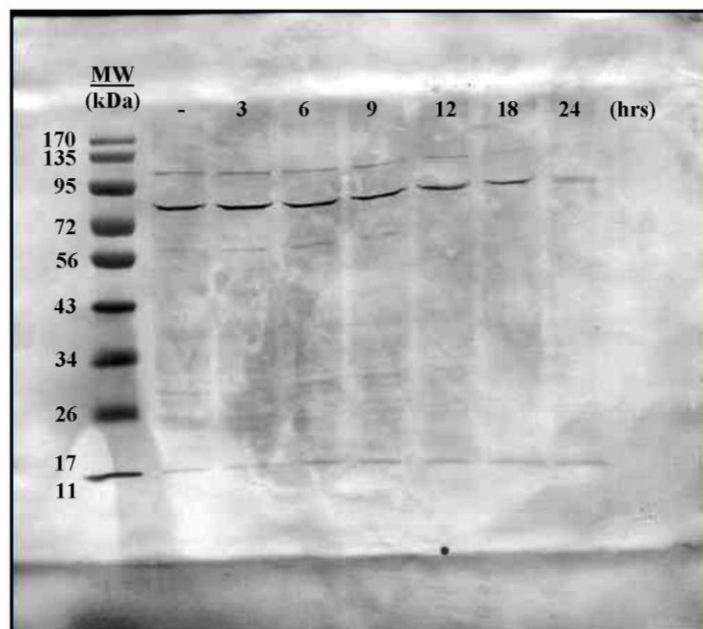
Expected molecular size: Approximately 26kDa.

**7.10.3.2 Cytochrome c protein expression in 0-24hrs cardamonin-induced HK-1 cells**



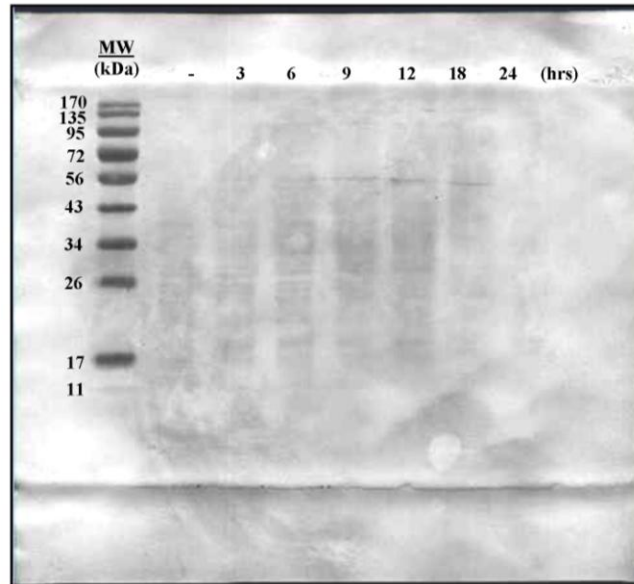
Expected molecular size: Approximately 12 kDa.

**7.10.3.3 Bcl-2 protein expression in 0-24hrs cardamonin-induced HK-1 cells**



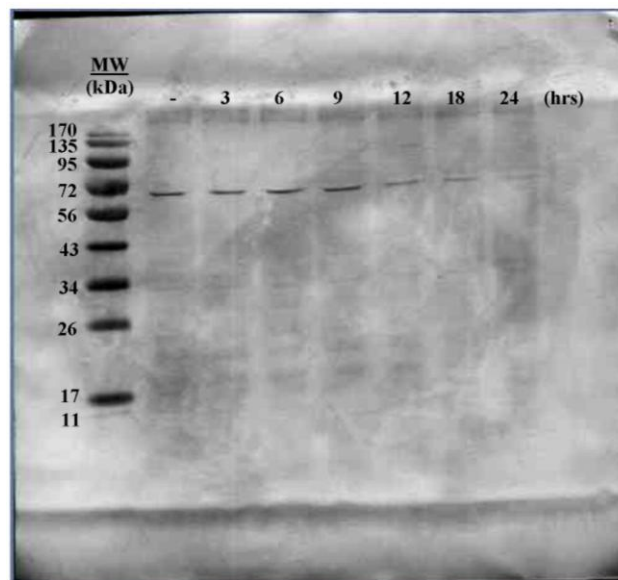
Expected molecular size: Approximately 26 kDa

**7.10.3.4 Bad protein expression in 0-24hrs cardamonin-induced HK-1 cells**



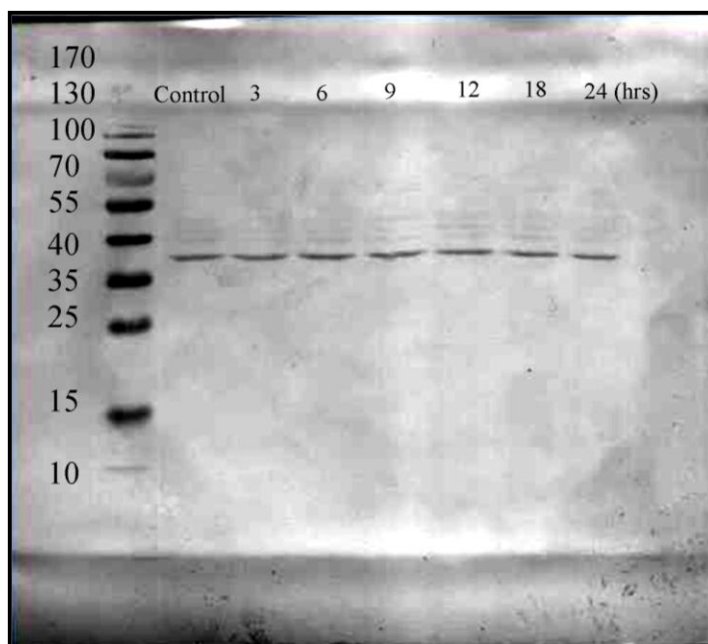
Expected molecular size: Approximately 19 kDa.

**7.10.3.5 Bax protein expression in 0-24hrs cardamonin-induced HK-1 cells**



Expected molecular size: Approximately 21 kDa.

### 7.10.3.6 GADPH (as loading control) protein expression in 0-24 hrs cardamonin-induced HK-1 cells



Expected molecular size: Approximately 37 kDa

### 7.10.4 Quantification of protein bands intensities

#### 7.10.4.1 Bcl2-L1 protein expression level

Cardamonin exposure (hrs)	1st read	2nd read	3rd read	Average intensity	% of control	Standard Deviation
-	120.48	113.97	114.88	116.44	100	3.525
3	112.50	110.86	111.21	111.52	95.77	0.8637
6	120.95	118.8	115.76	118.50	101.77	2.608
9	116.95	120.15	117.12	118.073	101.40	1.800
12	118.84	115.86	116.32	117.01	100.48	6.842
18	121.60	110.17	109.37	113.71	97.66	1.604
24	110.99	108.33	109.88	109.73	94.24	1.336

#### 7.10.4.2 Cytochrome c protein expression level

Cardamonin exposure (hrs)	1st read	2nd read	3rd read	Average intensity	% of control	Standard Deviation
-	139.38	134.73	133.80	135.97	100	2.990
3	136.17	130.30	134.03	133.50	98.18	2.971
6	142.66	141.61	146.05	143.44	105.49	2.320
9	137.60	136.44	133.92	135.99	100.01	1.881
12	127.37	125.26	125.64	126.09	92.73	1.125
18	119.46	118.56	116.74	118.25	86.97	1.386
24	106.30	105.47	106.83	106.20	78.11	0.6855

#### 7.10.4.3 Bcl-2 protein expression level

Cardamonin exposure (hrs)	1st read	2nd read	3rd read	Average intensity	% of control	Standard Deviation
-	164.50	155.68	162.59	160.92	100	4.640
3	154.33	151.17	158.52	154.67	96.12	3.687
6	150.60	152.33	158.06	153.66	95.49	3.905
9	139.56	137.96	149.58	142.37	88.47	6.298
12	139.40	142.36	152.58	144.78	89.97	6.915
18	114.35	116.19	128.48	119.67	74.37	7.682
24	112.71	115.03	119.43	115.72	71.91	3.413

#### 7.10.4.4 Bax protein expression level

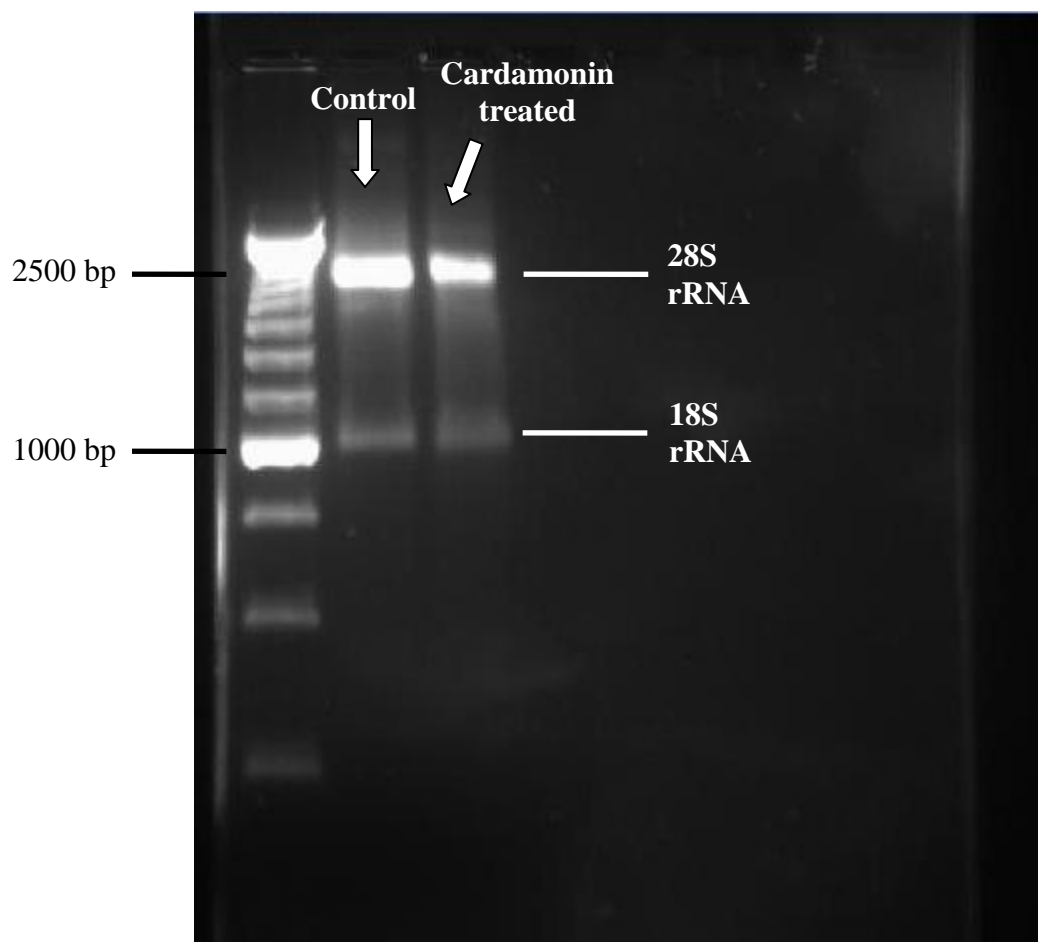
Cardamonin exposure (hrs)	1st read	2nd read	3rd read	Average intensity	% of control	Standard Deviation
-	70.92	77.72	73.82	74.15	100	3.412
3	55.65	55.47	56.78	55.97	75.47	0.7101
6	66.53	65.29	66.01	65.94	88.93	0.6227
9	81.14	81.15	84.45	82.25	110.91	1.908
12	64.95	67.27	70.93	67.72	91.32	3.015
18	64.18	65.67	68.14	66.00	89.00	2.000
24	62.96	64.50	62.21	63.22	85.26	1.167

## 7.11 Relative quantification of caspase-9 gene expression level using real-time PCR

### 7.11.1 Total RNA extraction from HK-1 cells

	Absorbance, $A_{260}$			Minus blank	[RNA] ( $\mu\text{g/mL}$ )
	1	2	Average		
<b>Blank(TE buffer)</b>	4.297	4.306	4.302	-	-
<b>Control</b>	4.319	4.349	4.334	0.033	66.61
<b>Cardamonin-treated</b>	4.341	4.301	4.321	0.020	40.42

### 7.11.2 Gel electrophoresis for total RNA extraction in HK-1 cells after 24 hrs





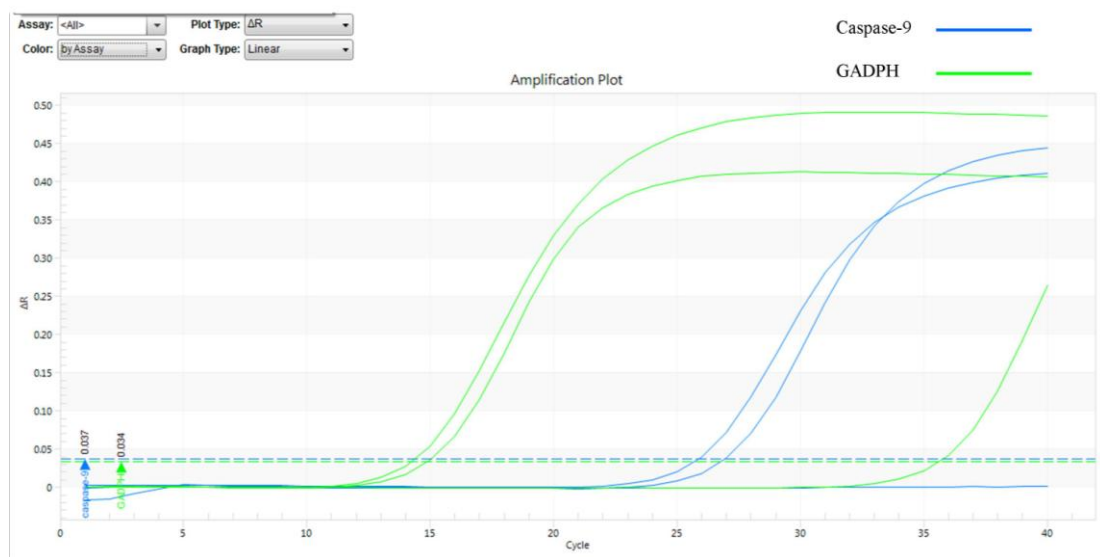
### 7.11.3 Mix preparation

<b>Caspase-9 (Gene of interest)</b>			
<b>Components</b>	<b>Volume (μL) for single tube reaction</b>		
	<b>Control</b>	<b>Cardamonin treated</b>	<b>Non template control (NTC)</b>
<b>Superscript<sup>®</sup> III RT/Platinum <i>Taq</i> Mix</b>	0.4	0.4	0.4
<b>2X SYBR Green Reaction Mix</b>	10	10	10
<b>Forward primer (10 μM)</b>	0.4	0.4	0.4
<b>Reverse primer (10 μM)</b>	0.4	0.4	0.4
<b>RNA template (1 ng/μL)</b>	0.3	0.5	0
<b>DEPC-treated water</b>	8.5	8.3	8.8
<b>Total</b>	20	20	20

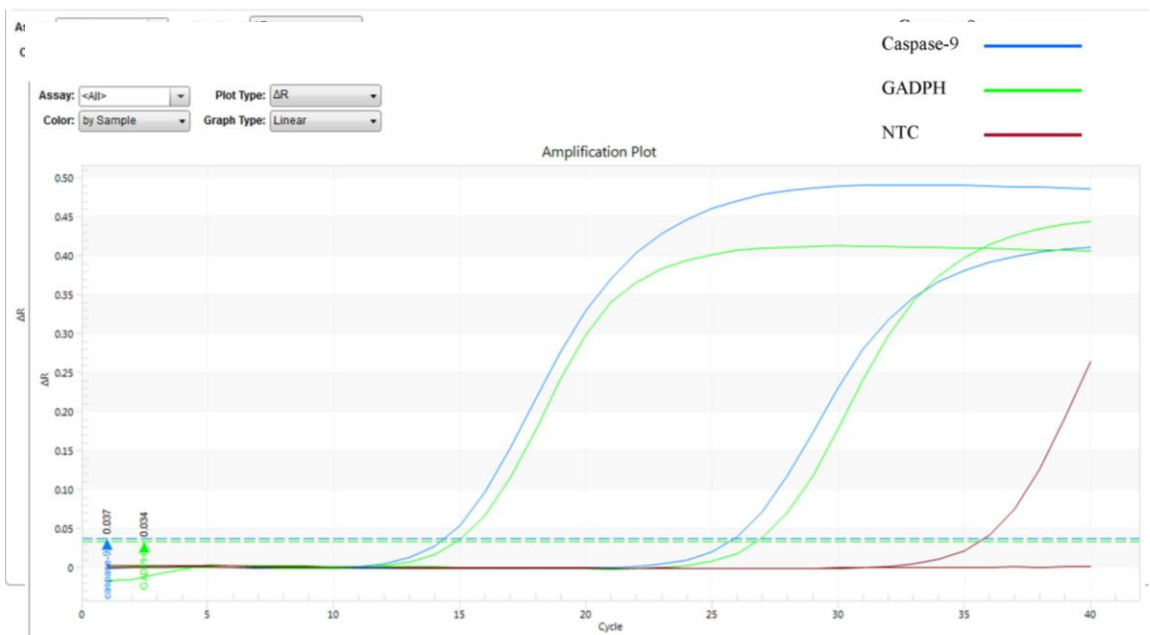
<b>GADPH (Reference gene)</b>			
<b>Components</b>	<b>Volume (μL) for single tube reaction</b>		
	<b>Control</b>	<b>Cardamonin treated</b>	<b>Non template control (NTC)</b>
<b>Superscript<sup>®</sup> III RT/Platinum <i>Taq</i> Mix</b>	0.4	0.4	0.4
<b>2X SYBR Green Reaction Mix</b>	10	10	10
<b>Forward primer (10 μM)</b>	0.4	0.4	0.4
<b>Reverse primer (10 μM)</b>	0.4	0.4	0.4
<b>RNA template (1 ng/μL)</b>	0.3	0.5	0
<b>DEPC-treated water</b>	8.5	8.3	8.8
<b>Total</b>	20	20	20

#### 7.11.4 Amplification plot in control and cardamonin-treated HK-1 cells (by assay)

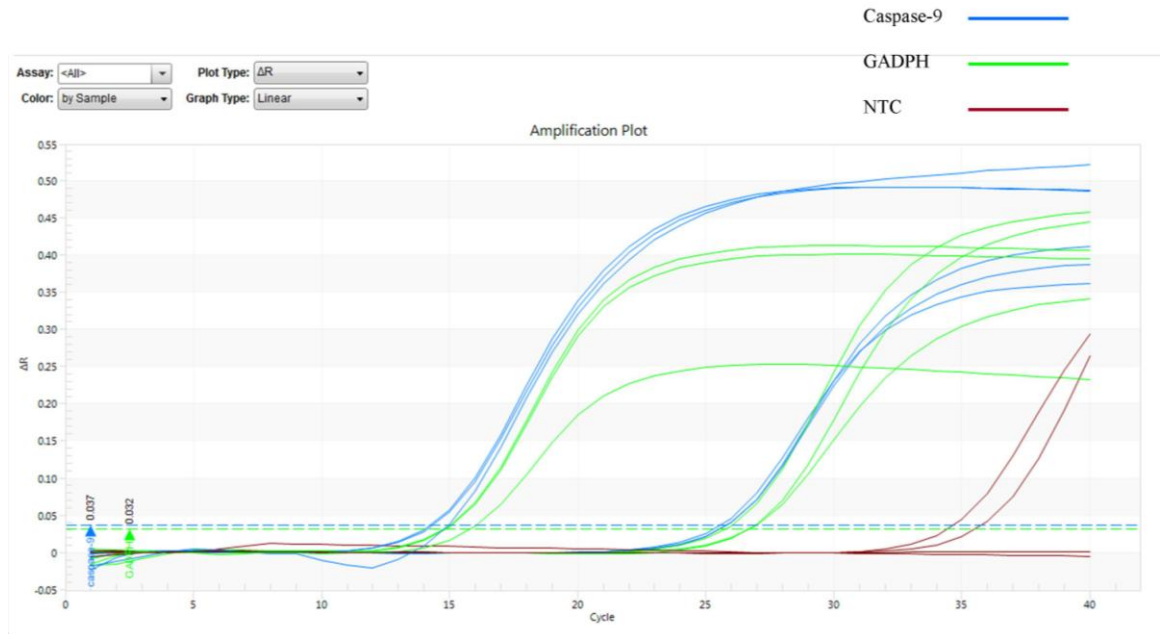
#### 7.11.5 Amplification plot in control and cardamonin-treated HK-1 cells (by assay repeats)



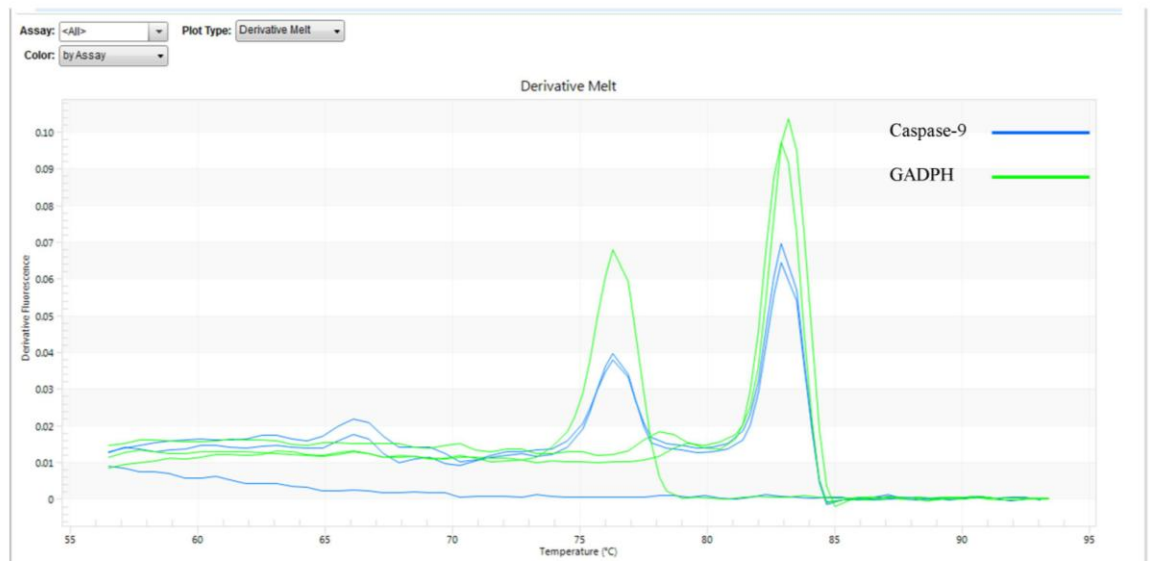
#### 7.11.6 Amplification plot in control and cardamonin-treated HK-1 cells (by sample)



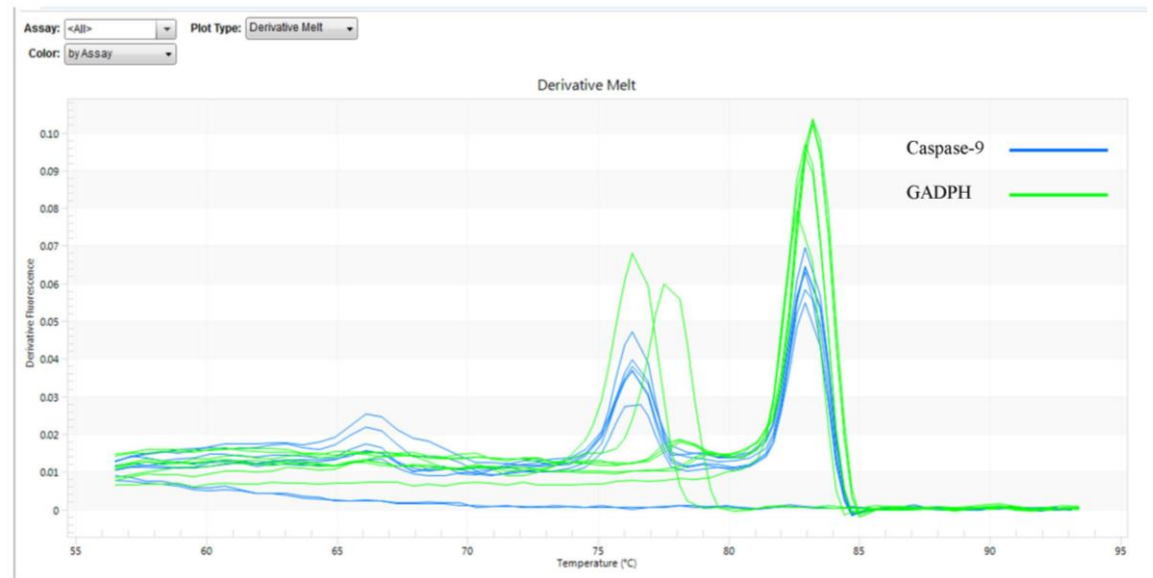
### 7.11.7 Amplification plot in control and cardamonin-treated HK-1 cells (by sample repeats)



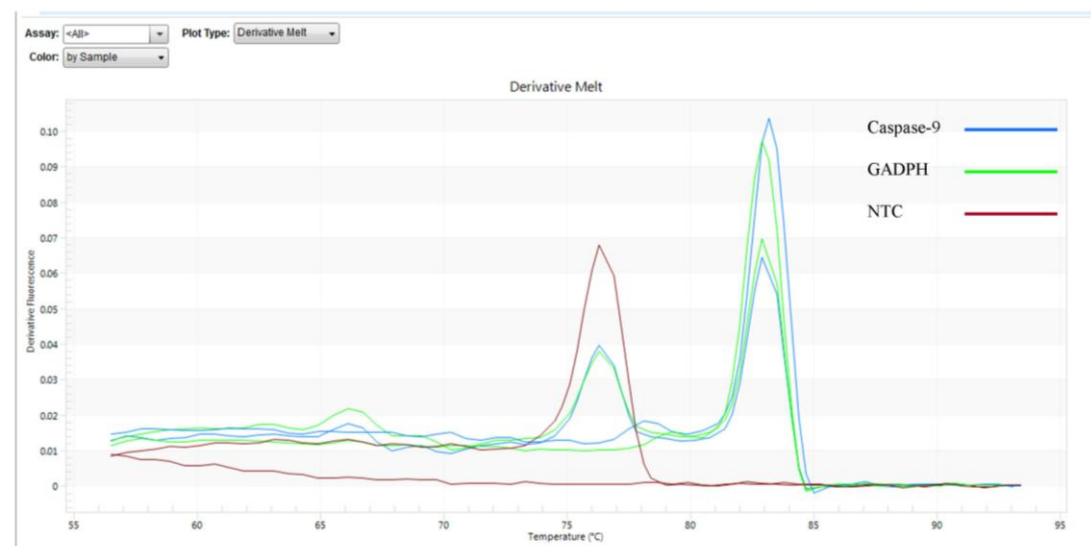
### 7.11.8 Derivative melt in control and cardamonin-treated HK-1 cells (by assay)



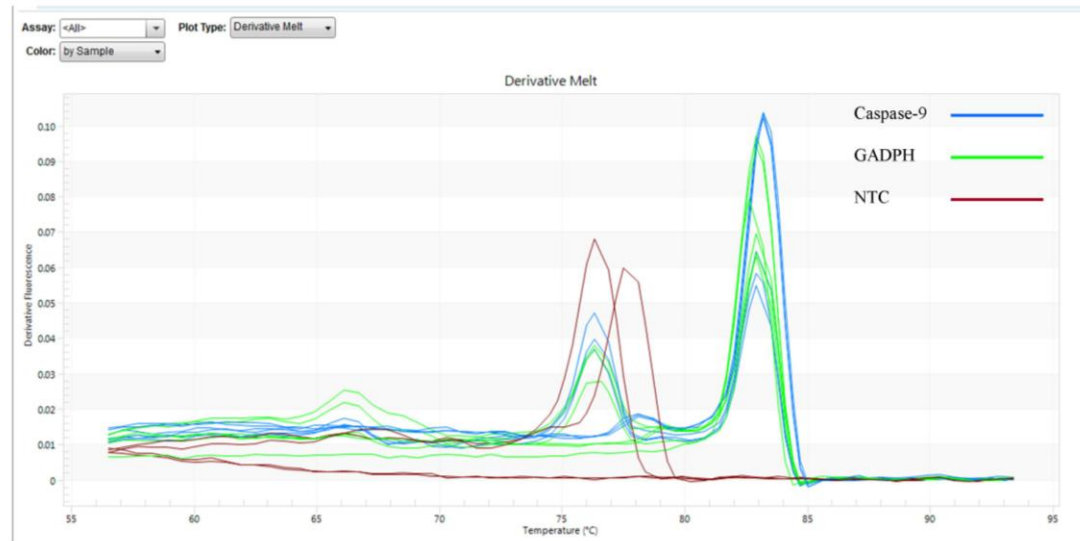
### 7.11.9 Derivative melt in control and cardamonin-treated HK-1 cells (by assay repeats)



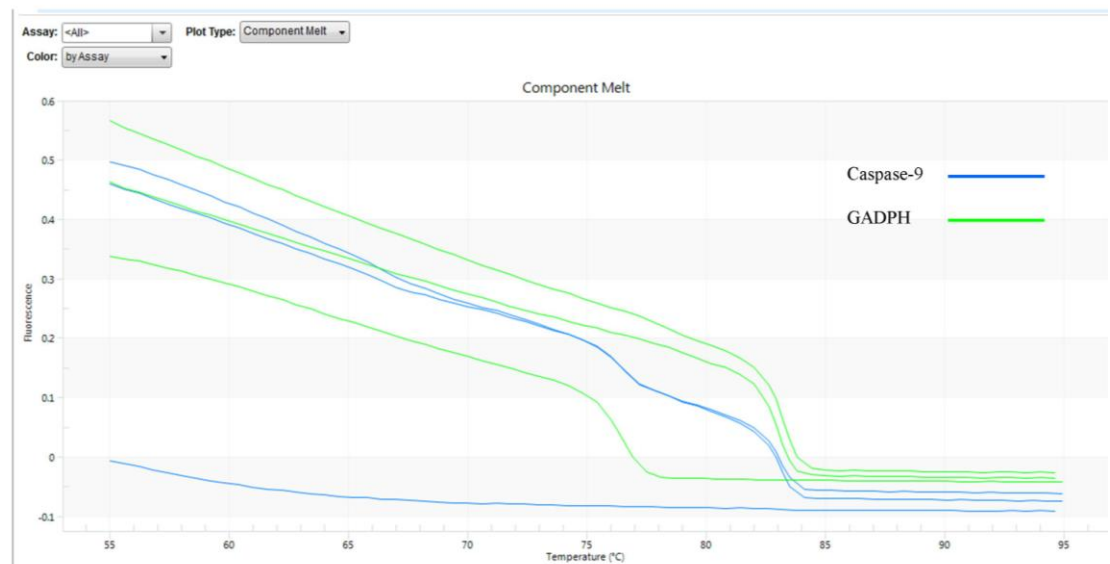
### 7.11.10 Derivative melt in control and cardamonin-treated HK-1 cells (by sample)



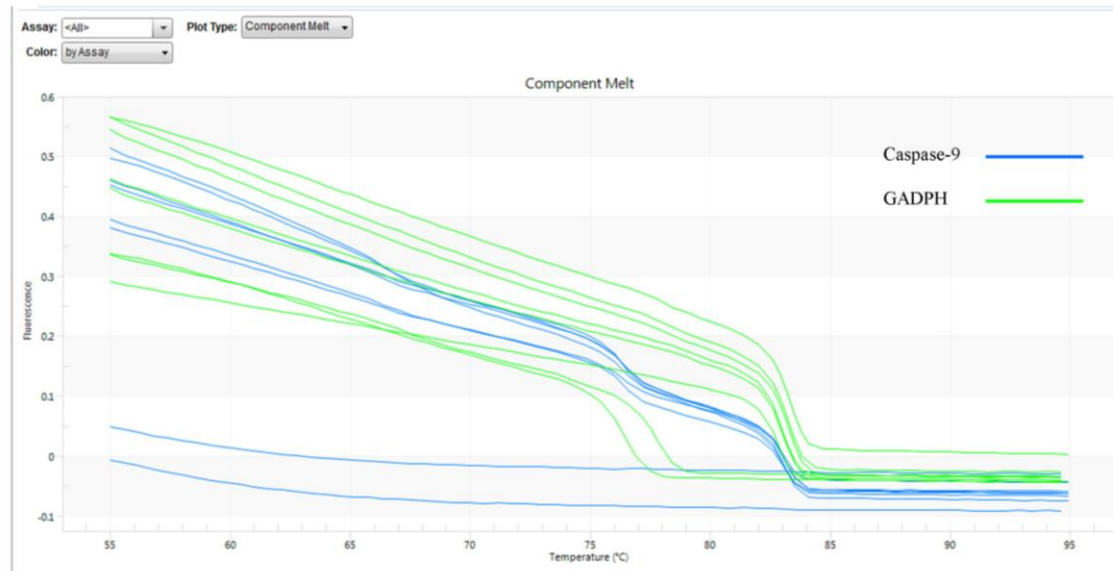
### 7.11.11 Derivative melt in control and cardamonin-treated HK-1 cells (by sample repeats)



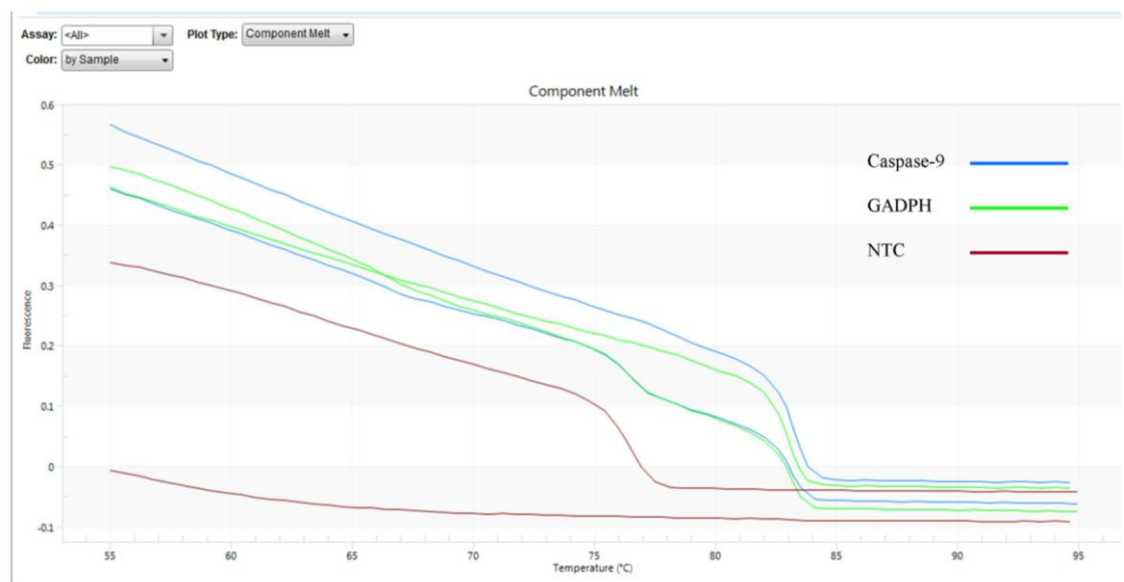
### 7.11.12 Component melt in control and cardamonin-treated HK-1 cells (by assay)



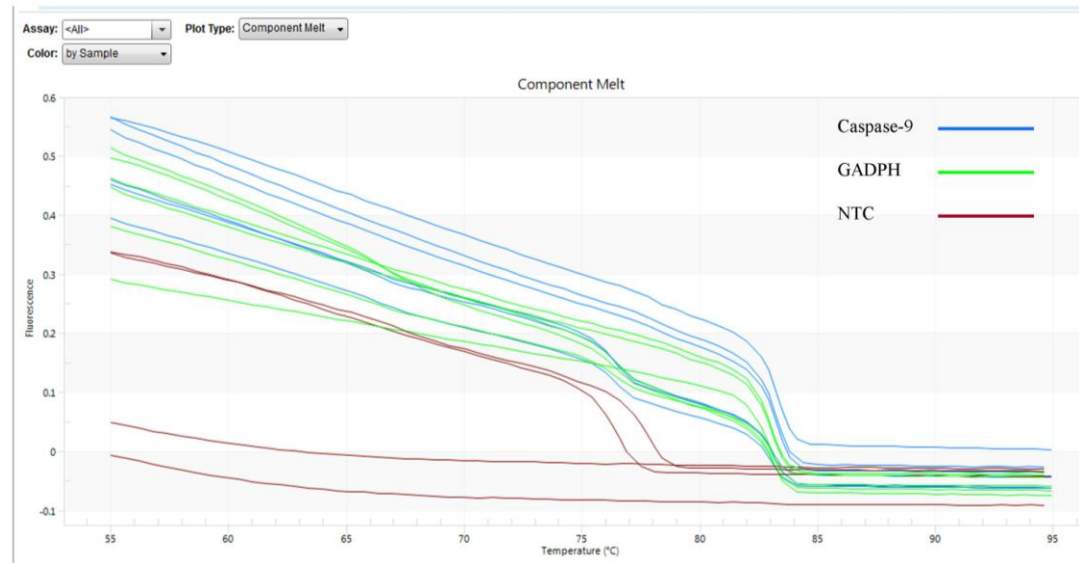
### 7.11.13 Component melt in control and cardamonin-treated HK-1 cells (by assay repeats)



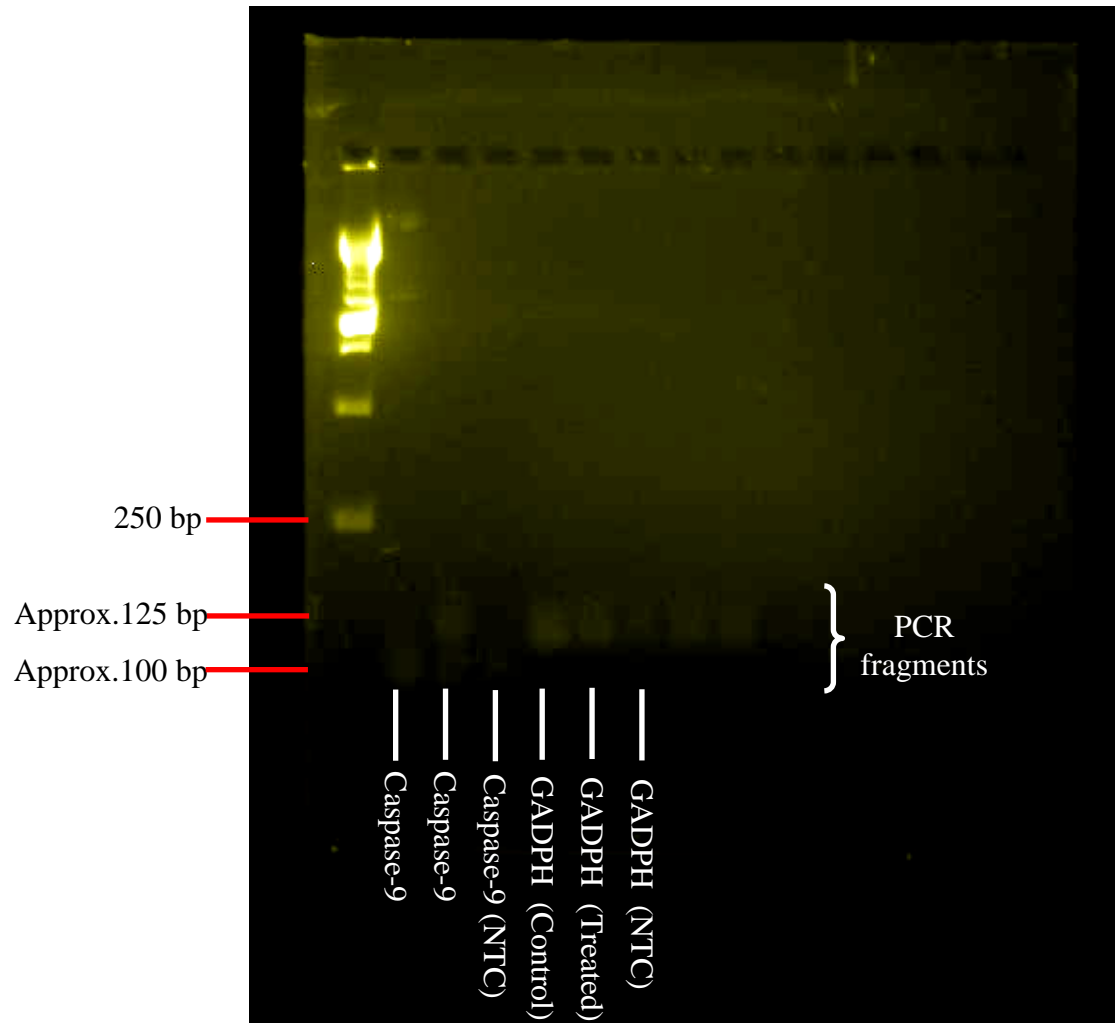
### 7.11.14 Component melt in control and cardamonin-treated HK-1 cells (by sample)



### 7.11.15 Component melt in control and cardamonin-treated HK-1 cells (by sample repeats)



### 7.11.16 Gel electrophoresis of amplicons





### 7.11.17 Relative quantification using Livak method

Using Livak method to quantify fold increase of caspase-9 gene expression,

**Step 1:** Normalize  $C_T$  (GOI) to  $C_T$  (reference gene)

$$\begin{aligned}\Delta C_T (\text{control}) &= \Delta C_T (\text{GOI}_{\text{control}}) - \Delta C_T (\text{reference gene}_{\text{control}}) \\ &= 14.33 - 25.75 \\ &= -11.42\end{aligned}$$

$$\begin{aligned}\Delta C_T (\text{cardamonin treated}) &= \Delta C_T (\text{GOI}_{\text{cardamonin treated}}) - \Delta C_T (\text{reference gene}_{\text{cardamonin treated}}) \\ &= 15.84 - 26.66 \\ &= -11.48\end{aligned}$$

**Step 2:** Normalize  $\Delta C_T$  of cardamonin treated group to control group

$$\begin{aligned}\Delta \Delta C_T &= \Delta C_T (\text{cardamonin treated}) - \Delta C_T (\text{control}) \\ &= (-11.48) - (-11.42) \\ &= -0.06\end{aligned}$$

**Step 3:** Calculate expression ratio/fold difference

$$\begin{aligned}\text{Normalized expression ratio} &= 2^{-\Delta \Delta C_T} \\ &= 2^{-(-0.06)} \\ &= +1.04 \quad (\text{positive indicates increase in fold} \\ &\quad \text{whereas negative value indicates} \\ &\quad \text{decrease in expression ratio})\end{aligned}$$

## Manuscripts

Elsevier Editorial System(tm) for Phytomedicine  
Manuscript Draft

Manuscript Number: PHYMED-D-15-00402

Title: Cardamonin induces apoptosis in human nasopharyngeal carcinoma cells via mitochondrial death pathway mediated by caspase-3 and caspase-8 activation, independent of caspase-9 signalling responses

Article Type: Original Article

Section/Category: Cancer

Keywords: Cardamonin; nasopharyngeal carcinoma (HK-1); caspases; mitochondrial-dependent apoptotic pathway.

Corresponding Author: Dr. Teng-Jin Khoo, PhD

Corresponding Author's Institution: University of Nottingham Malaysia Campus

First Author: Michelle Chiang, BSc.

Order of Authors: Michelle Chiang, BSc.; Teng-Jin Khoo, PhD; Chiew Foan Chin, PhD; Christophe Wiart, PhD

### Abstract: Background:

Cardamonin, a naturally occurring chalcone from *Alpinia* species has shown to exhibit anticancer effect on several cancer cell lines. In present study, the mechanism of cardamonin induced cell death in human nasopharyngeal carcinoma cell line, HK-1 was tested in vitro.

### Hypothesis:

Cardamonin triggers HK-1 cell death via mitochondrial-dependent cell death pathway.

### Methods:

Cell death induced by cardamonin was determined using different assays; MTT assay, caspase-3 and -8 detection assays, mitochondrial membrane potential assay, DNA fragmentation assay, cellular antioxidant assay (CAA), ATP/ADP ratio assay and cell cycle analysis by flow cytometer. Regulation of Bcl-2 family proteins were determined using western blot analysis and caspase-9 gene expression level was quantified by real-time PCR.

### Results:

Cardamonin exhibits a significant cytotoxic effect against human nasopharyngeal carcinoma cell line without affecting normal immortalized nasopharyngeal epithelial cell line, NP-69. Based on these results, IC50 22 µg/mL was used to further investigate the mechanisms of apoptosis. Up-regulation of caspase-3 and caspase-8 activities substantiated the induction of apoptosis through caspase-dependent signalling responses. There was no fold change in caspase-9 gene expression level suggesting that HK-1 cellular apoptosis occurred independent of caspase-9. Activation of caspase-3 was directly regulated by caspase-8 and does not require caspase-9. Present study also revealed up-regulation of pro-apoptotic protein, Bax and apoptotic signalling factor, cytochrome c resulting in down-regulation of anti-apoptotic protein, Bcl-2. Apoptotic cells induced by cardamonin were

illustrated by change in cellular morphology, increase in G2/M phase population and DNA fragmentation. Furthermore, cardamonin leads to a decrease in overproduction of reactive oxygen species (ROS), disruption in mitochondrial membrane potential and drop in intracellular ATP level in HK-1 cells.

**Conclusion:**

Current results indicate that caspase-3 and -8 activation of mitochondrial-dependent pathway play crucial roles in cardamonin-induced apoptosis in NPC cells. The data in present study demonstrate mode of actions of cardamonin which suggested its potential application as an anticancer agent against nasopharyngeal carcinoma.

19<sup>th</sup> March 2015.

Teng-Jin Khoo,  
Associate Professor,  
Center for Natural and Medicinal Product Research,  
School of Pharmacy, Faculty of Science,  
University of Nottingham Malaysia campus,  
Jalan Broga, 43500, Semenyih, Selangor.  
MALAYSIA

Dear Editor,

Re: Submission of Manuscript to Phytomedicine

I am writing to submit a manuscript entitled “Cardamonin induces apoptosis in human nasopharyngeal carcinoma cells *via* mitochondrial death pathway mediated by caspase-3 and caspase-8 activation, independent of caspase-9 signalling responses.” for consideration to publish in Phytomedicine.

The manuscript reports the anticancer activity of cardamonin from *Alpinia* species of ginger (Zingiberaceae) family. Nasopharyngeal carcinoma (NPC) cell line was treated with cardamonin in time-dependent manner and has been shown to exhibit cytotoxic effect. Induced cell death was illustrated by change in cellular morphology and DNA fragmentation. Up-regulation of caspase-3 and caspase-8 activities substantiated the induction of apoptosis through caspase-dependent pathway. Cell death in NPC after treatment by cardamonin was further justified through mitochondrial actions.

The research led to several significant findings. Cardamonin was found to exhibit cytotoxic effect against nasopharyngeal carcinoma without affecting normal nasopharyngeal cell line. The study was further substantiated by the activation of cell death through caspases signaling pathway which are responsible to regulate permeabilization of mitochondrial membrane. Up- and down-regulation of proteins associated with mitochondrial-dependent cell death pathway were detected and quantified.

The manuscript describes an original work and it is not being considered by any other journal. Please find the manuscript enclosed with this letter.

Thank you and looking forward to hear from you soon.

Regards,

*Khoo Teng Jin*

---

Teng-Jin Khoo

**Title**

Cardamonin induces apoptosis in human nasopharyngeal carcinoma cells *via* mitochondrial death pathway mediated by caspase-3 and caspase-8 activation, independent of caspase-9 signalling responses.

Michelle Chiang<sup>a</sup>, Chiew-Foan Chin<sup>b</sup>, Christophe Wiart<sup>a</sup> and Teng-Jin Khoo<sup>a,\*</sup>

<sup>a</sup>Center for Natural & Medicinal Product Research, School of Pharmacy,  
Faculty of Science, University of Nottingham, Malaysia Campus,  
Jalan Broga, 43500 Semenyih, Selangor, Malaysia.

<sup>b</sup>School of Biosciences, Faculty of Science, University of Nottingham, Malaysia Campus,  
Jalan Broga, 43500, Semenyih, Selangor, Malaysia.

\*Corresponding author

Teng-Jin Khoo, Center for Natural & Medicinal Product Research, School of Pharmacy,  
Faculty of Science, University of Nottingham, Malaysia Campus,  
Jalan Broga, 43500 Semenyih, Selangor, Malaysia  
Tel.: +603-89248213;  
Email address: tengjin.khoo@nottingham.edu.my

**Abstract**

*Background:*

Cardamonin, a naturally occurring chalcone from *Alpinia* species has shown to exhibit anticancer effect on several cancer cell lines. In present study, the mechanism of cardamonin induced cell death in human nasopharyngeal carcinoma cell line, HK-1 was tested *in vitro*.

*Hypothesis:*

Cardamonin triggers HK-1 cell death *via* mitochondrial-dependent cell death pathway.

*Methods:*

Cell death induced by cardamonin was determined using different assays; MTT assay, caspase-3 and -8 detection assays, mitochondrial membrane potential assay, DNA fragmentation assay, cellular antioxidant assay (CAA), ATP/ADP ratio assay and cell cycle analysis by flow cytometer. Regulation of Bcl-2 family proteins were determined using western blot analysis and caspase-9 gene expression level was quantified by real-time PCR.

*Results:*

Cardamonin exhibits a significant cytotoxic effect against human nasopharyngeal carcinoma cell line without affecting normal immortalized nasopharyngeal epithelial cell line, NP-69. Based on these results, IC<sub>50</sub> 22 µg/mL was used to further investigate the mechanisms of apoptosis. Up-regulation of caspase-3 and caspase-8 activities substantiated the induction of apoptosis through caspase-dependent signalling responses. There was no fold change in caspase-9 gene expression level suggesting that HK-1 cellular apoptosis occurred independent of caspase-9. Activation of caspase-3 was directly regulated by caspase-8 and does not require caspase-9. Present study also revealed up-regulation of pro-apoptotic protein, Bax and apoptotic signalling factor, cytochrome c resulting in down-regulation of anti-apoptotic protein, Bcl-2. Apoptotic cells induced by cardamonin were illustrated by change in cellular morphology, increase in G2/M phase population and DNA fragmentation. Furthermore, cardamonin leads to a decrease in overproduction of reactive oxygen species (ROS), disruption in mitochondrial membrane potential and drop in intracellular ATP level in HK-1 cells.

*Conclusion:*

Current results indicate that caspase-3 and -8 activation of mitochondrial-dependent pathway play crucial roles in cardamonin-induced apoptosis in NPC cells. The data in present study demonstrate mode of actions of cardamonin which suggested its potential application as an anticancer agent against nasopharyngeal carcinoma.

#### Keywords

Cardamonin; nasopharyngeal carcinoma (HK-1); caspases; mitochondrial-dependent apoptotic pathway.

#### Abbreviations

NPC, nasopharyngeal carcinoma; MTT, (3-[4,5-dimethylthiazol-2-yl]-2,5-diphenyltetrazolium bromide); ROS, reactive oxygen species; OMM, outer mitochondrial membrane; AO, acridine orange; PI, propidium iodide; ATP, adenosine triphosphate; JC-1, 5,5',6,6'-tetrachloro-1,1',3,3'-tetraethylbenzimidazolylcarbocyanine iodide.

### 1 Introduction

Nasopharyngeal carcinoma (NPC) consists of cancer cells that lie in the upper part of throat behind the nose and near the base of the skull called the nasopharynx. This type of cancer is fairly rare in most part of the world. Approximately 7 in every 1 million people in North America were diagnosed in the year 2012 (American Cancer Society). However, NPC is more common in parts of Asia, particularly in the southern China. Compared to other types of cancers, NPC is considered rare but it has been affecting certain ethnic in Southern China for decades. Besides ethnic background, it has been reported that NPC also arises due to dietary habits such as high consumption of alcohol and salted food (Ning et al., 1990). Since NPC is largely affected by dietary habits, we are interested to explore the possibility of utilizing food as a source of potential anticancer agent in NPC. Conventional anticancer drugs, paclitaxel and cisplatin have been used which worked synergistically with cetuximab to enhance the antitumor effect in NPC which down-regulates the over-expression of epidermal growth factor receptor (EGFR) (Sung et al., 2005). Several compounds isolated from plants have displayed anticancer effect against NPC (Lui et al., 2009; Lin et al., 2007; Kuo et al., 2011).

Cardamonin (Fig. 1A) was first extracted from cardamom spice and subsequently from other plants in Zingiberaceae family. The naturally occurring chalcone has been known to display diverse biological activities such as anticancer and anti-inflammatory activities (Chow et al., 2012; Qin et al., 2012; Park S et al., 2013; Park MK et al., 2013).

Caspases play an important role in mediation of nuclear apoptosis. The protease enzyme is mainly associated with formation of apoptotic bodies which occurred from a series of biological events that triggers cell death (Porter and Jänicke, 1999). Caspase-3 defective organisms are less likely to induce apoptosis although eventually typical signs of cell death did occur. Delay in cell death under deficiency of caspases provide strong evidence that caspases are important in the event to trigger apoptosis (Woo et al., 1998). Therefore, in the present study, we hypothesized that cardamonin induced cell death through up-regulation of caspases which subsequently induced apoptosis; thereby potentially demonstrates anticancer effect against NPC cells.

Mitochondria play important roles in activating apoptosis in mammalian cells as cell death is being regulated at cytosolic level (Wang and Youle, 2009). Studies have suggested that caspase-8 activation in cancerous cells leads to activation in mitochondrial dependent pathway through regulations of Bcl-2 family proteins (Lin et al., 2010). Hence, in this study we also investigate the mode of actions of cardamonin in triggering apoptotic effects in NPC

99 cells *via* activation of caspases and regulation of Bcl-2 family proteins in mitochondrial-  
100 dependent apoptotic pathway.

101

## 102 **2 Materials and Methods**

### 103 **2.1 Materials**

104 Human nasopharyngeal carcinoma (HK-1) and immortalized nasopharyngeal  
105 epithelial cell line (NP-69) cell lines were material transfer upon signing of collaboration  
106 with The University of Hong Kong through local collaboration with Institute of Medical  
107 Research (IMR) Malaysia. HK-1 was established from differentiated squamous carcinoma of  
108 nasopharynx of a Chinese male 17 ½ years after radiation therapy (Huang et al., 1980).

109 Cell culture media RPMI 1640 supplemented with 10% Fetal Bovine Serum (FBS),  
110 MTT (3-[4,5-dimethylthiazol-2-yl]-2,5-diphenyltetrazolium bromide) and ApoTarget Quick  
111 Apoptotic DNA Ladder Detection Kit were purchased from Gibco, Life Technologies, USA.  
112 Cardamonin ≥98% purity was obtained from Sigma-Aldrich Co. (St. Louis, MO). Propidium  
113 iodide (PI), acridine orange (AO), Caspase-3 DEVD-R110 Fluorometric and Colorimetric  
114 assay kit, Caspase-8 IETD-R110 Fluorometric and Colorimetric assay kit were purchased  
115 from Biotium Inc., Canada. Other assay kits include OxiSelect Cellular Antioxidant Activity  
116 Assay Kit (Green Fluorescence), Cell Biolabs, Inc., USA). JC-1 Mitochondrial Membrane  
117 Potential Assay Kit and ADP/ATP Ratio Assay Kit were obtained from Abnova,  
118 RNAqueous®-4PCR Total RNA Isolation Kit, SuperScript® III Platinum® SYBR®  
119 Green One-Step qRT-PCR Kit were purchased from Invitrogen, Life Technologies, USA.  
120 PRO-PREP protein extraction kit (iNtRON Biotechnology, Inc.), Anti-Bcl-2, Anti- Bcl2-L1,  
121 Anti-Bax, Anti-Bad, Anti-cytochrome c primary antibodies and Goat Anti-Rabbit IgG  
122 peroxidase-conjugated secondary antibodies were purchased from Abgent, Inc.. Primers were  
123 homo caspase-9 forward (F) primer (5' TGTCTACTCTACTTTCCCAGGTTTT 3'), homo  
124 caspase-9 reverse (R) primer (5' GTGAGCCCACTGCTCAAAGAT 3'), GADPH forward  
125 (F) primer (5' ACACCCACTCCTCCACCTTT 3') and GADPH reverse (R) primer (5'  
126 TAGCCAAATTCGTTGTCATACC) [16].

### 127 **2.2 Cell culture**

128 NPC HK-1 cells were cultured in RMPI media supplemented by 10% FBS and 5%  
129 penicillin-streptomycin. NP-69 cells were cultured in Keratinocyte-SFM containing 0.025%  
130 bovine pituitary extract, 0.014% recombinant epidermal growth factor (EGF) and 5%  
131 penicillin-streptomycin. Cells were maintained at 37°C in a humidified atmosphere with 5%  
132 CO<sub>2</sub>.

### 133 **2.3 Cell viability**

134 NPC HK-1 and NP-69 cell lines were seeded on a 96-well plate at  $7 \times 10^3$  cells per  
135 well. After 24 hrs, cardamonin was dissolved in DMSO at various concentrations (0, 3.125,  
136 6.25, 12.5, 25, 50, 100 and 200 µg/mL) before treated on the cells. After incubation times of  
137 24, 48 and 72 hrs, MTT solution was added.

### 138 **2.4 Fluorescence assay- cellular morphology microscopic observation**

139 HK-1 cells were seeded on a chamber slide (Thermo Scientific Nunc Lab Tek II) at  
140 cell density of  $6 \times 10^4$  cells per chamber. 10 µg/mL of acridine orange (AO) and 10 µg/mL of  
141 propidium iodide (PI) were added to each chamber. It was then observed under Fluoview  
142 1000 laser scanning confocal microscope (Olympus IX 81 Motorized Inverted Microscope).

### 143 **2.5 DNA fragmentation assay**

144 ApoTarget Quick Apoptotic DNA Ladder Detection Kit (Invitrogen) was used for cell  
145 DNA extraction. Extracted DNA was load on agarose gel and electrophoresis was run at 70V  
146 for 1-2 hrs before visualization using UV light illuminator (ChemiDoc XRS system, BioRad).

### 147 **2.6 Cell cycle analysis**

Cells were fixed in -20°C overnight prior to cell cycle analysis. RNase A solution (1 mg/mL) was added and incubate at 37°C for 15mins. Then, propidium iodide (PI) (1 mg/mL) was added to cells and left on ice in the dark for 10 mins prior to cell cycle analysis using CyAn™ ADP Analyzer flow cytometer (Beckman Coulter). The PI stained cells were analyzed using ModFit LT software for DNA cell cycle distribution and sub-G1 group as representative group of apoptosis.

#### 2.7 Caspase-3 and caspase-8 activity

Caspase-3 and caspase-8 activity were evaluated using Caspase-3 DEVD-R110 Fluorometric and Colorimetric Assay Kit and Caspase-8 IETD-R110 Fluorometric and Colorimetric Assay Kit (Biotium). Untreated cells and cells treated with 22 µM cardamonin were incubated for 24, 48 and 72 h at 37°C under 5% CO<sub>2</sub>. Fluorescence was measured at 470 nm excitation and 520 nm emission. A R110 reference standard was prepared to generate a standard curve to quantify the amount of caspase generated.

#### 2.8 Reactive Oxygen Species (ROS) production using Cellular Antioxidant Activity (CAA) assay

Evaluation of CAA was performed using OxiSelect Cellular Antioxidant Activity Assay Kit (Green Fluorescence), (Cell Biolabs, Inc., USA). Fluorescence reading was taken using Thermo Scientific Varioskan Flash multimode plate reader at 37°C with excitation wavelength of 480 nm and emission wavelength of 530 nm. Fluorescence was read at five-minute interval for a total one hour. Using the data generated from fluorescence values, the area under the curve (AUC) were integrated versus time. AUC values were used to determine cellular antioxidant activity (CAA) according to the formula below:

$$\text{CAA units} = 100 - [(\text{AUC}_{\text{antioxidant}} / \text{AUC}_{\text{control}}) \times 100]$$

From CAA versus concentration curve, half maximal effective concentration (EC<sub>50</sub>) values were generated.

#### 2.9 JC-1 Mitochondrial Membrane Potential Assay

Mitochondrial membrane potential was evaluated using JC-1 Mitochondrial Membrane Potential Assay Kit (Abnova). The ratio of fluorescent intensity of J-aggregates to monomers is used as an indicator of cell health. Changes in mitochondrial membrane potential stained with JC-1 were analyzed using Fluoview 1000 laser scanning confocal microscope (Olympus IX 81 Motorized Inverted Microscope). J-aggregates will emit intense red fluorescence whereas in cells with low mitochondrial membrane potential, JC-1 remains as monomers and emit green fluorescence.

#### 2.10 ADP/ATP Ratio Assay

Intracellular ATP level was evaluated using ADP/ATP Ratio Assay Kit (Abnova). ATP reagent was added to each well and after 1 min, luminescence (RLU A) was read using Thermo Scientific Varioskan Flash multimode plate reader. After 10 mins, luminescence was read again (RLU B). RLU B measures the background prior to ADP luminescence reading, also known as ATP residual signal. For ADP measurement, ADP reagent was added to each well and mixed well. After 1 min, luminescence (RLU C) was read. ADP/ATP ratio of each sample was calculated using the formula below:

$$\text{ADP/ATP} = \frac{\text{RLU C} - \text{RLU B}}{\text{RLU A}}$$

#### 2.11 Detection of mitochondrial-dependent pathway associated proteins using western blotting

30 µg of protein lysate were separated on 4-12% Tris-HCl SDS-PAGE gel and blotted onto a hybond ECL nitrocellulose membrane (GE Healthcare and Life Sciences). Membrane was blocked with 5% low fat milk in Tris Buffered Saline (TBS) containing 1% Tween-20 (TBST). Then, membrane was incubated with primary antibody (1:1500 dilution) for 2 hours



197 with agitation (60rpm) at room temperature. Membrane was washed with TBST prior to  
198 incubation with secondary antibody (1:1500 dilution). After that, membrane was washed with  
199 TMB Membrane Peroxidase Substrate Ready-To-Use (Rockland Immunochemicals Inc.)  
200 until protein bands were observed. Membrane was viewed using GS-800 calibrated  
201 densitometer.

## 202 2.12 Relative quantification of caspase-9 gene expression level using real-time PCR

203 To evaluate expression levels of gene of interest (caspase-9) and reference gene  
204 (GADPH), quantitative RT-PCR was performed in triplicates using Eco Real-Time PCR  
205 system (Illumina). Superscript III Platinum SYBR Green One-Step qRT-PCR kit (Invitrogen)  
206 with proprietary Superscript III Reverse Transcriptase (RT) and Platinum *Taq* DNA  
207 polymerase was performed in a single enzyme mix using SYBR Green I fluorescent dye.  
208 Thermal cycling conditions were set for cDNA synthesis for 3 mins hold at 50°C, followed  
209 by 5 mins activation of DNA polymerase and denaturation at 90°C. 40 cycles of annealing  
210 and amplification were performed at 95°C for 15 secs and 60°C for 30 secs respectively. The  
211 products were incubated for 1 min at 40°C prior to melting curve analysis. Eco Real-Time  
212 PCR system software v5.0 was employed for relative quantification to generate a real-time  
213 amplification plot based on the normalized fluorescence signal. Specific primers used were:  
214 Homo caspase-9 forward (F) primer (5' TGTCTACTCTACTTTCCCAGGTTT 3'), homo  
215 caspase-9 reverse (R) primer (5' GTGAGCCCACTGCTCAAAGAT 3'), GADPH forward  
216 (F) primer (5' ACACCCACTCCTCCACCTT 3') and GADPH reverse (R) primer (5'  
217 TAGCCAAATTCGTTGTCATACC).

## 218 2.13 Statistical analysis

219 The results of triplicate experiments were obtained and the values were presented in  
220 the form of mean  $\pm$  standard deviation (S.D.). One-way analysis of variance (ANOVA)'s  
221 Dunnett's Multiple Comparison Test and t-test were applied to analyze the difference from  
222 the respective controls for each experiment. All analyses were done using GraphPad Prism 5  
223 software and Microsoft Excel 2007. The signal intensities of various protein bands were  
224 quantified using Quantity One 1-D Analysis Software (Bio-Rad Laboratories, Munich,  
225 Germany).

## 227 3 Results

### 228 3.1 Cardamonin induces cell death and decreases cell viability in HK-1 cells

229 Results demonstrated that as the concentration of cardamonin increases, cell viability  
230 decreases (**Fig. 1B and 1C**). After 72 hrs, it was found that 50% of cardamonin-induced HK-  
231 1 cells proliferation inhibited at 22  $\mu$ g/mL.

### 232 3.2 Cardamonin induces morphological changes in HK-1 cells

233 HK-1 cells were treated with increasing concentration at 24 hrs to view the  
234 morphological changes using inverted microscope ( $\times 100$ ) (**Fig. 1D**). At cardamonin-induced  
235 concentration of 12.5  $\mu$ g/mL, HK-1 cells detached from adjacent cells forming clumps of  
236 cells floating in medium. Also, detached cells had uneven shape and unable to maintain their  
237 intact membranes (indicated by red arrows). Similar morphological changes were observed in  
238 HK-1 cells after 12 hrs of exposure to cardamonin (**Fig. 1E**).

### 239 3.3 Cardamonin-induced apoptosis in HK-1 cells leads to DNA fragmentation and 240 increase in G2/M and Sub-G1 cell populations

241 HK-1 cells treated with 22  $\mu$ g/mL of cardamonin at 24 and 48 hrs were stained with  
242 two DNA-binding dyes; acridine orange (AO) and propidium iodide (PI) to identify stages of  
243 apoptosis occurring in time-dependent manner (**Fig. 2A**). Acridine orange is able to pass  
244 through plasma membrane of viable cells and cells that are undergoing early apoptosis and  
245 stain DNA. From our results, HK-1 cells showed strong emission of green fluorescence in

untreated cells but when exposed to cardamonin for 24 hrs, cells emit orange red fluorescence more densely at the centre of the cells indicating late apoptosis. More dead cells were stained with PI after 48 hrs of cardamonin treatment emitting red fluorescence.

DNA from untreated and treated HK-1 cells were extracted at 24, 48 and 72 hrs and run on agarose gel for DNA separation (**Fig. 2B**). Nuclear fragmentation was observed in treated HK-1 cells. In untreated HK-1 cells, most DNAs were still intact with high molecular weight DNA strands being trapped on the gel. Cardamonin-treated cells showed DNA smearing with fragments at 48 and 72 hrs suggesting the occurrence of apoptosis. DNA sample from 5-fluorouracil-treated (positive control) showed DNA fragmentation after 24 hrs.

In current results, cardamonin induces cell cycle arrest at G2/M and Sub-G1 phase (apoptotic cells) (**Fig. 2C**). It was found that cardamonin-treated HK-1 cells after 12 hrs resulted in higher number of cells in G2/M phase (49.57%) compared to control group (2.56%) (**Fig. 2D**). Concurrently, cell population in G0/G1 phase after 12 hrs exposure to cardamonin showed a decrease (11.20%) in respect with control group (72.67%). An increase in apoptotic cells (Sub-G1 phase) was found after 12 hrs incubation with cardamonin. More than 36% HK-1 cells were accumulated in Sub-G1 phase compared to control group (2.99%).

#### 3.4 Cardamonin induces up-regulation of both caspase-3 and caspase-8 in HK-1 cells

Cardamonin has significantly enhanced the activity of caspase-3 in HK-1 cells compared to untreated cells within 24 hrs (**Fig.3A**). There was a slight decrease in caspase-3 activity at 48 hrs exposure but increased in the next 24 hrs. Similarly, caspase-8 activity was up-regulated within the first 24 hrs in cardamonin-treated HK-1 cells (**Fig. 3B**).

#### 3.5 Cardamonin decreases intracellular ROS production

Cardamonin decreases ROS production in HK-1 cells. Cardamonin-treated HK-1 cells revealed an increase in CAA as the concentration of cardamonin increases (**Fig. 3C**). Cardamonin was found to be effectively inhibiting radical-induced DCFH oxidation at 79.73  $\mu$ M (**Table 1**).

#### 3.6 Cardamonin induces loss of mitochondrial membrane potential and decreases intracellular ATP in HK-1 cells

A significant increase in mitochondrial membrane potential in HK-1 cells was observed after 3 hrs (**Fig. 3D**). Mitochondrial membrane potential increased five-fold compared to untreated control but decreased approximately three-fold after 6 hrs exposure to cardamonin. Changes in mitochondrial membrane potential after 3 and 6 hrs (**Fig. 3E**) showed strong J-aggregates and emit strong red fluorescence. However, in cardamonin-treated HK-1 cells, most of the cells observed were emitting green fluorescence indicating low mitochondrial membrane potential after 3 hrs.

In current research, an increase in intracellular ATP levels in control groups showed proliferating HK-1 cells. However, in cardamonin-treated HK-1 cells, a decrease in ATP levels was observed after 3 and 6 hrs (**Fig. 4A**). Changes in intracellular ATP level was further analysed by interpretation of ADP/ATP ratio. No significant increase in ADP levels with an elevated ATP levels in cardamonin-treated cells after 3 hrs in relative to control cells signify cells proliferation (ADP=, ATP $\uparrow$ ). After 6 hrs of exposure to cardamonin, it was observed that ADP/ATP ratio increased in comparison to control HK-1 cells (**Fig. 4B**).

#### 3.7 Cardamonin induces cell death *via* activations of mitochondrial-dependent pathway associated proteins

Effect of mitochondrial-dependent pathway associated proteins expression levels were summarized in **Fig. 4C**. A significant decrease in Bcl-2 proteins was observed after 6 hrs of cardamonin exposure (**Fig. 4D**) where as cytochrome c level was highest at 6 hrs of cardamonin exposure (**Fig. 4G**). Approximately 12% decrease in Bcl-2 protein expression

level was observed after 9 hrs of cardamonin exposure. Bcl-2 protein prevents the occurrence of apoptosis by inhibiting high release of cytochrome c between 3 to 6 hrs. However, as Bcl-2 proteins decreases, an increase in cytochrome c was observed at 6<sup>th</sup> hour. Our findings showed that there was no significant change in Bcl2-L1 (also known as Bcl2-X<sub>L</sub>) anti-apoptotic protein level (Fig. 4E). Bad pro-apoptotic protein was not detected within 24 hrs of cardamonin exposure. A significant increase in Bax pro-apoptotic protein expression level was observed between 3 to 9 hrs of cardamonin exposure (Fig. 4F). More than 25% increase in Bax proteins within first 9 hrs after treatment with cardamonin.

3.8 No change in caspase-9 gene expression level in HK-1 cells after treated with cardamonin: Mitochondrial-dependent apoptotic pathway occurs independent of caspase-9

Gene expression level of caspase-9 was measured in cardamonin-treated sample relative to control group. In addition, gene expression level of caspase-9 was normalized to the gene expression of a reference housekeeping gene, GAPDH based on C<sub>T</sub> values obtained in real time RT-PCR (Table 2). Relative quantification (RQ) was obtained and expressed as fold difference in respective to reference gene. Livak method was employed to quantify the fold change and based on current results, it has been found that the normalized gene expression ratio is 1.04 (Table 2). There was no change in gene expression level after HK-1 cells were treated with cardamonin after 24 hrs. Caspase-9 is not involved in cardamonin-induced HK-1 cell death.

#### 4 Discussion

Caspases play important roles in the activation of apoptosis and hence the activity of caspase-3 and caspase-8 were studied. Current results revealed that caspase activity was greatly amplified in HK-1 cells. An increase in caspase-3 activity triggers DNA fragmentation which is an indication of apoptosis as reported by Jänicke et al. (Jänicke et al., 1998). DNA extracted from cardamonin-treated HK-1 cells was found to be fragmented. It has been previously reported that caspase-3 is indeed required for DNA fragmentation leading to morphological changes in cancer cells. DNA is being fragmented at internucleosomal linker sites because these sites are easily accessible by Caspase-Activated DNase (CAD) enzyme. CAD forms a complex with an inhibitor, the Inhibitor of Caspase-Activated DNase (ICAD) which inactivates CAD. Caspase-3 cleaves the complex and leaving CAD to be in active form and hence degrades nuclear DNA (Enari et al., 1998). Therefore, caspase plays a crucial role in DNA fragmentation. It can be concluded that the up-regulation of caspase has greatly contributed to the distinct morphological changes in HK-1 cells i.e. DNA fragmentation.

Studies have suggested that caspase-8 mediates apoptosis in NPC which leads to activation of mitochondrial-dependent pathway through regulations of Bcl-2 family proteins (Lin et al., 2010). Regulation of pro-apoptotic and anti-apoptotic proteins belonging to Bcl-2 family has great influence in triggering cell death by promoting the cell's susceptibility to apoptotic stimuli (Wang and Youle, 2009). In our study, anti-apoptotic Bcl-2 proteins showed significant decrease whereas apoptosis inducer cytochrome c level was highest at 6 hrs of cardamonin exposure. Bad pro-apoptotic protein was not detected within 24 hrs of cardamonin exposure and hence this suggests that Bad pro-apoptotic was not involved in regulation of mitochondrial cell-death pathway. Previous literature suggested that this BH3-only member protein of Bcl-2 family may act as a sensitizer that binds to only pro-survival proteins to activate cell death. Hence, Bad protein was not entirely required for activation of mitochondrial-dependent apoptotic pathway (Willis and Adam, 2005).

Previous study showed that when Bcl-X<sub>L</sub>, an anti-apoptotic protein expression level decreases as Bax pro-apoptotic protein expression level increases, this regulation of Bcl-2

family proteins promote the release of cytochrome c and led to an up-regulation of caspase-3 thus triggered apoptosis in nasopharyngeal carcinoma cell lines (NPC-TW039 and NPC-TW076) treated with bioactive compound isolated from rhizomes of *Rheum palmatum* (Lin et al., 2010). Kuo *et al.* reported that when NPC-TW076 was exposed to a potent anticancer agent, curcumin in time-dependent manner, cell death pathway was activated. An up-regulation of Bax protein level accompanied by down-regulation of Bcl-2 protein level led to malfunction of mitochondria and subsequently triggered an activation of caspase-3 leading to cell death (Kuo et al., 2011). Bax undergoes homodimerization and translocates from cytosol to mitochondria causing a stimulated death in cell to be activated. Under circumstances where Bcl-2 is present, cells are protected by blocking the translocation of Bax pro-apoptotic proteins (Gross et al., 1998). Current results showed that Bax pro-apoptotic proteins contribute to cellular apoptosis in HK-1 cells.

Bcl-2 family proteins function as regulators that work collaboratively in regulation of cell death. This study demonstrates that mitochondrial cell-death pathway was triggered through an increase in Bax pro-apoptotic proteins by inhibiting Bcl-2 anti-apoptotic proteins to release death stimuli (an increase in cytochrome c expression level).

The permeability of mitochondrial membrane to allow protein translocation is greatly dependent on the activity of caspase. Caspase activation induces permeabilization of mitochondrial membrane to allow protein BID cleavage to an active fragment, tBID and thus being translocated to outer mitochondrial membrane (OMM). The initial signal triggered from caspase activation will be transmitted to release apoptogenic factors such as cytochrome c (Luo et al., 1998). These factors bind to apoptosis activating factor to form complex in order to activate the release of caspase-9 and hence stimulates apoptosis. We investigated changes of mitochondrial membrane potential and how it affects generation of ATP. Earlier results suggest that caspase-8 activity was significantly amplified in HK-1 cells within first 24 hrs after treated with cardamonin. Caspase-8 cleavage leads to translocation of pro-apoptotic protein, Bid to membrane of mitochondria. This causes recruitment of another pro-apoptotic protein, Bax to stimulate opening of mitochondrial PTP. Hence, we evaluate mitochondrial membrane potential ( $\Delta\Psi_m$ ) after exposure to cardamonin in time-dependent manner. Cardamonin induces loss of mitochondrial membrane potential in HK-1 cells. Loss of mitochondrial membrane potential is an initial requirement for cellular apoptosis. Loss in mitochondrial membrane potential greatly affects intracellular ATP level as mitochondria play role as energy generator. It was found that intracellular ATP level decreases concurrently as mitochondrial membrane potential drops in cardamonin-treated HK-1 cells. Loss in mitochondrial membrane potential within the few hours of cardamonin exposure was further justified by decline in intracellular ATP levels in HK-1 cells. Recent study reported that capsaicin isolated from chilli pepper causes disruption in mitochondrial membrane potential *via* mitochondrial cell death pathway which leads to inhibition of ATP synthesis in tumor cells (Skrzypski et al., 2014).

Mitochondrion is extensively studied and proven to be a major intracellular source of ROS. ROS production is due to partial inhibition of mitochondrial respiratory chain which leads to cell death (Fleury et al., 2002). ROS has long been associated with cancer because cancer cells are transformed cells and tend to generate more ROS for cell proliferation (Schumacker, 2006). Cancer cells normally overproduce ROS compared to normal cells (Szatrowski, 1991). Cellular Antioxidant Activity (CAA) assay was conducted to determine antioxidant properties of cardamonin against HK-1 cells. CAA activity increases as concentration of cardamonin increase. This may be due to the action of cardamonin as an antioxidant to scavenge and quench ROS. This shows that cardamonin reduces ROS production and does not contribute to HK-1 cell death.

Caspase-9, a final protein required before cleavage of apoptotic substrates, which is necessary to trigger apoptotic signal for permanent cell death was quantified by real-time PCR. Based on current finding, there was no fold change of caspase-9 gene expression level relative to control group. Despite recent evidences that prove caspase-9 is an important initiator to activate caspase-3 to trigger cell death (Yu et al., 2010; Jen et al., 2008; Bretnall et al., 2013), in current research our results proved otherwise. Although apoptotic-inducing factor, cytochrome c was shown to release from mitochondria in previous result, it did not function to induce caspase-9 to form apoptosome. Hence, caspase-9 was not involved in triggering HK-1 cell death. Instead, HK-1 cellular apoptosis was induced by the actions of caspase-3 and caspase-8.

Several literatures reported that caspase-9 was not required in some cellular apoptosis. Apoptotic death of platelets and megakaryocytes were shown to be independent of caspase-9. Caspase-9 deficient fetal liver cells in mice revealed that platelets and megakaryocytes still possess apoptotic function (White et al., 2012). Ekert *et al.* reported that Apaf-1 and caspase-9 are not required for apoptosis in drug-treated cells (Ekert et al., 2004). In hydrogen peroxide (H<sub>2</sub>O<sub>2</sub>)-induced apoptosis HeLa cells, caspase-3 was found to be activated by caspase-8 instead of caspase-9 in mitochondrial-dependent pathway (Wu et al., 2011). Similarly, cardamonin triggers apoptosis in HK-1 cells mediated by caspase-8 that activates caspase-3 directly. A summary of how cardamonin triggers apoptosis *via* activation of mitochondrial-dependent pathway mediated by caspase-8 ( - - - - ► ) that directly activates caspase-3 was illustrated in **Fig. 4**.

In conclusion, these studies demonstrate mode of actions of cardamonin-induced apoptosis in HK-1 cells mediated by caspase-8 activation and subsequently leads to cell death *via* mitochondrial-dependent apoptotic pathway *in vitro*.

#### Acknowledgements

This work was funded by Public Service Department of Malaysia (JPA) for Scholarship to Chiang Michelle. We would also like to thank Prof GSW Tsao, The University of Hong Kong and Dr Alan Khoo, Institute of Medical Research, Malaysia for providing the NP-69 and HK-1 cell lines.

#### Conflict of interest

The authors disclose that there is no financial and personal relationships with other party or institutions that may inappropriately influence our work.

#### References

- American Cancer Society, 2012. Cancer Facts & Figures, American Cancer Society. Atlanta, United States of America.
- Bretnall, M., Rodriguez-Menocal, L., De Guevara, R.L., Cepero, E., Boise, L.H., 2013. Caspase-9, caspase-3 and caspase-7 have distinct roles during intrinsic apoptosis. BMC Cell Biol. 14, 32.
- Chow, Y., Lee, K., Vidyadaran, S., Lajis, N.H., Akhtar, M.N., Israf, D.A., Syahida, A., 2012. Cardamonin from *Alpinia rafflesiana* inhibits inflammatory responses in IFN- $\gamma$ /LPS-stimulated BV2 microglia *via* NF- $\kappa$ B signalling pathway. Int. Immunopharmacology 12(4), 657-665.
- Ekert, P.G., Read, S.H., Silke, J., Marsden, V.S., Kaufmann, H., Hawkins, C.J., Gerl, R., Kumar, S., Vaux, D.L., 2004. Apaf-1 and caspase-9 accelerate apoptosis, but do not determine whether factor-deprived or drug-treated cells die. The J of Cell Biol. 165(6), 835-842.

442 Enari, M., Sakahira, H., Yokoyama, H., Okawa, K., Iwamatsu, A., Nagata, S., 1998. A  
 443 caspase-activated DNase that degrades DNA during apoptosis, and its inhibitor ICAD.  
 444 Nature 391, 43-50.

445 Fleury, C., Mignotte, B., Vayssière, J., 2002. Mitochondrial reactive oxygen species in cell  
 446 death signalling. Biochimie 84, 131-141.

447 Gross, A., Jockel, J., Wei, M.C., Korsmeyer, S.J., 1998. Enforced dimerization of BAX  
 448 results in its translocation, mitochondrial dysfunction and apoptosis. The EMBO J  
 449 17(14), 3878-3885.

450 Huang, D.P., Ho, J.H., Poon, Y.F., Chew, E.C., Saw, D., Lui, M., Li, C.L., Mak, L.S., Lai,  
 451 S.H., Lau, W.H., 1980. Establishment of a cell line (NPC/HK1) from a differentiated  
 452 squamous carcinoma of the nasopharynx. In: J Cancer 26(2), 127-132.

453 Jänicke, R.U., Sprengart, M.L., Wati, M.R., Porter, A.G., 1998. Caspase-3 is required for  
 454 DNA fragmentation and morphological changes associated with apoptosis. J of Biol.  
 455 Chem. 273(16), 9357-9360.

456 Jen, C., Lin, C., Huang, B., Leu, S., 2008. Cordycepin induced MA-10 mouse Leydig tumor  
 457 cell apoptosis through caspase-9 pathway. Evidence-Based Complementary and  
 458 Alternative Medicine 2011, Article ID 984537.

459 Kuo, C., Wu, S.Y., Ip, S., Wu, P., Yu, C., Yang, J., Chen, P., Wu, S.H., Chung, J., 2012.  
 460 Apoptotic death in curcumin-treated NPC-TW 076 human nasopharyngeal carcinoma  
 461 cells is mediated through ROS, mitochondrial depolarization and caspase-3-dependent  
 462 signalling responses. Int. J Oncology 39, 319-328.

463 Lin, M., Chen, S., Lu, Y., Liang, R., Ho, Y., Yang, C., Chung, J., 2007. Rhein induces  
 464 apoptosis through induction of endoplasmic reticulum stress and  $Ca^{2+}$ -dependent  
 465 mitochondrial death pathway in human nasopharyngeal carcinoma cells. Anticancer  
 466 Res. 27, 3313-3322.

467 Lin, M., Lu, Y., Chung, J., Li, Y., Wang, S., Ng, S., Wu, C., Su, H., Chen, S., 2010. Aloe-  
 468 emodin induces apoptosis of human nasopharyngeal carcinoma cells *via* caspase-8-  
 469 mediated activation of the mitochondrial death pathway. Cancer Lett. 291(1), 46–58.

470 Lui, V.W.Y., Yau, D.M.S., Wong, E.Y.L., Ng, Y-K., Lau, C.P.K., Ho, Y., Chan, J.P.L., Hong,  
 471 B., Ho, K., Cheung, C.S., Tsang, C-M., Tsao, S-W., Chau, A.T.C., 2009. Cucurbitacin I  
 472 elicits anoikis-sensitization, inhibits cellular invasion and *In Vivo* tumor formation  
 473 ability of nasopharyngeal carcinoma cells. Carcinogenesis 30, 2085-2094.

474 Luo, X., Budihardjo, I., Zou, H., Slaughter, C., Wang, X., 1998. Bid, a Bcl2 interacting  
 475 protein, mediates cytochrome c release from mitochondria in response to activation of  
 476 cell surface death receptors. Cell 94(4), 481–490.

477 Ning, J.P., Yu, M.C., Wang, Q.S., Henderson, B.E., 1990. Consumption of salted fish and  
 478 other risk factors for nasopharyngeal carcinoma (NPC) in Tianjin, a low-risk region for  
 479 NPC in the People's Republic of China. J Natl Cancer Inst. 82(4), 291-296.

480 Park, M.K., Jo, S.H., Lee, H.J., Kang, J.H., Kim, Y.R., Kim, H.J., Lee, E.J., Koh, J.Y., Ahn,  
 481 K.O., Jung, K.C., Oh, S.H., Kim, S.Y., Lee, C.H., 2013. Novel suppressive effects of  
 482 cardamonin on the activity and expression of transglutaminase-2 lead to blocking the  
 483 migration and invasion of cancer cells. Life Sci. 92, 154-160.

484 Park, S., Gwak, J., Han, S.J., Oh, S., 2013. Cardamonin suppresses the proliferation of colon  
 485 cancer cells by promoting  $\beta$ -catenin degradation. Biol. Pharmaceutical Bull. 36(6),  
 486 1040-1044.

487 Porter, A.G., Jänicke, R.U., 1999. Emerging roles of caspase-3 in apoptosis. Cell Death Diff.  
 488 6, 99-104.

489

490 Qin, Y., Sun, C., Lu, F., Shu, X., Yang, D., Chen, L., She, X., Gregg, N.M., Guo, T., Hu, Y.,  
 491 2012. Cardamonin exerts potent activity against multiple myeloma through blockade of  
 492 NF- $\kappa$ B pathway *in vitro*. Leukemia Res. 36, 514-520.

493 Schumacker, P.T., 2006. Reactive oxygen species in cancer cells: live by the sword, die by  
 494 the sword. Cancer Cell 10(3), 175-176.

495 Skrzypski, M., Sassek, M., Abdelmessih, S., Mergler, S., Grötzinger, C., Metzke, D.,  
 496 Wojciechowicz, T. , Nowak, K.W., Strowski, M.Z., 2014. Capsaicin induces  
 497 cytotoxicity in pancreatic neuroendocrine tumor cells *via* mitochondrial action. Cellular  
 498 Signalling 26, 41-48.

499 Sung, F.L., Poon, T.C.W., Hui, E.P., Ma, B.B.Y., Liong, E., To, K.F., Huang, D.P.W.S.,  
 500 Chan, A.T.C., 2005. Antitumor effect and enhancement of cytotoxic drug activity by  
 501 cetuximab in nasopharyngeal carcinoma cells. In vivo 19, 237-246.

502 Szatrowski, T.P., Nathan, C.F., 1991. Production of large amounts of hydrogen peroxide by  
 503 human tumor cells. Cancer Res. 51, 794-798.

504 Wang, C.X., Youle, R.J., 2009. The Role of Mitochondria in Apoptosis. Ann. Rev. Genetics  
 505 43, 95-118.

506 White, M.J., Schoenwaelder, S.M., Josefsson, E.C., Jarman, K.E., Henley, K.J., James, C.,  
 507 Debrincat, M.A., Jackson, S.P., Huang, D.C.S., Kile, B.T., 2012. Caspase-9 mediates  
 508 the apoptotic death of megakaryocytes and platelets, but is dispensable for their  
 509 generation and function. Platelets and Thrombopoiesis 119(18), 4283-4290.

510 Willis, S.N., Adams, J.M., 2005. Life in the balance: how BH3-only proteins induce  
 511 apoptosis. Curr. Opinion Cell Biol. 17(6), 617-625.

512 Woo, M., Hakem, R., Soengas, M.S., Duncan, G.S., Shahinian, A., Kägi, D., Hakem, A.,  
 513 McCurrach, M., Khoo, W., Kaufman, S.A., Senaldi, G., Howard, T., Lowe, S.W., Mak,  
 514 T.W., 1998. Essential contribution of caspase-3/CCP32 to apoptosis and its associated  
 515 nuclear changes. Genes Dev. 12, 806-819.

516 Wu, Y., Wang, D., Wang, X., Wang, Y., Ren, F., Chang, D., Chang, Z., Jia, B., 2011.  
 517 Caspase 3 is activated through caspase 8 instead of caspase 9 during H<sub>2</sub>O<sub>2</sub>-induced  
 518 apoptosis in HeLa cells. Cellular Physio Biochem. 27, 539-546.

519 Yu, F., Yang, J., Yu, C., Lu, C., Chiang, J., Lin, C., Chung, J., 2010. Safrole induces  
 520 apoptosis in human oral cancer HSC-3 cells. J Dental Res. 90(2), 168-174.

521

522

523

524

525

526

527

528

529

530

531

532

533

534

535

536

537

538



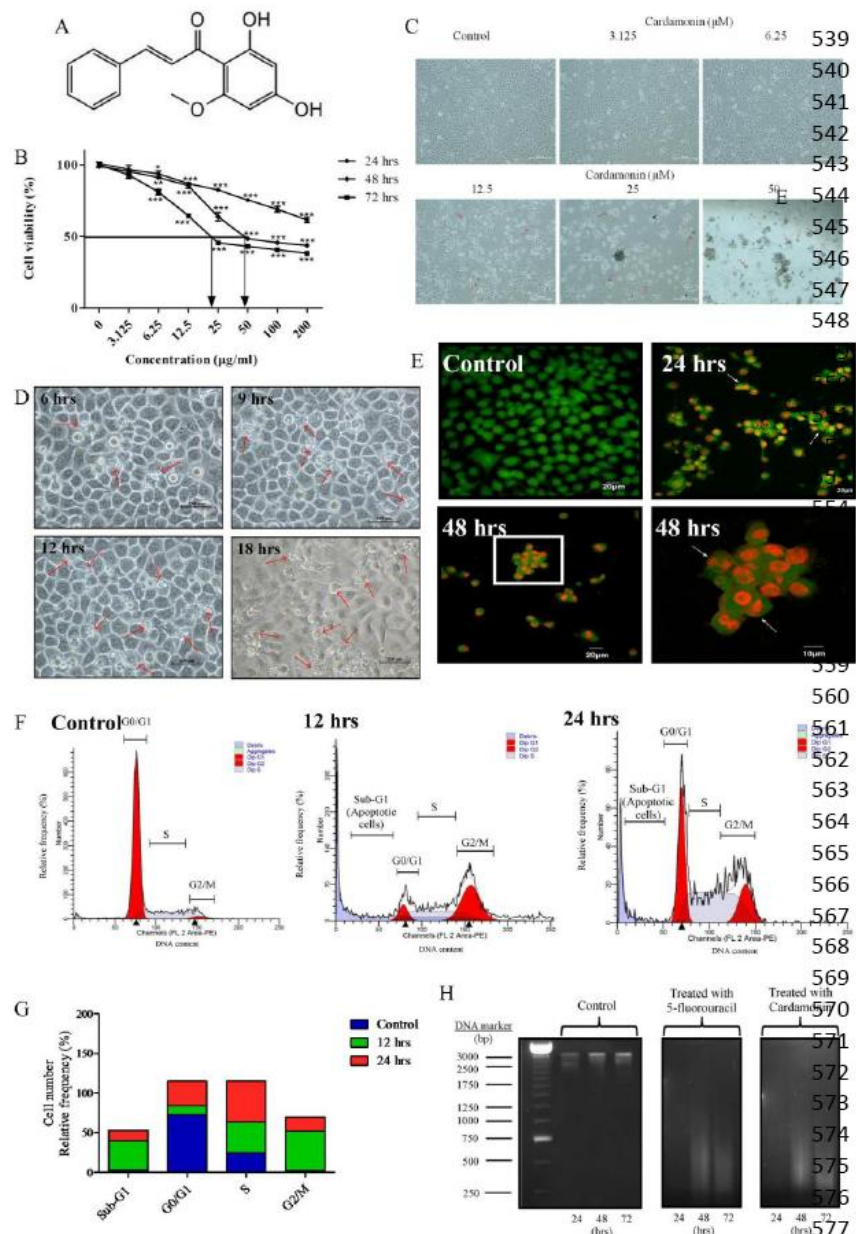


**Fig. 1.** (A) Structure of cardamomin. (B) Cytotoxic effect of various concentrations of cardamomin on HK-1 cell viability at 24, 48 and 72 hrs. Each point represents the mean  $\pm$  standard deviation (S.D.) from three independent experiments (n=3). \*\*\*P < 0.001, \*\*P < 0.05 and \*P < 0.01 indicate the statistical significant difference with respect to untreated control group. (C & D) Changes in cell morphology were examined by inverted microscope ( $\times 100$ ). (E) HK-1 cells stained with AO and PI were observed using laser confocal microscope ( $\times 400$ ). (F) DNA fragmentation of HK-1 cells when untreated, treated with 19  $\mu$ M of anticancer drug, 5-fluorouracil (5-FU) and 22  $\mu$ M of cardamomin at 24, 48 and 72 hrs. (G & H)



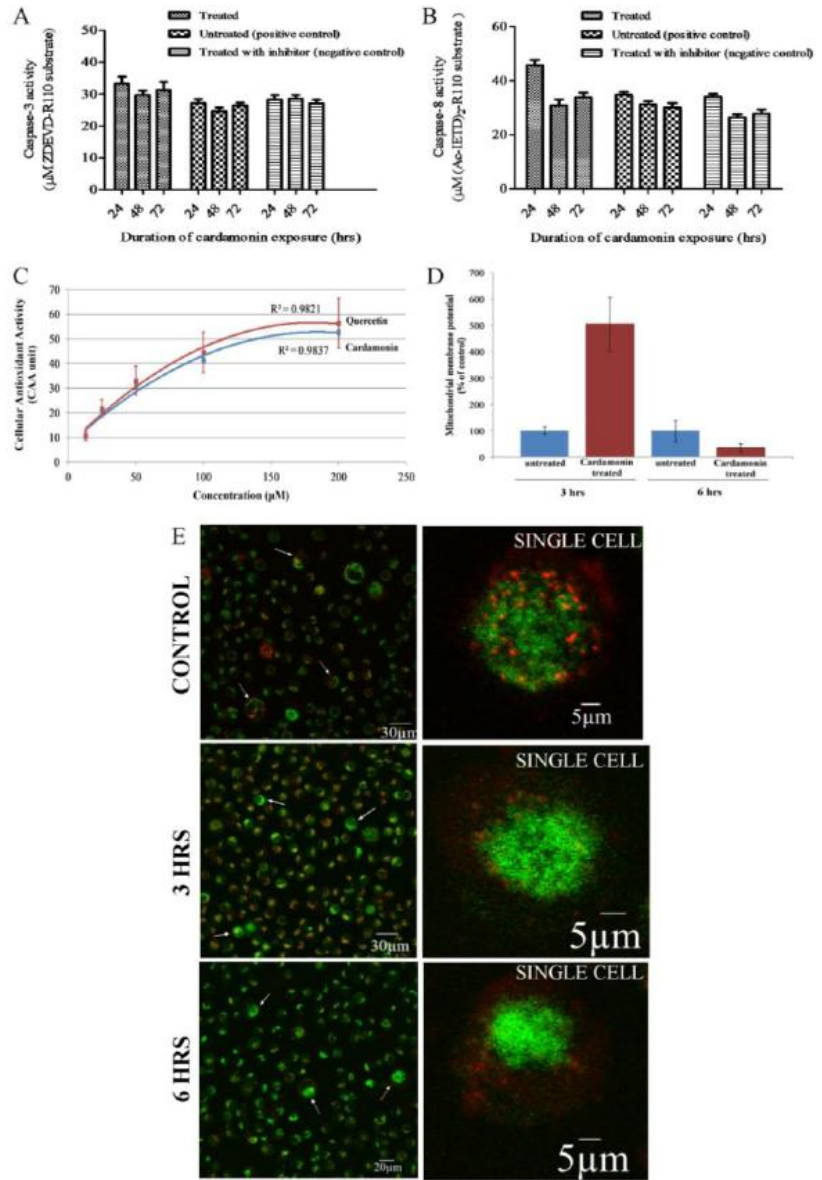


**Fig. 2.** (A) Caspase-3 and (B) Caspase-8 activity in HK-1 cells when untreated, treated with 22 µg/mL of cardamonin and caspase-3 inhibitor at 24, 48 and 72 hrs. (C) Dose-response curve of quercetin standard and cardamonin in HK-1 cells. Each bar or point represents mean  $\pm$  standard deviation (S.D.) from three independent experiments (n=3). \* $P < 0.05$  and \*\*\* $P < 0.001$  indicate the statistical significant difference with respect to untreated control group. (D) Effect of cardamonin on mitochondrial membrane potential in HK-1 cells after 3 and 6 hrs. (E) Mitochondrial membrane potential in HK-1 cells (control group) after 3 and 6 hrs ( $\times 400$ ). Untreated cells showing strong J-aggregation and emits red fluorescence (indicated by white arrows).

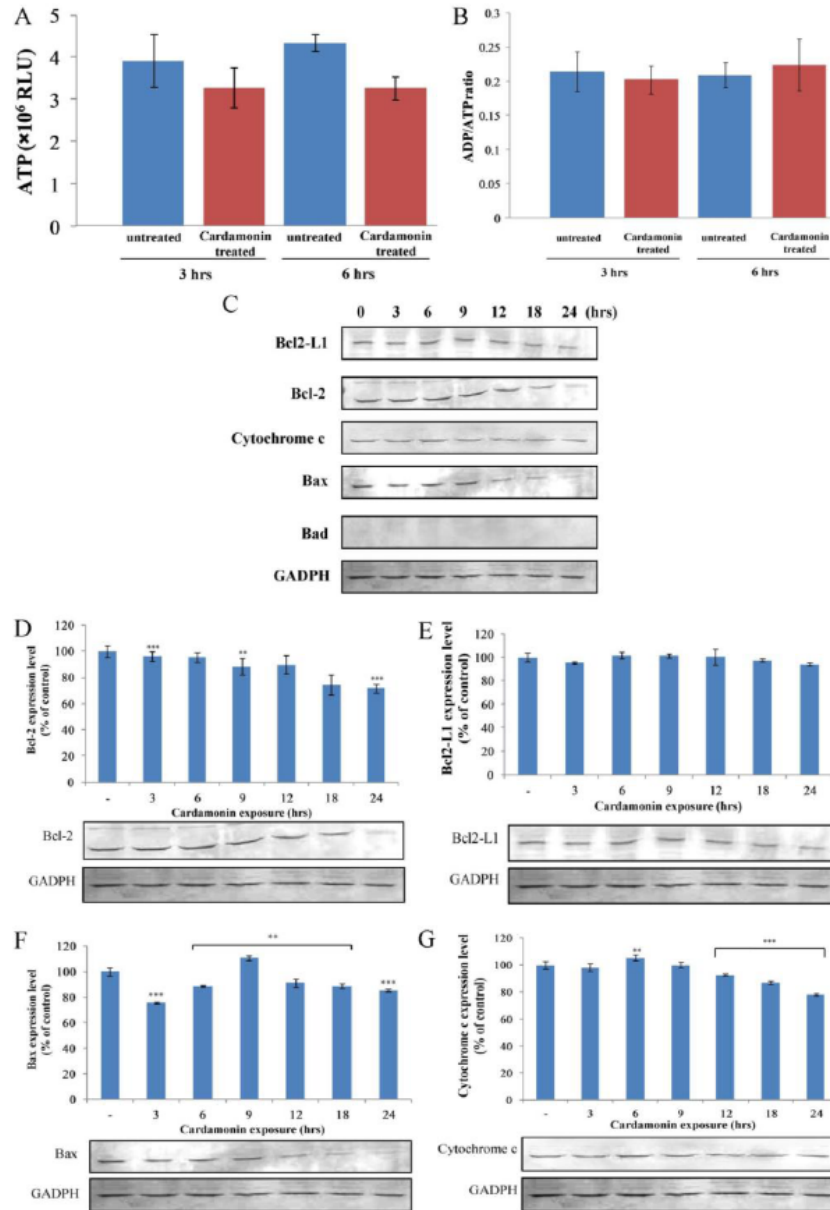
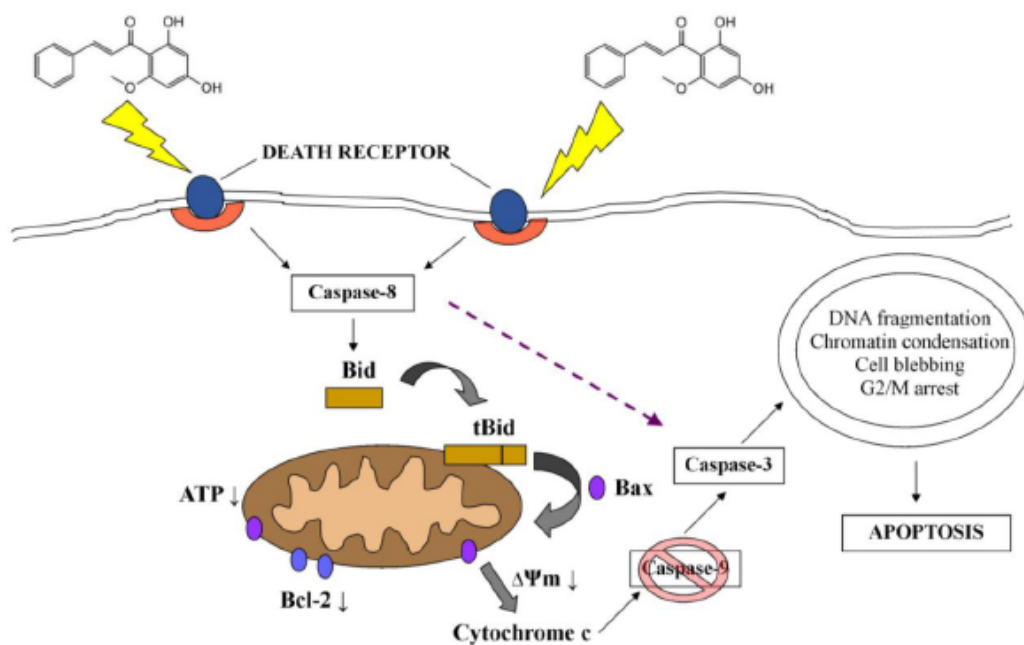


**Fig. 3.** (A) Effect of cardamonin on intracellular ATP levels and (B) ADP/ATP ratio in HK-1 cells after 3 and 6 hrs. Each bar represents mean  $\pm$  standard deviation (S.D.) from there independent experiments (n=3). (C) Changes in mitochondrial dependent pathway-associated protein expression levels were analyzed qualitatively by Western blotting. (D) Effect of cardamonin on Bcl-2, Bcl2-L1 (E), Bax (F), cytochrome c (G) proteins expression level in time-dependent manner. Each bar represents the mean  $\pm$  standard deviation (S.D.) derived from three replicates reading. \*\*\* $P$ <0.001 and \*\* $P$ <0.01 indicate the statistical significant difference with respect to control.

663



664

665

666 **Fig.4.** This diagram illustrates mode of actions of cardamonin in activation of mitochondrial-  
667 dependent pathway mediated by caspase-8 against nasopharyngeal carcinoma (HK-1) cells.

668

669

**Table 1. EC<sub>50</sub> values from dose-response curve.**

Standard/Sample	EC <sub>50</sub> (μM)
Quercetin	89.27
Cardamonin	79.73

670

671 **Table 2. Normalized gene expression ratio of caspase-9 and GADPH in control and**  
672 **cardamonin-treated groups.**

	Threshold cycle (C <sub>T</sub> ) values		Normalized gene expression ratio
	Gene of interest (Caspase-9)	Reference gene (GADPH)	
Control	25.75 ± 0.15	14.33 ± 0.40	-
Cardamonin treated	26.66 ± 0.55	15.18 ± 0.57	1.04

673

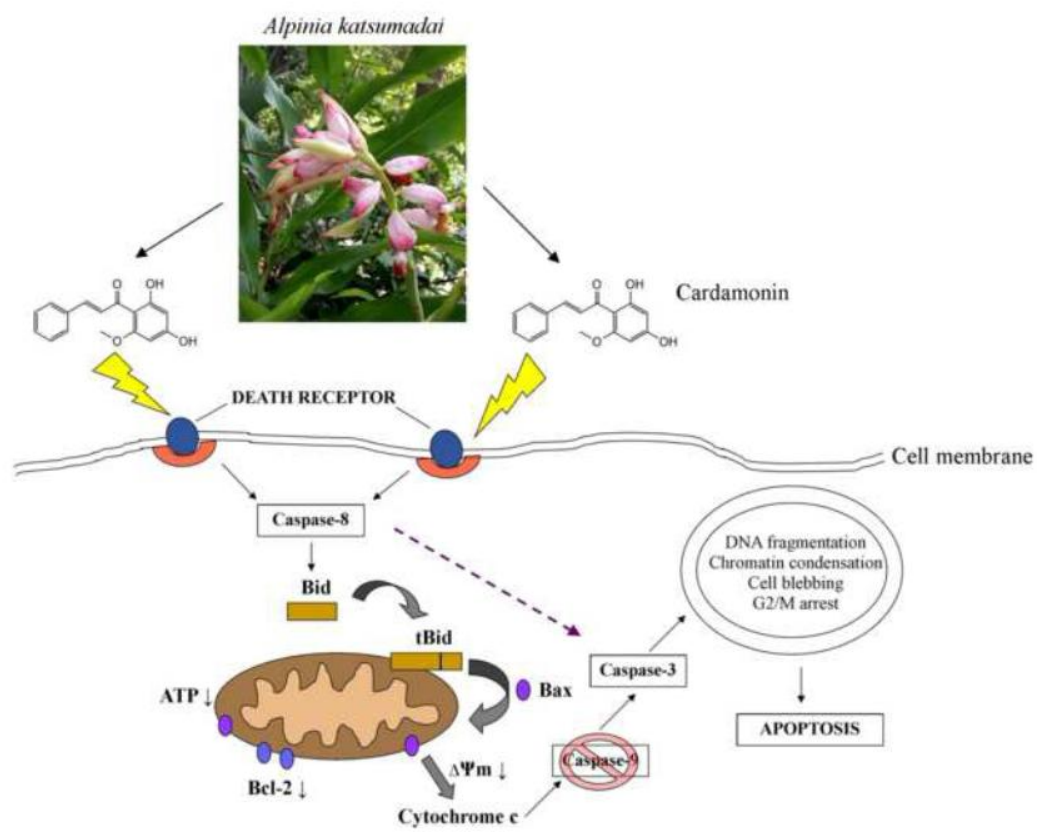


Figure 1  
[Click here to download high resolution image](#)

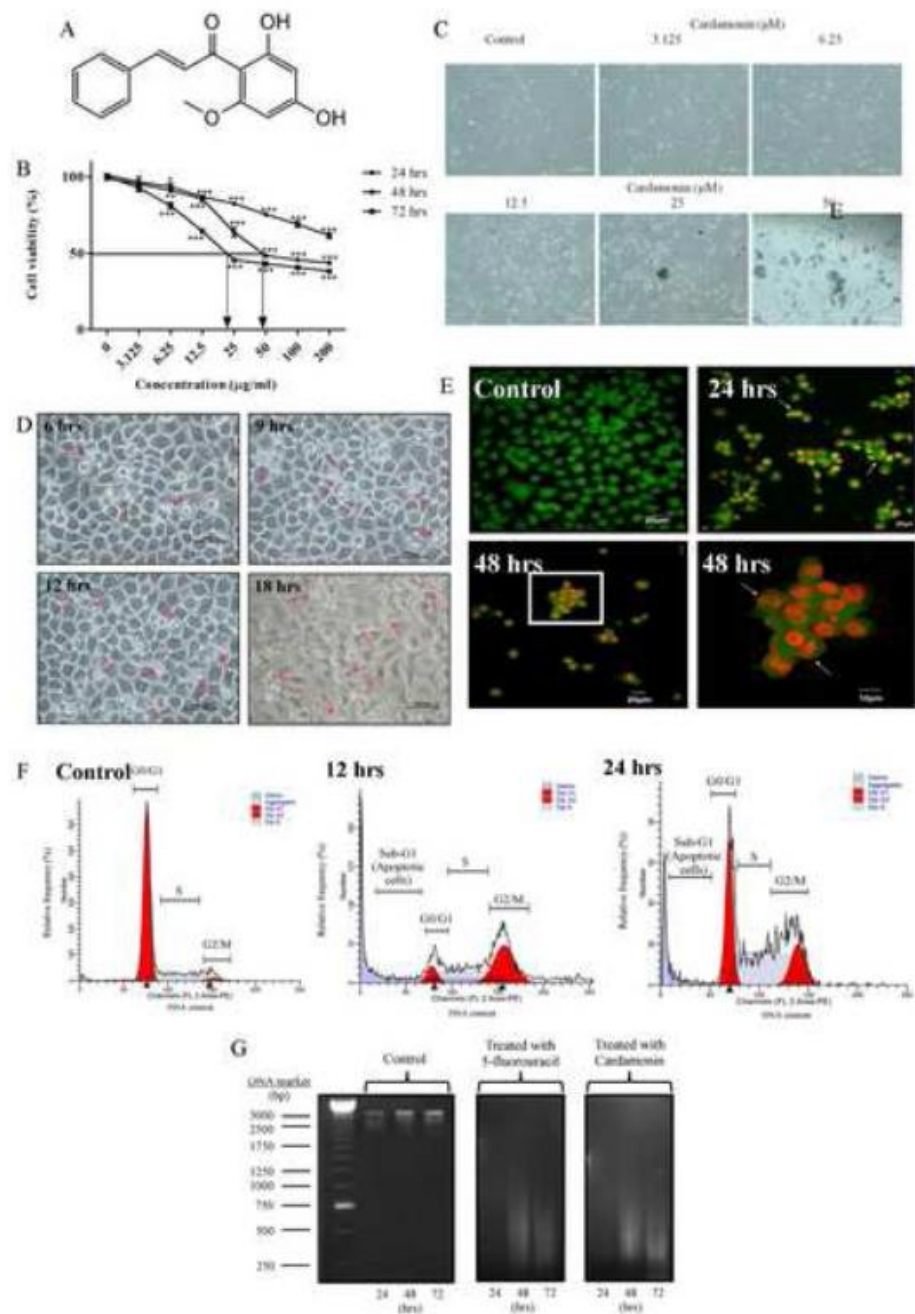




Figure 2  
[Click here to download high resolution image](#)

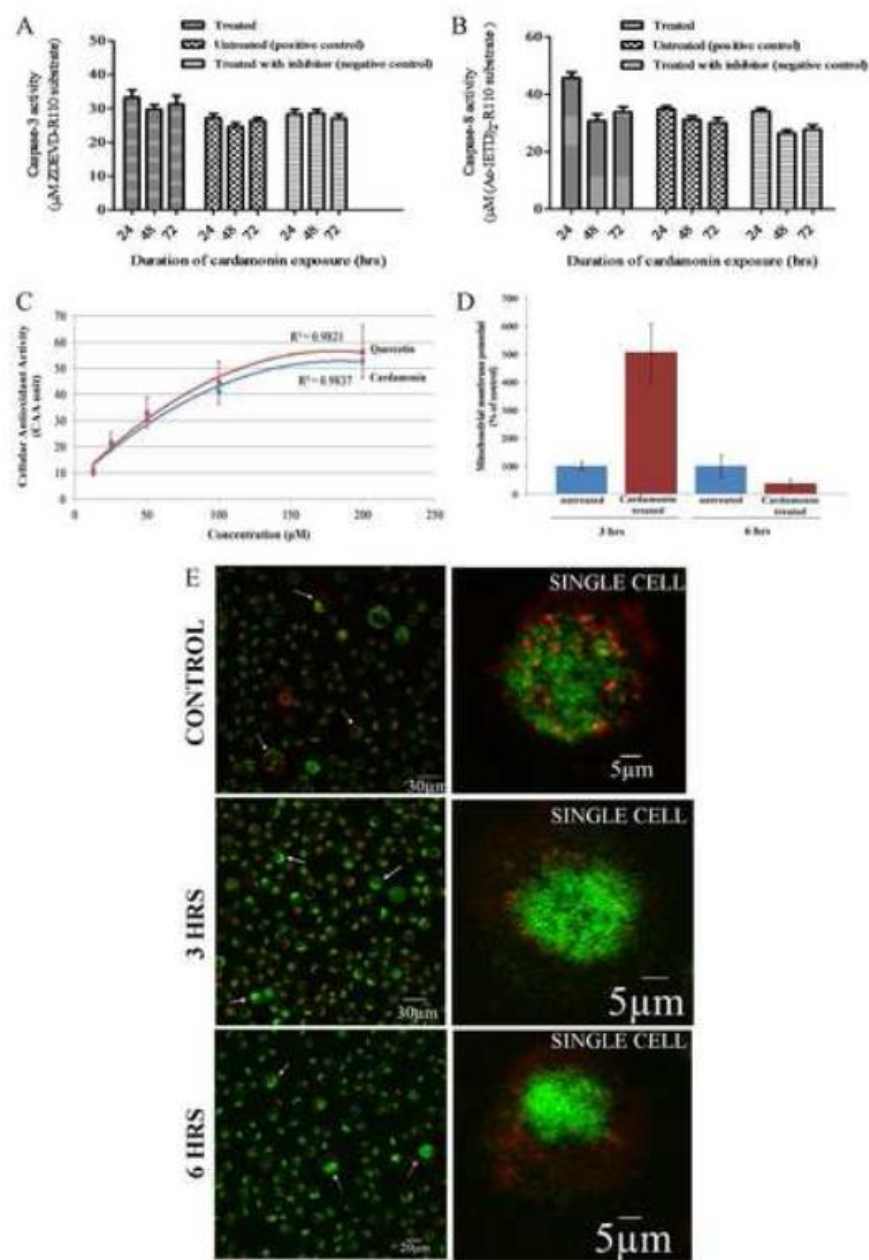
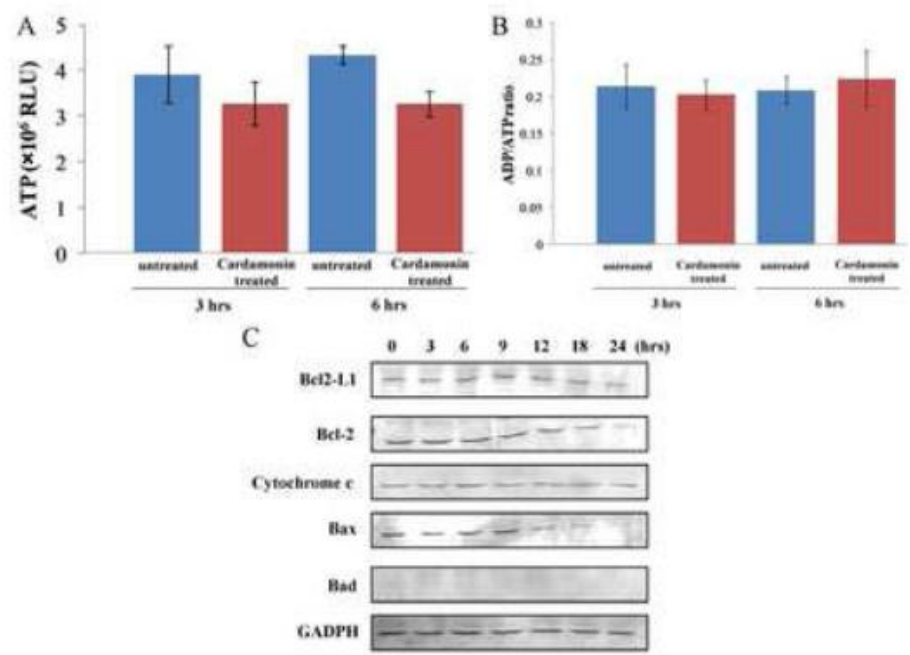


Figure 3  
[Click here to download high resolution image](#)



**Table 1**  
[Click here to download high resolution image](#)

Standard/Sample	EC <sub>50</sub> (μM)
Quercetin	89.27
Cardamonin	79.73



Table 2  
[Click here to download high resolution image](#)

	Threshold cycle (C <sub>T</sub> ) values		Normalized gene expression ratio
	Gene of interest (Caspase-9)	Reference gene (GADPH)	
<b>Control</b>	25.75 ± 0.15	14.33 ± 0.40	-
<b>Cardamonin treated</b>	26.66 ± 0.55	15.18 ± 0.57	1.04

## Author Agreement

### Author Agreement

Submission of work requires that the piece to be reviewed has not been previously published. Upon acceptance, the Author assigns to Phytomedicine the right to publish and distribute the manuscript as part or entirely. The Author's name will always be included with the publication of the manuscript.

The Author has the following nonexclusive rights: (1) to use the manuscript in the Author's teaching activities; (2) to publish the manuscript, or permit its publication, as part of any book the Author may write; (3) to include manuscript in the Author's personal or institutional database or on-line site; and (4) to license reprints of the manuscript to third persons for educational photocopying. The Author also agrees to properly credit the Phytomedicine as the original place of publication.

The Author hereby grants Phytomedicine full and exclusive rights to the manuscript, with consent from the Author (s).

I hereby accept the terms of the above Author Agreement.

Khoo Teng-Jin

---

Author:- Teng-Jin Khoo

Date:- 2<sup>nd</sup> April 2015

1   **Title**

2   Chemical- and Cell-based Antioxidant Capacity of Methanolic Extracts of Three Commonly  
3   Edible Plants from Zingiberaceae Family.

4

5   **Authors**

6   Michelle Chiang<sup>1</sup>, Yasin Kurmoo<sup>2</sup> and Teng-Jin Khoo<sup>1\*</sup>

7

8   **Author Affiliations**

9   <sup>1</sup>Centre for Natural & Medicinal Product Research, School of Pharmacy, Faculty of Science,  
10   The University of Nottingham Malaysia Campus, Jalan Broga, 43500, Semenyih, Selangor,  
11   Malaysia.

12   <sup>2</sup>Faculty of Science, School of Pharmacy, University of Nottingham, University Park,  
13   Nottingham, NG7 2RD.

14

15   \*Corresponding Author:

16

17   Centre for Natural & Medicinal Product Research, Faculty of Science, School of Pharmacy,  
18   The University of Nottingham Malaysia Campus, Jalan Broga, 43500, Semenyih, Selangor,  
19   Malaysia. (phone: +603-89248213; email: tengjin.khoo@nottingham.edu.my)

20

**Abstract**

Methanolic extracts of three edible plants in Zingiberaceae family; namely *Boesenbergia rotunda*, *Phaeomeria imperialis* and *Zingiber officinale* were evaluated to determine their phenolics and flavonoids contents and further compare their antioxidant properties. Conventional DPPH (2,2-diphenyl-1-picryl-hydrazyl), revolutionary CUPRAC (cupric ion reducing antioxidant capacity) and cellular antioxidant activity (CAA) in vitro assays were employed to evaluate the antioxidant activities of methanolic plant extracts for the first time. DPPH and CUPRAC antioxidant assays resulted in similar trend to total flavonoid content in the order *Z. officinale* > *P. imperialis* > *B. rotunda* where as *P. imperialis* revealed highest phenols content and displayed highest CAA. Methanolic extract of *Z. officinale* showed highest free radical scavenging ability hence flavonoids present may potentially act as natural source of antioxidant.

**Keywords:** Antioxidant, methanolic extracts, phenolics, flavonoids, Zingiberaceae.

## 18    **Introduction**

19    Human metabolism (oxidative phosphorylation) generates endogenous free radicals and reactive  
20    oxygen species (ROS), giving rise to oxidative stress (1) which will then give rise to chronic dis-  
21    eases, such as heart disease, neurodegenerative diseases and cancer (2). Upon ROS formation,  
22    lipid peroxidation can occur; leading to formation of toxic peroxides. These series of reactions  
23    cause direct tissue damage. ROS can also source nitrosation and deamination of amino groups in  
24    DNA point mutations and potentially, tumor formation (3,4). Antioxidants are molecules that  
25    inhibit oxidation of other molecules. They scavenge free radicals by donating an electron, in or-  
26    der to pair up the unpaired electron. They are essentially reducing agents (5). For centuries, edi-  
27    ble plants are commonly used in traditional remedy to treat a variety of diseases (6). Increasing  
28    antioxidants in the body will reduce ROS numbers and lower the risk of developing the afore-  
29    mentioned diseases. Consumption of foodstuffs containing antioxidants has proven effective in  
30    increasing plasma antioxidant concentration (7).

31  
32    There are approximately 1500 known species in Zingiberaceae family and the Malesian region  
33    contains 650 of those species (8). They grow in tropical and subtropical areas, which are damp,  
34    humid and shady. Delin and Larsen describe these plants as, “Herbs perennial, terrestrial, rarely  
35    epiphytic, aromatic, with fleshy, tuberous or non-tuberous rhizomes, often with tuber-bearing  
36    roots. Stems are usually short, replaced by pseudostems formed by leaf sheaths.” (9). Zingibera-  
37    ceae family was selected for investigation based on several reasons. Sabli et al. reported the abil-  
38    ity of the genus *Etlingera* and *Zingiber* to scavenge free radicals and act as natural antioxidants  
39    (10). A host of publications have demonstrated the antioxidant activity of *Z. officinale*. DPPH  
40    assay has shown a radical inhibition percentage of over 50% for the extracts of rhizomes from  
41    two varieties of *Z. officinale* (11). *Z. officinale* has also been shown to reduce lipid peroxidation

42 as much as the natural antioxidant ascorbic acid (12). The antioxidant potential of these three ed-  
43 ible plants have been looked into many times previously, with positive results in several antioxi-  
44 dant assays, such as ABTS decolourisation, FRAP assay and DPPH assay (13). ORAC assay has  
45 also been tested on the rhizomes which reported high antioxidant activity (14).

46

47

48 Methanol was utilized for maceration to extract polar compounds from the three edible plants as  
49 polyphenols and flavonoids extracted from polar solvents will result in high composition in the  
50 extract. In previous work published by Hassim et al. methanol extract was proven to contain  
51 higher polyphenols and flavonoids as compared to lesser polarity solvent such as ethanol and wa-  
52 ter (15). Hence, in current research we will utilize methanol to macerate and extract polar com-  
53 pounds which will be tested for their antioxidant capacities.

54

55 In 2004, Apak et al. successfully employed cupric ion reducing antioxidant capacity (CUPRAC)  
56 chromophore called the Cu(I)-neocuproine (Nc) chelate which formed when undergoing redox  
57 reaction with antioxidant to evaluate antiradical activity in plant extracts. This electron-transfer  
58 based assay measures the capacity of antioxidant in reduction of an oxidant which is substantiat-  
59 ed by colour change (15). Yildiz et al. solely used CUPRAC assay to associate flavonoid content  
60 with antioxidant functions (16). A relatively new antioxidant assay, Apak et al. reported various  
61 advantages of CUPRAC assay over other conventional antioxidant assays. One that distinguishes  
62 it from others is the effectiveness of CUPRAC assay in quantification of total antioxidants direct-  
63 ly from plant and food extracts. The chromogenic radical reagent is versatile and generally sta-  
64 ble, applicable to almost all antioxidants detection in plant extracts (17).

65 Antioxidant activity can also be evaluated using biological assay where by the activity is being  
66 measured *in vitro*. Cellular antioxidant activity (CAA) assay is a cell-based assay employed to  
67 measure the antioxidant activity within a cell. A fluorogenic dye is used to quantify the reactive  
68 oxygen species (ROS) within the cell cytosol (18).

69

70 Therefore, current research aimed to quantify phenol and flavonoid content and to evaluate the  
71 antioxidant activity using conventional DPPH free radical scavenging, revolutionary CUPRAC  
72 assay alongside with cellular antioxidant activity (CAA) assay in three commonly consumed  
73 plants in the family of Zingiberaceae.

74

## 75 **Materials and Methods**

76

### 77 **Plants and Chemicals**

78 *Z. officinale*, *B. rotunda* and *P. imperialis* were obtained from Pasar Tani, Prima Saujana, Ka-  
79 jang, Malaysia (3°0'25''N, 101°48'26''E). The following chemicals are of analytical reagent  
80 grade and were supplied from the corresponding sources: DPPH (2,2-diphenyl-1-picryl-  
81 hydrazyl), neocuproine (2,9-dimethyl-1,10-phenanthroline), Folin-Ciocalteu reagent, ascorbic  
82 acid, BHA (Butylated hydroxyanisole), gallic acid and quercetin: Sigma Aldrich (Steinheim,  
83 Germany); sodium carbonate, monopotassium phosphate (KH<sub>2</sub>PO<sub>4</sub>), disodium phosphate  
84 (Na<sub>2</sub>HPO<sub>4</sub>) and aluminium trichloride: R&M Chemicals (Selangor, Malaysia); Methanol and  
85 ethanol: RCI Labscan (Mueng Samutsakorn, Thailand); Copper (II) chloride dihydrate  
86 (CuCl<sub>2</sub>.2H<sub>2</sub>O), ammonium acetate: Merck (Darmstadt, Germany) and hydrogen peroxide (30%

87 v/v); System® (Selangor, Malaysia); OxiSelect Cellular Antioxidant Activity (CAA) Assay Kit  
88 (Cell Biolabs, Inc.).

89

#### 90 Apparatus

91 Absorption measurements were made either in quartz cuvettes using a Biochrom (Libra S12)  
92 UV-vis spectrophotometer (Cambridge, United Kingdom) or in a Varioskan Flash plate reader  
93 from Thermo Scientific (Massachusetts, USA). Rotary evaporation was performed in a Rotavap-  
94 tor-210 evaporator (BUCHI, Switzerland).

95

#### 96 Cell line

97 Human nasopharyngeal carcinoma (HK-1) cell line was material transferred upon signing of col-  
98 laboration with Department of Anatomy, The University of Hong Kong through local collabora-  
99 tion with Institute of Medical Research (IMR) Malaysia.

100

#### 101 Plant Extraction

102 All three plants were left to dry for one week, after which were pulverized, subjected to macera-  
103 tion in methanol for 3 days, in a 1:10 ratio (1 g in 10 mL of solvent). After maceration, each ex-  
104 tract was filtered through Whatman filter paper and the solvent evaporated via rotary evaporation  
105 at 37°C (19) to yield oily plant crude extracts. Each extract was kept in -4°C for further bioas-  
106 says.

107



108    Total Phenolic Content

109    100 µL of stock extract was placed in a test tube. 2 mL of 2% (w/v) sodium carbonate (Na<sub>2</sub>CO<sub>3</sub>)  
110    was added and was mixed vigorously. While mixing, 100 µL of 1:1 dilution of Folin-Ciocalteu  
111    reagent was added and test tube was allowed to stand for a minimum of 30 mins at room temper-  
112    ature. The absorbance against blank (0 µL of the standard gallic acid standard solution) was de-  
113    termined at 750 nm using Thermo Scientific Varioskan Flash multimode plate reader. Gallic ac-  
114    id with concentrations 25, 50, 100, 200 and 400 µg/mL were used as standard for determination  
115    of total phenolic compounds in plant extracts. Total phenolic content was expressed as mg gallic  
116    acid equivalents per g of sample (20, 21).

117

118    Total Flavonoid Content

119    100 µL of stock extract was placed in a test tube. 100 µL of 2% (w/v) aluminium trichloride  
120    (AlCl<sub>3</sub>) was added to test tube and incubated for 10 mins in the dark at room temperature. The  
121    absorbance against reagent blank (0 µL of the standard quercetin standard solution) was deter-  
122    mined at 415 nm using Thermo Scientific Varioskan Flash multimode plate reader. Quercetin  
123    with concentrations 25, 50, 100, 200 and 400 µg/mL were used as standard for determination of  
124    total flavonoid content in plant extracts. Total flavonoid content was expressed as mg quercetin  
125    equivalents per g of sample (22).

126

127    DPPH(2,2-diphenyl-1-picryl-hydrazyl) Radical Scavenging Assay

128    0.5 mL of plant methanolic extract was added to 0.2 mL of 0.1 mM ethanolic DPPH solution.  
129    The mixture was left to react in the dark at room temperature for 30 mins and measured spectro-

130 photometrically at 518 nm (23). DPPH radical scavenging activity (%) was calculated using the  
131 following formula:

132

133  $(1 - (\text{Absorbance of sample} - \text{Absorbance of blank sample}) / (\text{Absorbance of control sample})) \times 100$

134 where blank sample contained 0.2 mL of ethanol + 0.5 mL of sample/standards as positive con-  
135 trol and control sample contained 0.2 mL of 0.1 mM DPPH solution + 0.5 mL ethanol.

136 (24)

137

138 Cupric Ion Reducing Antioxidant Capacity (CUPRAC) Antioxidant Assay

139  $\text{CuCl}_2$  solution ( $1.0 \times 10^{-2}$  M) was prepared by dissolving 85.24 mg of  $\text{CuCl}_2 \cdot 2\text{H}_2\text{O}$  in 50 mL

140  $\text{H}_2\text{O}$ . Ammonium acetate buffer (pH 7.0, 1.0 M) was prepared by dissolving 3.854 g  $\text{NH}_4\text{Ac}$  in

141 50 mL  $\text{H}_2\text{O}$ . Neocuproine (Nc) ( $7.5 \times 10^{-3}$  M) was prepared by dissolving 78 mg of Nc in 50 mL

142 of 96% EtOH. Samples were prepared to a final concentration of 50  $\mu\text{g/mL}$  in  $\text{H}_2\text{O}$ . The proce-

143 dure highlighted by Apak and et al. was summarized as follows:

144

145 Add 1 mL  $10^{-2}$  M  $\text{Cu}^{2+}$  + 1 mL  $7.5 \times 10^{-3}$  M neocuproine + 1 mL 1 M  $\text{NH}_4\text{Ac}$  + x mL antioxidant  
146 solution +  $(1.1 - x)$  mL  $\text{H}_2\text{O}$ ; final volume 4.1 mL

147 (17)

148 The mixture was incubated at room temperature for 30 mins and read spectrophotometrically at

149 450 nm against a reagent blank.

150

151 Cellular Antioxidant Activity (CAA) Assay

152 CAA of plant methanolic extracts was measured using OxiSelect Cellular Antioxidant Activity

153 (CAA) Assay Kit (Cell Biolabs, Inc.) in nasopharyngeal carcinoma cell line (HK-1).  $2 \times 10^4$  HK-

154 1 cells were seeded in a clear bottom black 96-well plate for 24 hrs. All media was removed and

155 washed gently with phosphate buffered saline (PBS) for 3 times. 50  $\mu$ L of 2',7'-

156 dichlorodihydrofluorescein diacetate (DCFH-DA) probe was added to all wells before treated

157 with 50  $\mu$ L of plant methanolic extracts at different concentrations 31.3, 62.5, 125, 250, 500,

158 1000 and 2000  $\mu$ M.

159 Plate was incubated for 60 mins. After incubation, all solutions were removed and wells were

160 washed three times with PBS. 100  $\mu$ L of free radical initiator solution was added to each well.

161 Fluorescence was read at 37°C with excitation wavelength 480 nm and emission wavelength 530

162 nm for 60 mins with 5 mins intervals.

163

## 164 Results and Discussion

165

### 166 Total Phenolic and Flavonoid Content

167 Phenolics and flavonoids contents of three edible plants are presented in Table 1. *P. imperialis*

168 has the highest phenol content, followed by *B. rotunda* and *Z. officinale*. On the contrary, *Z. of-*

169 *ficinale* contained most flavonoids, followed by *P. imperialis* and *B. rotunda*. It can be deduced

170 that flavonoids present in *Z. officinale* are 7-fold the amount of phenolics. High flavonoids con-

171 tent present in *Z. officinale* methanolic extract compared to other edible plants may further ce-

172 ment a promising antioxidant property.

173 Both phenols and flavonoids are bioactive compounds present in most plants and possess robust  
174 antioxidant activity. A significant finding reported that increasing phenol content leads to an in-  
175 creased antioxidant activity (25). Recent research suggested the association between both flavo-  
176 noids and phenols content and antioxidant activity. It is likely that the plant with the highest con-  
177 centration of one or both moieties will exhibit most potent antioxidant activity (11).

178

#### 179 DPPH (2,2-diphenyl-1-picryl-hydrazyl) Radical Scavenging Assay

180 This is a very common method to determine radical scavenging capabilities. DPPH itself is a rad-  
181 ical and, in ethanol solution, has a deep violet colour, with a strong peak at approximately  
182 520nm. When DPPH is mixed with a reducing agent, i.e. a substance that can donate a hydrogen  
183 atom, it becomes the reduced form of DPPH. The violet colour is replaced with a dull yellow  
184 colour and has a lower absorption at 520nm (23).

185

186 The DPPH radical scavenging activity of the edible plant methanolic extracts and standard anti-  
187 oxidants increased in the order of *B. rotunda* < *P. imperialis* < quercetin < BHA < gallic acid <  
188 *Z. officinale* < ascorbic acid (Figure 2). *Z. officinale* methanolic extract displayed higher radical  
189 scavenging activity than two other plant extracts. The actions of radical scavenging may be con-  
190 tributed by high flavonoids present in *Z. officinale* methanolic extract.

191

#### 192 Cupric Ion Reducing Antioxidant Capacity (CUPRAC) Antioxidant Assay

193 It has been previously reported that CUPRAC has effectively demonstrated various advantages  
194 over other antioxidant assays. It is relatively more sensitive and environment where reaction oc-

195 curs is near to physiological pH (15). In present findings, reducing power decreased in the order  
196 of gallic acid > ascorbic acid > quercetin > BHA > *Z. officinale* > *P. imperialis* > *B. rotunda*  
197 (Figure 3). All there methanolic edible plant extracts showed lower reducing capability than  
198 standard antioxidants. However, antioxidant capacity of *Z. officinale* methanolic extract was  
199 shown to be highest among all plant extracts.

200

#### 201 Cellular Antioxidant Activity (CAA) Assay

202 HK-1 cells were pre-incubated with cell-permeable DCFA-DA fluorescence probe and quercetin  
203 (antioxidant standard) or methanolic plant extracts.

204 2,2'-Azo-bis-amidinopropane (ABAP), a free radical initiator causes generation of peroxy radicals  
205 which leads to a rapid oxidation of DCFH to highly fluorescent 2'7'-  
206 dichlorodihydrofluorescein (DCF). Antioxidant present in plant extracts will quench these per-  
207 oxy radicals by preventing the generation of DCF (Figure 1). Therefore, CAA assay measures  
208 the ability of antioxidants to inhibit oxidation of DCFH to DCF. The conversion from non-  
209 fluorescent DCFH to fluorescent DCF act as an oxidative stress indicator. Quercetin was em-  
210 ployed as standard for CAA assay because it is pure, relatively stable and widely found in fruits  
211 and vegetables (18).

212

213 CAA assay is greatly dependent on the properties of antioxidants and their interactions with  
214 cells. Antioxidant can react by inhibiting peroxy radical chain on cell surface or react intracellu-  
215 larly. The structural properties of flavonoids and other phytochemicals such as polarity also de-  
216 termine the interactions on the cell membrane (26). It has been proven previously that flavonoid

217 such as quercetin contains 2,3-double bond and 4-oxo group displayed high CAA (18). Current  
218 finding showed that cellular antioxidant activity (CAA) of the edible plant methanolic extracts  
219 and quercetin standard antioxidant decreased in the order of quercetin > *P. imperialis* > *Z. offici-*  
220 *nale* > *B. rotunda* (Figure 4). Methanolic extract of *P. imperialis* contains highest phenols con-  
221 tent and highest CAA compared to *Z. officinale* and *B. rotunda*. CAA values were reported to be  
222 significantly correlated with total phenolics content in common fruits (27). Current result sug-  
223 gests that phenolics content in *P. imperialis* may contribute to CAA in nasopharyngeal carcino-  
224 ma, HK-1 cells.

225

## 226 **Conclusion**

227

228 From this study, we can conclude that methanolic extract of *Z. officinale* revealed highest flavo-  
229 noid content and displayed most effective antioxidant capability in DPPH and CUPRAC antioxi-  
230 dant assays compared to *B. rotunda* and *P. imperialis* in Zingiberaceae family. Methanolic ex-  
231 tract of *P. imperialis* contains highest phenols content which associated with high antioxidant  
232 activity (CAA assay). Future work involves elucidation of the compound responsible to trigger  
233 the actions of radical scavenging.

234

## 235 **Acknowledgments**

236 This work was funded by Public Service Department of Malaysia (JPA) for Scholarship to  
237 Chiang Michelle. We would also like to thank Prof GSW Tao, The University of Hong Kong and  
238 Dr Alan Khoo, Institute of Medical Research, Malaysia for providing the HK-1 cell line.

239 **Author Contributions**

240 All authors contributed equally from participation in experimental designs, execution of labora-  
241 tory experiments to writing up the manuscript. All authors read and approved the final manu-  
242 script.

243

244 **Conflict of interest**

245 The authors declare that they have no competing interests.

246

247 **References**

- 248 1. Zheng W, Wang SY. Antioxidant activity and phenolic compounds in selected herbs. J of Agr  
249 and Food Chem. 49: 5165-5170 (2001).
- 250 2. Astley SB. Dietary antioxidants past, present and future. Trends in Food, Sci and Tech. 14: 93-  
251 98 (2003).
- 252 3. Mylonas C. Kouretas D. Lipid peroxidation and tissue damage. *In Vivo*. 13(3): 295-309  
253 (1999).
- 254 4. Aruoma OI, Cuppett SL. Antioxidant Methodology: *In-Vivo and Iv-Vitro* Concepts. Illinois,  
255 USA. American Oil Chemists (1997).
- 256 5. Panglossi HV. Antioxidants: New Research. New York, USA. Nova Science Publishers, Inc.  
257 (2006).
- 258 6. Tepe B, Sokmen M, Akpulat HA, Sokmen A. Screening of the antioxidant potentials of six  
259 *Salvia* species from Turkey. Food Chem. 95: 200-204 (2006).
- 260 7. Walton NJ, Brown DE. Chemicals from plants: Perspectives on Plant Secondary Products.  
261 London, UK. Imperial College Press (1999).
- 262 8. Sirirugsa P. Thai Zingiberaceae: Species Diversity And Their Uses. Pure and Applied Chem.  
263 IUPAC, 70 (1999).
- 264 9. Delin W, Larsen K. (2000). Zingiberaceae. Flora of China. 24: 322-377 (2000).  
265

- 266 10. Sabli F, Mohamed M, Rahmat A, Ibrahim H, Abu Bakar MF. Antioxidant Properties of Se-  
267 lected *Etlingera* and *Zingiber* Species (Zingiberaceae) from Borneo Island. *Int J of Biol Chem.*  
268 6(1): 1-9 (2012).  
269
- 270 11. Ghasemzadeh A, Jaafar HZE, Rahmat A. (2010). Antioxidant Activities, Total Phenolics and  
271 Flavonoids Content in Two Varieties of Malaysia Young Ginger (*Zingiber officinale* Roscoe).  
272 *Molecules.* 15, 4324-4333 (2010).
- 273 12. Ahmed RS, Seth V, Banerjee BD. Influence of dietary ginger (*Zingiber officinales* Rosc) on  
274 antioxidant defence system in rat: comparison with ascorbic acid. *Indian J of Exp Biol.*  
275 38(6):604-606 (2000).  
276
- 277 13. Jing LJ, Mohamed M, Rahmat A, Abu Bakar AF. Phytochemicals, antioxidant properties and  
278 anticancer investigations of the different parts of several gingers species (*Boesenbergia rotunda*,  
279 *Boesenbergia pulchella* var *attenuata* and *Boesenbergia armeniaca*). *J of Med Plant Res.*  
280 4(1):27-32 (2010).  
281
- 282 14. Isa NM, Abdelwahab SI, Mohan S, Abdul AB, Sukari MA, Taha MME, Syam S, Narrima P,  
283 Cheah SC, Ahmad S, Mustafa MR. *In vitro* anti-inflammatory, cytotoxic and antioxidant activi-  
284 ties of boesenbergin A, a chalcone isolated from *Boesenbergia rotunda* (L.) (fingerroot). *Brazili-*  
285 *an J of Med and Biol Res.* 45(6): 524-530 (2012).
- 286 15. Apak R, Guclu K, Ozyurek M, Karademir SE. Novel Total Antioxidant Capacity Index for  
287 Dietary Polyphenols and Vitamins A and E, Using Their Cupric Ion Reducing Capability in the  
288 Presence of Neocuproine: CUPRAC Method. *J of Agri and Food Chem.* 52: 7970-7981 (2004).  
289
- 290 16. Yildiz L, Baskan KS, Tutem E, Apak R. Combined HPLC-CUPRAC (cupric ion reducing  
291 antioxidant capacity) assay of parsley, celery leaves, and nettle. *Talanta.* 77(1): 304-13 (2008).
- 292 17. Apak R, Guclu K, Ozyurek M, Celik SE. Mechanism of antioxidant capacity assays and the  
293 CUPRAC (cupric ion reducing antioxidant capacity) assay. *Microchim Acta.* 160: 413-419  
294 (2008).  
295
- 296 18. Wolfe KL, Liu RH. Cellular Antioxidant Activity (CAA) Assay for Assessing Antioxidants,  
297 Foods, and Dietary Supplements. *J of Agri and Food Chem.* 56: 8896-8907 (2007).  
298
- 299 19. Furuse AY, Peutzfeldt A, Asmussen E. Effect of evaporation of solvents from one-step, self-  
300 etching adhesives. *J of Adhe Dent.* 10(1): 35-9 (2008).
- 301 20. Singleton VL, Orthofer R, Lamuela-Raventos RM. Analysis of total phenols and other oxida-  
302 tion substrates and antioxidants by means of folin-ciocalteu reagent. *Methods Enzymol.* 299:152-  
303 178 (1999).
- 304 21. Ainsworth EA, Gillespie KM. Estimation of total phenolic content and other oxidation sub-  
305 strates in plant tissues using Folin-Ciocalteu reagent. *Nat Protoc.* 2: 875-877 (2007).



306 22. Papoti VT, Xystouris S, Papagianni G, Tsimidou MZ. "Total Flavonoid" Content Assessment  
307 Via Aluminium [AL(III)] Complexation Reactions. What We Really Measure? Italian J of Food  
308 Sci. 23(3): 252 (2011).

309 23. Molyneux P. The use of the stable free radical diphenylpicrylhydrazyl (DPPH) for estimating  
310 antioxidant activity. Songklanakarin J of Sci and Tech. 26(2): 211-219 (2004).

311 24. Li Y, Jiang B, Zhang T, Mu W, Liu J. Antioxidant and free radical-scavenging activities of  
312 chickpea protein hydrolysate (CPH). Food Chem. 106: 444-450 (2007).  
313

314 25. Velioglu YS, Mazza G, Gao L, Oomah BD. Antioxidant Activity and Total Phenolics in Se-  
315 lected Fruits, Vegetables, and Grain Products. J of Agri and Food Chem. 46: 4113-4117 (1998).

316 26. Oteiza PI, Erlejman AG, Verstraeten SV, Keen CL, Fraga CG. Flavonoid-membrane interac-  
317 tions: a protective role of flavonoids at the membrane surface. Clin and Dev Immunol. 12(1): 19-  
318 25 (2005).

319 27. Wolfe KL, Kang X, He X, Dong M, Zhang Q, Liu RH. Cellular Antioxidant Activity of Common  
320 Fruits. J of Agri and Food Chem. 56: 8418-8426 (2008).  
321

322

323

324

325

326

327

328

329

330

331

332

333

334

335

336

337 **Tables**

338

339 Table 1: Total phenolic and flavonoid contents of methanolic extract in three edible plants of  
340 Zingiberaceae family.

341

342

Edible plant	Total phenolics (mg GAE/g sample)	Total flavonoid (mg QE/g sample)
<i>Z. officinale</i>	15.76±0.003	111.68±0.004
<i>B. rotunda</i>	30.11±0.002	42.63±0.002
<i>P. imperialis</i>	42.65±0.002	67.84±0.007

343

344

345

346

347 Values are presented in mean±SD (n=3). Total phenolics was expressed as mg gallic acid  
348 equivalent (mg GAE) in 1 g of dry sample and total flavonoid was expressed as mg quercetin  
349 equivalent (mg QE) in 1 g of dry sample.

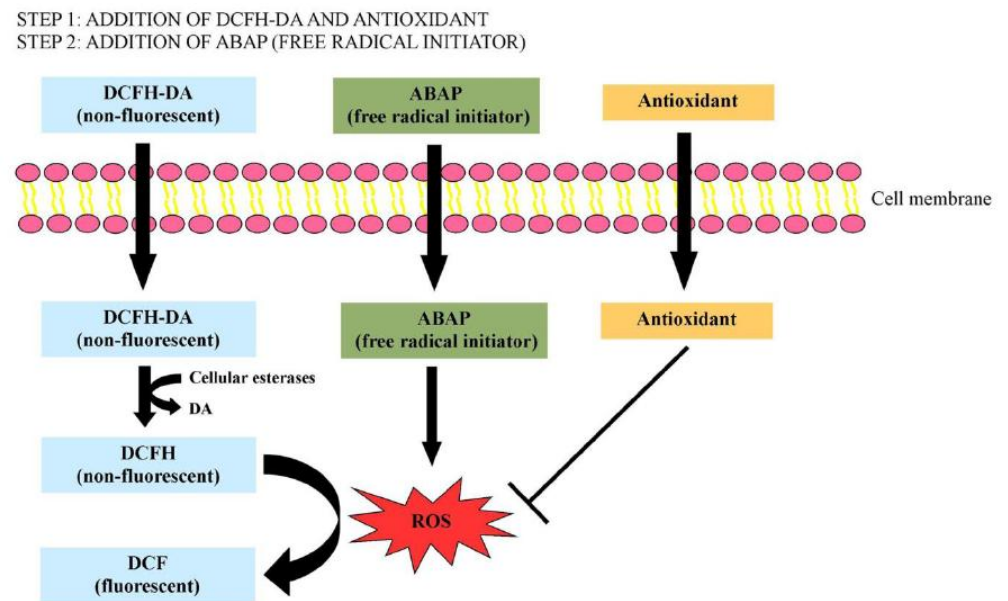
350

351

352

353

354 **Figures**



355

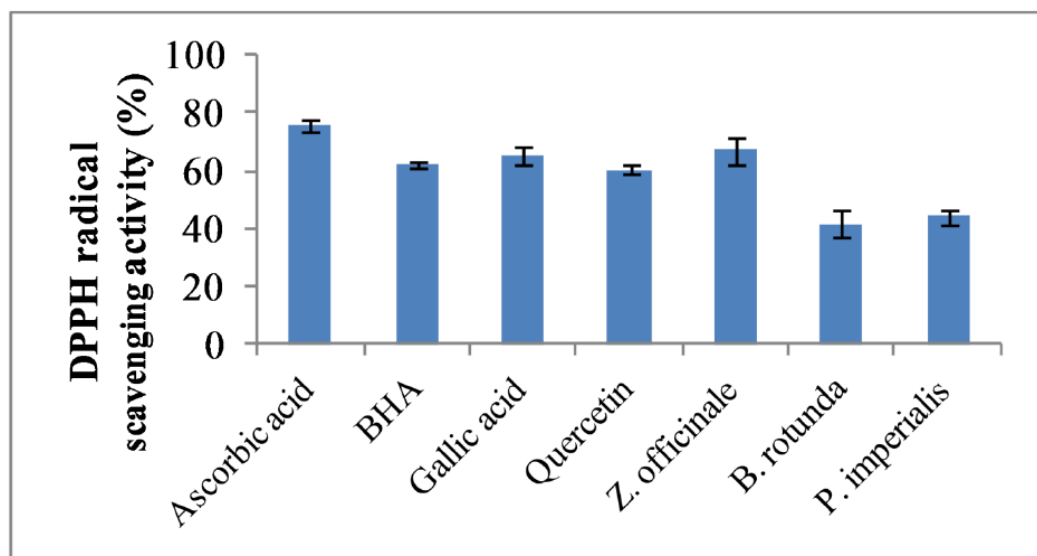
356 Figure 1: Schematic diagram illustrates steps in Cellular Antioxidant Activity (CAA) assay.

357

358

359

360



361

362 Figure 2: DPPH radical scavenging activity of Z. officinale, B. rotunda, P. imperialis and antiox-  
 363 idant standards.

364

365

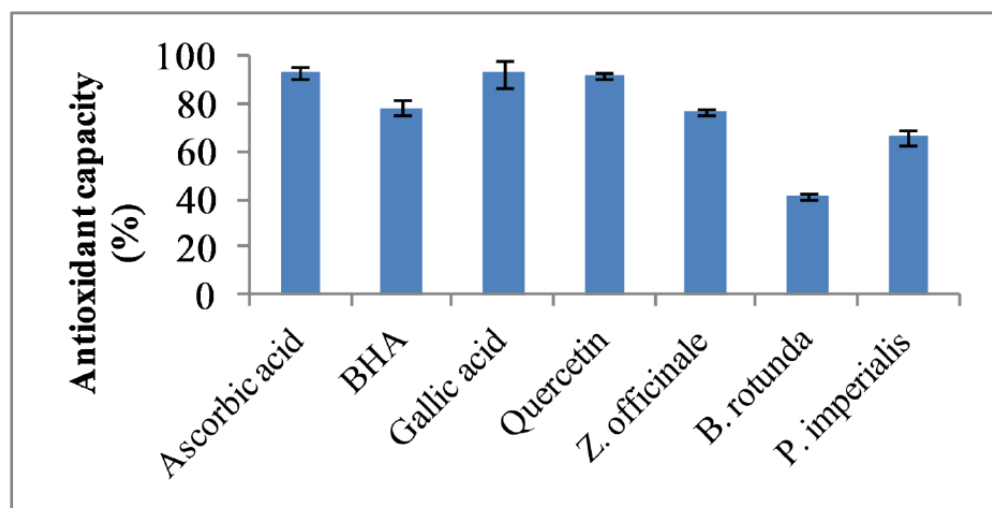
366

367

368

369

370



371 Figure 3: CUPRAC antioxidant capacity of *Z. officinale*, *B. rotunda*, *P. imperialis* and standard  
372 antioxidants.

373

374

375

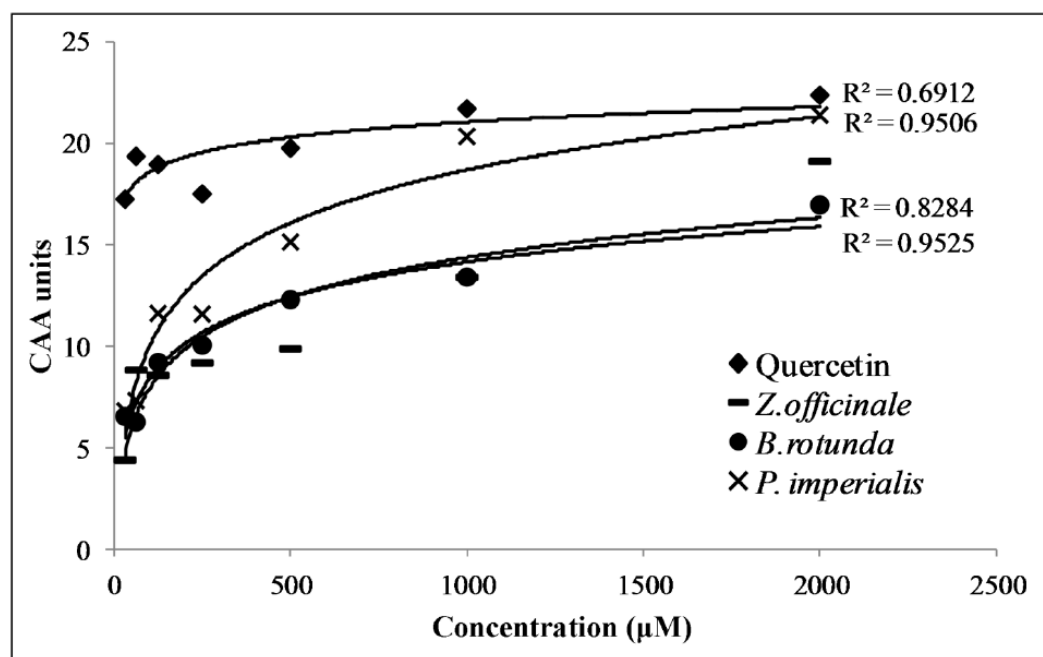
376

377

378

379

380



381

382 Figure 4: Dose-response curve of cellular antioxidant activity (CAA) of Z. officinale, B. rotunda,

383 P. imperialis and quercetin antioxidant standard.